

**Engineering Polymer Networks for Enhanced Loading and Extended Release of
Therapeutics via Molecular Imprinting**

by

Arianna Tieppo Rappo

A dissertation submitted to the Graduate Faculty of
Auburn University
in partial fulfillment of the
requirements for the Degree of
Doctor of Philosophy

Auburn, Alabama
December 14, 2013

Keywords: ocular therapy, molecular imprinting, controlled drug delivery,
polymer hydrogels, cognitive polymers

Copyright 2013 by Arianna Tieppo Rappo

Approved by

Mark E. Byrne, Chair, Daniel F. & Josephine Breeden Associate Professor of Chemical
Engineering

Christopher B. Roberts, Uthlaut Professor of Chemical Engineering

Maria L. Auad, Associate Professor of Polymer and Fiber Engineering

Elizabeth Lipke, Assistant Professor of Chemical Engineering

Abstract

Conventional topical ocular therapies such as eye drops and ointments are the current “go to” therapy, and account for over 90% of the market. However, topical drug delivery results in very low drug bioavailability, ranging from 1-7%. Therefore, there is a significant unmet need in the ocular therapeutic market for effective drug delivery mechanism. This study focused on the rational design and engineering of novel contact lenses via molecular imprinting techniques, capable of tailorable loading and extended release of ocular therapeutics.

Poly(HEMA-co-DEAEM-co-PEGnDMA) hydrogels imprinted with the non-steroidal anti-inflammatory, diclofenac sodium (DS), were engineered exploiting ionic and hydrogen bonding non-covalent interactions to better understand the effect of various compositional parameters, such as amount and length of crosslinking monomers, template concentration, and functional monomer concentration, on their macromolecular structure and subsequently their binding and transport properties. Varying the compositional parameters had diverse effects on the imprinted hydrogel properties. For example, an increase in the amount of crosslinking resulted in ~3.0 times smaller mesh size, ~1.6 times lower template binding capacity, ~1.3 times lower template binding affinity, and ~1.8 times lower transport diffusion coefficients. When the release studies were performed in artificial lacrimal solution, the presence of salts and ions altered interactions between the anionic template molecule and the cationic functional monomer. A controlled and extended release of diclofenac sodium was achieved for up to 72 hours in artificial lacrimal solution. Moreover, the diffusion coefficients of diclofenac sodium through

weakly crosslinked imprinted poly(HEMA-co-DEAEM-co-PEG200DMA) lenses were further controlled by adjusting the functional monomer to template (FM/T) ratio (1, 3.5 and 10.5). There was an inverse correlation between the FM/T ratio and the diffusion coefficient. Extended and controlled release of therapeutically relevant concentrations of diclofenac was achieved for up to 6 days in lacrimal solution at *in vitro* ocular flowrates.

A polyvinyl alcohol (PVA) macromer, Nelfilcon A, which has ~4.4 times larger chain building blocks than poly(HEMA-co-DEAEM-co-PEG200DMA), was used as a backbone monomer to engineer a daily disposable contact lens to tailor the release rate of diclofenac sodium, permitting the study of the imprinting effectiveness in this large network structure. Additionally, silicone hydrogel contact lenses were engineered with varying hydrophobic:hydrophilic ratios as well as including additional crosslinking monomers. As the hydrophobic:hydrophilic ratio increased, the diffusion coefficient of diclofenac decreased up to ~36 times. Release was delayed due to a combination of increased hydrophobic to hydrophilic composition and the inclusion of additional structural constraints, both of which decreased the polymer volume fraction in the swollen state.

The study also demonstrated the successful *in vivo* extended release of an anti-histamine drug, ketotifen fumarate, from molecularly imprinted, therapeutic contact lenses. This is the first time that a steady, effective concentration of drug was maintained in the tear film from a contact lens for an extended period of time for the entire duration of lens wear. The results showed that the imprinted lenses exhibited ~100 times greater bioavailability than eye drops and a dramatic increase in ketotifen mean residence time (MRT).

Finally, variations in the release conditions (e.g., volume, mixing rate, and temperature) and their effect on the release of a wide spectrum of both hydrophilic and hydrophobic drugs

(ketotifen fumarate, diclofenac sodium, timolol maleate, and dexamethasone) from conventional hydrogel lenses and silicone hydrogel lenses were studied. It was found that volume had the biggest effect on the release profile, which incidentally is the least consistent variable throughout the literature. Faster release rates of up to 12 times were observed when the volume was changed from 2 mL to 200 mL.

Acknowledgements

I would like to thank my advisor, Dr. Mark Byrne, whose encouragement, guidance and support, allow me to pursue my doctoral degree. His contributions to develop my understanding of different aspects of my research field have been fundamental. I would also like to thank my committee members, Dr. Chris Roberts, Dr. Elizabeth Lipke, and Dr. Maria L. Auad, for their willingness to serve on my committee and their extraordinary patience and support. I would like to thank Dr. Jacek Wower for his willingness to serve as my outside reader. I would also like to acknowledge the chemical engineering staff, Karen Cochran, Sue Allen, Georgetta Dennis, and Jennifer Harris for helping me with academic, financial and logistic matters.

My fellow lab mates have been a tremendous source of technical and moral support and to them I extend my gratitude. I especially want to thank Matthew Eggert and Dr. Vishal Salian for their guidance and their assistance when I first started in the lab. I want also to acknowledge my undergraduate and REU students, Amanda Paine, Aarika Boggs, Kayla Pate and Payam Pourjavad for their contributions to the work presented in this dissertation.

My greatest thanks are to my family and friends, especially my parents, Susana Rappo, Rafael Pagán and Reinaldo Tieppo, my sister, María José Pagán, my aunt, Enriqueta Silva, my cousin, Dunia Cortés and my friends, Maria Adela Ansaldi, Xiu Wang and Min Kim. I cannot possibly thank you enough for taking care of my baby, Santiago, while doing my experiments in the lab. I would also like to thank my aunt, Judith Chaffee, for reviewing my dissertation.

Last but not least, I would like to thank my husband, Hector Galicia for his friendship, advice and for being my support structure in Auburn. This is as much your achievement as it is mine and this work is dedicated to you and to our son, Santiago.

Financial support for this work was provided by OcuMedic Inc., and CIBA Vision Inc. I would like to thank Ciba Vision personnel, Dr. Lynn Winterton, Dr. John Pruitt and Jared Nelson for their support of this work.

Table of Contents

Abstract.....	ii
Acknowledgments.....	v
List of Tables	xiii
List of Figures.....	xv
1.0 Introduction.....	1
2.0 Drug Delivery of Ocular Therapeutics	5
2.1 Barriers to Ocular Transport, Ocular Bioavailability and Pharmacokinetics	7
2.1.1 Routes of Ocular Drug Delivery to the Anterior Segment	8
2.1.1.1 Lipophilic drugs	11
2.1.1.2 Hydrophilic drugs	11
2.1.1.3 Ionizable drugs.....	12
2.1.2 Routes of Ocular Drug Delivery through the Blood Ocular Barriers	13
2.1.3 Routes of Ocular Drug Delivery to the Posterior Segment.....	14
2.2 Current Trends of Ocular Drug Delivery to the Anterior Segment	16
2.2.1 Eye Drops and Ointments	16
2.2.2 Inserts and In-situ Gel Systems.....	18
2.2.3 Contact Lenses	19
3.0 Contact Lenses as Platform for Drug Delivery.....	26
3.1 Drug Soaked Lenses	29

3.2 Supercritical Solvent Impregnation	32
3.3 Diffusion Barriers	33
3.4 Inclusion of Chemistry and Network Design.....	35
3.4.1 Direct Embedding	35
3.4.2 Cyclodextrins	36
3.4.3 Ion-ligand Mechanism	37
3.4.4 Polymer Degradation	39
3.5 Particle-laden Strategies.....	40
3.6 Molecular Imprinting	44
4.0 Characterization of Imprinted Contact Lenses	52
4.1 Diffusion through an Imprinted Hydrogel	52
4.1.1 Theoretical Model for Diffusion	53
4.2 Structural Characterization of Imprinted Hydrogels.....	55
4.2.1 Equilibrium Swelling Theory	56
4.2.2 Rubber Elasticity Theory	58
4.3 Determination of Template Binding Parameters	60
5.0 Effect of Crosslinker Diversity on Drug Loading, and Drug Release from Molecularly Imprinted Hydrogels	63
5.1 Creating Memory in Hydrophilic Hydrogels via Imprinting Techniques	65
5.2 Materials and Methods.....	66
5.2.1 Materials and Reagents	66
5.2.2 Synthesis of Molecularly Imprinted Poly(HEMA-co-DEAEM-co-PEGnDMA) Hydrogels.....	66
5.2.3 Equilibrium Swelling Studies and Mechanical Properties.....	68

5.2.4 Template Binding Experiments and Analysis of Binding Parameters.....	69
5.2.5 Dynamic Template Release Studies and Diffusion Coefficient Determination	70
5.3 Results and Discussion	70
5.3.1 Structural Analysis for Imprinted Poly(HEMA-co-DEAEM-co-PEGnDMA).....	70
5.3.2 Diclofenac Sodium Loading Studies for Imprinted Poly(HEMA-co-DEAEM-co-PEGnDMA)	72
5.3.3 Dynamic Release Studies for Imprinted Poly(HEMA-co-DEAEM-co-PEGnDMA)	74
5.3.4 Imprinted Poly(HEMA-co-DEAEM-co-PEG200DMA).....	75
5.3.5 Assessment of the Molecular Imprinting Technique and Release Studies in Lacrimal Solution.....	79
5.4 Conclusions.....	83
6.0 <i>In Vitro</i> Controlled Release of Diclofenac Sodium from HEMA Lenses under Physiological Ocular Tear Flow	93
6.1 Materials and Methods.....	95
6.1.1 Materials and Reagents	95
6.1.2 Synthesis of Molecularly Imprinted Contact Lenses	96
6.1.3 Diclofenac Sodium Loading Studies	97
6.1.4 Lens Mechanical Properties, Structural Studies, and Optical Clarity Studies	98
6.1.5 <i>In Vitro</i> Diclofenac Release Studies	99
6.1.6 Design and Fabrication of Microfluidic Device	100
6.1.7 Analysis of Drug Release from Contact Lenses	100
6.2 Results and Discussion	101
6.2.1 Diclofenac Sodium Loading Studies	101
6.2.2 Dynamic Release Studies.....	103

6.2.2.1 Infinite sink release studies	103
6.2.2.2 Release studies under physiological flow conditions	104
6.2.2.3 Release analysis for daily disposable lenses	106
6.2.3 Structural Analysis.....	108
6.3 Conclusions.....	109
7.0 Engineering Therapeutic Contact Lenses for Delivery of Non-Steroidal Anti-Inflammatory Drugs.....	117
7.1 Creating Memory in Nelfilcon A Lenses.....	119
7.2 Materials and Methods.....	121
7.2.1 Reagents.....	121
7.2.1.1 Nelfilcon A.....	122
7.2.1.2 Lotrafilcon B.....	123
7.2.1.3 Synthesis of acrylanidomethyl- β -cyclodextrin (β -CD-NMA).....	123
7.2.2 Synthesis of Nelfilcon A Contact Lenses	124
7.2.3 Synthesis of Silicone A Contact Lenses	126
7.2.4 Diclofenac Sodium Loading Studies	127
7.2.5 Dynamic Release Studies.....	128
7.2.5.1 Effect of ionic strength in the release of diclofenac sodium.....	129
7.2.6 Swelling Studies and Tensile Studies	129
7.2.7 Optical Clarity Studies.....	130
7.3 Results and Discussion	131
7.3.1 Dynamic Release of Diclofenac Sodium from Nelfilcon A Lenses	131
7.3.2 Structural Analysis of Nelfilcon A-DS Lenses.....	140
7.3.3 Dynamic Release of Diclofenac Sodium from Lotrafilcon B Lenses.....	142

7.4 Conclusions.....	147
8.0 Sustained <i>In Vivo</i> Release of Ketotifen Fumarate from Imprinted Therapeutic Contact Lenses	166
8.1 Materials and Methods.....	167
8.1.1 Rabbit Purchase, Handling, and Ophthalmic Evaluation.....	167
8.1.2 Synthesis of Imprinted Lenses and Ketotifen Loading.....	169
8.1.3 Transport and Structural Characterization Studies	170
8.1.4 In vitro Dynamic Therapeutic Release Studies.....	171
8.1.5 Fitting of Lenses and In vivo Release Studies	172
8.1.6 Pharmacokinetic Parameters of Ketotifen Fumarate in Tear Fluid	173
8.2 Results and Discussion	173
8.3 Conclusions.....	179
9.0 Effects of Sink Conditions on Release Kinetics of Ocular Therapeutic from Contact Lenses	185
9.1 Materials and Methods.....	187
9.1.1 Materials and Reagents	187
9.1.2 Synthesis of Therapeutic Hydrogels Films	188
9.1.3 Drug Loading of Hydrogel Films	189
9.1.4 Dynamic Therapeutic Release Study.....	190
9.2 Results and Discussion	191
9.2.1 Release Studies from Hydrophilic, Conventional Hydrogels	191
9.2.2 Release Studies from Silicone Hydrogels.....	194
9.2.3 Effect of Temperature and Mixing Rate	196
9.3 Conclusions.....	196

10.0 Conclusions.....	207
References.....	212
Appendix A: Nelfilcon A Lenses.....	243
Appendix B: Silicone Lenses.....	253

List of Tables

Table 2.1: Summary of the global ophthalmic forecast by diseases class for 2009 and 2014.....	6
Table 5.1: Equilibrium swelling parameters of imprinted poly (HEMA-co-DEAEM-co-PEGnDMA)	71
Table 5.2: Structural parameters of imprinted poly(HEMA-co-DEAEM-co-PEGnDMA).....	71
Table 5.3: Binding capacities and affinities, and diffusion coefficients for imprinted poly(HEMA-co-DEAEM-co-PEGnDMA).....	73
Table 5.4: Equilibrium swelling parameters of imprinted poly(HEMA-co-DEAEM-co-PEG200DMA)	76
Table 5.5: Structural parameters of imprinted poly(HEMA-co-DEAEM-co-PEG200DMA).....	76
Table 5.6: Binding capacities, affinities and diffusion coefficients for diclofenac sodium in imprinted poly(HEMA-co-DEAEM-co-PEG200DMA)	77
Table 5.7: Binding capacities, affinities and diffusion coefficients for diclofenac sodium in poly(HEMA-co-DEAEM-co-PEG200DMA)	80
Table 5.8: Structural parameters of poly(HEMA-co-DEAEM-co-PEG200DMA)	82
Table 6.1: Partition coefficients, binding capacities and affinities for diclofenac sodium in poly(HEMA-co-DEAEM-co-PEG200DMA) hydrogels	102
Table 6.2: Summary of diffusion coefficients, power law exponents and swelling data	104
Table 6.3: Equilibrium swelling parameters of poly(HEMA-co-DEAEM-co-PEG200DMA) ...	108
Table 6.4: Structural parameters of poly(HEMA-co-DEAEM-co-PEG200DMA)	109

Table 7.1: Silicone contact lens formulations.....	126
Table 7.2: Physical parameters of the silicone contact lenses in swollen state	127
Table 7.3: Diclofenac sodium diffusion coefficient and release order from imprinted Nelfilcon A lenses with varying DADMAC proportions	134
Table 7.4: Equilibrium weight swelling values compared for lenses containing DADMAC and MAPTAC.....	136
Table 7.5: Equilibrium swelling parameters and transmittance values of Nelfilcon A-DS lenses with functional monomers	141
Table 7.6: Structural parameters of Nelfilcon A-DS lenses with functional monomers	142
Table 7.7: Diffusion coefficient, equilibrium swelling parameters and structural parameters of silicone contact lenses.....	145
Table 8.1: Pharmacokinetic parameters calculated from the concentration time profiles of ketotifen fumarate in tear fluid	176
Table 9.1: Formulation of hydrophilic, conventional hydrogel films	188
Table 9.2: Formulation of silicone hydrogel films	188
Table B.1: Silicone lens formulations.....	254
Table B.2: Silicone lens formulations with functional monomers	255
Table B.3: Silicone lens formulations with functional monomers	255

List of Figures

Figure 2.1: Pathway of the drug administered by topical formulations	21
Figure 2.2: Transport of drugs through the surface of the eye.....	22
Figure 2.3: Transport of drugs through the anterior segment of the eye.	23
Figure 2.4: Transport of drugs through the posterior segment of the eye.....	24
Figure 2.5: Ocular tear film drug concentration based on delivery method.	25
Figure 3.1: Classification of contact lenses on the basis of material, modalities and use.	49
Figure 3.2: Demonstration of release mechanisms used within contact lenses.	50
Figure 3.3: General schematic of the imprinting technique.....	51
Figure 5.1: Functional monomers and crosslinking monomers.....	84
Figure 5.2: Equilibrium binding isotherms for diclofenac sodium by imprinted hydrogels with varying length of crosslinker	85
Figure 5.3: Fractional diclofenac released in DI water from imprinted poly(HEMA-co-DEAEM-co-PEGnDMA)	86
Figure 5.4: Diffusion coefficient and binding parameters of imprinted poly(HEMA-co-DEAEM-co-PEGnDMA) hydrogels	87
Figure 5.5: Equilibrium binding isotherms for diclofenac sodium by imprinted poly(HEMA-co-DEAEM-co-PEG200DMA) hydrogels with varying concentrations of crosslinker	88
Figure 5.6: Fractional release of diclofenac sodium in DI water from imprinted poly(HEMA-co-DEAEM-co-PEG200DMA) hydrogels with varying concentrations of crosslinker.	89

Figure 5.7: Diffusion coefficient and binding parameters of imprinted poly(HEMA-co-DEAEM-co-PEG200DMA) hydrogels	90
Figure 5.8: Equilibrium binding isotherm for poly(HEMA-co-DEAEM-co-PEG200DMA) hydrogels.....	91
Figure 5.9: Fractional release of diclofenac sodium in lacrimal solution from poly(HEMA-co-DEAEM-co-PEG200DMA) hydrogels.....	92
Figure 6.1 Microfluidic chip design with physiological ocular flow.....	110
Figure 6.2: Equilibrium binding isotherm for poly(HEMA-co-DEAEM-co-PEG200DMA)	111
Figure 6.3: Infinite sink drug release of diclofenac sodium for poly(HEMA-co-DEAEM-co-PEG200DMA) contact lenses	112
Figure 6.4: Cumulative and fractional diclofenac release from imprinted contact lenses in a physiological flow.....	113
Figure 6.5: Zero-order of release for imprinted lenses in physiological flow	114
Figure 6.6: Release rate for 24 hours for poly(HEMA-co-DEAEM-co-PEG200DMA) contact lenses.....	115
Figure 6.7: Relative constant diclofenac concentration for 24 hours for poly(HEMA-co-DEAEM-co-PEG200DMA) contact lenses	116
Figure 7.1: Chemical structures of interest in diclofenac releasing Nelfilcon A lenses	149
Figure 7.2: Synthesis of Nelfilcon A macromer from PVA	150
Figure 7.3: Monomers in the LFB formulation	151
Figure 7.4: Cumulative mass release of diclofenac from Nelfilcon A contact lenses	152
Figure 7.5: Cumulative mass release of diclofenac from Nelfilcon A lenses comparing different loading concentrations of diclofenac	153
Figure 7.6: Optical clarity of Nelfilcon A lenses synthesized with diclofenac	154

Figure 7.7: Cumulative and fractional diclofenac release from Nelfilcon A lenses with different proportions of HEMA	155
Figure 7.8: Cumulative release of diclofenac from imprinted Nelfilcon A lenses with different proportions of DADMAC	156
Figure 7.9: Fractional release of diclofenac from imprinted Nelfilcon A lenses with different proportions of DADMAC	157
Figure 7.10: Zero-order release analysis from imprinted Nelfilcon A lenses with different proportions of DADMAC	158
Figure 7.11: Effect of ionic strength on diclofenac release profiles from Nelfilcon A lenses	159
Figure 7.12: Cumulative release of diclofenac from imprinted Nelfilcon A lenses with MAPTAC	160
Figure 7.13: Cumulative release of diclofenac from imprinted Nelfilcon A lenses with β -CD-NMA10	161
Figure 7.14: Cumulative release of diclofenac from imprinted Nelfilcon A lenses with DEAE-Dextran as diffusion barrier	162
Figure 7.15: Cumulative release of diclofenac from imprinted Nelfilcon A lenses with BAK	163
Figure 7.16: Cumulative and fractional diclofenac release from LFBs lenses with different hydrophobic:hydrophilic ratios	164
Figure 7.17: Cumulative release from LFB4 lenses with a 2.18:1 Macromer/TRIS:DMA mass ratio and 2 wt.% EGDMA	165
Figure 8.1: Loading, transport, and structure of imprinted networks	181
Figure 8.2: Conventional infinite sink drug release from imprinted (■) and non-imprinted (●) poly(HEMA-co-AA-co-AM-co-NVP-co-PEG200DMA) contact lenses	182

Figure 8.3: In vivo ketotifen fumarate tear fluid concentration profile from contact lenses and topical eye drops in a white New Zealand rabbit.....	183
Figure 8.4: In vivo drug release results: (a) First study of imprinted lenses releasing timolol, and (b) silicone hydrogel lenses releasing ketotifen fumarate.....	184
Figure 9.1: Typical volumes used in release studies of contact lenses.....	198
Figure 9.2: Chemical structures and physicochemical properties of drugs.	199
Figure 9.3: Drug release in small volumes from hydrophilic, conventional hydrogel films.....	200
Figure 9.4: Release of ketotifen fumarate from hydrophilic, conventional hydrogel films in 2 mL and 5 mL small volumes	201
Figure 9.5: Release of ketotifen fumarate from hydrophilic, conventional hydrogel films in small and large volumes.	202
Figure 9.6: Data fit for hydrophilic, conventional hydrogel films releasing ketotifen fumarate in the 2 mL volume.	203
Figure 9.7: Cumulative mass released from hydrophilic, conventional hydrogel films.....	204
Figure 9.8: Cumulative mass released from silicone hydrogel films.....	205
Figure 9.9: Effect of mixing rate and temperature in the release kinetics	206
Figure A.1. Cumulative mass release of diclofenac from Nelfilcon A lenses at different stir rates	244
Figure A.2. Comparison of dissolution apparatus protocol and replacement method for the release of diclofenac from Nelfilcon A lenses	245
Figure A.3. Comparison of dissolution apparatus protocol and replacement method for the release of diclofenac from Nelfilcon A lenses with different proportions of NVP and DEAEM	246
Figure A.4. Fractional mass release of diclofenac from Nelfilcon A lenses with different loading concentrations of diclofenac sodium	247

Figure A.5. Optical clarity of Nelfilcon A pre-polymer solutions.....	248
Figure A.6 Long time cumulative mass release of diclofenac from Nelfilcon A lenses with different proportions of HEMA	249
Figure A.7. Cumulative release of diclofenac sodium from Nelfilcon A lenses with different proportions of DADMAC.....	250
Figure A.8. Cumulative release of diclofenac from Nelfilcon A lenses in artificial lacrimal solution.....	251
Figure A.9. Cumulative release of diclofenac from Nelfilcon A lenses with DADMAC and HEMA in artificial lacrimal solution	252
Figure B.1: Equilibrium binding isotherms for diclofenac sodium by silicone hydrogels lenses.....	256

Chapter 1

Introduction

The global ophthalmic therapeutic market is expected to be worth \$20.6 billion by 2014, growing by a compound annual growth rate (CAGR) of 5.9% [1] . Topical eye drops in the forms of suspensions and solutions are the most widely used platform for delivering ocular therapeutics. Together with ointments, they account for over 90% of currently administered ocular drugs [2-4]. Typically, less than 7% of drug delivered through eye drop formulations is absorbed, while the rest is removed by the clearance mechanisms of the corneal surface, such as lacrimation, tear dilution and tear turnover; leading the drug to the systemic circulation, resulting in very low drug bioavailability in the eye [5, 6]. To overcome low bioavailability, topical formulations have remained effective by the administration of high concentrations of drug multiple times a day. Variations in the effectiveness of topically applied drugs occur by patient non-compliance, that is when patients fail to follow the dosage regimen, this situation can lead to poor prognosis and ocular side effects [7].

There is an unmet need in the ocular therapeutic market for effective drug delivery. It is imperative to develop novel methods and devices that enable the precise delivery of medications at therapeutic concentrations to the target site. It is essential to load therapeutically relevant concentrations of drug and to control the drug transport for a successful prolonged pharmacological effect.

An emerging and interesting alternative to overcome low drug bioavailability and patient non-compliance, is the use of soft contact lenses as drug delivery devices. In the US, current

contact lens wearers are estimated at nearly 50 million, with more than 170 million people needing corrective lenses (contact lenses or eyeglasses). The whole contact lenses (corrective and cosmetic) generated approximately \$7.3 billion in revenues worldwide in 2012, and it is expected to increase to nearly \$7.9 billion by 2017 [8].

Delivering ocular medications via contact lenses can solve problems such as low bioavailability and patient compliance. However, this has not become a reality due to the inability of commercial contact lenses to load and release significant concentration of drug so as to have a therapeutically relevant effect. This can be attributed to lack of functionality at the molecular level, which would enhance carrier-drug interactions.

This study focused on the rational design and engineering of novel, hydrogel contact lenses capable of tailorable loading and extended release of a non-steroidal anti-inflammatory (NSAID), diclofenac sodium, via imprinting techniques. Molecular imprinting techniques were used to introduce “macromolecular memory” within hydrogels and to increase the tailorability of the macromolecular structure by producing networks with intrinsic affinity and capacity for a template, drug molecule.

Hydrogels are water-insoluble polymers, which have been used as carriers for drug delivery due to their controllable physical and chemical properties. Synthesis of hydrogels with particular chemistry at the molecular level can result in desirable properties at the macromolecular level. The advantage of tuning co-polymer network functionality is the ability to manipulate the macromolecular structure and chemistry on the therapeutic level, thus providing enhanced template loading and better control over the template transport. This would result in soft contact lenses capable of loading therapeutically relevant amounts of specific ocular drugs and the extended release of those drugs.

Imprinted contact lenses as a platform for drug delivery offer a more effective method of ocular therapy by providing a constant and optimal dosage of medication with increased drug bioavailability to the eye. This novel system could be used with a wide spectrum of drugs and it has enormous potential in designing and engineering of the next generation of drug delivery carriers. A thorough understanding of weakly crosslinked imprinted hydrogels might lead to the rational design of imprinted polymer networks for not just drug delivery but for a wide variety of other applications.

Chapters 2 and 3 of the Dissertation, offer an overview of the ocular therapeutic delivery process and the use of soft contact lenses as platform for ocular drug delivery. Chapter 4, gives a description of the methods used to characterize the structure of hydrogels, as well as the methods used to study their template binding and transport properties. In Chapter 5, you will find how molecularly imprinted hydrogel networks via non-covalent interactions were synthesized (poly(HEMA-co-DEAEM-co-PEGnDMA) hydrogels) by varying the length and amount of crosslinking monomers to analyze the effect on the network architecture and the subsequent impact on template binding and transport properties. Diclofenac sodium, a negatively charged small molecule at physiological pH ($pK_a \sim 4$), was selected as the template molecule. Chapter 6, describes methods to enhance loading and control release of diclofenac sodium by varying the functional monomer to template (FM/T) ratio. A microfluidic device, which mimics the physiological flow rate in the eye, was used for dynamic release studies. In Chapter 7, you will find how a polyvinyl alcohol (PVA) macromer, Nelfilcon A, was used as a backbone monomer to engineer a daily disposable lens to tailor the release rate of diclofenac sodium. Additionally how, silicone hydrogels were engineered to study the transport of diclofenac sodium molecules through a biphasic (hydrophobic/hydrophilic) polymer network. Chapter 8, explains the

successful *in vivo* extended release of ketotifen fumarate, an anti-histamine, from molecularly imprinted, therapeutic contact lenses. Finally, Chapter 9 compares the widespread experimental conditions used for ocular drug release kinetic studies via contact lenses throughout literature.

Chapter 2

Drug Delivery of Ocular Therapeutics

Several eye diseases like cataracts, glaucoma, and retinal degenerative maladies can be the leading cause of partial and complete blindness, affecting millions of people around the world, with a significant economic impact [9]. Other diseases such as ocular inflammation, ocular allergy, dry eye syndrome, and bacterial conjunctivitis do not lead to complete loss of vision, but they affect the quality of life for millions of people by causing blurred vision as well as discomfort, requiring the patients to stick to a therapeutic dosage regime for a long period of time, where high concentrations of drug need to be applied multiple times a day with a low payload, leading to undesirable side effects.

For the front of the eye or anterior therapy, most treatments require non-invasive, topically applied drugs, such as solutions or suspensions in the form of eye drops or ointments. For the back of the eye or posterior therapy, drugs are typically administered by intravitreal injections and systemic routes [10]. All these treatments present limitations that mainly involve the eye's natural anatomical and physiological barriers, which restrict the transport of foreign molecules.

The global ophthalmic therapeutic market was valued at \$15.5 billion in 2009, with growth rate of more than 2.5 times that of the overall pharmaceutical industry. The sector is expected to grow to \$20.6 billion by 2014, at compound annual growth rate (CAGR) of 5.9% [1]. Table 2.1 outlines a summary of the global ocular forecast by diseases class for 2009 and 2014.

Table 2.1: Summary of the global ophthalmic forecast by diseases class for 2009 and 2014

Disease Class	Ocular Location Affected	Global Forecast	
		2009	2014
Glaucoma	Anterior	\$5.8 billion	\$6.6 billion
Wet AMD	Posterior	\$2.4 billion	\$3.9 billion
Dry eye	Anterior	\$1.8 billion	\$2.7 billion
Infection or risk of infection	Anterior	\$1.35 billion	\$2.2 billion
Inflammatory	Anterior	\$900 million	\$1.3 billion
Combo (infective + inflamm)	Anterior	\$700 million	\$800 million
Allergy	Anterior	\$1.45 billion	\$1.9 billion
Other	Anterior/Posterior	\$1.1 billion	\$1.2 billion

Data reproduced from [1].

There are numerous factors limiting patient compliance in ocular drug delivery including: high dose frequency, an inconvenient administration, intolerance of side effects and adverse reactions, and forgetfulness. Many ophthalmic medications such as those used to treat allergic conjunctivitis have high dose frequencies such as four times daily. The impact of non-compliance is far reaching and includes decrease in efficacy and reliability of medications, increasing progression of the condition, and increasing the overall economic cost.

An ideal ocular drug delivery system should possess crucial properties, including: (i) a controlled sustained release profile to provide a therapeutically relevant concentration of the drug for an extended period of time to reduce the frequency of administration; (ii) precise targeting and prolonged retention to improve therapeutic efficacy and diminish side effects; and (iii) patient-friendly delivery routes.

2.1 Barriers to Ocular Transport, Ocular Bioavailability and Pharmacokinetics

The eye is one of the most accessible organs, it can be examined without invasive procedures; however, from a drug delivery perspective, due to its physiology, the bioavailability of an applied drug is generally low. In order to function as an organ, it is of vital importance for the eye to maintain a highly regulated environment for the visual cells and transparent tissues. The eye has anatomical and physiological barriers, which restrict and regulate the intake of fluids and solutes, and help to protect and maintain vital ocular functions [11]. The eye has two anatomical regions: the anterior segment, in which the cornea, conjunctiva, iris, ciliary body, and anterior chamber are the main structures, and the posterior segment, which includes the vitreous humor, retina, choroid, and optic nerve [12].

There are several possible routes of drug delivery into the ocular tissues. The variables that may select the route include the rate-limiting barriers to the target tissue and the physiochemical characteristics of the drug, such as lipophilicity, shape, molecular weight, degree of ionization, charge and solubility [13]. Frequently, topical and subconjunctival administrations are used for anterior therapy, whereas for posterior therapy intravitreal injections, or systemic delivery are used [10].

Conventional topical ocular therapies account for 90% of all ophthalmic formulations on the market [2]. Topical delivery of the drug to the ocular surface have low bioavailability, due to lacrimation, tear dilution, tear turnover, nasolacrimal drainage, spillage from the eye, metabolic degradation and nonproductive adsorption/absorption as a result from a relative impermeability of the corneal epithelial membrane [4] (Figure 2.1). Under normal tear volume and turnover rate, an aqueous instilled dose, leaves the precorneal area within 30 min of its application [10], while the contact time of the drug on the ocular surface (cornea and sclera) is often 1 hour or less [4].

Due to these physiological and anatomical constraints, only around 1-7% of the applied drug reaches the aqueous humor, and the rest enters systemic circulation, resulting in many cases in undesirable side effects [6, 14, 15].

Drugs delivered systemically to the eye are detained by blood-ocular barriers which prevent the transportation of the drug to the eye's interior; this route of drug administration is extremely inefficient and exposes the body to a potential toxicity and unwanted side effects, because of the need to administer extremely large doses of antibiotics, antiviral medication or steroids [10, 16]. Blood-ocular barriers, along with liver metabolism, limit the bioavailability of orally or intravenously administered drugs [4]. As a result, only between 1-2% of the drugs administered reach the vitreous cavity [12].

2.1.1 Routes of Ocular Drug Delivery to the Anterior Segment

An optimal function of the eye depends on the presence of a stable precorneal tear film and an ocular tear system, which provide a regular and smooth surface for the cornea [17]. A normal tear film consists of three main layers -a hydrophilic mucin layer, an aqueous layer, and a superficial lipid layer-. The hydrophilic mucin layer (0.01-0.07 μm thick), which lies adjacent to the corneal epithelium, lubricates the eye from the shearing force applied by blinking ensuring wettability and maintains the integrity of the surface by trapping and removing foreign matter [18, 19]. The middle layer is a 6-7 μm thick aqueous layer with dissolved oxygen, nutrients and proteins [20]. The superficial layer comprises a 0.1 μm thick film of lipids that prevents excessive evaporation of the aqueous film [21].

The movement of fluid in the eye depends on the flow of the aqueous phase, which is secreted by the lacrimal glands above the eye, spread over the eye's surface through blinking and

surface tension, and which drains out of the eye through the lacrimal punctum with the aid of a pumping mechanism [22]. Under normal physiological conditions, the tear volume ranges from 7 to 30 μL , with a tear turnover rate of 0.5-2.2 $\mu\text{L}/\text{min}$ [6, 23]. Up to 95% of topically applied drugs can get washed away from the eye's surface within minutes [24]. In addition to providing comfort, the tear fluid aids in the transport of oxygen to the eye. The rate of oxygen diffusion is approximately $7.8 \mu\text{L}\cdot\text{hr}/\text{cm}^2$ [25]. This is an important factor in both ocular health and comfort.

The cornea is a transparent, dome-shape structure covering the front of the eye [4]. Human corneal structure consists mainly in three layers: corneal epithelium (a major hydrophilic barrier), the stroma (a highly hydrophilic tissue) and the endothelium (a minor lipophilic barrier), which restrict the ocular entry of drug molecules. The cornea is relatively impermeable to solutes with a molecular size larger than 1 kDa [15].

The conjunctiva is a vascularized mucous membrane which covers the anterior part of the sclera (the tough, opaque, white of the eye) and lines the inner surface of the eyelids [4, 26]. The conjunctiva is implicated in the production and maintenance of the precorneal tear film [27, 28]. New studies have demonstrated that several transporters (e.g. P-glycoprotein, amino acid, etc) play a critical role in achieving influx and efflux transport of drugs through the conjunctiva. Intraocular drug delivery via the conjunctival route is now well documented [12, 26]. For many compounds, conjunctival permeabilities are higher than corneal permeabilities, due to a wider intercellular space in the conjunctival epithelium [27]. The sclera is more permeable than the cornea and its permeability is not dependent on drug lipophilicity. The reader is referred to an excellent review that compiles ocular tissue permeability measurements [29].

When a drug reaches the corneal or conjunctival epithelium, it must find a pathway through the layers of cells. For a drug to take a transcellular route (i.e., through the cells), it

needs to enter the cell either by facilitated transport, which requires particular chemical interactions with transporters native to the cell, or by passive diffusion through the lipid bilayer, which is influenced by various factors, such as the lipophilicity, molecular weight, degree of ionization of the drug and the cell membrane thickness [4, 13]. The paracellular route (i.e., around the cells) is limited by the presence of tight junctions at the most superficial corneal epithelial cells [11]. Studies prove that increasing molecular size of the permeating substance decreases the rate of paracellular permeation [30].

Drugs transport through the stroma is relatively equivalent for all ocular drugs. The stroma has a relatively open structure; and drugs with a molecular weight up to 500 kDa can diffuse freely through it [31].

After passing through the ocular surface barriers, the drug reaches the aqueous humor, an anterior segment between the cornea and the lens. The aqueous humor is a clear fluid secreted by the iris-cilary body that circulates through the anterior chamber at approximately 1 % per minute and drains out via the trabecular meshwork. It supplies nutrients and antioxidants to the cornea and lens without interfering with visual clarity [4]. Typically, less than 3% of the topically instilled drug reaches this point. Drugs delivered via the corneal route can be diluted to the point of inefficacy, even before moving into the posterior segment. Drugs are eliminated from the anterior chamber via aqueous humor turnover, metabolic pathways and/or blood circulation of the anterior uvea [14, 31].

In addition to the physical barriers, ocular tissue contains metabolic enzymes, such as esterases, aldehyde and keton reductases [32], which may break down the drug molecules that manage to penetrate into the tissue, reducing the efficacy of the treatment.

2.1.1.1 Lipophilic drugs

Highly lipophilic drugs cannot be formulated in an aqueous medium and need to be prepared as emulsions or suspensions. These formulations often suffer stability problems. Particle sizes should be under 10 μm in diameter for maximum comfort, so as to minimize irritation and reflex tearing [33]. The discomfort they cause in the patients may lead to blinking, hence the loss of a considerable amount of drug. On the other hand, the remaining drug on the precorneal surface will have to diffuse into the lacrimal fluid before it can penetrate the corneal barriers [2, 34] (Figure 2.2).

The transcellular pathway is the main route for lipophilic drug transport from the lacrimal fluid to the aqueous humor [26, 35]. At the corneal epithelium, lipophilic drugs can quickly move through transcellular route, due to the lipophilic nature of the barrier (Figure 2.3). For the most lipophilic drugs the stroma is a rate limiting barrier, this is not due to the hydrophilic nature of the stroma, but rather to the slow partitioning of lipophilic compounds from the epithelium to the stroma. However, for highly lipophilic drugs, the stroma is rate limiting and determines corneal permeability. Actually, the stroma can act as a reservoir from which the drug will be slowly delivered to the aqueous humor [27, 36]. Finally, the drug transport through the endothelium depends on the partitioning behavior of the drug.

2.1.1.2 Hydrophilic drugs

Hydrophilic drugs can be easily presented as aqueous eye-drop solutions; however, they encounter some difficulties passing from the tear film to the corneal/conjunctival epithelium, having a low residence time over the precorneal surface [34] (Figure 2.2).

The paracellular pathway is the most common way to transport hydrophilic drugs through corneal and non-corneal (conjunctival/scleral) epithelium [3]. The intercellular spaces at the most superficial corneal epithelial cells have tight junctions that serve as a selective barrier between adjacent cells, thus, this paracellular route is limited to very low molecular weight of hydrophilic compounds or ions (< 350 Da) [4, 27, 37]. Results in studies of absorption by the non-corneal route, found that the conjunctiva is a leakier epithelium, which plays an important role in the absorption of large hydrophilic drugs such as proteins and peptides (i.e., poor corneal permeability compounds) [12, 38, 39]. The conjunctiva may allow the permeation of hydrophilic compounds with a molecular weight up to 20 kDa [27], whose molecular radius is around 4.9 nm [40], and the sclera may allow a molecular size up to 70kDa [10]. Finally, the endothelium has large intercellular junctions, which make it a not rate limiting barrier for hydrophilic compounds. It has been estimated that drugs with molecular size up to 20 nm can diffuse across normal endothelium [41]. The non-corneal pathway is favored for delivery of hydrophilic drugs, bypassing the anterior chamber and permitting direct access to the intraocular tissues of the posterior segments.

Ocular barriers limit the utility of hydrophilic drugs in ocular therapies. Since hydrophilic drugs penetrate much easier via the paracellular pathway, transcellular transport is possible by using a limited range of transporters present on the corneal and conjunctival epithelial cells [4].

2.1.1.3 Ionizable drugs

Permeation of ionizable drugs (weak bases and weak acids) depend on the chemical equilibrium between the ionized and unionized molecules of the drug [42]. The unionized molecule usually penetrates the lipophilic membranes more easily than the ionized ones. In the

case of ionized molecules, the charge of the molecule also affects their corneal permeation [43]. The corneal epithelium is negatively charged at physiological pH (or above its isoelectric point: 3.2); as a result, negatively charged molecules permeate slower than positively charged and neutral molecules [44].

2.1.2 Routes of Ocular Drug Delivery through the Blood Ocular Barriers

The blood ocular barriers consist of the blood-aqueous barrier, which is located in the anterior part of the eye, and the blood-retinal barrier that is located in the posterior part of the eye. These barriers separate the eye from the rest of the body by using tight junctions and efflux proteins. The blood aqueous barrier (BAR) is formed by the epithelial cells of the iris-ciliary body and the blood-retinal barrier (BRB), which is composed of two parts: the outer part consists of the retinal pigment epithelium (RPE) and the inner part of the retinal endothelial cells [16, 32].

In the posterior segment the tissues support the retina and encase the vitreous humor, a highly viscous fluid. The choroid, a vascularized tissue, is inside the sclera and nourishes the outermost layers of the retina. The retina is inside the choroid and it is made up of several layers which can be classified into two major groups: the neural retina and the RPE that rest on the Bruch's membrane, the innermost layer of the choroid [4].

The BRB limits drug distribution from the blood stream to the posterior ocular tissues and is selectively permeable to more lipophilic molecules [12], however, it is impermeable to polar or charged compounds in the absence of a transport mechanism [10]. It has similar features with the blood-brain barrier (BBB).

The RPE is capable of a number of specialized transport processes. It allows selective exchange of nutrients between the choroid and retina [32]. The RPE has tight junctions that form a strong barrier to the permeation of hydrophilic drugs from the sclera or systemically delivered drugs from the choroid into the neural tissue and the vitreous humor [4] (Figure 2.4), but, in the case of small lipophilic drugs, the sclera and RPE have similar permeabilities [45].

The retinal endothelial cells prevent drugs to reach the neural retina coming from the circulatory system. The retinal endothelial cells have intercellular tight junctions limiting the paracellular transport of compounds (Figure 2.4). The retinal vessel walls have poorly permeation of small hydrophilic molecules and proteins, while lipophilic compounds can penetrate more easily [11].

2.1.3 Routes of Ocular Drug Delivery to the Posterior Segment

Drug delivery to the posterior eye is a considerably more challenging problem, which can follow numerous routes. The natural anatomic and physiological limitations of the eye make this a particularly difficult tissue to target.

When using topical administrations, drugs that are absorbed into the eye through the corneal route first enter the aqueous humor and are then distributed to the intraocular tissues, (i.e., iris-ciliary body, vitreous and choroid-retina) and drugs that penetrate into the eye via non-corneal routes enter the conjunctiva and sclera, reach the vitreous and must pass across choroid and RPE without entering the aqueous humor [16, 38]. Consequently, these drugs will generally be diluted or eliminated to a sub-therapeutic dosage.

The most common alternatives to reach the posterior segment of the eye involve injecting the drug, inserting a drug delivery device into the vitreal cavity of the eye, or the use of a

periocular route of delivery and relying on trans-scleral transport [4]. These techniques are efficient in delivering the drug; however, they are invasive and may carry serious complications such as postoperative endophthalmitis, intravitreal hemorrhage and retinal detachment [4, 46]. Anterior segment complications, such as, cataracts, strabismus and high intraocular pressure, have developed in some patients following periocular injections [12]. Additionally, some drugs are delivered through the systemic circulation by oral administration or intravenous injections. However, minute amounts of the drug reach the posterior segment of the eye, exposing the body to systemic toxicity [47].

Intravitreal injections can be introduced into the vitreous in solution, in a depot formulation or dispersed in microparticles. Linear and globular shaped molecules, especially protein and peptide drugs, with molecular weights greater than 40 and 70 kDa, respectively, tend to cause longer retention in vitreous humor [12]. As the diameter of particles rises to 50 nm, the light scattering interferes with vision [3]. Drugs are eliminated from the vitreous humor via: i) the anterior chamber by diffusion across the vitreous to the posterior chamber and elimination via the aqueous turnover and iris blood vessels, or ii) across the blood-retina barrier into systemic circulation [35]. Subconjunctival injections can deliver drug into the sclera while bypassing the epithelial barriers. The drug can diffuse laterally through the sclera and reach the choroid and the retina. The design of improved drug delivery systems should help to overcome these anatomical and physiological barriers that act as rate-limiting steps in achieving an effective drug bioavailability.

2.2 Current Trends of Ocular Drug Delivery to the Anterior Segment

The central objective of a delivery system is to release therapeutics at the desired anatomical site and to maintain the drug concentration within a therapeutic range for a desired duration (Figure 2.5). Efficient ocular delivery rests on two important factors- (i) enhancing drug bioavailability by improving retention of drug on the ocular surface thereby limiting loss by lacrimation, tear turnover, and drainage, and (ii) increasing drug transport through ocular barriers such as the cornea, the sclera, and the conjunctiva

2.2.1 Eye Drops and Ointments

Topical formulations such as solutions and suspensions in the form of eye drops have been in use for centuries [48], and they are still the most common treatment approach used today. Along with ointments, they both account for 90% of ophthalmological formulations on the market today [2]. Eye drops are easy to manufacture at low cost and they are non-invasive and relatively simple to apply by patients, yet, the effectiveness of topical therapy is limited by several issues. Factors such as ocular protective mechanisms, nasolacrimal drainage, spillage from the eye, lacrimation and tear turnover, metabolic degradation, etc., reduce the residence time of topically applied drugs within the tear fluid, often to 1 hour or less [4]. Typically, less than 7% of a drug delivered through eye drop formulations is absorbed, the rest enters the systemic circulation resulting in very low drug bioavailability [35]. To overcome most of these protective mechanisms and low drug bioavailability, topical formulations have remained marginally effective by administering very high concentrations of the drug multiple times on a daily basis, leading to drug wastage and, more importantly leading to negative effects such as

burning, itching, gritty sensations, and systemic intake, which can induce undesirable side effects as well as increased toxicity.

Variations in the effectiveness of topically applied drugs are also introduced through the application technique, the type of eye drop carrier, and patient non-compliance (i.e., when patients fail to follow the dosage regimen) [7]. Typically, patients using topical eye drops have large variations in medication from application to application due to insufficient dosages, skipping dosages, and/or over administering dosages. A typical ocular drug concentration profile for eye drops is presented in Figure 2.2. A high concentration of the drug is applied via eye drops and is quickly reduced. To maintain effective concentration of drug, eye drops must be applied often. If the dose is missed, long periods of ineffective drug concentration can occur.

Improved methods have focused on increasing the residence time of the drug and thus the bioavailability. Viscosity enhancers such as methylcellulose compounds, polyvinyl alcohol, and polyvinyl pyrrolidone have been used in topical formulation to increase the viscosity of the tear fluid and decrease the tear drainage rate, increasing the result residence time of the drug on the eye surface [49]. A considerable increase in viscosity produces ointments which can lead to a slightly increased bioavailability over eye drops; however, they are difficult to apply, uncomfortable to use, and severely reduce vision [2, 50, 51]. Thus, they are used to a much lesser extent than eye drops and are typically used at night.

Apart from viscosity enhancers, mucoadhesive polymers have been explored. They interact with the mucin layer on the tear film and adhere to the ocular surface which leads to higher residence time of the drug [52, 53]. Mucoadhesive polymers can be applied directly to the eye as a vehicle for drug, or they can be used to attach inserts to the eye. Major disadvantages of

these delivery systems are blurred vision and an uncomfortable feeling due to the sticky nature of these polymers.

Several solid particle suspensions have also been explored for their ability to increase transport, and supposedly to increase residence time [54]. These systems mainly include liposomes [55-60] (i.e., vesicles made of concentric phospholipids bilayers), microspheres [61-66] (i.e., particles containing drug dispersed within a polymer), dendrimers [67-69] (i.e., highly branched, star-shaped macromolecules), and micro- or nanoemulsions [70-72] (i.e., sub-micron colloidal dispersion of drug stabilized by surfactants). Major issues concerning these systems are the stability and sterilization for mass production, making them quite ineffective for use. Additionally, cyclodextrins (CDs), which are cyclic oligosaccharides with a high concentration of hydroxyl groups in a ring structure (hydrophobic cavity), can form inclusion complexes by taking up the guest molecule or a lipophilic moiety of the molecule into their central hydrophobic cavity [73]. Cyclodextrins are used to improve aqueous solubility of poorly soluble therapeutics, and they can act as a permeation enhancer by increasing the drug retention at the surface of the corneal epithelium [74-76]. Although, all these strategies may increase the drug residence time and, thus the bioavailability, they cannot completely satisfy the need for treatments of ocular diseases, especially when long term therapy is needed.

2.2.2 Inserts and In-situ Gel Systems

Inserts are designed to be installed into the cul de sac (pocket formed where the palpebral and the ocular conjunctiva meet in either the lower or upper eyelid). These systems can lead to a programmed delivery of the drug onto the ocular surface for extended period of time [77-81]. However, potential drawbacks with these systems have been reported, such as foreign body

sensation, ocular irritation, hyperemia, hypersensitivity, eyelid edema, vision interference, sometimes the insert can be self-expelled from the eye, and some require a professional to place and remove them. This type of device may also present fragmentation and membrane rupture with a burst of drug being released into the eye [10].

In-situ gel forming systems are liquid for easy application, but go through phase transition attaining a gel-like consistency when they encounter the eye's physiological environment. Gellation can be triggered by a change in temperature [82-84], by a change in pH [85, 86], and by the presence of mono or divalent ions [86, 87]. The polymer solution is mixed with the desired drug and installed in the cul-de-sac, where it gels. Research has focused in optimizing the phase transition and gaining better control over gellation times (e.g. combination of the triggering mechanisms), extending the drug release, on top of reducing the amount of the polymer needed in a dosage [88-90].

2.2.3 Contact Lenses

Using soft hydrogel contact lenses as drug delivery device was suggested since their conception [91]. In 1965, Otto Wichterle described hydrophilic, weakly crosslinked polymer gels in the first soft contact lens patent. In the document, he stated that “bacteriostatic, bacteriocidal or otherwise medicinally active substances such as antibiotics may be dissolved in the aqueous constituent of the hydrogels to provide medication over an extended period via diffusion” [91].

Since then, delivering ocular drugs via contact lenses has been considered an effective alternative to topical application via eye drops [92]. This idea comes from the observation that drug molecules have longer residence time in the tear film, when loaded into contact lenses than when they are administered through eye drops. This longer residence time enhances drug

permeation through the cornea and minimizes drug absorption into the blood stream through the conjunctiva or nasolacrimal drainage [54].

Thus far, most data involving drug release from contact lenses has been from drug soaked contact lenses, which have involved taking a conventional lens and soaking it within a concentrated drug solution. This approach has the main disadvantage of insufficient drug loading and a lack of a controlled release mechanism (Figure 2.2) [93]. This has been the primary reason why drug release from contact lenses has not become a clinical or commercial success.

In recent years, the development of new approaches, a greater understanding of polymeric structural properties as well as network formation, have produced a number of techniques that are considerably different than past efforts (i.e., drug soaked contact lenses) [93-95]. Controlling and tailoring the release of drugs via novel contact lenses can help to overcome the eye's physiological barriers. Benefits of such technology are the increased drug bioavailability, patient compliance, and reduced eye and systemic side effects. These methods have included molecular imprinting as well various forms of mediated release via carriers, surfactants, inclusion complexes, and molecular barriers. A detailed analysis of soft contact lenses as drug delivery devices is presented in Chapter 3.

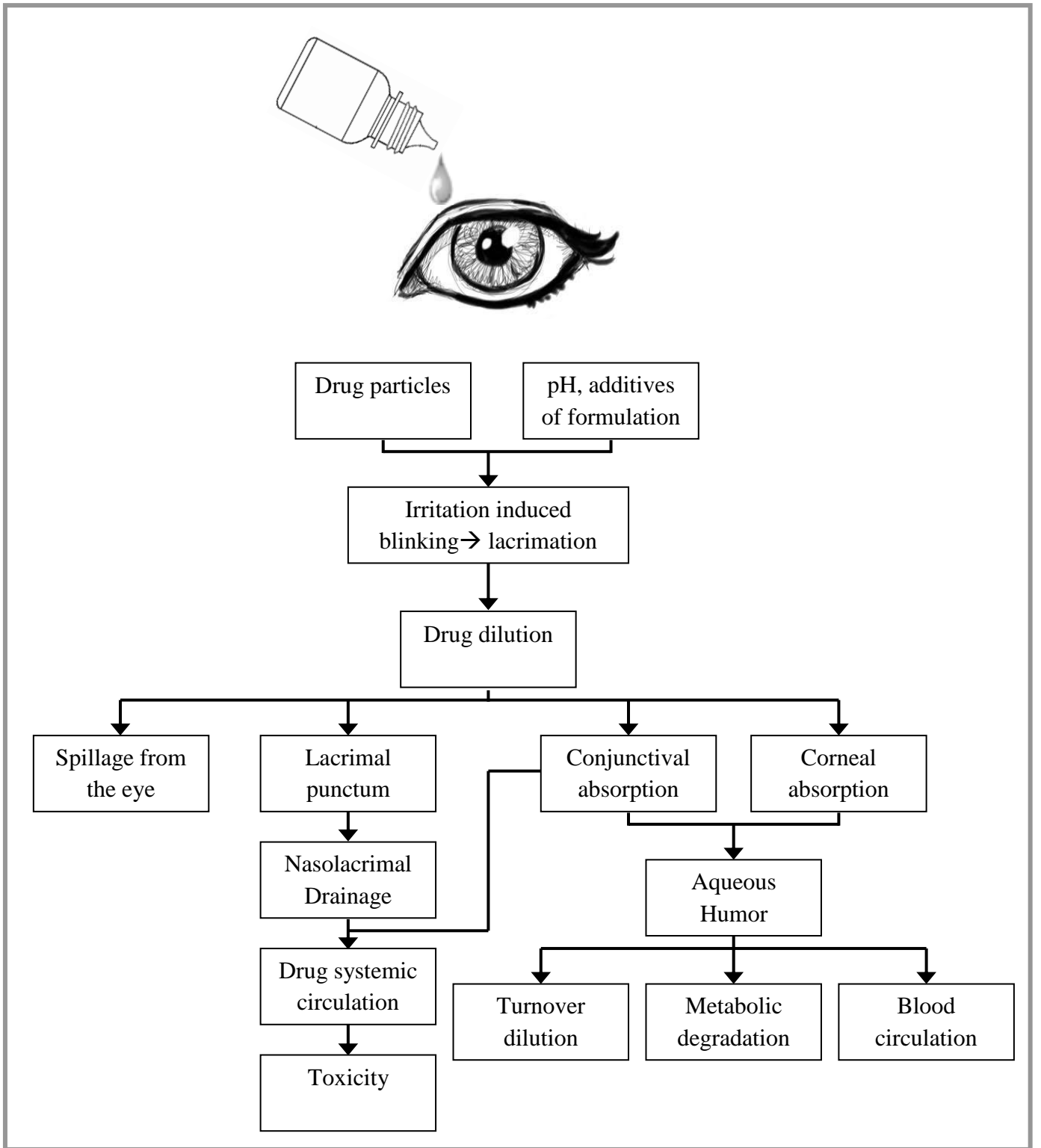


Figure 2.1: Pathway of drug administered by topical formulations

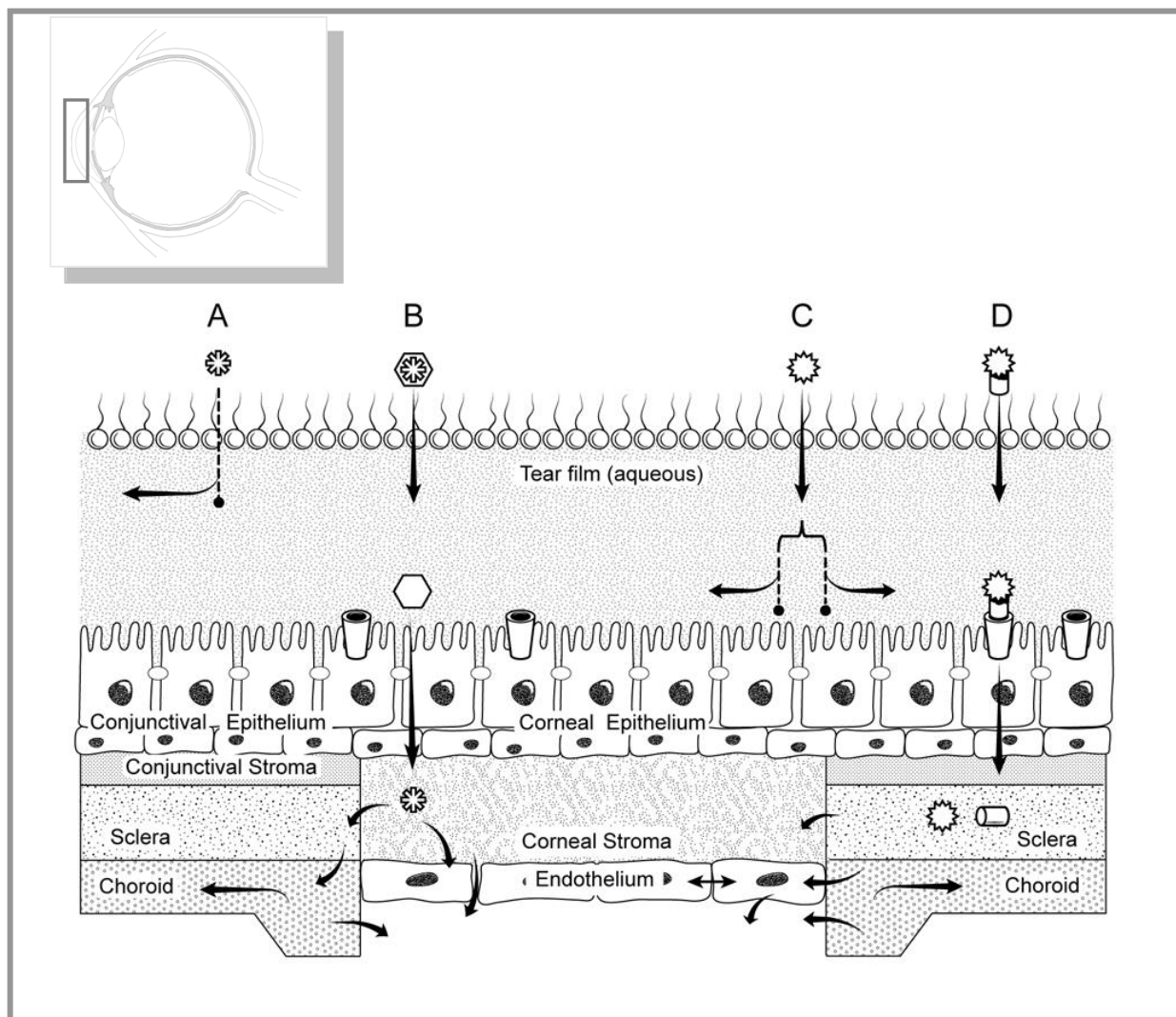


Figure 2.2: Transport of drugs through the surface of the eye

[A] is a lipophilic drug which cannot easily penetrate the tear film and is washed away.

[B] is a lipophilic drug in the central cavity of a cyclodextrin molecule. The cyclodextrin solubilizes in the tear film and reaches the ocular epithelium. The lipophilic drug partitions out of the cyclodextrin and into lipid membrane of the epithelium.

[C] is a hydrophilic drug that solubilizes in the tear film and reaches the epithelium. It cannot cross the epithelium transcellularly (because of lipid membrane) or paracellularly (because of tight junctions), and eventually washes away from the eye surface.

[D] is a hydrophilic pro-drug which penetrates the epithelium transcellularly with the aid of a membrane transporter. Once in the ocular tissue, it is converted into the drug by enzymes.

Drugs that penetrate the epithelia can easily move between ocular tissues such as the corneal and conjunctival stroma, the sclera, the vascularized choroid, and the leaky endothelium. From there they can diffuse into the anterior chamber or laterally through the sclera to the posterior segment.

The corneal and conjunctival epithelia contain several layers of cells not shown in the figure.

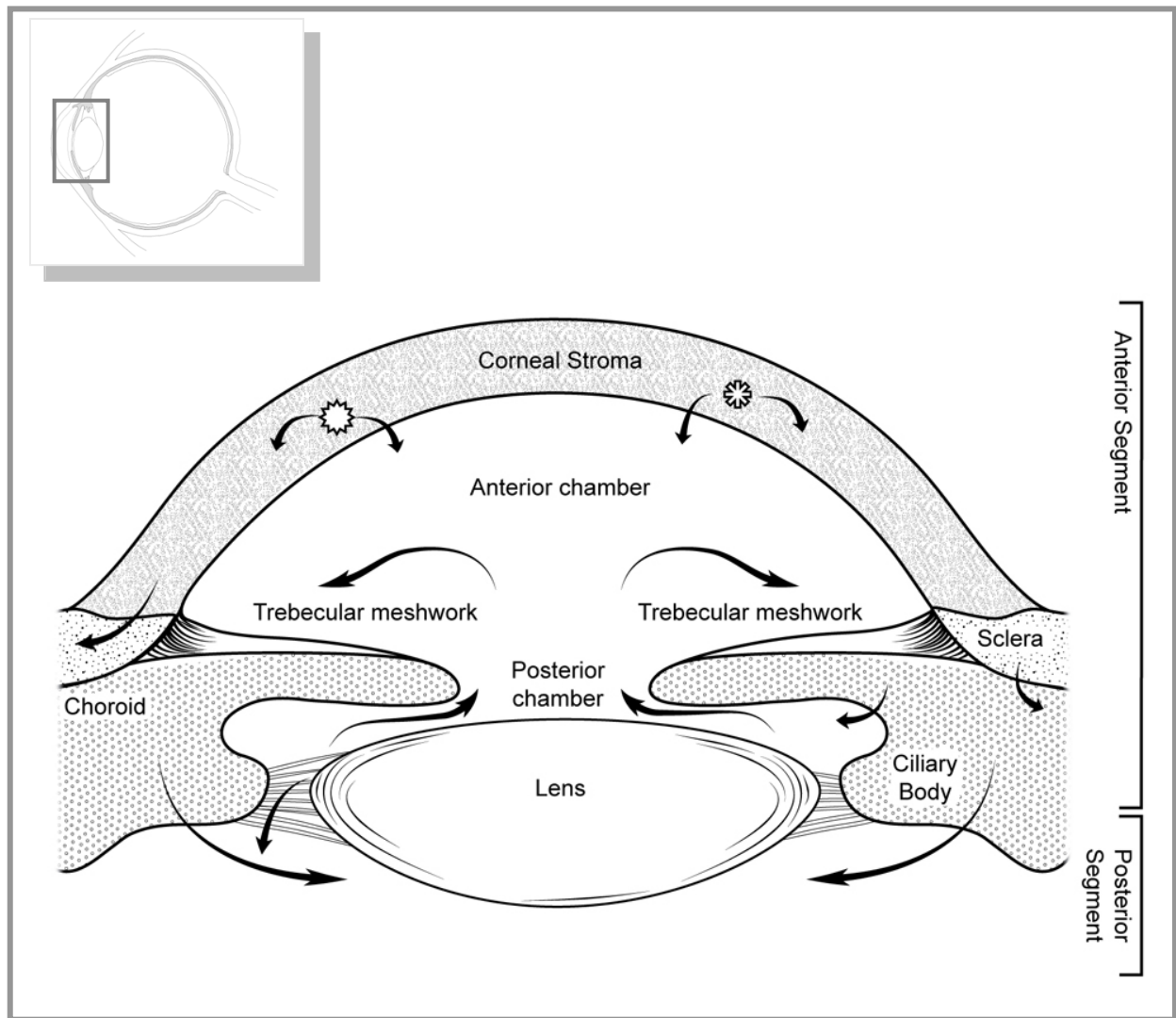


Figure 2.3: Transport of drugs through the anterior segment of the eye

Both hydrophilic and lipophilic drugs pass through the permeable stroma and sclera into the choroid and the posterior segment. They also penetrate to the ciliary body, transfer to the secreted aqueous humor and circulate around the anterior and posterior chamber before draining away through the trebeccular meshwork.

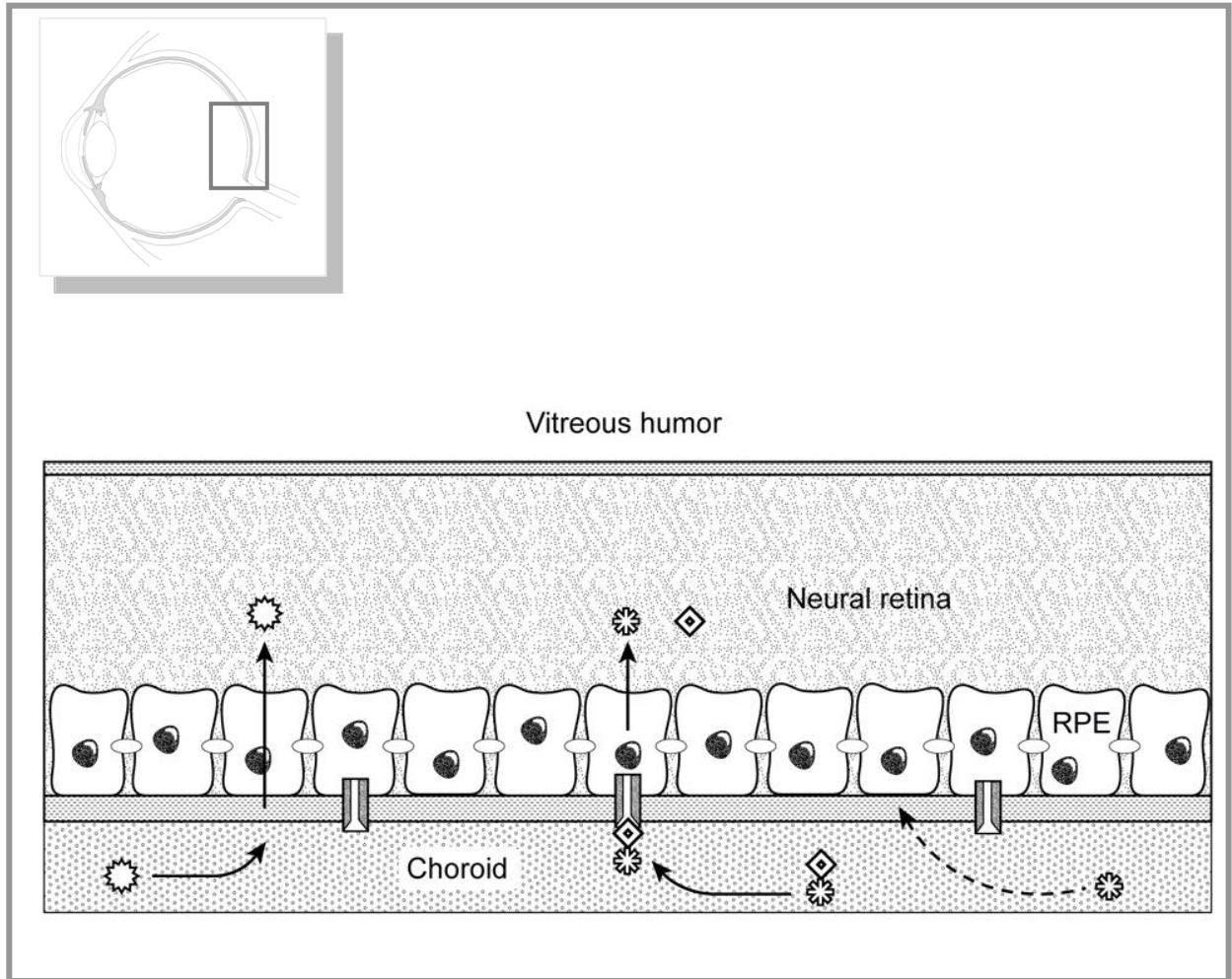


Figure 2.4: Transport of drugs through the posterior segment of the eye

Typically delivered drugs diffuse through the sclera to the vascularized choroid to the posterior segment of the eye. A layer of tight-junctioned cells, the retinal pigment epithelium (RPE),..... prevent drugs from penetrating into the retina. Small lipophilic drugs penetrate the lipid membrane easily but large and hydrophilic drugs require assistance either from transporters or from permeation enhancers. When the drug reaches the neural retina, it acts upon the target cells. The retinal vasculature is lined with endothelial cells bound by tight-junctions to prevent blood borne drugs and pathogens from reaching the neural retina. Together, the retinal vascular endothelium and the RPE form the blood-retinal barrier.

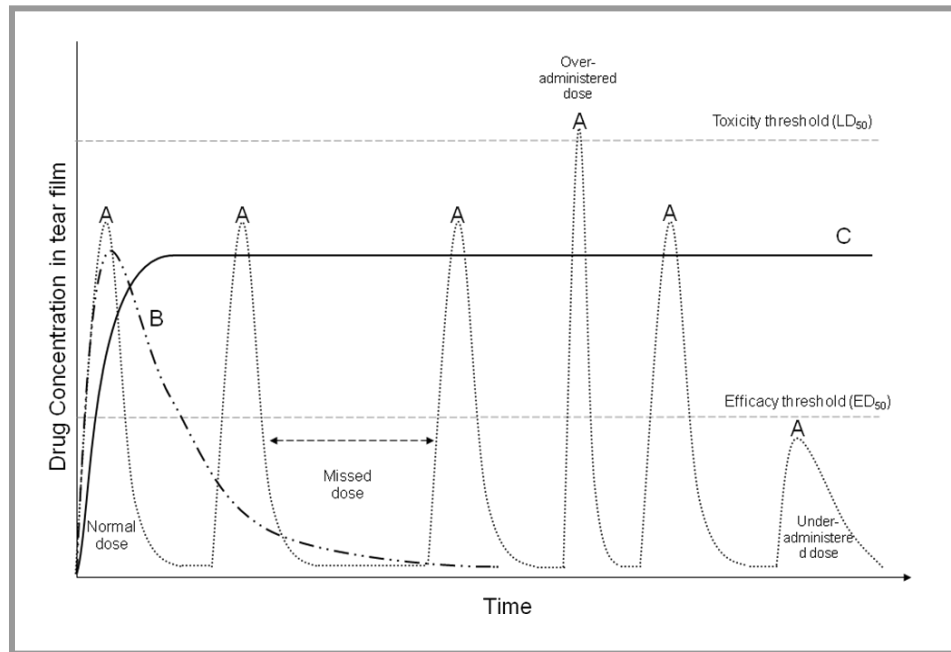


Figure 2.5: Ocular tear film drug concentration based on delivery method

(A) Tear film drug concentration quickly reaches a maximum value when applied by eye drops. Lacrimation, drainage and absorption of the drug quickly reduce the concentration below therapeutic levels until another drop is applied. To maintain effective concentration of drug, eye drops must be applied multiple times a day. (B) Drug release from drug soaked lenses has been shown to load small amounts of drug and release drug quickly. However, (C) an unmet need exists for a drug delivery device that provides a controlled and sustained drug release where a constant concentration of drug can be achieved for an extended period of time.

Chapter 3

Soft Contact Lenses as Platform for Drug Delivery

Contact lenses can be classified on the basis of their materials into: (i) soft contact lenses, which are subclassified in conventional lenses (hydrophilic hydrogels) and silicone hydrogel lenses; (ii) rigid gas permeable lenses (RGP), which are made of durable oxygen-permeable polymers; (iii) hybrid contact lenses, in which the central optical zone is made of a RGP material and then surrounded by an edge of soft lens material. Both, hybrid and RGP lenses maintain a presence in the contact lens market but can be considered specialty lenses, along with (iv) hard contact lenses which are made with polymethyl methacrylate (PMMA), a hard plastic with poor oxygen permeability, which are now virtually obsolete.

The development of different contact lens materials has allowed several wear modalities, which are: daily disposable, continuous wear, and extended continuous wear. Daily disposable lenses are designed to forego the need for daily cleaning and storage of contact lenses by the user. A new lens is worn daily while the old lens is discarded. Daily disposable lenses are recommended for patients with ocular allergies, to prevent the accumulation of dust and other allergens on the lens [96]. Continuous wear lenses are designed for daily use, must be removed nightly, and discarded every two weeks or sooner. Extended continuous wear lenses can be worn up to 30 days consecutively without removal, and must be discarded monthly.

Contact lenses can be divided further into purpose of use, which includes: vision correction, cosmetics, therapeutic, and bandage lenses. Corrective lenses are used to correct the same conditions that eyeglasses do, such as myopia (nearsightedness), hyperopia

(farsightedness), astigmatism (blurred vision due to the shape of the cornea) and presbyopia (inability to see close up). Cosmetics lenses are color lenses, which change the appearance of the cornea. Contact lenses used as bandages typically remain on the eye continuously for several weeks protecting the cornea from rubbing associated with blinking to promote faster corneal healing after disease or trauma [97-99]. Contact lenses soaked in antibiotics or steroids and placed onto the eye to assist in dealing with inflammation or infection occurring from the corneal trauma are called therapeutic lenses. Figure 3.1 shows the classification of contact lenses on the basis of material, modalities and purpose of use.

Hydrogels are the leading materials for soft contact lenses because of their biocompatibility and unique properties such as optical clarity (good transmission of visible light), high chemical and mechanical stability, oxygen permeation, and resistance to accumulation of protein and lipid deposits, to name a few. Hydrogels are water-swollen weakly crosslinked homo- or hetero-co-polymers capable of absorbing significant amounts of water, but insoluble in it. They have generated a lot attention due to their ability to control the diffusion behavior of molecules in or through them, their ability to amplify the microscopic events occurring at the molecular level into macroscopic phenomena [100, 101], and the dramatic implications they have had in drug delivery [100, 102-105].

Soft contact lenses were first developed by Otto Wichterle in 1965 [91, 92]. In his patent, he briefly discussed the potential for soft contact lenses to act as drug delivery platforms through diffusion mechanisms. This essentially involved the transport barrier properties of the polymer chains within the crosslinked networks to limit the diffusion of the drug molecule. Conventional hydrogel soft contact lenses are hydrophilic polymers, that commonly consist of poly(2-hydroxyethyl methacrylate) (pHEMA). Other lens materials include polyvinyl alcohol (PVA), or

HEMA copolymerized with other monomers such as methacrylic acid (MA), methyl methacrylate (MMA), N-vinyl-2-pyrrolidone (NVP), and glycidyl methacrylate (GMA). For conventional hydrogel lenses water content must be high for adequate oxygen diffusion and lens comfort. Water content for these lenses can be up to 70%.

In the 1980's studies found that continuous wear of these lenses could damage the eye through oxygen starvation. As a result, in 1989, the FDA voided the used of these lenses for extended continuous wear (30 days) [106]. Ever since, an interest in hydrogels with higher oxygen permeability has existed. To maintain ocular health in open eyes the lens oxygen transmissibility (Dk/t) should be above 100 barrer (1 barrer is equivalent to 1×10^{-11} (cm²/s)*(mlO₂/ml mmHg). Below 85 barrer, damage could occur with prolonged lens wear [107].

The need for a highly oxygen permeable material resulted in the development of polydimethyl siloxane (PDMS) [106]. This material has high oxygen permeability (600 barrers) due to the bulkiness of the siloxane group (-Si(CH₃)₂-O-) and the chain mobility. In 1980, Dow Corning developed the first commercial soft silicone lens (elastofilcon A), which contained no water, and lacked the necessary properties for ions and water transport to be used as a successful lens. In the late 1990's silicone hydrogels were developed and are the most recent generation of contact lenses [106]. Unlike conventional hydrogel lenses, which are largely hydrophilic, silicone hydrogel lenses are biphasic systems. The silicone component (hydrophobic portion) of the lens material provides extremely high oxygen permeability, while the hydrogel component (hydrophilic portion) facilitates flexibility, wettability and water and ion transport, making them ideal for continuous wear (i.e. 5-7 days) and extended continuous wear (i.e. up to 30 days).

Silicone hydrogel lenses are typically copolymers made of high oxygen permeability silicone monomers, such as polydimethyl siloxane macromers (PDMS) and methacryloxypropyl-tris-(trimethylsiloxy) silane (TRIS), along with a high ion permeability hydrophilic monomer, such as dimethyl acrylamide (DMA) or N-vinyl 2-pyrrolidinone (NVP). Water content for these lenses can be up to 35%.

The development of daily wear lenses, daily disposable lenses, and the newer extended continuous wear lenses has increased interest in controlled drug delivery, particularly for release durations which are related to the duration of lens wear. Increasing the drug reservoir within the lens to sustain a controlled release for an extended period of time has been challenging. Therefore, a tremendous need exists to increase drug loading to ensure a sufficient supply of the drug to maintain longer release periods of therapeutically relevant concentrations. In recent years, many strategies have tried to enhance the drug loading capability and to control the release rate of therapeutics in contact lenses (Figure 3.2). These strategies include the incorporation of chemistry [108-110] or cyclodextrins [111, 112] able to interact with drugs, long chain molecule eluting lenses [113], molecules used as diffusion barriers [114], supercritical solvent impregnation [115, 116], nanospheres [117], and (poly[lactic-*co*-glycolic acid]) coatings [118, 119] . Another approach has been molecular imprinting, which has shown to improve loading and considerably extended and controlled the release [120-122]. This chapter gives review and discussion of these technologies.

3.1 Drug Soaked Lenses

Since the development of soft contact lenses as a potential drug delivery device [123], drug soaking has remained the most sought method to achieve drug delivery [93]. However, a

sufficient reservoir of drug for a therapeutically relevant effect is hard to attain. Drug release from drug soaked lenses is purely a diffusion process, depending on differences in drug concentration, steric hindrance, drug partitioning, and drug solubility in the lens. However, drug soaked lenses have been produced for a variety of drugs and used in a number of *in vitro* and *in vivo* studies. In the overwhelming majority of these cases, the drug was released very quickly with no control over the release profile and only slight improvements over topical eye drops have been demonstrated [93, 124-132].

To emphasize the low potential for drug soaked lenses, the uptake and release of cromolyn sodium, ketotifen fumarate, ketorolac tromethamine, and dexamethasone sodium phosphate were compared using commercially available HEMA based and silicone hydrogel contact lenses [124]. The study resulted in overwhelming evidence that drug soaked lenses lack significant control over drug release rates and load insufficient drug concentrations necessary for use as therapeutic contact lenses, regardless of material. Drug release was performed in 2 mL of saline and the uptake of cromolyn sodium, ketorolac tromethamine, and dexamethasone sodium phosphate was rapid and release was complete in less than an hour. Similar results were observed when the study was performed using ciprofloxacin and dexamethasone [130, 131]. Another investigation showed the uptake and release of ketotifen fumarate from 14 different commercially available contact lenses (silicone hydrogels and conventional hydrogels lenses) [133]. The results in that study revealed that the drug uptake and release was dependent on the lens materials. Drug release was performed over a 24 hour period using 6 mL of borate buffered solution, with no replacement of fresh solvent. Silicone drug-soaked lenses showed a ketotifen fumarate release of less than three hours, while conventional drug-soaked lenses had a complete release in less than an hour. In another study, where epidermal growth factor was used in a

rabbit model, results showed that the drug uptake and release was dependent of the lens materials [134] .

High water content (up to 75%), in conventional hydrogel lenses, leaves plenty of free volume to load hydrophilic drugs [95]. However, the hydrophilic structure and high water content reduces the partitioning of hydrophobic drugs into these lenses. Thus, for hydrophobic molecules, loading will be very low and far from the values needed to sustain release. For hydrophilic molecules, however, the solubility limit of the drug in the solution will be the major factor. The equilibrium drug partitioning of hydrophilic drugs into hydrophilic lenses has repeatedly been shown to be lower than necessary to attain sustained release [93, 124].

On the other hand, silicone hydrogels contain hydrophobic areas within the lens structure. Potentially, hydrophobic molecules could partition into the lens via drug soaking and lead to a more sustained release. The more hydrophobic the drug and the more hydrophobic regions within the lens structure, the higher amounts of drug that could be loaded and which would reside in the hydrophobic areas of the lens. However, loading significant hydrophobic drug concentration is difficult and control over the release rate for extended periods is questionable with other methods invariably needed to control the release. In addition, silicone hydrogel materials have significantly lower water content that reduces the volume to load hydrophilic drugs [106]. If silicone hydrogels are used for continuous or extended wear (i.e., 7, 30 days), the hydrophobic interactions would not be enough to sustain or control drug release at therapeutically relevant values for significant durations.

When the molecular weight of the loaded molecule is rather large, release can be delayed by the polymer structure alone; however, large molecular weight molecules cannot be loaded via soaking methods. As the molecular weight increases, the loading amount will decrease. Thus, the

drug reservoir (i.e., the amount of drug to be released over the duration period) is low, and a sustained release of a therapeutically relevant amount cannot be achieved.

The duration of lens wear is an important metric when considering release methods. Drug soaked lenses clearly do not extend release for sufficient time, and topical eye drops have remained the ‘go to’ products. It is important to note that drug soaking has been around as long as soft contact lenses have existed [91]. The most telling fact of their non-superiority to topical therapy is that after 46 years, no contact lens product that loads or releases drug this way, has made it to market.

3.2 Supercritical Solvent Impregnation

In recent years, supercritical techniques have been used to impregnate and disperse drugs into contact lenses [115, 135]. The drugs are dissolved in compressed highly volatile solvents (e.g., carbon dioxide (CO₂), water, and ethanol) at their critical temperatures and pressures. Supercritical CO₂-drug solutions were used to enhance loading of timolol maleate and flurbiprofen into commercially available lenses. Timolol maleate, glaucoma drug, was selected as a model hydrophilic drug, while flurbiprofen, a non-steroidal anti-inflammatory drug (NSAID), was selected as a hydrophobic drug. The cumulative mass release of flurbiprofen from pHEMA lenses (methafilcon A) loaded by supercritical CO₂ was 5-6 times greater than the mass released from drug soaked lenses [115]. This method enhanced the loading; however, drug release from this type of lens was purely a diffusion process with no control, and did not extend drug elution time compared to control lenses.

In separate studies, the effectiveness of supercritical solvents in loading anti-glaucoma drugs within lenses was compared by immersing lenses in supercritical water-drug and

supercritical ethanol-drug solutions. Acetazolamide loading increased when immersed in supercritical ethanol compared to supercritical water, loading 50 and 20 $\mu\text{g}/\text{lens}$, respectively. Immersing a lens in a supercritical ethanol solution increased loading of timolol maleate by a factor of 20 when compared to soaking in an ethanol solution [135]. However, the amount of drug loaded with this method was lower than using other techniques [112, 120]. Other studies also demonstrated that supercritical techniques in addition to a controlled drug delivery method may be an effective way to increase loading of some drugs onto different lens materials [116, 136]; however, no control over release rate was observed.

This technique provides the opportunity to incorporate both hydrophilic and hydrophobic drugs into contact lenses, and the amount of drug incorporated in the polymer matrix can be tailored by altering the operational pressure and temperature, and selecting the appropriate solvent, without altering the physical, chemical and mechanical properties of the lenses. However, it does not increase release duration, and has little control over release, indicating no true benefits over drug soaked lenses.

3.3 Diffusion Barriers

Another approach for controlled release of drugs from contact lenses has been developed by creating transport barriers. A diffusion barrier can be any biocompatible material that can be dispersed in the polymer network of the lens without changing its mechanical and physical properties. In theory, drug elution would be slowed by loading sufficient quantities of the barrier molecule to eliminate the free volume within the lens removing the unhindered transport of loaded drug. As a consequence, loading the barrier drug decreases volume available for any secondary drug resulting in lower drug mass uptake

Vitamin E, a high molecular weight molecule, was used as the diffusion barrier into different silicone commercial lenses. Drugs with different physicochemical properties such as timolol, dexamethasone 21-disodium phosphate, and fluconazole were investigated [114]. As a large molecule, vitamin E, constrained the free movement of these drugs and increased the residence time of the drug within the lens. Release studies were carried out in 2 mL of PBS (no replacement of release media was stated by the authors), showing a release from hours to several days. The release duration is questionable due to the small volume used. When the release study is performed in small volumes, a boundary layer between the film and the surrounding solvent is formed. The bulk concentration of the drug in the solvent is non-negligible, and increases as drug releases with time. The release becomes delayed as this concentration gradient (driving force) decreases. When the release is close to equilibrium, the concentration gradient becomes insufficient, causing a decrease in the release rate and extending the duration of the release (Chapter 9 further highlights this issue). Even that an extended release of the drug was stated by the authors, non-therapeutically doses were reached over time [114]. Furthermore, the rate of release is strongly dependent on the concentration of the diffusion barrier molecule. However, the barrier molecule also diffuses from the lens and as time increased, the effectiveness of the blockage decreased.

The use of Vitamin E as a diffusion barrier has been also investigated by the same authors to load and release dexamethasone [137], cyclosporine A [138], and anesthetics drugs, such as bupivacaine, lidocaine, and tetracaine [139].

Recently, the same group performed *in vivo* studies in beagle dogs, releasing timolol from commercial daily disposable silicone contact lenses (ACUVUE® TruEye™) [140], and extended continuous silicone contact lenses (NIGHT & DAY™) [141]. The addition of vitamin

E did not improve the IOP reduction in these studies. Timolol delivered from contact lenses achieved the same efficacy as eye drops, but with one-fifth [140] or one-third [141] of the drug administered via eye drops.

In recent work, hyaluronic acid (HA) (35kDa and 132kDAa) was incorporated into conventional hydrogel films and hydrogels containing silicone monomers to control the release of ciprofloxacin and dexamethasone phosphate. No statistical difference was observed in the release rates among lenses with and without HA. Moreover, ciprofloxacin lenses showed low optical clarity [142].

3.4 Inclusion of Chemistry and Network Design

Recent studies have included methods which work with the incorporation of specific chemistry or inclusion molecules along the polymer chains to increase the loading of ocular therapeutics and control their release.

3.4.1 Direct Embedding

One means to overcome low drug loading is to disperse the molecule into the pre-polymer formulation. Once polymerization occurs, a network will form around the molecules embedding them in the free volume within the polymer chains. This method can be used with high or low molecular weight molecules. While these are not drug-soaked lenses, the drug transport is similar the same as their drug-soaked counterparts.

Currently, there are two commercially daily disposable lenses that used this procedure. CIBA Vision's FOCUS DAILES® are designed to release a comfort molecule (polyvinyl alcohol, PVA) to sequester water on the anterior surface of the eye. Release is controlled via

solubility and reptation of the PVA in the Nelfilcon A network, a PVA based macromer. The reported release duration is ~16 hours [44, 45]. Recently, a variation of the FOCUS DAILES® lenses was launched, the DAILIES® AquaComfort Plus® contact lenses, where polyethylene glycol (PEG), a low molecular weight lubricant, binds to the embedded PVA, and further extends its release. These lenses are packed in a saline solution that contains a low molecular weight of hydroxypropyl methylcellulose (HPMC), which promotes initial comfort upon insertion. A clinical trial with 81 subjects wearing these lenses at least 8 hr/day and 4 days/week was performed [143]. Common contact lens-related symptoms such as, tired eyes or irritated eyes, blurred vision, redness, discomfort, deposits/lens needs cleaning, and dryness were examined. An average of 46% of subjects who reported symptoms at baseline experienced a reduction in the frequency of symptoms. The three symptoms that showed the most improvement in terms of the percentage of patients experiencing reduced frequency throughout the 4-week study were blurred vision (58% of patients), tired eyes (58% of patients), and dryness (54% of patients) [143].

Other studies with long chain comfort agents demonstrated the release of PVP from poly(HEMA-co-EGDMA) lenses capable of daily disposable wear [46]. Results showed a release of PVP for ~ 3 days, but had very little demonstrated control over the release rate of PVP.

3.4.2 Cyclodextrins

Cyclodextrins (CDs) are cyclic oligosaccharides with a high concentration of hydroxyl groups in a ring structure (hydrophobic cavity). CDs are capable of forming a high affinity inclusion complex with several drug moieties through non-covalent interactions [73]. Cyclodextrins have been used in a number of topical ophthalmic formulations and recently have

been formulated into hydrogels. HEMA hydrogels which had been prepared by copolymerization with glycidyl methacrylate (GMA) and β -cyclodextrins (β -CDs) were grafted to the network by reaction with GMA, then, the films were loaded with diclofenac sodium (DS) by soaking in aqueous diclofenac sodium solution [111]. The data showed that the grafted β -CD did not alter the Tg, swelling optical clarity, or oxygen transmissibility of the networks. Release studies were carried out in 10-20 mL of artificial lacrimal solution without fluid replacement at 25°C, showing an extended release for up to 11 days. However, the small volumes used might delay the release of the drug, showing a deceitful extended release (Chapter 9). As GMA concentration in the lens increased from 0 to 360 $\mu\text{mol GMA/g lens}$, a higher loading was observed [111]. However, these films were significantly thicker than commercial lenses. In Fickian release kinetics, the diffusion coefficient scales to the reciprocal of thickness squared, thus decreasing lens thickness by 10 will increase the release rate by a factor of 100. Reducing the hydrogel films to adequate thickness will greatly increase the release rate and decrease the loading of diclofenac. Another group synthesized mono-methacrylated- β -CD (MA- β -CD) and copolymerized with a polyvinyl alcohol (PVA) based hydrogel [144]. Puerarin and acetazolamide were used as model drugs to evaluate the drug loading and the *in vitro* release of the hydrogels. As the content of β -CD was increased in the pPVA- β -CD hydrogels, more drug was loaded. Drug release was performed in 10 mL of PBS without fluid replacement. The release profiles were Fickian with an exponentially decreasing release rates, and the films were twice as thicker than commercial lenses [144].

3.4.3 Ion-ligand Mechanism

Ion ligand-containing polymeric hydrogels have been used to release drugs from lenses by ion exchange. Published work has demonstrated controlled release of azulene by hydrogels

containing cationic functional groups in their side chain (i.e., copolymerization of methacrylamide propyltrimethylammonium chloride (MAPTAC) and HEMA) [108]. A drawback from this system was that before and after the release a significant size change occurred. However, the addition of an anionic monomer such as methacrylic acid (MAA) or 2-methacryloxyethyl acid phosphate (MOEP) to the initial composition was effective in preventing the size change [108]. In other work, naphazoline, a cationic drug, was loaded into lenses composed of HEMA and methacrylamide (MAM) with MOEP or methacrylic acid MAA as ionic monomer. Naphazoline release into saline from 3 mole% monomer containing lenses reached completion in 4 hours (MAA) and 12 hours (MOEP) [145]. This method, which greatly extended the release in DI water, is dramatically limited in the presence of other ions, especially among those ions common in lacrimal fluid. Any ion absorbed from the ocular environment can interact with the drug, ionic monomer or both, preventing the pairing between the network ion and drug ion pair to delay release.

Recently, an *in vivo* study on a rabbit model was performed comparing eye drops and contact lenses synthesized using the ion-ligand mechanism [146]. Two antibiotics, gatifloxacin and moxifloxacin, were tested. The results showed that lenses released antibiotics for up to 3 days with no control over the release. Moreover, a fast release of ~ 90% of the drug loaded into the lenses was detected in the first couple of hours (i.e., burst release), and the concentration of the drug decreased exponentially over time, causing a variable concentration of the drug in the cornea, aqueous humor and crystalline lens.

3.4.4 Polymer Degradation

Tailoring release through controlled polymer degradation has also been studied. Initially, drug elution is stopped via size exclusion but as the polymer degrades, the mesh size increases allowing more drug to elute. Polymers used for this method are usually poly(lactic-co-glycolic acid) (PLGA) or polylactic acid (PLA) since they are well studied, approved for use, can be controlled quite well, and have non-toxic degradation products.

In a recent study, researchers sandwiched a layer of ciprofloxacin containing PLGA film in between pHEMA sheets as a mimic of a contact lens [118]. The inner core thickness of PLGA film measured 200-250 μm . Thus, the completed lenses were 450 μm thick (dry state). A very high loading of ciprofloxacin into the PLGA phase was measured (up to 20 mg of ciprofloxacin). Release was performed in 15 mL of PBS solution. Zero order release (concentration independent release, ideal for release devices) was reported by the authors for both ciprofloxacin and fluorescein, but significant standard deviation was observed in the measurements. Each concurrent error bar completely overlapped with the preceding error bar. Given such a significant deviation in measurements, any confident conclusions about release order are dubious and difficult to accept [118]. The same group used this approach to release an antifungal drug, econazole, which has not been yet approved by the FDA to be used for ocular therapy [119]. These devices suffer from several deficiencies including large thickness, low oxygen and ion permeability due to the thick PLGA layer, loss of transparency in the peripheral region which contains PLGA, etc. Additionally, these lenses cannot be autoclaved or packaged in PBS because of PLGA degradation [118, 119].

3.5 Particle-Laden Strategies

This technique is based on incorporation of drug-loaded colloidal particles (micro-emulsions, liposomes, nanoparticles, etc.) into the matrix of contact lenses.

Micro-emulsions are commonly used in ocular topical formulations to increase the solubility of drugs and as carriers to deliver drugs to specific targets. Emulsifiers and surfactants are commonly used in ocular formulations, especially in eye drops as preservatives and stabilizers. Researchers have been dispersing micro- and nano-emulsion drops of ophthalmic drugs into soft hydrogels. The use of emulsifiers and surfactants as well as liposomes has found application to delivery drug from hydrogels to control drug release rate and increase loading. Hydrogel films have been synthesized and the drugs are encapsulated into thermodynamically stable micelles or drug particles and mixed with the pre-polymer solution. These nanoparticles are best employed where high partitioning occurs between two phases. As a result, the hydrogels are conceptually limited to the release of hydrophobic drugs from hydrophilic hydrogels or hydrophilic drugs from hydrophobic regions of hydrogels. It is hypothesized that the colloidal nanoparticles provide additional resistance to drug release. The drug must first diffuse through the nanoparticle and penetrate the particle surface to reach the hydrogel matrix.

A pHEMA hydrogel was used to release a hydrophobic model drug, lidocaine (an anti-arrhythmic drug commonly used for heart patients) [147] The lidocaine, which is insoluble in hydrophilic materials, was encapsulated in the lenses with Brij 97 and the addition of an oil phase consisting of hexadecane and octadecyltrimethoxysilane. Films were 1,000 μm thick, far outside commercial tolerances. Lenses containing between 3 wt.% and 0.55 wt.% oil, released in DI water $\sim 100 \mu\text{g}$ lidocaine (50 %) in less than 6 hours, $\sim 70 \%$ release at one day after which the rate of release dropped to $\sim 10 \mu\text{g}$ lidocaine/day for 4 days. The volume used for the release

studies, which is a variable that influences the duration of the release (Chapter 9), was not stated by the authors. Moreover, these surfactant particles could be sensitive to ions and pH. Also, as the films were 10 times thicker than commercial lenses, scaling the thickness down would greatly reduce the loading of these systems and significantly reduce release times.

The same group investigated ways to encapsulate lidocaine in dimyristoyl phosphatidylcholine (DMPC) liposomes, and the drug-laden liposomes were dispersed in the pHEMA hydrogels [148]. A high loading was achieved compared with their previous work. Release studies were performed in 20 mL DI water without fluid replacement at ~26°C. After 3-4 days, the rate of drug release leveled to around 65 % of theoretical loading and no further release was observed. Explanations for this include the possibility that the drug is sequestered in the liposomal drug carriers, that theoretical loading was not as high as expected, or that the release medium of 20 mL of DI water was too small a volume for complete release, delaying the release rate.

Another hydrophobic drug, timolol (anti-glaucoma drug), was encapsulated in different formulations of Pluronic F127 and sodium caprylate with ethyl butyrate oil [149]. Films were formed to a thickness of 200 μm . The systems displayed extremely high loading. Release studies were conducted in 3 mL of DI water, which was replaced daily, or in 3 mL of phosphate buffered saline (PBS) solution. Timolol releases performed in PBS or saline solutions reached completion in less than a day. It was concluded that the timolol laden films were not feasible to release in physiological ocular condition.

Cyclosporine A nanoparticles were dispersed in the pre-polymerization solution to synthesize pHEMA films with thicknesses of 100, 200, 400, and 800 μm [150]. Brij 78, 97, 98 and 700 were used to stabilize the drug particles. Release was performed in 3.5 mL of PBS.

Increasing surfactant concentration seemed to decrease loading of cyclosporine A, while extending release duration, but it did not significantly alter the release rate. A decaying release rate was shown for all the formulations. Release of cyclosporine from Brij 78 films delivered ~0.7-1 µg/day when loaded with 8 and 2 wt % Brij 78, respectively. The addition of 2 and 8 wt % Brij 97 extended release by 7-10 days beyond the control films without Brij 97 and rates of mass release were 3 and 2 µg/day. Release rates of Brij 700 laden lenses at 2 wt% concentration were indistinguishable from control samples. Rates for 8 and 4 wt% delivered ~1.5 and ~1.75 µg cyclosporine/day, respectively. Release profiles were independent of surfactant concentration and structure. These films released only 50-70 % of the calculated loaded mass, presenting another concern with this system [150]. It was found that the transparency of micro-emulsion-loaded HEMA films decreased with increasing micro-emulsion loading. It may not be possible to load sufficient drug to deliver effective drug concentrations for more than 2-3 days. Other drawbacks are that the system was unstable during preservation and transportation because the loaded drugs diffused into the gel matrix. Typically, the carrier is not covalently linked to any part of the polymer network, and it also elutes from the lens. The carrier can then cause irritation or could be toxic to the eye.

In another study, timolol loaded highly crosslinked ropoxylated glyceryl triacrylate (PGT), ethylene glycol dimethacrylate (EGDMA) or surfactants (Pluronic F127) nanoparticles were synthesized [151]. The nanoparticles were dispersed in the pre-polymerization solution. pHEMA films with a thickness of 100 or 200 µm were synthesized. As the amount of nanoparticles increased in the gels, the storage modulus increased and the water content decreased to values not suitable for commercial contact lenses. Hence, a low amount of PGT nanoparticles (4.6%) was dispersed in the HEMA pre-polymerization solution and polymerized

afterward for further studies. Release studies were carried out in 1.75 and 3.5 mL of PBS and no replacement of fresh PBS was stated in the procedure. Hence, an extended *in vitro* release of timolol was stated by the authors (~25 days). As mentioned before, the small volume used by the authors to perform the release studies might not be adequate for a complete release, delaying the release rate and resulting in false conclusions (Chapter 9).

Due to the fact that pHEMA lenses are not suitable for an extended continuous wear, the same group, dispersed the timolol loaded PGT nanoparticles in silicone hydrogels films, and soaked commercial silicone contact lenses (Acuevue® Oasys®) in a timolol-PGT nanoparticle solution[152]. Mechanical experiments showed that as the content of PGT nanoparticles increased the storage modulus increased to values (~5-22 MPa) not suitable for commercial use as a soft contact lens. Hence, Vitamin E was incorporated into the films, resulting in a decrease of the storage modulus (1.07 MPa) and similar release rates when compared to films without Vitamin E. Release studies were performed in 1.75 mL and 3.5 mL of PBS, apparently with no replacement of fresh release media. A release at room temperature of ~ 22 days and ~ 50 days was achieved for commercial silicone lenses and silicone films (100 and 200µm), respectively. However, when the commercial silicone lenses loaded with timolol-PGT nanoparticles were tested *in vivo* in glaucomatous dogs [152], the IOP reduction was attained for just 2 days and slightly improvement was observed when compared to control lenses. Furthermore, no comparison with eye drops was shown.

In another study, drug-loaded nanocarriers were immobilized on the surface of functionalized contact lenses. Levofloxacin liposomes were immobilized on commercial contact lenses (Hioxifilcon B, pHEMA lens). Polyethylenimine was covalently bounded onto the hydroxyl groups present on the surface of the lens, followed by NHS-PEG-biotin molecules

being attached onto the surface amine groups by carbodiimide reaction. Then, NeutrAvidin was bonded onto the PEG-biotin layer, and liposomes containing PEG-biotinylated lipids were docked onto the surface of immobilized NeutrAvidin. Further addition of NeutrAvidin and liposomes layers allowed multilayers to be formed [153]. When 2 levofloxacin- liposome layers were immobilized onto the surface of the lens, a complete release was achieved in 30 hours, while levofloxacin- liposomes of 5 or 10 layers maintained a sustained release for up to 120 hours [154]. Release studies were carried out in 3 mL of a saline solution with no replacement of fresh release media. However, the small volumes used might delay the release of the drug, showing a deceitful extended release (Chapter 9). Moreover, the multilayer arrangement of liposomes reduced the oxygen and carbon dioxide permeabilities.

3.6 Molecular Imprinting

The concept of molecular imprinting involves the creation of macromolecular memory for a template molecule within a polymer network. Molecular imprinting involves polymerization in the presence of the template, which directs the growth and formation of the polymer structure. Effective self-assembly of the functional monomer(s)-template complex is crucial toward imprinting efficacy. The template molecules act as sites of nucleation and organize the polymer chains around them. The propagating polymer chains are constrained into conformations which correspond to the three dimensional topology of the template molecule. The binding site as such is composed of functional groups oriented precisely in the polymer structure so that they can form non-covalent bonds with the template molecule. The main non-covalent interactions responsible for template recognition in molecularly imprinted networks are hydrogen bonding, hydrophobic interactions, Van der Waals forces of attraction, London

dispersion forces, metal-ion coordination bonds, ion pairing interactions, and π - π or cation- π interactions, and in a given system, two or more of these forces might influence binding [102]. Once the polymer network is formed, the unreacted monomers and template molecule are washed out from the network with a thermodynamically compatible solvent. The polymer structure now consists of microscopic template-specific cavities or “macromolecular memory sites” wherein the chemical functional groups are precisely oriented such that they can recognize and bind the template molecule, while the backbone of the polymer network provides the necessary rigidity to maintain the size, overall shape and relative positioning of the functional groups (Figure 3.3).

Macromolecular memory is primarily due to two synergistic effects: (i) mesh size cavities that match the template molecule, which provide stabilization of the chemistry in a crosslinked matrix, and (ii) chemical groups oriented on multiple polymer chains that form multiple non-covalent complexation points with the template. Successfully imprinting within hydrogels depends on structural considerations and the underlying flexibility of polymer chains as well as limiting the expansion or collapse of polymer chains due to solvation or desolvation forces. It also depends on the number of template molecules in relation to the number of functional monomeric species, the level of diversity of functional monomeric species that interact with the template, the strength of the monomer template interactions, and the polymerization reaction.

The selection of monomers involved in the imprinting process is critical for effective imprinting. Biomimesis is the processes of mimicking biological recognition or exploiting biological mechanisms. The active site of the binding molecule is examined for amino acids that are critical for binding to the template molecule. Analogous acrylate or methacrylate monomers are selected by comparing the chemistry of the acrylates to the critical amino acids. The acrylate

monomers with functional groups most similar to the critical amino acids are likely to form the best memory sites within the hydrogel.

Selective binding of template molecules combined with stability and cost effectiveness make molecular imprinting polymers (MIPs) attractive for many analytical applications, including catalysis, sensing, solid-phase extraction, chromatography, and binding assays [155-157]. Recently, the potential of molecularly imprinted polymers for new applications in the pharmaceutical field as carriers for drugs, peptides, and proteins has gained increased attention [158, 159]. A relatively new area of application of MIPs is in the field of drug delivery, due to their potential for enhanced drug loading and controlled drug release [160]. The reader is directed to reviews on the conventional applications of molecular imprinting [161, 162], as well as bio-focused and drug delivery reviews [102, 163-165].

The first imprinted hydrogel created for use in contact lenses was published in 2002 [59]. The gel released timolol HEMA hydrogels were formulated with methacrylic acid (MAA) or methyl methacrylate (MMA) as imprinting monomers. Complete release of the loaded timolol was achieved between 6 and 10 hours in artificial lacrimal solution, and correlated to a Fickian release profile. The results showed increased loading of timolol over non-imprinted lenses, especially in lenses containing 100 mM MAA, which loaded 12 mg of timolol/g of dry hydrogel. This was a 3 fold increase in loading over control HEMA hydrogels. Timolol release was once again explored with variations in the backbone polymer network based on relative hydrophilicity at similar ratios and formulations with varying concentrations of crosslinkers [60]. In 2005, the monomer to template (M/T) ratio was shown to affect the release rate of imprinted hydrogels [61]. At optimal M/T ratios, more interactions occur and slow template transport. At very high M/T ratios, there is no organized orientation of the monomers and the functional groups are

randomly oriented and no difference is seen in imprinted and non-imprinted lenses. At low M/T ratios, functional monomers are spread widely apart and the number of interactions is low enough that no effect is seen in template transport. The same group published an *in vivo* study, showing the release of timolol in rabbit eyes using 14 mm wide diameter, 80 μm thick imprinted contact lenses [166]. Imprinted lenses showed higher timolol concentration in the tear layer of the rabbits, but did not manage to extend release past 90 minutes. Thus, these imprinted lenses showed marginal improvement over conventional eye drops with enhanced bioavailability [166].

In 2005 our group demonstrated that greater control could be gained by including several different functional monomers which interact differently. Four different functional monomers were used (N-vinyl pyrrolidone (NVP), Acrylic acid (AA), Acrylimide (AM), and HEMA) to synthesize 400 μm and 700 μm films, which loaded 8 times the amount of drug from single imprinted monomer networks [121, 167]. The multiple monomers outperformed single monomers and loaded 6 times the amount of ketotifen fumarate over non-imprinted lenses. Therapeutically relevant amounts of drug were released *in vitro* at 25°C over multiple days (5 days) [167]. This included a relatively constant release in artificial lacrimal solution with ocular flow rates [168]. The release studies were performed in 30 mL of lacrimal solution with replacement of fresh media after measured time intervals to maintain infinite sink conditions, in order to sustain the greatest driving force.

Our group also synthesized imprinted lenses to controllably release hyaluronic acid. This was the first imprinted contact lens for a large molecular weight molecule [122]. Films of ~ 120 μm thickness lenses were composed of CIBA Vision's Nelfilcon A macromer, AM, NVP, and 2-(diethylamino) ethyl methacrylate (DEAEM) and controlled release of HA was demonstrated for 24 h. Effective control of the diffusion coefficient for HA was demonstrated by varying the

concentration and variety of imprinting monomers. This diffusion coefficient with diverse monomers was lowered 1.5 times compared to a single monomer and 1.6 over non-imprinted lenses. Altering the M/T ratio reached a critical value which sequestered HA chains inside the lens and did not release them until the pH was altered to interfere and disrupt the HA-DEAEM interactions. Such devices were designed to deliver a therapeutic amount of HA into the eye to treat contact lens induced dry eye symptoms and increase wettability and the comfort of lenses. In more recent work, 120 KDa hydroxypropyl methylcellulose (HPMC) was used as the template macromolecule for development of comfort enhanced, molecularly imprinted, extended wear, silicone hydrogel contact lenses [169]. Using acrylic acid, significant control over the release rate was achieved. Altering the M/T ratio allowed for significant control over the release rate and could be formulated to deliver the HPMC reservoir over the entire spectrum of lens wear. A lens with a thickness of $\sim 100 \mu\text{m}$ and the HPMC content of $1,000 \mu\text{g HPMC/lens}$ was tested at physiological flow rate. The release in DI water reached completion in 60 days where the rate of release was observed to approximately constant at a rate of $16 \mu\text{g/day}$ under physiological flow rates.

Diclofenac sodium, which is used to treat inflammation, was released from imprinted hydrogels synthesized via living polymerization reactions. The imprinting of living polymerization formed networks led to 54 % increase in loading over traditional radically polymerized hydrogels and a 269 % increase in loading over non-imprinted lenses [170]. Controlled living imprinting delayed release for 5 days in DI water with release profiles approaching zero order release. The controlled polymerizations slowed the polymerization reactions and lead to chain orientation around the template [170].

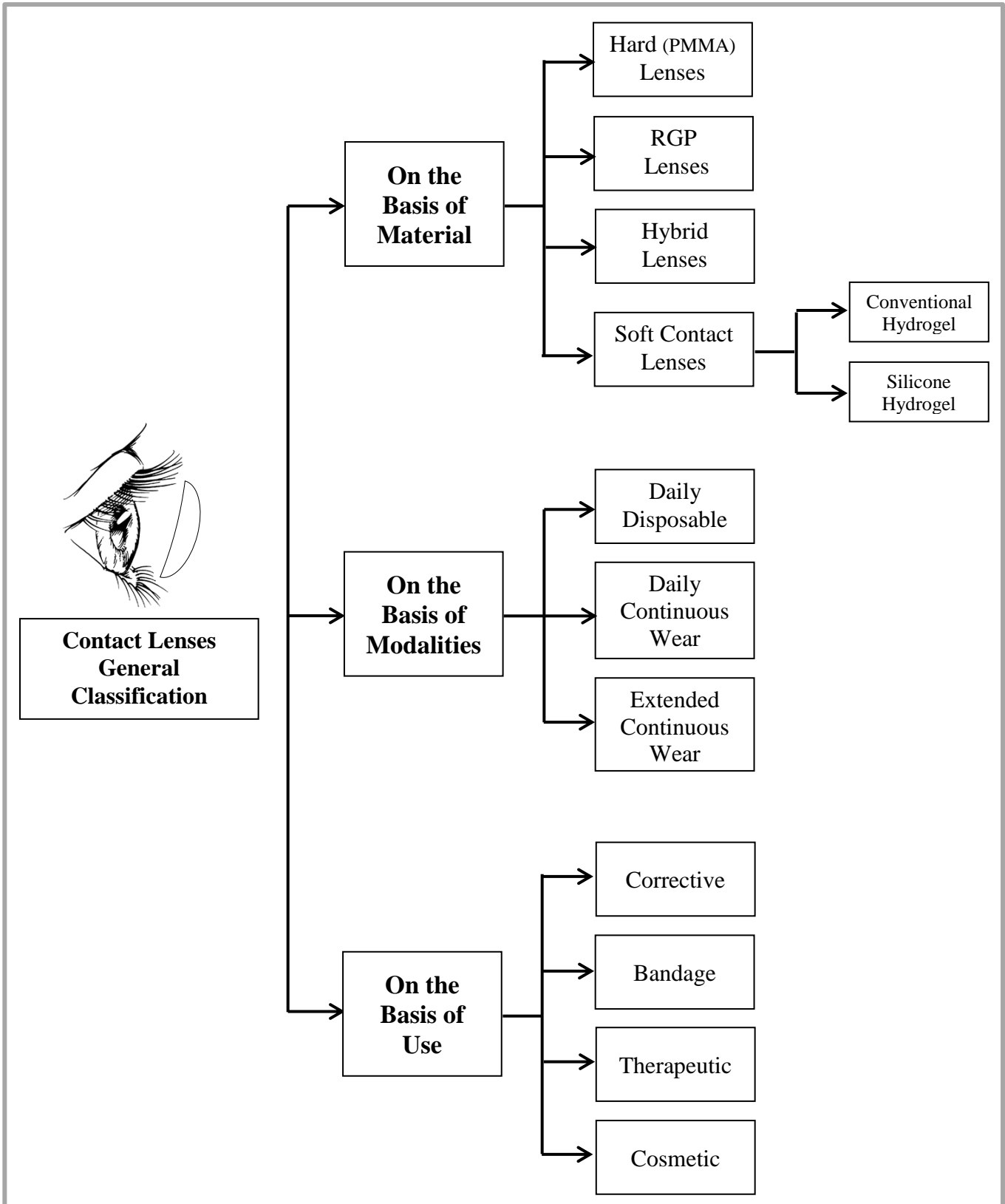


Figure 3.1: Classification of contact lenses on the basis of material, modalities and use

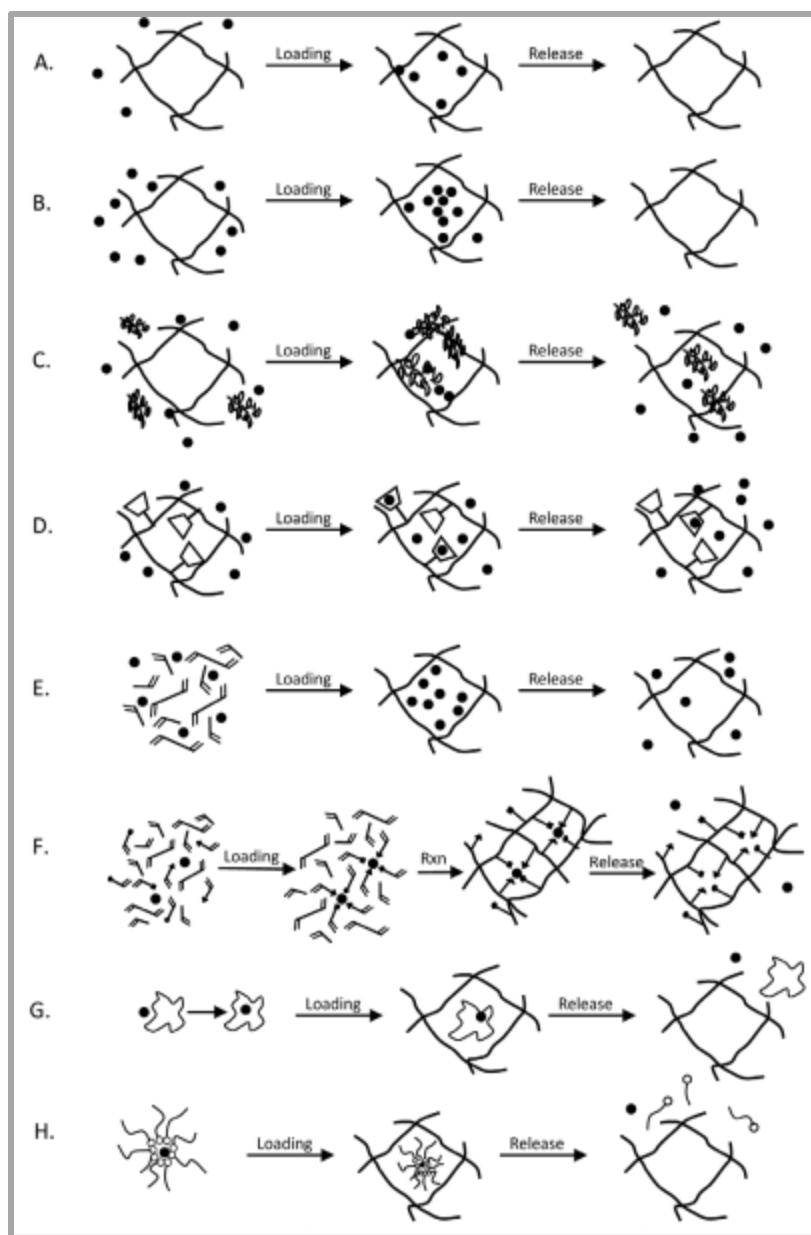


Figure 3.2: Demonstration of release mechanisms used within contact lenses

Drug loading and release within contact lenses varies according to the method used. Therapeutic contact lenses have been produced by (A) soaking lenses in a drug solution, (B) immersion of a lens in a supercritical fluid-drug solution to increase loading, (C) including high molecular weight barrier molecules to slow elution of a small molecular weight drug, (D) incorporating cyclodextrins into lens formulations to create inclusion complexes that slow the release rate, (E) dispersing drug into the pre-polymer lens formulation or direct embedding of drug to increase drug loading, (F) molecular imprinting drugs to control release rate and increase drug loading, (G) addition of a carrier to load and release insoluble drugs as well as (H) using micelles to disperse insoluble drugs to increase their loading.

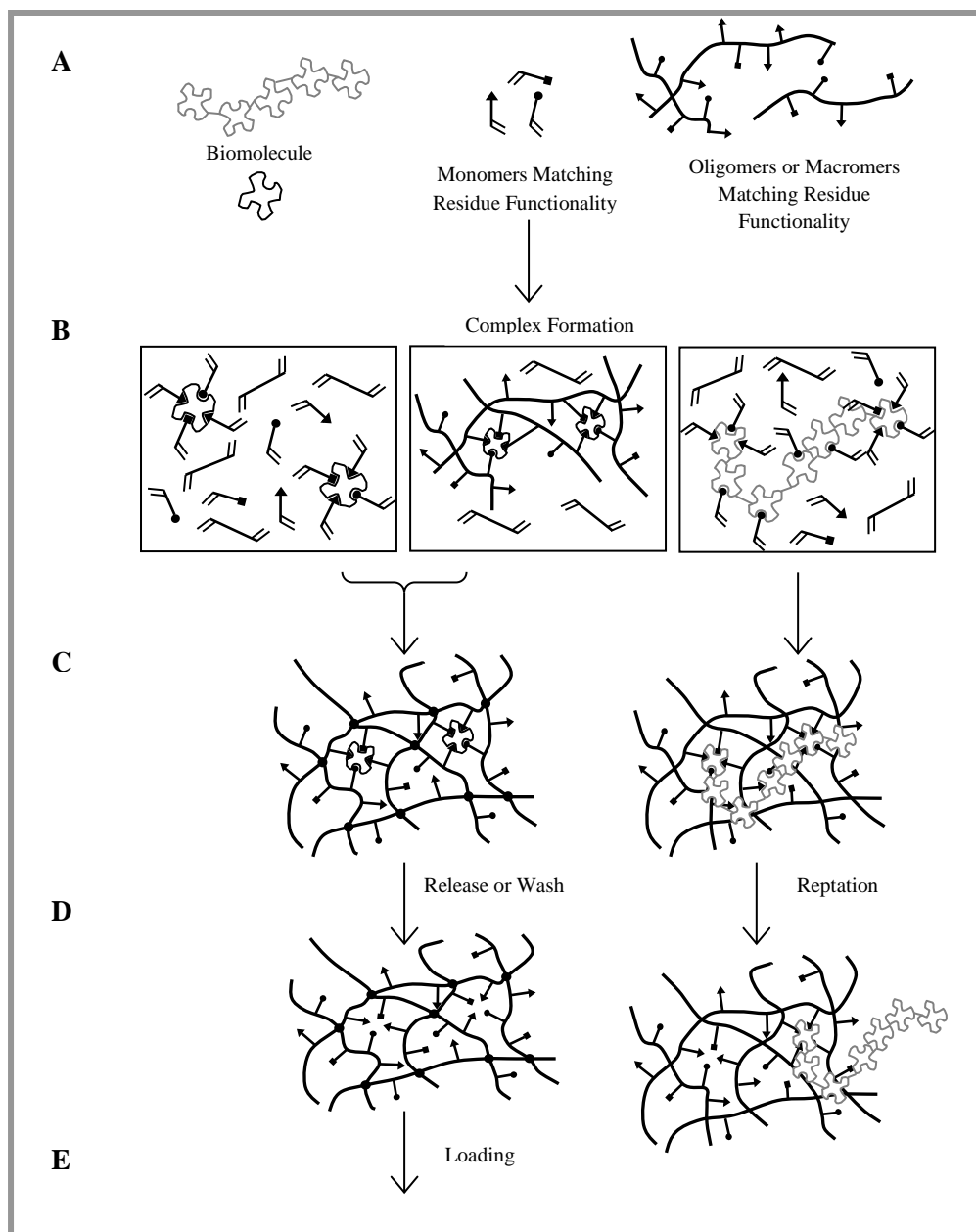


Figure 3.3: General schematic of the imprinting technique

Diverse chemical functionalities are incorporated at the molecular level in the network, which maximizes the non-covalent interactions with the drug. The drug acts as a template and organizes the growing polymer chains during the formation of the network, and hence “imprints” or creates macromolecular memory within the polymer for the template drug molecule.

Chapter 4

Characterization of Imprinted Hydrogels

To evaluate imprinted hydrogels as drug delivery devices, it is crucial to analyze their template binding, structural parameters and transport properties. Therefore, specific experiments and theoretical analysis are needed. The sections below provide the methods used herein to characterize imprinted polymer structures.

4.1 Diffusion through an Imprinted Hydrogel

Diffusion of particles is the random transport of particles from regions of high concentration to low concentration. The concept of diffusion is tied to that of mass transfer driven by a concentration gradient in order to bring the system to thermodynamic equilibrium.

Template transport through a polymer occurs in the solvent filled domains between the network chains. The mean free path length and residence time of the template diffusing through the network is dependent on various factors which can affect either the organization of the network chains within the polymer (i.e., mesh size, which is the correlation distance between two adjacent crosslinking or junction points), or the strength and quality of non-covalent interactions experienced by the template as it passes through the network. These factors include the polymer chain mobility, size and chemistry of the template, the electronic interactions between the template and pendant functional groups, and the macro/micro porosity (which is reflected the amount of water absorbed by the hydrogel), and tortuosity of the polymer [171]. Clearly, the

template diffusion is impaired in highly crosslinked networks, where mesh sizes are small, or when the hydrodynamic radius of the template is comparable to the mesh size of the network. In particular, the polymer chains have the propensity to strongly influence template diffusion characteristics. The polymer chains can also increase the frictional drag on the template [171].

Transport of the template through an imprinted hydrogel will depend on a number of structural and physiochemical considerations. For imprinted hydrogels prepared in solvent (i.e., macro or microporous hydrogels), the template diffusion coefficient will be primarily related to the porosity and tortuosity within the hydrogel, as in conventional hydrogels [100, 101]. For imprinted hydrogels prepared with no solvent the “tumbling hypothesis” was proposed by Byrne and colleagues, and explains that when a molecule tumbling through an imprinted network with multiple, organized functionalities and an appropriate mesh size, experiences heightened, transient interactions with memory sites and shows delayed transport kinetics. This could also be partially due to bound template temporarily obstructing free template transport [121]. Thus, the structural plasticity of polymer chains (i.e., the organization of functional groups into memory sites) may be responsible for an extended release.

4.1.1 Theoretical Model for Diffusion

The transport of a particle through a hydrogel can be mathematically modeled. In all the hydrogels studied the aspect ratios (exposed surface length/thickness) were much greater than 10; therefore, the edge effects can be ignored and the problem can be approached as a one-dimensional process [172]. Diffusion of a drug from a thin hydrogel can be approximated to a flat slab and can then be described by application of Fick’s Second Law by the following differential equation, initial conditions, and boundary conditions.

$$\frac{\partial C}{\partial t} = \frac{\partial}{\partial x} \left(D \frac{\partial C}{\partial x} \right) \quad (4.1)$$

$$C(x, t) = C_0 \quad \text{when } t = 0 \quad (4.2)$$

$$\frac{\partial C}{\partial t} = 0 \quad \text{while } t > 0 \text{ and } x = 0 \quad (4.3)$$

$$C = C_s \quad \text{while } t > 0 \text{ and } x = \pm L/2 \quad (4.4)$$

where C_0 represents the initial drug concentration (assumed to be uniform) in the homogenous hydrogel, x represents the distance from the center of the sample to the surface, C_s represents the surface concentration, D is the diffusion coefficient independent of position and concentration, t is time, and L is the thickness of the gel.

The solution of the PDE is given by [172]

$$\frac{C - C_0}{C_s - C_0} = 1 - \frac{4}{\pi} \sum_{n=0}^{\infty} \frac{(-1)^n}{2n+1} e^{-\frac{(2n+1)^2 \pi^2 D t}{4L^2}} \cos \frac{(2n+1)\pi x}{2L} \quad (4.5)$$

If M_t is the total cumulative mass of therapeutic released at time t and M_∞ represents the total cumulative mass of therapeutic at infinite time, M_t / M_∞ represents the fractional release of therapeutic with respect to the value at infinite time,

$$\frac{M_t}{M_\infty} = 1 - \sum_{n=0}^{\infty} \frac{8}{(2n+1)^2 \pi^2} e^{-\frac{(2n+1)^2 \pi^2 D t}{4L^2}} \quad (4.6)$$

The above expression is cumbersome to estimate a value of the diffusion coefficient, and hence, a solution is obtained in terms of error functions.

$$\frac{M_t}{M_\infty} = 4 \left[\frac{Dt}{L^2} \right]^{\frac{1}{2}} \left[\frac{1}{\pi^{1/2}} + 2 \sum_{n=1}^{\infty} (-1)^n \operatorname{ierfc} \left(\frac{nL}{2\sqrt{Dt}} \right) \right] \quad (4.7)$$

At short times ($M_t / M_\infty < 0.6$) the expression can be simplified to

$$\frac{M_t}{M_\infty} = 4 \left[\frac{Dt}{\pi L^2} \right]^{\frac{1}{2}} \quad (4.8)$$

An effective way to compare the release profiles of different hydrogels is to compare their fractional release profiles. Then, by plotting the fractional release of the template versus $(t^{0.5}/L)$, the diffusion coefficient can be calculated from the slope. It can also be measured how well the data matches a Fickian release by using the empirical Power Law equation:

$$\frac{M_t}{M_\infty} = kt^n \quad (4.9)$$

where the variables k and n are constants related to diffusion coefficients and the specific transport mechanism. The equation can be linearized by plotting the log of the fractional release versus the log of the time, where the slope corresponds to the diffusional exponent, n . For planar geometries an exponent value of 0.5 describes Fickian behavior, indicating diffusion controlled drug release, and a value of 1 indicates zero-order release or independent of concentration and time (case II transport); with $|n-1|$ corresponding to the order of release.

4.2 Structural Characterization of Imprinted Hydrogels

Hydrogels in solvent are subject to a number of thermodynamic influences. Factors such as the amount, size and flexibility of crosslinking monomer in the network, and the type of chemical groups that comprise the polymer chains, primarily affect the swelling and mesh structure of imprinted hydrogel structures. Typically, imprinted hydrogels containing more hydrophilic moieties tend to swell more than hydrogels containing hydrophobic groups, which will minimize their chain exposure to aqueous solvent. Higher crosslinked imprinted hydrogels have a tighter mesh structure and swell to a lesser extent than weakly crosslinked hydrogels. As

polymers solvate in water, their tendency to elongate is resisted by the chemical bonds that make up the polymer chain. Equilibrium swelling and rubber elasticity theories can help to characterize the structural parameters of imprinted hydrogel.

4.2.1 Equilibrium Swelling Theory

Flory-Rehner theory states that a crosslinked polymer gel in equilibrium is subject to two opposing forces, the thermodynamic force of mixing and the elastic, restrictive force of the polymer chains [173, 174]. At equilibrium, the total Gibbs free energy is zero and these two forces are equal.

$$\Delta G_{total} = \Delta G_{mixing} + \Delta G_{elastic} \quad (4.10)$$

Differentiating equation 4.10 with respect to the number of solvent molecules, while keeping the temperature and pressure constant, will yield an equivalent equation in terms of chemical potential. At equilibrium, the chemical potential of the solvent outside and inside the gel must be equal. The change in chemical potential due to elastic restrictive forces of the polymer chains can be determined from the theory of rubber elasticity [173], and the change in chemical potential due to mixing can be expressed using the heat and entropy of mixing. Essentially, this measures the interaction and compatibility of the polymer chains with the solvent molecules. By equating these two contributions, an expression can be written for the determination of the molecular weight between two adjacent crosslinks of a neutral, non-ionized, imprinted polymer gel prepared without solvent,

$$\frac{1}{M_c} = \frac{2}{M_n} - \frac{\left(\bar{v}/V_1\right) \left[\ln(1 - \nu_{2,s}) + \nu_{2,s} + \chi_1 \nu_{2,s}^2 \right]}{\nu_{2,s}^{1/3} - \left(\frac{\nu_{2,s}}{2}\right)} \quad (4.11)$$

where \overline{M}_c is the average molecular weight between crosslinks, \overline{M}_n is the average molecular weight of the polymer chains prepared under identical conditions in the absence of crosslinking agent, V_1 is the molar volume of solvent (e.g., V_1 for water is 18.1 cm³/mol), \overline{v} is the specific volume of the polymer (i.e., the reciprocal of density), χ_1 is the Flory polymer-solvent interaction parameter, and $v_{2,s}$ is the polymer volume fraction in the swollen state.

The polymer volume fraction in the swollen state is related to the volume swelling ratio, Q , which can be calculated from equilibrium swelling experiments as follows:

$$Q = \frac{1}{v_{2,s}} = \frac{V_{2,s}}{V_{2,d}} \quad (4.12)$$

where $V_{2,s}$ is the swollen gel volume at equilibrium, and $V_{2,d}$ is the volume of the dry polymer. The volume of the polymer in the swollen or dry state can be obtained as the reciprocal of the density by using Archimedes buoyancy principle [100].

$$\rho_x = \frac{W_a \times \rho_h}{W_a - W_h} \quad (4.13)$$

where, ρ_x is the density of the sample, W_a is the mass of the sample in air, ρ_h is the density of heptane (0.684 g/mL at a temperature of 25°C), and W_h is the weight of the sample in heptane.

If the imprinted network is prepared in the presence of solvent, the Peppas and Merrill equation must be used [100]. It is a modification of the Flory-Rehner theory to include the presence of solvent, which modifies the chemical potential due to elastic forces.

$$\frac{1}{\overline{M}_c} = \frac{2}{\overline{M}_n} - \frac{(\overline{v}/V_1) [\ln(1 - v_{2,s}) + v_{2,s} + \chi_1 v_{2,s}^2]}{v_{2,s} \left[\left(\frac{v_{2,s}}{v_{2,r}} \right)^{1/3} - \frac{1}{2} \left(\frac{v_{2,s}}{v_{2,r}} \right) \right]} \quad (4.14)$$

where $v_{2,r}$ represents the polymer volume fraction in the relaxed state, which is defined as a physical property of the polymer immediately after crosslinking before swelling or collapse of the network.

If the imprinted network contains a number of ionic moieties, an ionic contribution is added to the expression of chemical potential. We direct the reader to the following references [175, 176] for the derivation of the equations for both anionic and cationic gels prepared in the presence of solvent.

4.2.2 Rubber Elasticity Theory

Polymers demonstrate elastomeric behavior so when a constant stress is applied to a hydrogel, it will undergo a change in shape and reach an equilibrium strain. The average molecular weight between crosslinks, \overline{M}_c of imprinted polymer gels can be determined from the theory of rubber elasticity [173, 174]. For an isotropic, swollen, imprinted polymer gel synthesized with no solvent, with a constant deformation volume, equation 4.15 is valid for short elongation ratios of up to 2:

$$\tau = RT \left(\frac{v_{2,s}^{1/3}}{vM_c} \right) \left(1 - \frac{2\overline{M}_c}{M_n} \right) \left(\alpha - \frac{1}{\alpha^2} \right) \quad (4.15)$$

where R is the universal gas constant, T is the absolute temperature, τ is the stress, and α is the deformation of a network structure by elongation which is equivalent to the stretched length over initial length ($\alpha = L/L_0$).

If $\overline{M}_c \ll \overline{M}_n$, $\left(1 - \frac{2\overline{M}_c}{M_n} \right) \rightarrow 1$, and equation 4.15 becomes,

$$\tau = RT \left(\frac{\nu_{2,s}^{1/3}}{\nu \overline{M}_c} \right) \left(\alpha - \frac{1}{\alpha^2} \right) \quad (4.16)$$

Sillman, Peppas and Merrill [100] deduced a relationship for hydrogels prepared in the presence of solvent,

$$\tau = RT \left(\frac{1}{\nu \overline{M}_c} \right) \left(1 - \frac{2\overline{M}_c}{M_n} \right) \left(\alpha - \frac{1}{\alpha^2} \right) \left(\frac{\nu_{2,s}}{\nu_{2,r}} \right)^{1/3} \quad (4.17)$$

where $(\nu_{2,s}/\nu_{2,r})$ is the ratio of the fractions of the swollen and relaxed state.

Stress-strain data is typically obtained by performing tensile studies on a dynamic mechanical analyzer. Strain values are converted into the elongation function $(\alpha - 1/\alpha^2)$ and the slope can be used to calculate \overline{M}_c .

The \overline{M}_c can now be used to calculate the correlation length (ξ) between two adjacent crosslinks in a swollen hydrogel (i.e., mesh size or pore size),

$$\xi = Q^{1/3} \left(\frac{2C_n \overline{M}_c}{M_r} \right)^{1/2} l \quad (4.18)$$

where C_n is the rigidity factor of Flory characteristic ratio, l is the length of the bond along the polymer backbone (which is equal to 1.54 Å for vinyl polymers, i.e., carbon-carbon bond), and M_r is the molecular weight of repeating units from which the polymer chain is composed. For heteropolymers, this can be a weighted average of the monomers that make up the polymer chains assuming equal reactivity.

4.3 Determination of Template Binding Parameters

Imprinting effectiveness can be determined by assessment of the binding parameters, such as template binding affinity, capacity of loading and selectivity. Proper template washing procedures and verification of template removal is very important in the analysis of binding parameters. Binding characterization can be incorrect if post-polymerization washing of template is not completed.

Binding affinity is a measure of how well the template molecule is attracted to the macromolecular binding site or how well a ligand is hold to the receptor site formed between the macromolecule chains. The equilibrium dissociation constant, K_d , or equilibrium association constant, K_a , provide a quantitative measure of this level of attraction. Ligands with low K_d or high K_a values bind tightly to the receptor and have high affinity. Conversely, high K_d and low K_a values are indicative of weak template binding. The loading capacity, Q , is the maximum ligand bound per mass or volume of polymer, and the selectivity, α , is the ability to differentiate between the ligand and other molecules.

Template affinity and loading capacity can be estimated from equilibrium binding isotherms analyzing template bound versus the equilibrium concentration of template in the solution. It is common knowledge that imprinting leads to a distribution of binding sites of varying affinity. The distribution has been demonstrated in a number of systems to be bi-modal, but affinity distribution models have been successfully applied [177, 178] and better approximate the heterogeneity of binding cavities within imprinted networks. Analysis has been conducted in a number of ways using theoretical or empirical based binding isotherms. Care must be taken when applying the best isotherm based on the fit of the data but also on the inherent assumptions in the underlying equations, especially if a theoretical is used.

Imprinted networks have been analyzed via limiting slope Scatchard analysis [179], Langmuir isotherms [120, 180-182], Freundlich isotherms [181-183], bi-[184, 185] and tri-[186] Langmuir isotherms, and Langmuir-Freundlich isotherms [185, 187-189]. More recently, isothermal titration calorimetry has thermodynamically verified differences in the binding enthalpy of template within imprinted and non-imprinted gels [190]. The reader is directed to the following review which classifies typical dissociation constants of molecularly imprinted polymers and those of common classes of receptor-ligand interactions [158].

Equilibrium binding studies will be carried out keeping clean hydrogels immersed in varying concentrations of drug solution until equilibrium is reached. The resulting binding curves will be then compared with an appropriate binding isotherm which best fits the system to calculate the binding parameters (binding affinity and capacity) for the hydrogels. Once the equilibrium concentration of the solution is determined, a mass balance yields the bound concentration.

The Scatchard equation is represented by the following equation:

$$\frac{Q}{C_e} = -K_a Q + Q_{\max} \quad (4.19)$$

where Q is the bound amount of template, C_e is the equilibrium concentration of template in the solution, the template equilibrium binding affinity is represented by K_a , and Q_{\max} is the maximum template loading capacity. The affinity and the maximum template loading capacity are calculated via linear regression of the data.

The Langmuir isotherm is represented by the following equation:

$$Q = \frac{K_a C_e Q_{\max}}{1 + K_a C_e} \quad (4.20)$$

Linear regression of the Langmuir equation is used to find the binding affinity and capacity. The Langmuir isotherm assumes that there is uniform one-layer adsorption of the template molecule, equilibrium conditions, and that the surface is homogeneous.

The Freundlich isotherm is an empirical equation that can have multiplicity of sites on a surface and can be applied to heterogeneous surfaces. However, it just demonstrates excellent fit to adsorption isotherm data in the low concentration region (nM-mM) [187], therefore, it is unable to model saturation behavior and diverges from experimental isotherms in high concentration regions. The Freundlich isotherm is shown in equation 4.21.

$$Q = k_f C_e^n \quad (4.21)$$

where additional parameters not defined previously are the Freundlich equilibrium template binding affinity constant, k_f , and the heterogeneity index, n . The Freundlich affinity constant and the heterogeneity index are found from a linear regression of this equation.

The Langmuir-Freundlich (LF) isotherm is a versatile isotherm expression that can simulate both Langmuir and Freundlich behaviors. It provides heterogeneity information and is capable to model adsorption behavior over the entire concentration region up to saturation. The LF isotherm is shown in equation 4.22

$$Q = \frac{Q_{\max} (K_a C_e)^n}{1 + (K_a C_e)^n} \quad (4.22)$$

The heterogeneity index, n , varies from 0 to 1. For homogeneous materials, n is equal to 1, whereas is less than 1 for heterogeneous materials. Mathematically, when $n=1$ the LF isotherm reduces to the Langmuir isotherm (Equation 4.20) and, on the other hand, as either K_a or C_e approaches 0, the LF isotherm reduces to the Freundlich isotherm (Equation 4.21)

Chapter 5

Effect of Crosslinker Diversity on Drug Loading, and Drug Release from Molecularly Imprinted Hydrogels

Molecular imprinting techniques comprise the creation of macromolecular memory for a template molecule within a polymer network. Molecular imprinting involves polymerization in the presence of the template, which directs the growth and formation of the polymer structure. Effective self-assembly of the functional monomer(s)-template complex is crucial towards imprinting efficacy. Decreased flexibility in imprinted polymers is assumed to favor binding as it helps maintain the shape of the binding cavity. This is especially true for non-covalently imprinted polymers where the primary interaction between the template and the polymer chains is via hydrogen bonding. Variations in the network structure itself have been demonstrated to influence template binding and control the size of the imprinted cavities [164, 191-193]. For example, maximizing crosslinker content has been shown to improve selectivity of molecular imprinted polymers (MIPs) [194]. However, little work has been done when the primary interaction is ionic. Therefore, the aim of this research was to study how structural changes within imprinted hydrogels affect the stability of the memory site when the primary interaction between the template and the hydrogel chains is ionic.

Hydrogels are flexible polymer networks at temperatures above their glass transition, where the amorphous portions are in the rubbery state. Thus, they can be deformed and respond as an elastic body. Crosslinks (known as tie-points or junctions) are primarily responsible for

preventing the dissolution of the hydrogels in solvent [100, 101], and they can be covalent bonds, permanent physical entanglements, non-covalent interactions, or microcrystalline regions incorporating various chains. For hydrogels with covalent crosslinks, the number of double bonds, the crosslinker length (i.e., linear size), and the crosslinker concentration (i.e., the percentage of crosslinking monomer reacted in network) influence imprinting effectiveness. When a dry hydrogel is immersed in a thermodynamically compatible solvent, the movement of the solvent into the hydrogel polymer chains leads to considerable volume expansion and macromolecular rearrangements, depending on the nature and extent of crosslinking within the network. The expansion of polymer chains increases the free volume available for template transport, but it can decrease the effectiveness of the imprinting site created by multiple polymer chains. Equilibrium is reached when the swelling force is counterbalanced by the retractive force due to crosslinking points in the network structure. Typically, higher crosslinked imprinted hydrogels have a tighter mesh structure and swell to a lesser extent than weakly crosslinked hydrogels. There have been many excellent reviews characterizing hydrogel structures [100, 101].

In this chapter, imprinted poly(hydroxyethyl methacrylate-co-diethylaminoethyl methacrylate-co-poly(ethyleneglycol)-n-dimethacrylate) (poly(HEMA-co-DEAEM-co-PEGnDMA)) hydrogels with varying crosslinking monomer lengths and concentrations were synthesized and characterized. A molecular imprinting strategy was employed for the choice of functional monomers, exploiting predominantly ionic non-covalent interactions [170]. The concentration and length of the crosslinking monomer are important factors in determining the strength and the flexibility of the resultant network as well as the stability of the binding cavity formed by the imprinting process. Therefore, the effects of altering the chain building blocks on

the imprinting effectiveness of poly(HEMA-co-DEAEM-co-PEGnDMA)) hydrogels, as well as, template loading and transport were also studied.

5.1 Creating Memory in Hydrophilic Hydrogels via Imprinting Techniques

The template (drug molecule) selected was diclofenac sodium (DS), a non-steroidal anti-inflammatory drug (NSAID), which is a small molecule with a hydrodynamic radius in water of $\sim 4.3 \text{ \AA}$. In the human body, diclofenac sodium acts on the enzyme cyclooxygenase-2 (COX-2) to inhibit the production of prostaglandins, unsaturated carboxylic acids that have a variety of physiological effects, including the inflammatory response. The carboxylate of diclofenac forms two strong hydrogen bonds to the side chains of Tyr-385 and Ser-530 at the apex of the cyclooxygenase active site. In addition, the inhibitor forms extensive van der Waals interactions with several hydrophobic protein residues within the active site [195]. Tyrosine contains a 4-hydroxy-phenyl group which features aromatic behavior with some hydrogen bonding capabilities and serine contains a hydroxyl group for hydrogen bonding. At physiological pH (7.4), diclofenac sodium is dissociated to more than 99% (negatively charged) ($pK_a \sim 4$) [196]. However, its distribution coefficient in n-octanol/aqueous buffer ($\log D_{7.4}$) is 1.1 [197], and its chemical structure (two chloride phenyl rings) suggest a hydrophobic nature of the molecule. The X-ray analysis of diclofenac shows an intramolecular hydrogen bond between the carboxyl oxygen and the amino hydrogen [198, 199].

By applying the principles of molecular imprinting and examining these amino acid residues and the non-covalent interactions between the template and the active site, such as, H-bonding (H-bond donors and acceptors) and ionic interactions, monomers with similar chemical functionalities were chosen to mimic the natural receptor sites. Acrylate and methacrylate

monomers capable of similar non-covalent interactions and similar functional groups as those of tyrosine and serine were sought. Monomers with similar chemical groups are diethylaminoethyl methacrylate (DEAEM) and 2-hydroxyethylmethacrylate (HEMA). The hydroxyl group of HEMA can be seen as an analog for that of serine with hydrogen-binding capability. Diethylaminoethyl methacrylate, DEAEM, is a cationic acrylate with a pKa of 9.5 and at physiological pH is expected to form an ionic non-covalent bond with diclofenac sodium.

5.2 Materials and Methods

5.2.1 Materials and Reagents

Diethylaminoethyl methacrylate (DEAEM), 2-hydroxyethylmethacrylate (HEMA), ethylene glycol dimethacrylate (EGDMA) and azobisisobutyronitrile (AIBN) were purchased from Sigma-Aldrich (Milwaukee, WI). Diclofenac sodium salt (DS) was purchased from Sigma-Aldrich (Saint Louis, MO). Polyethylene glycol (200) dimethacrylate (PEG200DMA), and polyethylene glycol (600) dimethacrylate (PEG600DMA) were purchased from Polysciences, Inc (Warrington, PA). EGDMA, DEAEM and HEMA, had inhibitors removed via inhibitor removal packing sieves (Sigma-Aldrich, Milwaukee, WI) prior to polymerization. The rest of the chemicals were used as received.

5.2.2 Synthesis of Molecularly Imprinted poly (HEMA-co-DEAEM-co-PEG_nDMA) Hydrogels

Crosslinking monomers were chosen with different chain length between the two vinyl ends (PEG_nDMA), to allow structural changes in the polymer network (e.g. mesh size). EGDMA has a single ethylene glycol unit between two vinyl groups. PEG200DMA and

PEG600DMA have an average of 4.5 and 13.5 ethylene glycol repeating units between the two vinyl groups, respectively.

Imprinted poly(HEMA-co-DEAEM-co-PEG_nDMA) hydrogels films were synthesized by varying the length and concentration of the crosslinking monomer. When the length was varied, hydrogels consisted of 90 mole% of the backbone monomer, HEMA, 5 mole% of the functional monomer, DEAEM, and 5 mole% of crosslinking monomer (PEG600DMA, PEG200DMA or EGDMA). Whereas, when the concentration of the crosslinker monomer was changed, hydrogels consisted of 5 mole% of the functional monomer, DEAEM, the concentration of the crosslinker monomer (PEG200DMA) was set to be 1 mole%, 5 mole% 10 mole% and 50 mole%, totaling to 100 mole% with the backbone monomer, HEMA. All the solutions were mixed with 0.472 mmol of diclofenac sodium (template drug) to attain a constant DEAEM to diclofenac mole (FM/T) ratio of 3.5 for all formulations.

The reaction solutions were vortexed and sonicated (15-20 min) until no phase separation occurred in the mixture. The solutions were transferred to an inert (nitrogen) atmosphere (MBraun Labmaster 130 1500/1000 Glovebox (Stratham, NH)) and left uncapped and open to the nitrogen atmosphere until the oxygen levels inside reached negligible levels (<1.0 ppm) (MBraun Oxygen Analyzer , MB-0X-SE-1). Thin films were prepared by pipetting the monomer solutions into glass plates (6" x 6") coated with trichloromethylsilane (to prevent strong adherence of the polymer matrix to the glass) and separated by 0.25 mm Teflon spacers. The free radical UV photopolymerization reaction was carried out for 8.5 minutes (separate differential photocalorimetry (DPC) studies revealed exact reaction times) with a light intensity of 40 mW/cm², measured using a radiometer (International Light IL1400A), at a constant temperature of 35°C. After polymerization, the glass plates were submerged into a DI water bath

(Millipore, 18.2 M Ω cm, pH 6.2); the thin film was peeled from the glass surface and cut into circular films of 13.5 mm diameter, using a size 10 cork borer. The films were washed with DI water until the template and unreacted monomers could no longer be detected by spectroscopic monitoring (Synergy Biotek UV–Vis Spectrophotometer, BioTek Instruments, Winooski, VT), and then dried at room temperature for 24 hours, followed by vacuum drying oven (28 in Hg, 32–34°C) until the disc weight change was less than 0.1wt%.

5.2.3 Equilibrium Swelling Studies and Mechanical Properties

Hydrogel structural analysis was obtained by swelling and tensile studies. The hydrogel films were subject to the analysis described in section 4.2.1. The mass of the dry hydrogels were weighted in air and heptane. After being weighted in the dry state, hydrogels were placed in DI water and allowed to swell to equilibrium. The experiment was repeated for swollen hydrogels. Once measurements were taken, Archimedes buoyancy principle [200] was used to calculate the density of the dry and swollen hydrogels as shown in equation 4.13. The specific volume of the hydrogel was calculated as the reciprocal of density. The volume swelling ratio (Q) and the polymer volume fraction in the swollen state ($v_{2,s}$) were calculated. Q is the ratio of the swollen to dry volumes of the hydrogel, $v_{2,s}$ is the inverse of the volume swelling, and $(1 - v_{2,s})$ gives the fractional water content of the hydrogel.

Stress–strain data were obtained by performing tensile studies with a RSA III Dynamic Mechanical Analyzer (DMA), (TA Instruments, New Castle, DE). A linear load stress at a constant rate of 4 mm/min was applied to hydrated imprinted hydrogels prepared in strips (8mm \times 30 mm \times 0.25mm, in triplicate). The average molecular weight between crosslinks ($\overline{M_c}$) was determined from the theory of rubber elasticity [173] (Section 4.2.2). The slope of the normal

stress applied, τ , versus the elongation term $(\alpha-1/\alpha^2)$, obtained from the tensile tests, is the Shear modulus and enables to calculate $\overline{M_c}$. Equation 4.16 was used to calculate $\overline{M_c}$, which accounts for swollen hydrogel synthesized in the absence of solvent [100]. The ideal gas constant used is $R= 8:314472 \text{ cm}^3\text{MPa}^{-1}\text{mol}^{-1}$, the temperature of experimental conditions is $T=295 \text{ K}$, and the specific polymer volume is $\overline{v}=0.909$.

From $\overline{M_c}$, the mesh size (ξ) can be determined using Equation 4.18 [100], where M_r is the effective molecular weight of the repeating unit (determined by a weighted average of the copolymer composition) and $l = 1.54 \text{ \AA}$. For poly(DEAEM-co-HEMA-co-PEGnDMA) hydrogels the typical average value of the characteristic ratio is, $C_n = 11$ [201-203].

5.2.4 Template Binding Experiments and Analysis of Binding Parameters

A variety of concentrations of diclofenac sodium in DI water (0.05, 0.10, 0.15, 0.20, and 0.25 mg/mL) were prepared. Initial absorbance of each concentration was measured using a Synergy UV–Vis spectrophotometer at 276 nm, the wavelength of maximum absorption. After the initial absorbance was taken, a dry, washed poly(DEAEM-co-HEMA-co-PEGnDMA) polymer disk was inserted into 5 mL of solution placed in a vial, and the vials were gently agitated on an ocelot rotator (Fisher Scientific; Chicago, IL) at 75 rpm and 12° tilt angle. Separate experiments were conducted to assure equilibrium was reached. After equilibrium was reached over an 11-day period, the solutions were vortex for 10 seconds; the bound concentration in the gel was determined by mass balance. All gels were analyzed in triplicate, and all binding values are based upon the dry weight of the gel. The Langmuir-Freundlich isotherm (Equation 4.22) was used to determine binding parameters, such as template binding capacity (Q_{max}) and template binding affinity (K_a), because gave the best fit to the experimental.

5.2.5 Dynamic Template Release Studies and Diffusion Coefficient Determination

Imprinted poly(DEAEM-co-HEMA-co-PEGnDMA) hydrogels, loaded with diclofenac sodium at a concentration of 0.25 mg/mL, were placed in 30 mL of DI water or artificial lacrimal fluid (6.78 g/L NaCl, 2.18 g/L NaHCO₃, 1.38 g/L KCl, 0.084 g/L CaCl₂·2 H₂O, pH 8), which was continuously agitated on an ocelot rotator (Fisher Scientific; Chicago, IL) at 75 rpm and 12° tilt angle at 25°C. After measured time intervals, the lenses were extracted and deposited into fresh release media to maintain infinite sink conditions. The absorbance of the solution was measured using a Synergy UV–Vis spectrophotometer at 276 nm. Fractional drug release (M_t/M_∞) profiles were calculated for all the hydrogels by taking the amount of template released at specific times, M_t , divided by the amount of diclofenac released during the experiment, M_∞ . Template diffusion coefficients were calculated using Fick's law, which describes one-dimensional planar solute release from gels [172] (Section 4.1). In all the films studied in this work, the diameter (length) over thickness was much greater than 10; therefore, slab geometry was considered for the analysis. Equation 4.8 gives the solution of Fick's law for short times of diffusion.

5.3 Results and Discussion

5.3.1 Structural Analysis for Imprinted Poly(HEMA-co-DEAEM-co-PEGnDMA)

In order to verify that a structural change was achieved, swelling studies and mechanical analysis were performed to obtain information about the network structure. The volume swelling ratio and the polymer volume fraction in the swollen state were calculated for all imprinted poly(HEMA-co-DEAEM-co-PEGnDMA) hydrogels and are summarized in Table 5.1.

Table 5.1: Equilibrium swelling parameters of imprinted poly (HEMA-co-DEAEM-co-PEGnDMA)

Crosslinker monomer	q (Equilibrium weight swelling ratio)	Q (Equilibrium volume swelling ratio)	$v_{2,s}$ (Equilibrium polymer volume fraction in the swollen state)
EGDMA	1.142±0.024	1.266±0.110	0.794±0.024
PEG200DMA	1.423±0.026	1.566±0.062	0.639±0.012
PEG600DMA	1.734±0.011	1.906±0.009	0.525±0.002

The data are presented as mean ± SD (n=3).

The results showed that as the crosslinking length is increased, the equilibrium swelling ratio increased, suggesting that different macromolecular architectures are available for free volume transport. The expansion of polymer chains increases the free volume available for template transport, but it can decrease the effectiveness of the imprinting site created by multiple polymer chains. Equilibrium is reached when the swelling force is counterbalanced by the retractive force due to crosslinking points in the network structure.

Structural parameters were obtained and summarized in Table 5.2.

Table 5.2: Structural parameters of imprinted poly(HEMA-co-DEAEM-co-PEGnDMA)

Crosslinker monomer	Young's Modulus (MPa)	Shear Modulus (MPa)	Mc (g/mol)	Mesh Size (Å)
EGDMA	5.74±0.86	2.01±0.31	1210.3±245.4	21.88±0.89
PEG200DMA	3.61±0.22	1.30±0.05	1806.7±149.0	29.52±0.63
PEG600DMA	3.08±0.23	1.05±0.04	2164.6±151.1	32.43±0.38

The curves obtained to calculate the modulus and Mc had excellent correlation coefficients (>0.99). The data are presented as mean ± SD (n=3).

As expected from the equilibrium polymer volume fraction values (Table 5.1), hydrogels prepared with EGDMA showed the highest modulus, confirming that imprinted poly(HEMA-co-DEAEM-co-EGDMA) hydrogels had the most rigid structure, hence, the smallest mesh size (21.88±0.89 Å) with the tightest network. Similar mesh size values were obtained for hydrogels prepared with PEG200DMA and PEG600DMA (29.52±0.63 Å and 32.43±0.38 Å, respectively).

Variations in network structure itself have been demonstrated to influence template binding and control the size of the imprinted cavities [164, 191-193]. The hydrodynamic radius of diclofenac sodium is 4.3 Å, making it amenable to imprint via multiple polymer chains and diffusion through the network.

5.3.2 Diclofenac Sodium Loading Studies for Imprinted poly(HEMA-co-DEAEM-co-PEGnDMA)

Diclofenac sodium equilibrium binding isotherms for imprinted poly(HEMA-co-DEAEM-co-PEGnDMA) hydrogels prepared varying the crosslinker ethylene glycol content with EGDMA, PEG200DMA, and PEG600DMA at a fixed 5% molar concentration, are presented in Figure 5.2. Imprinted hydrogels prepared with PEG200DMA exhibited the highest loading over the rest of the crosslinking monomers. Imprinted poly(HEMA-co-DEAEM-co-PEG200DMA) showed a 70% and 22% increase in maximum loading over imprinted poly(HEMA-co-DEAEM-co-EGDMA) and imprinted poly(DEAEM-co-HEMA-co-PEG600DMA), respectively, when placed in a 0.25mg/mL diclofenac solution. Furthermore, the results show that the amount of drug bound can be tuned by altering the concentration of the binding solutions.

The template binding capacity and affinity for all hydrogels were calculated and summarized in Table 5.3. Hydrogels prepared with PEG200DMA as crosslinker demonstrated, by far, the highest template binding capacity ($Q_{\max}=6.25\pm0.06 \times 10^{-2}$ mmol/g) when compared with the corresponding hydrogels prepared with EGDMA and PEG600DMA as crosslinkers ($Q_{\max}=3.39\pm0.03 \times 10^{-2}$ mmol/g, and $4.51\pm0.06 \times 10^{-2}$ mmol/g, respectively). On the other hand, the template binding affinity, K_a , increases as the crosslinking monomer length is reduced (Table 5.3).

Table 5.3: Binding capacities and affinities, and diffusion coefficients for imprinted poly(HEMA-co-DEAEM-co-PEGnDMA)

Crosslinker monomer	K_a (mM⁻¹)	Q_{max} (×10² mmol/g)	Diffusion Coefficient (×10¹¹ cm²/s)
EGDMA	16.77±0.43	3.39±0.03	7.97±0.09
PEG200DMA	15.74±0.12	6.25±0.06	7.96±0.22
PEG600DMA	14.63±0.35	4.23±0.06	15.14±0.16

The data are presented as mean ± SD (n=3).

While, imprinted poly (HEMA-co-DEAEM-co-EGDMA) hydrogels (the most rigid structure) achieved the highest template binding affinity, these hydrogels had the lowest template binding capacity. However, with a slight increase in flexibility (hydrogels prepared with PEG200DMA) a better binding capacity can be achieved without losing a considerable amount in the binding affinity. Nonetheless, if the length of the crosslinker is further increased (hydrogels prepared with PEG600DMA), both the binding capacity and affinity are adversely affected.

Conventionally, decreased flexibility in imprinted polymers was assumed to favor binding as it helped maintain the shape of the binding cavity. This is especially true for non-covalently imprinted polymers where the primary interaction between the template and the polymer chains is via hydrogen bonding. However, when the primary interaction is ionic, such as the diclofenac ion and the charged ammonium group contributed by DEAEM, the results showed that not just rigidity (supposedly better preservation of the binding cavity) but certain amount of flexibility of the binding site is required to better imprint diclofenac sodium, a charged molecule. The results showed that PEG200DMA might be an ideal crosslinker that may produce a final network that it is more ideal in terms of the mesh size, flexibility and orientation of the polymer chains, maximizing both the binding capacity and affinity, delaying the release rate. Therefore, a certain amount of flexibility of the polymer chains during polymerization may allow greater

freedom to continue to interact with the template throughout the polymerization reaction which may result in the formation of more binding sites. An increase in the number of binding sites in the polymer network increases the probability and amount of temporary binding events between the template and the polymer chains, as proposed in the tumbling hypothesis [121], slowing the elution of template out of the hydrogel.

5.3.3 Dynamic Release Studies for Imprinted poly(HEMA-co-DEAEM-co-PEGnDMA)

Release studies in DI water were conducted with the solvent replacement method to achieve infinite sink conditions in order to sustain the greatest driving force. Fractional mass release studies for diclofenac sodium imprinted poly(HEMA-co-DEAEM-co-PEGnDMA) hydrogels are shown in Figure 5.3. As the crosslinking monomer length is decreased, a slower fractional release of the template was observed. For example, polymers prepared with EGDMA in the pre-polymerization solution released 60% of the loaded template in approximately 152 hours, while the hydrogels prepared with PEG200DMA, and PEG600DMA released 60% of loaded template in approximately 128 hours and 84 hours, respectively.

Within a Fickian diffusion process, the fractional mass released depends linearly on $t^{0.5}/L$ at short times or fractional release less than 0.6 with a slope directly proportional to the diffusion coefficient. There was no statistical difference in the diffusion coefficient of imprinted poly(HEMA-co-DEAEM-co-EGDMA) and poly(HEMA-co-DEAEM-co-PEG200DMA) hydrogels (Table 5.3). Hydrogels synthesized with PEG600DMA showed the fastest diclofenac sodium transport; thus, the higher diffusion coefficient. The imprinted poly(HEMA-co-DEAEM-co-PEG600DMA) hydrogels exhibited a diclofenac sodium diffusion coefficient in DI water of $15.14 \pm 0.16 \text{ cm}^2/\text{s}$, that is 1.9 times faster than the diffusion coefficient of hydrogels synthesized

with PEG200DMA and EGDMA (Table 5.3). The slightly slower diclofenac sodium transport through hydrogels prepared with EGDMA (Figure 5.3) may be due to their smaller mesh sizes ($21.88 \pm 0.89 \text{ \AA}$) compare to the mesh sizes of hydrogels prepared with PEG200DMA ($29.52 \pm 0.63 \text{ \AA}$). However, the difference in diclofenac sodium transport through hydrogels prepared with PEG200DMA and PEG600DMA might be related to two circumstances – the higher binding capacity and affinity of hydrogels prepared with PEG200DMA, and the slightly difference in their mesh sizes (Table 5.2).

5.3.4 Imprinted poly(HEMA-co-DEAEM-co-PEG200DMA)

It was found that imprinted poly(HEMA-co-DEAEM-co-PEG200DMA) hydrogels with 5 mole% of crosslinking monomer had an optimal conformation of the macromolecular memory sites, which provided the most favorable binding to the drug, therefore, delaying the diclofenac sodium transport through the hydrogels, resulting in similar diffusion coefficients in DI water, than imprinted hydrogels with smaller mesh size (i.e., hydrogels prepared with 5% EGDMA) (Figure 5.4). Thus, in further studies, the mesh size was altered by changing the molar ratio of PEG200DMA to 1%, 5%, 10% and 50% of the total monomer concentration.

In order to verify structural changes among the hydrogels prepared with different molar ratios of PEG200DMA, swelling studies and mechanical analysis were performed to obtain information about the network structure. Equilibrium swelling parameters were calculated for all imprinted hydrogels and are summarized in Table 5.4. It was observed that increasing the crosslinking content generally resulted in hydrogels with lower equilibrium swelling ratios. As the equilibrium volume swelling ratio is the reciprocal of the polymer volume fraction in the swollen state, the polymer volume fraction increased as the crosslinking content was increased.

The presence of crosslinking points has been demonstrated to constrict the ability of a hydrogel to solvate in a favorable solvent resulting in lower equilibrium swelling ratios. Since water is a favorable solvent for the imprinted poly(HEMA-co-DEAEM-co-PEG200DMA) hydrogels, these results are consistent with other reported results [121].

Table 5.4: Equilibrium swelling parameters of imprinted poly(HEMA-co-DEAEM-co-PEG200DMA)

molar% of PEG200DMA	q (Equilibrium weight swelling ratio)	Q (Equilibrium volume swelling ratio)	$v_{2,s}$ (Equilibrium polymer volume fraction in the swollen state)
1%	1.988±0.017	2.138±0.048	0.468±0.017
5%	1.423±0.026	1.566±0.062	0.639±0.012
10%	1.258±0.035	1.495±0.114	0.672±0.054
50%	1.029±0.018	1.037±0.022	0.964±0.020

The data are presented as mean ± SD (n=3).

Structural parameters for imprinted poly(HEMA-co-DEAEM-co-PEG200DMA) hydrogels were obtained and are summarized in Table 5.5.

Table 5.5: Structural parameters of imprinted poly(HEMA-co-DEAEM-co-PEG200DMA)

molar% of PEG200DMA	Young's Modulus (MPa)	Shear Modulus (MPa)	Mc (g/mol)	Mesh Size (Å)
1%	1.48±0.03	0.53±0.02	3980.8±179.2	48.88±1.10
5%	3.61±0.22	1.30±0.05	1806.7±149.0	29.52±0.63
10%	4.61±0.21	1.68±0.12	1398.9±115.3	24.73±1.01
50%	5.70±0.23	1.96±0.07	1275.2±170.3	16.67±1.12

The curves obtained to calculate the modulus and Mc had excellent correlation coefficients (>0.99). The data are presented as mean ± SD (n=3).

As expected from the equilibrium polymer volume fraction values (Table 5.4), as the content of the crosslinker monomer was increased the Young and Shear modulus increased, hence, the mesh size decreased. Polymers prepared with 1% PEG200DMA in pre-polymerization

solution exhibited a mesh size of $48.88 \pm 1.10 \text{ \AA}$, while the corresponding polymers with 50% PEG200DMA exhibited a mesh size of $16.67 \pm 1.12 \text{ \AA}$

Equilibrium binding isotherms for imprinted hydrogels with varying amounts of PEG200DMA, ranging from 1% to 50% of the total monomer content, are shown in Figure 5.5, and the binding capacity (Q_{\max}) and binding affinity (K_a) for all hydrogels were calculated using the Langmuir-Freundlich isotherm and are listed in Table 5.6.

Table 5.6: Binding capacities, affinities and diffusion coefficients for diclofenac sodium in imprinted poly(HEMA-co-DEAEM-co-PEG200DMA)

molar% of PEG200DMA	K_a (mM^{-1})	Q_{\max} ($\times 10^2 \text{ mmol/g}$)	Diffusion Coefficient ($\times 10^{11} \text{ cm}^2/\text{s}$)
1%	15.17 \pm 0.25	6.76 \pm 0.04	12.70 \pm 0.10
5%	15.74 \pm 0.15	6.25 \pm 0.06	7.96 \pm 0.22
10%	14.95 \pm 0.23	4.33 \pm 0.02	8.27 \pm 0.11
50%	11.93 \pm 0.19	0.94 \pm 0.03	7.09 \pm 0.04

The data are presented as mean \pm SD (n=3).

For imprinted hydrogels prepared with 1% and 5% of PEG200DMA, there were no statistically significant differences on either the template binding capacity or the binding affinity of the hydrogels. However, as the amount of crosslinking was increased, the template binding capacity decreased. Hydrogels prepared with 50% PEG200DMA in the pre-polymerization solution demonstrated a binding capacity of $0.94 \pm 0.03 \times 10^{-2} \text{ mmol/g}$ which was a factor of 6.7 lower than the binding capacity of hydrogels prepared with 5% PEG200DMA ($Q_{\max} = 6.25 \pm 0.06 \times 10^{-2} \text{ mmol/g}$). The template binding affinity showed a smaller 32% decrease. This makes sense for capacity if one considers that an increase in crosslinker content means less backbone monomer is added to the formulation at a fixed template to functional monomer ratio, thus less binding sites are formed. The binding affinity decreased as crosslinking is increased, which is counterintuitive, as less mobility in the polymer network is expected to lead to more stable

binding sites. Therefore, when the primary non-covalent interaction is ionic, the preservation of the binding cavity is less vital, and certain amount of mobility/flexibility in the polymer network is needed. In addition, as the percentage of crosslinking content is increased, gel formation begins early and may result in the loss of available binding sites.

Figure 5.6 shows the fractional mass released in DI water from imprinted poly(HEMA-co-DEAEM-PEG200DMA) hydrogels with varying amounts of crosslinker (1%, 5%, 10%, 50%) in the pre-polymerization solution. Increasing the crosslinking monomer content resulted in a delayed release of the template. Nonetheless, similar release profiles were observed for hydrogels prepared with 5% and 10% of PEG200DMA. Hydrogels with 1% PEG200DMA released 60% of the loaded template in approximately 96 hours while the polymers with 5%, 10% and 50% PEG200DMA released 60% of loaded template in approximately 128 hours, 152 hours, and 168 hours, respectively. Imprinted hydrogels prepared with 1% PEG200DMA, showed the fastest diclofenac sodium transport in DI water; thus, the higher diffusion coefficient ($D=12.70\pm 0.10 \times 10^{-11} \text{ cm}^2/\text{s}$), which was 1.60, 1.55 and 1.80 times faster than the diffusion coefficient of hydrogels synthesized with 5%, 10% and 50% PEG200DMA, respectively (Table 5.6).

The slower template transport through the high crosslinked hydrogels can be attributed to the decrease in the mesh size of the hydrogel network and a decrease in the free volume available for transport as the number of crosslinking points is increased. Polymers prepared with 50% PEG200DMA in pre-polymerization solution exhibited a 2.9, 2.0 and 1.7, times smaller mesh size than the corresponding polymers with 1%, 5% and 10% of PEG200DMA, respectively. The observed increase in polymer volume fraction (Table 5.4) as the amount of crosslinking was

increased supports the decrease in diffusion coefficients for template transport through the hydrogels.

Findings revealed that 5 mole% of PEG200DMA might be the ideal concentration of the crosslinking monomer, which might produce a final network that it is more ideal in terms of the flexibility and orientation of polymer chains that produce the template binding site. The results showed similar diffusion coefficients in DI water, than imprinted hydrogels with smaller mesh sizes (i.e., hydrogels prepared with 10% PEG200DMA and 50% PEG200DMA), but maximizing the binding parameters (Figure 5.7).

5.3.5 Assessment of the Molecular Imprinting Technique and Release Studies in Lacrimal Solution.

The creation of macromolecular memory sites and their enhanced template loading and transport were examined via equilibrium binding studies, mechanical analysis, and release studies. For these studies, imprinted and non-imprinted (control) poly(HEMA-co-DEAEM-co-PEG200DMA) thin films were prepared with 5 mole% PEG200DMA in the pre-polymerization solution. Non-imprinted films were prepared in exactly the same manner than the imprinted hydrogels, except that the template molecule, diclofenac sodium, was not included in the pre-polymerization formulation.

Diclofenac sodium equilibrium binding results for weakly crosslinked poly(HEMA-co-DEAEM-co-PEG200DMA) imprinted and control (non-imprinted) hydrogels with 5% molar ratio of crosslinking monomer to total monomer concentration are presented in Figure 5.8. It is clear that the imprinted network exhibited increased loading over the control network. The imprinted hydrogels showed a 50% increase in maximum loading over the control hydrogels, when placed in a 0.25mg/mL diclofenac solution. As stated before, the amount of template

bound can be tailored by altering the concentration of the binding solutions, thus loading can be tuned by the concentration of the original drug solution.

The calculation of binding parameters (Table 5.7) revealed an increase in both the number of binding sites (Q_{\max}) and binding affinity (K_a) in imprinted hydrogels over the corresponding control hydrogels, indicating the successful creation of macromolecular memory in the imprinted hydrogels, showing 15% higher binding capacity and 44% higher binding affinity over the control hydrogels. These results are consistent with those reported by our group previously [170].

Table 5.7: Binding capacities, affinities and diffusion coefficients for diclofenac sodium in poly(HEMA-co-DEAEM-co-PEG200DMA)

5% PEG200DMA	K_a (mM^{-1})	Q_{\max} ($\times 10^2$ mmol/g)	Diffusion Coefficient ($\times 10^{11}$ cm^2/s) DI water	Diffusion Coefficient ($\times 10^{11}$ cm^2/s) Lacrimal
Imprinted	15.74 \pm 0.12	6.25 \pm 0.06	7.96 \pm 0.22	71.14 \pm 8.42
Control	10.87 \pm 0.20	5.44 \pm 0.04	13.36 \pm 0.32	104.43 \pm 14.32

The data are presented as mean \pm SD (n=3).

Furthermore, Figure 5.8 shows that imprinted poly(HEMA-co-DEAEM-co-PEG200DMA) hydrogels exhibited around five times higher loading of diclofenac over similar imprinted hydrogels prepared without DEAEM (i.e. poly(HEMA-co-PEG200DMA)), which were outperformed by even the poly(HEMA-co-DEAEM-co-PEG200DMA) control hydrogels. This can be attributed to the absence of DEAEM and as a result the ionic interactions between the template and the polymer chains were missing. Results indicate that the ionic interaction has a greater influence on binding, even though diclofenac sodium also has a proton donor group. However, the X-ray analysis of diclofenac shows an intramolecular hydrogen bond between the carboxyl oxygen and the amino hydrogen [198, 199]. Thus, diclofenac is not significantly receptive to extra-molecular hydrogen bonding, even though HEMA has strong proton accepting

groups. This explains the extremely low binding demonstrated for the imprinted poly(HEMA-co-PEG200DMA) network (Figure 5.8).

These results indicate that the poly(HEMA-co-DEAEM-co-PEG200DMA) network uses primarily ionic bonding for diclofenac sodium loading. Ionic bonds are the strongest non-covalent bonds with bond strengths of 5–35 kcal/mol, approaching a third of covalent bond strength, and they are 4–30 times stronger than hydrogen bonds [204, 205].

Dynamic release studies were conducted to achieve infinite sink conditions in order to sustain the greatest driving force. Diclofenac sodium fractional release studies in DI water of imprinted and control (non-imprinted) poly(HEMA-co-DEAEM-co-PEG200DMA) hydrogels with 5mole% of the crosslinking monomer and previously loaded in a 0.25mg/mL diclofenac solution, are shown in Figure 5.9. Imprinted hydrogels exhibited a slower diclofenac sodium transport when compared to the control hydrogels.

Imprinted poly(HEMA-co-DEAEM-co-PEG200DMA) hydrogels exhibited a diclofenac sodium diffusion coefficient of $7.96 \pm 0.22 \times 10^{-11} \text{ cm}^2/\text{s}$ in DI water, which was a factor of 1.68 less than the control hydrogels (Table 5.7). Since the presence of salts and ions in lacrimal solution might alter the interactions between diclofenac and the cationic monomer. Therefore, release studies were also conducted in an artificial lacrimal solution. Figure 5.9 shows a faster diclofenac sodium transport through the hydrogels when the release was performed in lacrimal solution, nonetheless under these conditions a sustained linear release was achieved. Imprinted poly(HEMA-co-DEAEM-co-PEG200DMA) hydrogels exhibited a diclofenac sodium diffusion coefficient of $71.14 \pm 8.42 \times 10^{-11} \text{ cm}^2/\text{s}$ in lacrimal solution, which was a factor of 1.48 less than the control hydrogels, and ~ 9 times faster than the release in DI water (Table 5.7). The presence of competitive agents in the lacrimal solution (i.e. ions) promoted the dissociation of diclofenac

sodium:functional monomer complexes, resulting in a faster release of the drug compared to those in DI water. However, a controlled release was attained in lacrimal solution. Imprinted poly(HEMA-co-DEAEM-co-PEG200DMA) hydrogels exhibited an extended release profile for duration of 24 hours in lacrimal solution, releasing 60% of loaded template in approximately 12 hours, which resulted in a delay of the template release by 2.2 fold over that of the control hydrogels (drug was completely released in ~11 hours, releasing 60% of loaded template in ~ 6 hours).

In order to verify that molecular imprinting was responsible for the enhanced loading and delayed release, swelling studies and mechanical analysis were also performed on the control hydrogels. Equilibrium volume swelling ratios were similar for imprinted and control hydrogels (Table 5.8). Thus, the equilibrium polymer volume fraction in the swollen state was not statistically different among the hydrogels, which suggest that similar macromolecular architectures were available for free volume transport. Comparable values in the mesh sizes were obtained for imprinted and control hydrogels (Table 5.8).

Table 5.8: Structural parameters of poly(HEMA-co-DEAEM-co-PEG200DMA)

5% PEG200DMA	Q (Equilibrium volume swelling ratio)	$v_{2,s}$ (Equilibrium polymer volume fraction in the swollen state)	Young's Modulus (MPa)	Mesh Size (Å)
Imprinted	1.566±0.062	0.639±0.012	3.609 ± 0.217	29.51 ± 0.63
Control	1.538 ± 0.002	0.650 ± 0.001	3.695 ± 0.277	29.49 ± 1.18

The curves obtained to calculate the modulus and M_c had excellent correlation coefficients (>0.99). The data are presented as mean ± SD (n=3).

The enhance loading and transport delay of the template achieved by the imprinted hydrogels along with the fact that there is no indication of a change in the hydrogels network when compared to the control hydrogels, offers evidence of macromolecular memory affecting these parameters.

5.4 Conclusions

The research work presented in this chapter examined the effects of crosslinker diversity on the structure of imprinted hydrogels and subsequently on their drug binding and transport properties.

Findings reveal that an increase in the length of the crosslinker resulted in decreased binding affinity and faster template transport through the hydrogel, which corresponded with increased equilibrium swelling ratios, lower polymer volume fractions and increased mesh size. On the other hand, increase in the amount of crosslinking in the hydrogels resulted in a decrease in the template binding capacity and slower template transport with smaller reductions in template binding affinity. This corresponded with lower equilibrium swelling ratios and smaller mesh sizes of the solvated hydrogels.

Results found that in imprinted films with no DEAEM, there was negligible binding indicating that DEAEM is most likely the most important monomer interacting with the template. This demonstrates the importance of the ionic interaction to facilitate template binding in the system.

Among the different lengths and amounts of crosslinking monomers, it was found that imprinted hydrogels with a mesh size around 30 Å (i.e., hydrogels prepared with 5% PEG200DMA) had an optimal conformation of the macromolecular memory sites, which provided the most favorable binding to the drug, resulting in similar diffusion coefficients in DI water, than imprinted hydrogels with smaller mesh size (i.e., hydrogels prepared with 5% EGDMA, 10% PEG200DMA and 50% PEG200DMA).

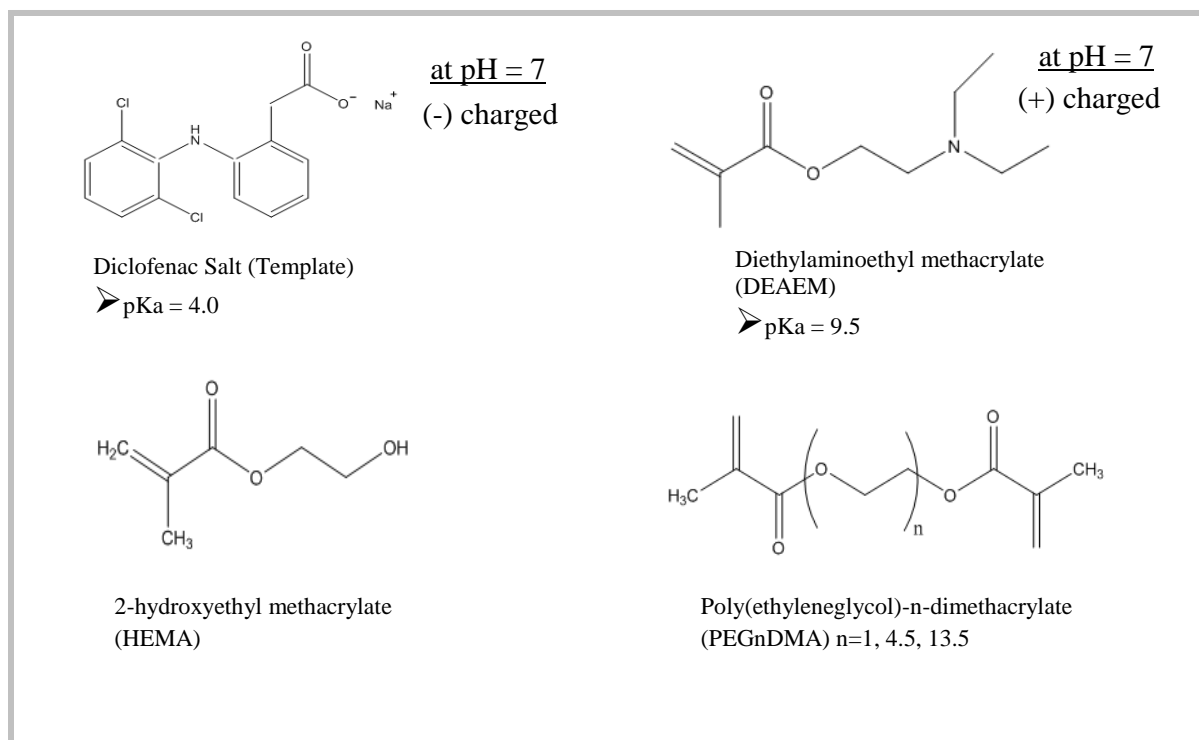


Figure 5.1: Functional monomers and crosslinking monomers

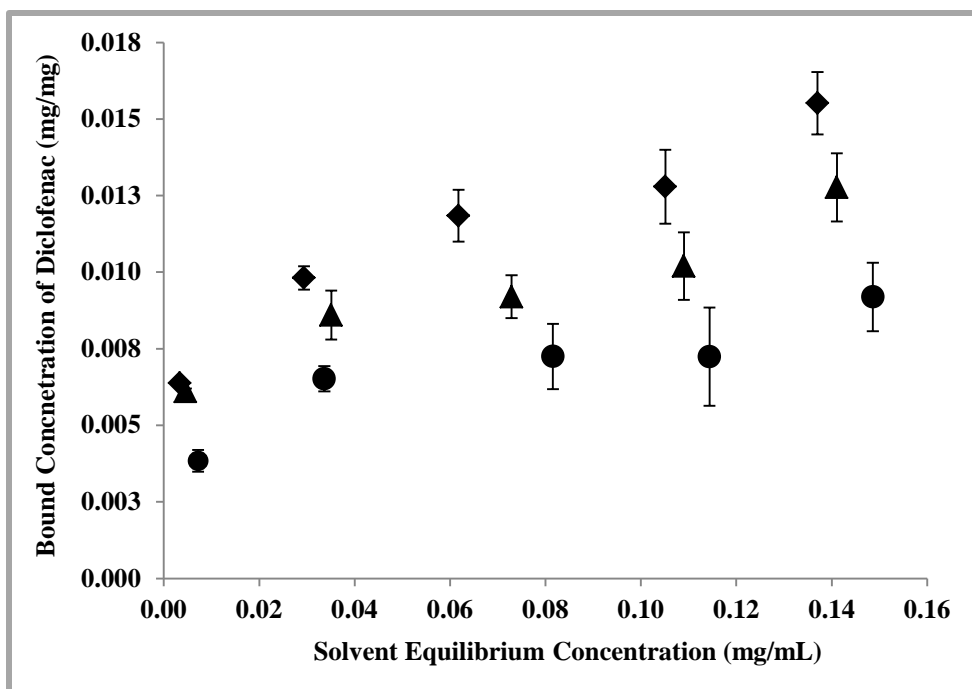


Figure 5.2: Equilibrium binding isotherms for diclofenac sodium by imprinted hydrogels with varying length of crosslinker

Imprinted poly(HEMA-co-DEAEM-co-PEGnDMA) hydrogels prepared with EGDMA (●); PEG200DMA(◆), and PEG600DMA(▲) as crosslinking monomers. Crosslinker content= 5 mole%. The data is plotted as the mean \pm SD (n=3).

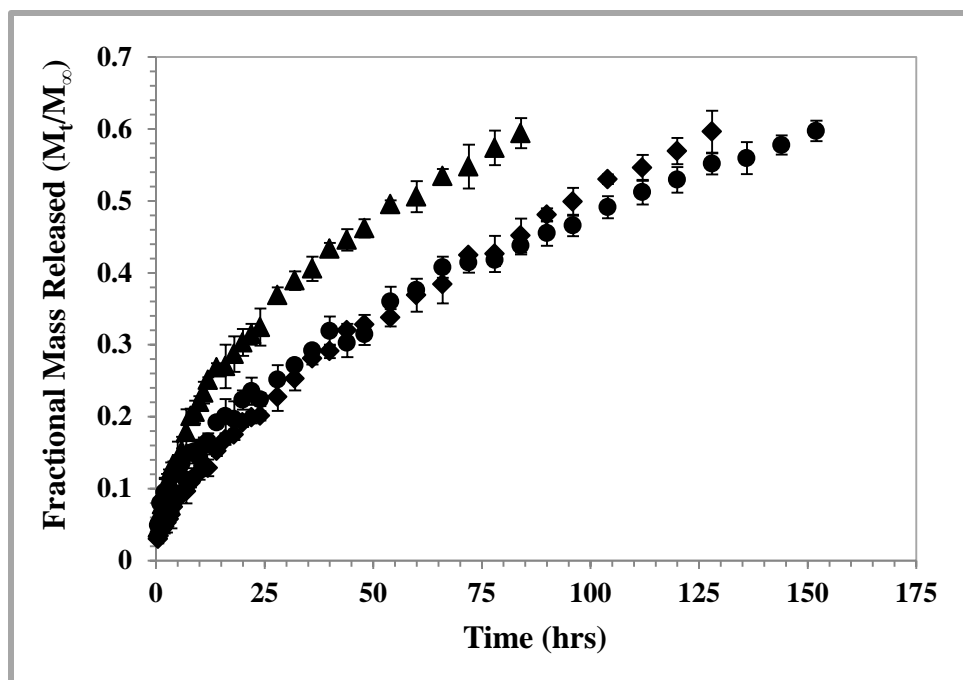


Figure 5.3: Fractional diclofenac released in DI water from imprinted poly(HEMA-co-DEAEM-co-PEGnDMA)

Imprinted poly(HEMA-co-DEAEM-co-PEGnDMA) hydrogels prepared with EGDMA (●), PEG200DMA(◆), and PEG600DMA(▲) as crosslinking monomers. Crosslinker content= 5 mole%. The data is plotted as the mean \pm SD (n=3). T=25°C.

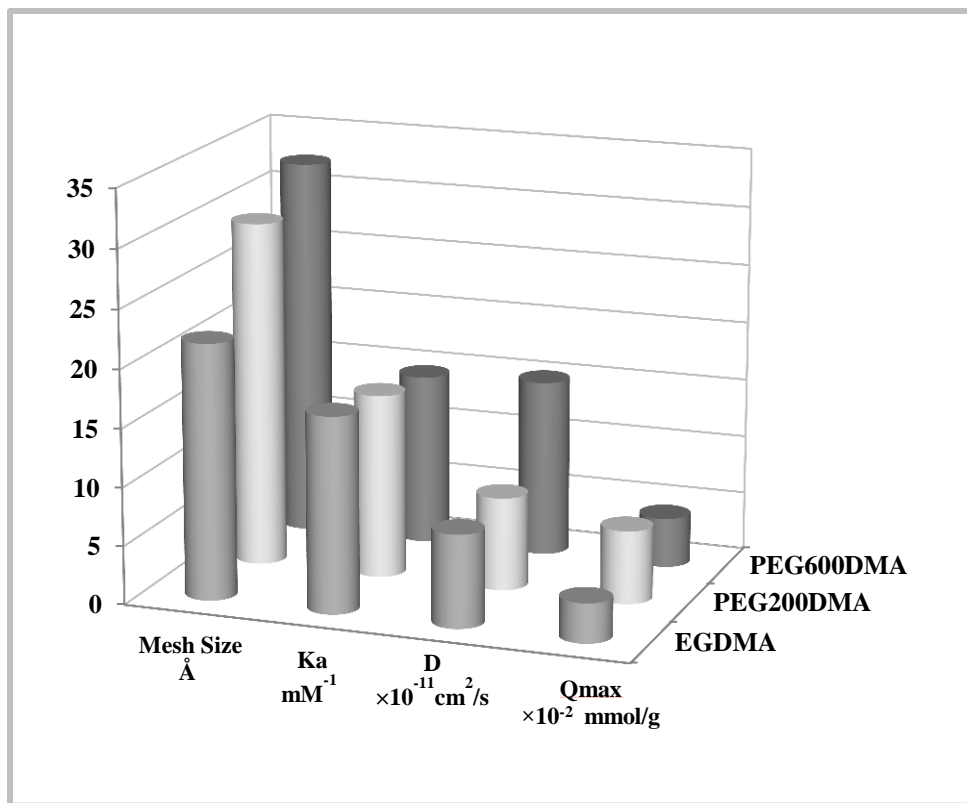


Figure 5.4: Diffusion coefficient and binding parameters of imprinted poly(HEMA-co-DEAEM-co-PEGnDMA) hydrogels

Imprinted poly(HEMA-co-DEAEM-co-PEGnDMA) hydrogels prepared with EGDMA (■), PEG200DMA(■), and PEG600DMA(■) as crosslinking monomers. Imprinted hydrogels prepared with PEG200DMA had an optimal conformation of the macromolecular memory sites, which provided the most favorable binding to the drug, thus delaying diclofenac sodium through the hydrogels, resulting in similar diffusion coefficients in DI water, than imprinted hydrogels with smaller mesh size (5% EGDMA) Crosslinker content= 5 mole%. The data is plotted as the mean \pm SD (n=3).

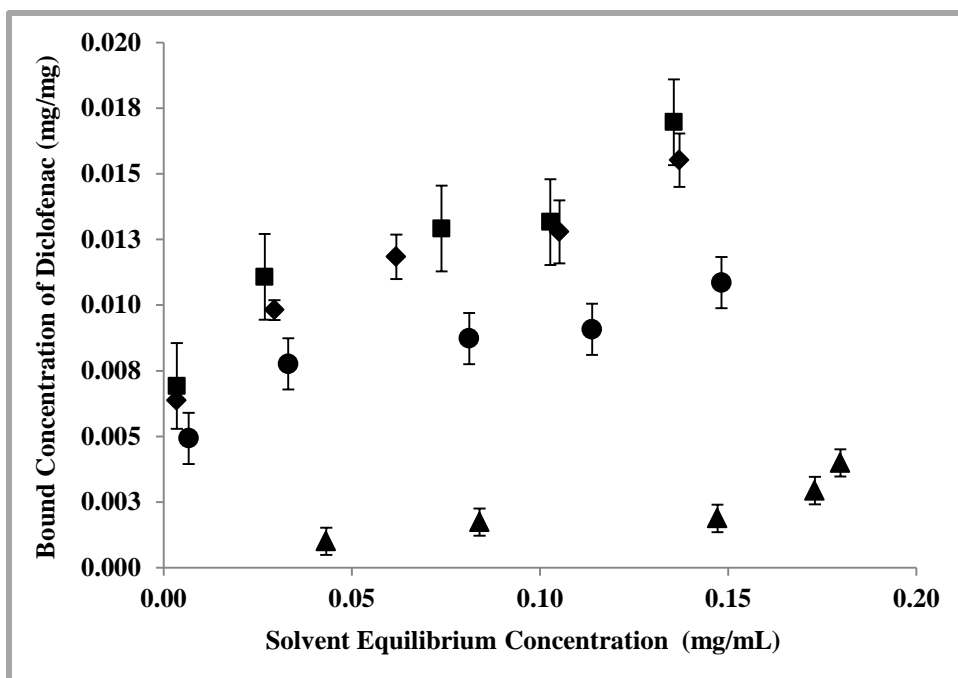


Figure 5.5: Equilibrium binding isotherms for diclofenac sodium by imprinted poly(HEMA-co-DEAEM-co-PEG200DMA) hydrogels with varying concentrations of crosslinker

Imprinted poly(HEMA-co-DEAEM-co-PEG200DMA) hydrogels prepared with varying concentrations of crosslinker in feed: PEG200DMA molar content = 1% (■), 5% (◆), 10% (●), and 50% (▲). The data is plotted as the mean \pm SD (n=3).

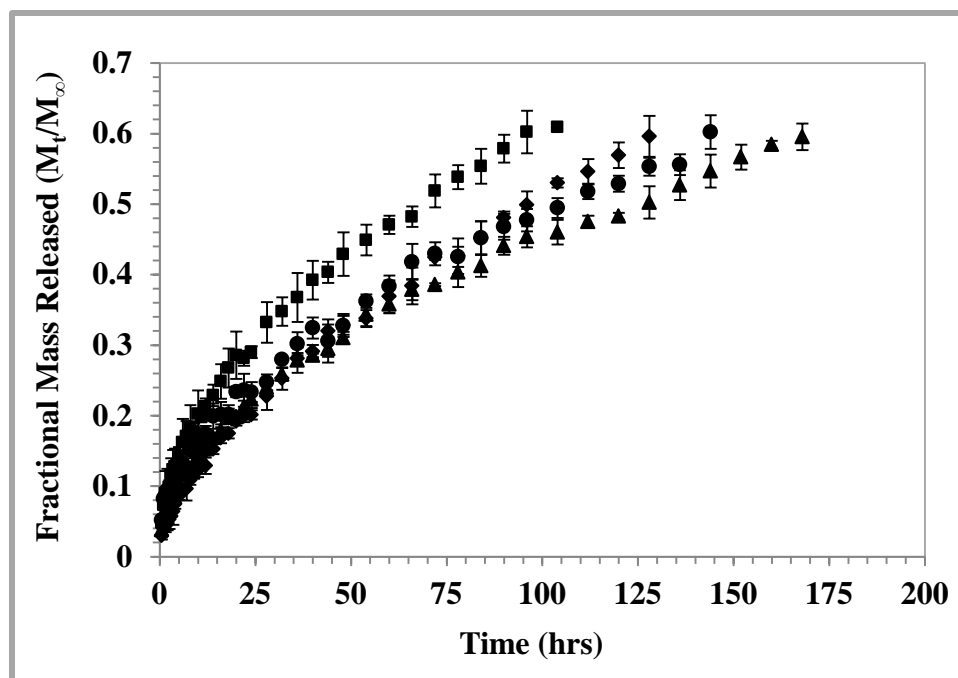


Figure 5.6: Fractional release of diclofenac sodium in DI water from imprinted poly(HEMA-co-DEAEM-co-PEG200DMA) hydrogels with varying concentrations of crosslinker

Imprinted poly(HEMA-co-DEAEM-co-PEG200DMA) hydrogels prepared with varying concentrations of crosslinker in feed: PEG200DMA molar content = 1% (■), 5%(◆), 10%(●), and 50%(▲), T=25°C. The data is plotted as the mean \pm SD (n=3).

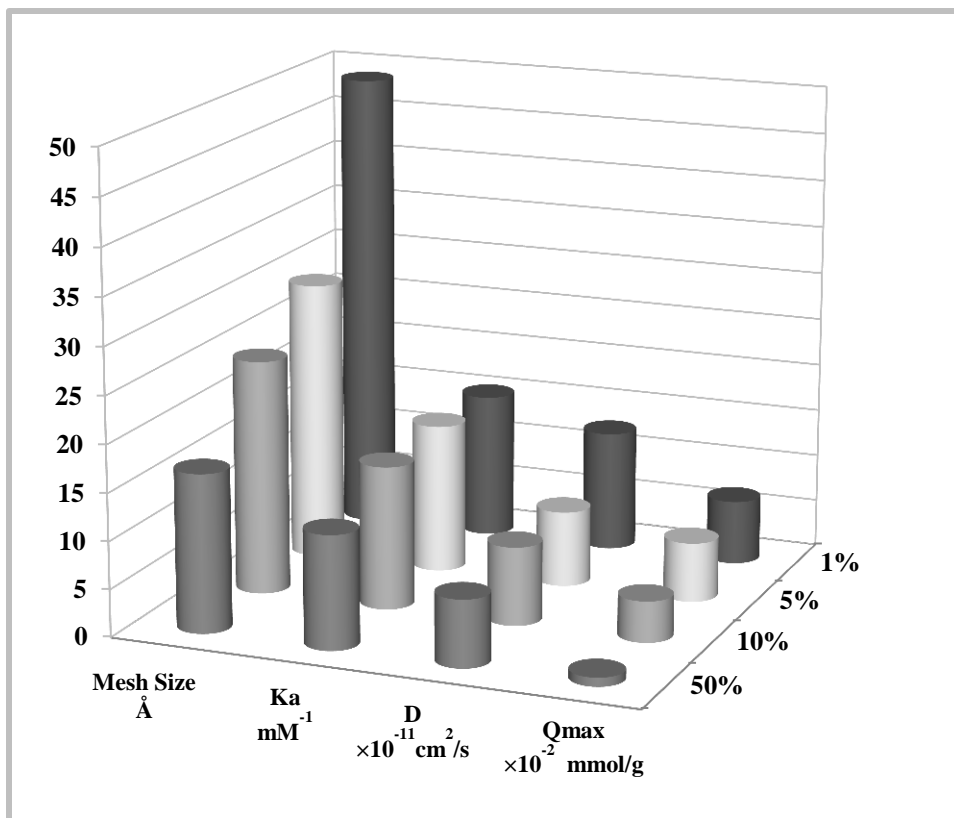


Figure 5.7: Diffusion coefficient and binding parameters of imprinted poly(HEMA-co-DEAEM-co-PEG200DMA) hydrogels

Imprinted poly(HEMA-co-DEAEM-co-PEG_nDMA) hydrogels prepared with: PEG200DMA molar content = 1% (■), 5% (■), 10% (■), and 50% (■). Imprinted hydrogels prepared with 5% PEG200DMA had an optimal conformation of the macromolecular memory sites, which provided the most favorable binding to the drug, thus delaying diclofenac sodium transport through the hydrogels, resulting in similar diffusion coefficients in DI water, than imprinted hydrogels with smaller mesh size (i.e., hydrogels prepared with 10% PEG200DMA and 50% PEG200DMA). The data is plotted as the mean ±SD (n=3).

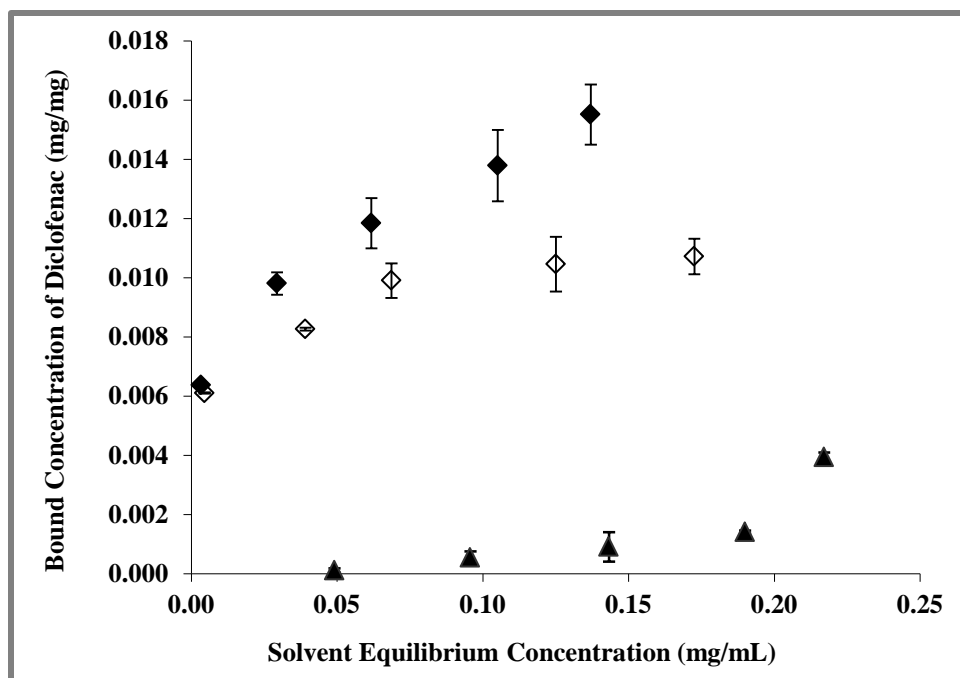


Figure 5.8: Equilibrium binding isotherm for poly(HEMA-co-DEAEM-co-PEG200DMA) hydrogels

Imprinted hydrogels (◆) bound more diclofenac sodium compare with control (non-imprinted) hydrogels (◇), and imprinted poly(HEMA-co-PEG200DMA) hydrogels (▲). These results indicate the successful creation of macromolecular memory in the imprinted hydrogels Crosslinker content=5 mole%. The data is plotted as the mean \pm SD (n=3).

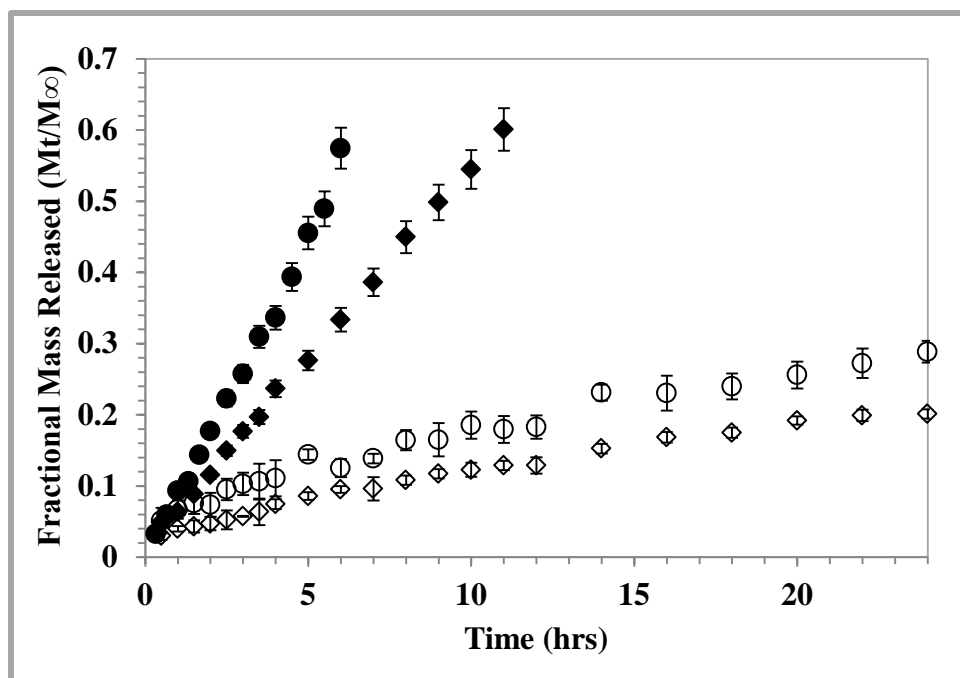


Figure 5.9: Fractional release of diclofenac sodium in lacrimal solution from poly(HEMA-co-DEAEM-co-PEG200DMA) hydrogels

Fractional release from poly(HEMA-co-DEAEM-co-PEG200DMA) in artificial lacrimal solution: imprinted (♦) and control (●), and in DI water: imprinted (◇) and control (○) The presence of competitive agents in the lacrimal solution promoted the dissociation of diclofenac sodium: functional monomer complexes, resulting in a fast release of the drug. However, a controlled release was attained. Crosslinker content= 5 mole%. The data is plotted as the mean \pm SD (n=3). T=25°C

Chapter 6

***In Vitro* Controlled Release of Diclofenac Sodium from HEMA Lenses under Physiological Ocular Tear Flow**

In Chapter 5, the effects of altering the chain building blocks on the imprinting effectiveness of poly(HEMA-co-DEAEM-co-PEG_nDMA) hydrogels as well as diclofenac sodium loading and transport properties were presented. It was found that the imprinted poly(HEMA-co-DEAEM-co-PEG200DMA) hydrogels with a 5 mole% of crosslinking monomer may produce a final network that it was more ideal in terms of the flexibility and orientation of polymer chains that produced the template binding site. More importantly, an extended controlled release of diclofenac sodium was achieved in lacrimal solution.

Imprinted hydrogels with enhanced affinity for specific molecules could be used as the basis for rate controlled release, triggered or, even, feedback-regulated drug delivery devices. Therefore, the aim of this study was to synthesize hydrophilic soft contact lenses so as to control the release of diclofenac sodium for an extended period of time. Poly(HEMA-co-DEAEM-co-PEG200DMA) hydrogels with 5 mole% of crosslinking monomer were chosen as the ideal network. Further analysis of template loading and template transport were performed when template-monomer interactions were altered by varying the functional monomer to template (FM/T) ratio. The monomer to template (M/T) ratio has shown to affect release rate of imprinted hydrogels [61].

Diclofenac sodium is used for the treatment of ocular inflammation. Clinicians typically prescribe anti-inflammatory medication when trauma has occurred to the eye. For example, two

areas have substantial markets: anti-inflammatory is prescribed at a dosage of 1-2 drops four times daily for two weeks after cataract surgery, whereas dosage for corneal refractive surgery (Lasik) recommends 1 drop every hour during the first day and 1-2 drops four times daily for up to one week. The medication controls post-operative inflammation and temporarily relieves pain and photophobia following surgery. Cataract surgery and corneal refractive surgery (Lasik) are among the most common surgeries performed worldwide [206, 207]. Cataract surgery is the most frequently performed surgery in the United States [206], with over 2.5 million surgeries done every year [208]. Also it is estimated that ~1 million patients undergo Lasik surgery every year [207].

The benefit of therapeutic contact lenses could be in the delivery of the correct dose of medication at an approximately constant rate, thereby eliminating the application of a topical eye drop medication multiple times a day and, more importantly, providing patient benefit with substantially increased efficacy..

In the field of controlled therapeutic delivery, drug release from delivery devices typically agrees with the Fickian model of release kinetics, which means that the release rate of the drug is proportional to the concentration gradient between the drug source and the surroundings [100, 121]. In practical terms, this means that as the finite drug source is depleted, the rate of drug release decreases until there is no more drug in the device, whereupon the rate is zero. For delivery devices, a zero-order (i.e., independent of concentration) release rate is preferable because medication is delivered at a constant rate for an extended, tunable amount of time. The challenge is to use a finite drug source to achieve an extended zero-order release.

Typically, in both modeling and experimental work, infinite sink conditions are assumed, and the accumulation of drug in the solution surrounding the hydrogel is considered to be

negligible. However, most drug-eluting lens systems described in the literature to date have used small volumes (i.e., 2-4 mL), which are not well mixed [93]. An infinite sink with good mixing assures that a concentration gradient is the main driving force for elution, and it corresponds to the fastest possible release. Under normal lacrimation and blinking rate, the human eye has a tear volume that ranges from 7.0 to 30.0 μL , with a normal tear turnover rate of $1.51 \pm 0.58 \mu\text{L}/\text{min}$. After 6 hours of contact lens wear the turnover rate is $2.82 \pm 1.45 \mu\text{L}/\text{min}$ [23]. Due to the small tear volume and flow rates encountered *in vivo*, infinite sink conditions do not adequately describe drug release kinetics on the eye. In these types of physiological situations, it is imperative that microfluidic models be used to characterize the release profiles.

Previous work from our lab showed the first zero-order release profiles from imprinted thin films, using a microfluidic device [168]. It was demonstrated that under physiological flow conditions similar to those in the human eye, the release time of the drug was increased and provided a more linear and sustained release profile. In this chapter, the release kinetics using an improved microfluidic device is presented, that allows the study of contact lenses with the dimensions and thickness of commercial lenses.

6.1 Materials and Methods

6.1.1 Materials and Reagents

Diethylaminoethyl methacrylate (DEAEM), 2-hydroxyethylmethacrylate (HEMA) and azobisisobutyronitrile (AIBN) were purchased from Sigma-Aldrich (Milwaukee, WI). Diclofenac sodium salt (DS) was purchased from Sigma-Aldrich (Saint Louis, MO). Polyethylene glycol (200) dimethacrylate (PEG200DMA) was purchased from Polysciences, Inc (Warrington, PA). All chemicals were used as received.

6.1.2 Synthesis of Molecularly Imprinted Contact Lenses

Hydrogel contact lenses were synthesized varying the functional monomer to template molar ratios in a temperature controlled non-oxidative environment using free-radical UV photopolymerization. All polymer compositions consisted of 90 mole% of the backbone monomer, HEMA, 5 mole% of the functional monomer, DEAEM and 5 mole% of crosslinking monomer, PEG200DMA. The solution was mixed with various amounts of diclofenac (template drug) to achieve different DEAEM to diclofenac mole (FM/T) ratios of 1, 3.5 and 10.5. Non-imprinted control lenses were prepared in exactly the same manner except the template molecule, diclofenac sodium, was not included in the formulation. The reaction solutions were sonicated (15-20 min) until no phase separation occurred in the mixture. The solutions were purged with nitrogen for 15 minutes and then transferred to a MBraun Labmaster 130 1500/1000 glovebox, which provided an inert (nitrogen) atmosphere, where the solutions were left uncapped and open to the nitrogen atmosphere until the oxygen levels inside reached negligible levels (<1.0 ppm) (MBraun Oxygen Analyzer , MB-0X-SE-1). Contact lenses with a base curve of 8.6 ± 0.2 mm, a diameter of 15.0 ± 0.2 mm and center thickness of 105 ± 5 μm were synthesized using polypropylene contact lens molds (CIBA Vision Inc., Duluth, GA).

The polymerization reaction was carried out for 8 minutes with a light intensity of 40 mW/cm^2 , measured using a radiometer (International Light IL1400A), at a constant temperature of 35°C. Lenses were washed with deionized water (Millipore, 18.2 $\text{M}\Omega\text{cm}$, pH 6.2) until the template and unreacted monomers could no longer be detected by spectroscopic monitoring (Synergy Biotek UV–Vis Spectrophotometer, BioTek Instruments, Winooski, VT).

6.1.3 Diclofenac Sodium Loading Studies

Equilibrium binding studies were conducted to examine the creation of memory and the enhanced loading potential of the hydrogels. For these studies, imprinted and control (non-imprinted) thin films were prepared by pipetting the monomer solution into glass plates (6" x 6") coated with trichloromethylsilane (to prevent strong adherence of the polymer matrix to the glass) and separated by 0.25 mm Teflon spacers. After polymerization, the glass plates were submerged into a deionized water bath; the thin film was peeled from the glass surface and cut into circular films of 13.5 mm diameter. The films were washed following the procedure described above and then dried at room temperature for 24 hours, followed by vacuum drying ($T=30\text{ }^{\circ}\text{C}$, 28 in. Hg vacuum), until the weight change was less than 0.1 wt%. A variety of concentrations of diclofenac sodium in DI water (0.05, 0.10, 0.15, 0.20, and 0.25 mg/mL) were prepared. Initial absorbances of each concentration were measured using a Synergy UV-Vis spectrophotometer at 276 nm, the wavelength of maximum absorption. After the initial absorbance was taken, a dry, washed poly(HEMA-co-DEAEM-co-PEG200DMA) film was inserted into 5 mL of solution placed in a vial, and the vials were gently agitated on an ocelot rotator (Fisher Scientific; Chicago, IL) at 75 rpm and 12° tilt angle. Separate experiments were conducted to assure equilibrium was reached. After equilibrium was reached, the solutions were vortexed for 10 seconds, the bound concentration in the gel was determined by mass balance. All gels were analyzed in triplicate, and all binding values are based upon the dry weight of the gel.

The diclofenac partition coefficient (K_d) was calculated as the ratio of the equilibrium diclofenac concentration within the lens to the equilibrium solution concentration. This was found by soaking the lenses in an aqueous drug solution (0.25mg/mL) until an equilibrium weight uptake was achieved. The Langmuir-Freundlich isotherm (Equation 4.22) was used to

determine binding parameters, such as template binding capacity (Q_{\max}) and template binding affinity (K_a), because gave the best fit to the experimental.

6.1.4 Lens Mechanical Properties, Structural Studies, and Optical Clarity Studies

Hydrogel structural analysis was obtained by swelling and tensile experimental studies. The hydrogel contact lenses were subject to the analysis described in section 4.2.1. The volume swelling ratio (Q) and the polymer volume fraction in the swollen state ($v_{2,s}$) were calculated. Q is the ratio of the swollen to dry volumes of the hydrogel, $v_{2,s}$ is the inverse of the volume swelling, and $(1- v_{2,s})$ gives the fractional water content of the hydrogel. The volume of the gel in the swollen or dry state was calculated by using Archimedes buoyancy principle [200].

Stress–strain data were obtained by performing tensile studies with a RSA III Dynamic Mechanical Analyzer (DMA), (TA Instruments, New Castle, DE). A linear load stress at a constant rate of 4 mm/min was applied to hydrated hydrogels prepared in strips (8mm \times 30 mm \times 0.25mm, in triplicate). The average molecular weight between crosslinks (\overline{M}_c) was determined from the theory of rubber elasticity [173] (Section 4.2.2). Equation 4.16 was used to calculate \overline{M}_c , which accounts for swollen hydrogel synthesized in the absence of solvent [100]. The normal stress applied is τ , the ideal gas constant used is $R= 8.314472 \text{ cm}^3\text{MPa}^{-1}\text{mol}^{-1}$, the temperature of experimental conditions is $T=298 \text{ K}$, and the specific polymer volume is $\bar{v} = 0.909$.

The slope of τ versus the elongation term $(\alpha-1/\alpha^2)$ is the Shear modulus and enables to calculate \overline{M}_c . From \overline{M}_c , the mesh size (ξ) can be determined using Equation 4.18 [100], where $C_n=11$, $l=1.54 \text{ \AA}$, and $M_r = 144.09 \text{ g/mol}$ were selected for this structure.

Optical transmission studies were conducted by cutting small diameter films and placing in the bottom of a 96-well plate where absorbance values were measured via spectrophotometric monitoring (BioTek, Winooski, VT). All films were fully hydrated and tested at wavelengths of visible light (380 to 780 nm). The absorbance value of each well in water was calculated and subtracted from the data. Percent transmission values were calculated from the absorbance data.

6.1.5 *In Vitro* Diclofenac Release Studies

Dynamic release studies were conducted using two different *in vitro* methods, the conventional sink model and the physiological flow model using a microfluidic device. In the infinite sink model, the drug-loaded lenses, loaded at a template concentration of 0.25 mg/mL, were placed in 450 mL of artificial lacrimal fluid (6.78 g/L NaCl, 2.18 g/L NaHCO₃, 1.38 g/L KCl, 0.084 g/L CaCl₂·2 H₂O, pH 8), kept at a constant temperature of 34 °C and continuously agitated at 45 rpm, in a dissolution apparatus from SOTAX Inc. (Hopkinton, MA). Preliminary studies were conducted to determine the amount of fluid and mixing speed needed to approximate infinite sink analysis.

In the physiological flow model, the drug-loaded lens was placed within the chamber of the microfluidic device. A KDS101 infusion pump from KD Scientific (Holliston, MA) was used to pump lacrimal fluid through the device. It has been assessed that after 6 hours of contact lens wear the turnover rate could be 2.82±1.45 μL/min [23], therefore, the syringe pump was set to pump at the physiological flow rate of 3 μL/min. The samples were collected at regular time intervals. Release of diclofenac sodium was monitored at specific time intervals using a Synergy UV-Vis Spectrophotometer at 276 nm. The absorbance was recorded for three samples, averaged, and corrected by subtracting the relevant controls.

6.1.6 Design and Fabrication of Microfluidic Device

A microfluidic device was engineered and fabricated using polydimethylsiloxane (PDMS). A mixture of 10:1 ratio of Sylgard 184 Silicone base and curing agent was prepared and stirred manually for 3-5 minutes. The mixture was placed under vacuum for an hour and was then poured into a mold constructed to create an inner chamber and two channels for flow. The inner chamber had a radius of curvature of 9.00 ± 0.10 mm. The device was then cured at 60°C for 6 hours. A drug-loaded lens was placed over a mount with radius of curvature of 8.75 ± 0.10 mm and the device was sealed against a glass plate. A schematic of the microfluidic device is presented in Figure 6.1. The device is designed to mimic the flow rate of tears but does not fully reproduce other ocular conditions. In the human eye, the mixing and flow of tears is complicated by the presence of contact lenses. The tear film is thinner and varies in thickness by evaporation between blinks and tear breakup. These factors may also affect drug release, but relative to tear flow rate these effects are small [6, 209].

6.1.7 Analysis of Drug Release from Contact Lenses

Fractional drug release (M_t/M_∞) profiles were calculated for the diclofenac imprinted and control lenses by taking the amount of template released at specific times, M_t , divided by the maximum amount of diclofenac released during the experiment, M_∞ . Template diffusion coefficients were calculated using Fick's law, which describes one-dimensional planar solute release from gels [172] (Section 4.1). In all the contact lenses studied in this work, the diameter (length) over thickness was much greater than 10; therefore, slab geometry was considered for the analysis. Equation 4.8 gives the solution of Fick's law for short times of diffusion.

The diffusional exponent, n , was also calculated using the empirical relationship $M_t/M_\infty=kt^n$ [210] (Section 4.1). For planar systems an exponent value of 0.5 describes Fickian behavior, indicating diffusion controlled drug release, and a value of 1 indicates zero-order or independent of concentration and time, with $n-1$ corresponding to the order of release.

6.2 Results and Discussion

6.2.1 Diclofenac Sodium Loading Studies

Diclofenac sodium equilibrium binding results for the poly(HEMA-co-DEAEM-co-PEG200DMA) imprinted and control (non-imprinted) hydrogels are presented in Figure 6.2. It is clear that the imprinted networks exhibited increased loading over the control networks. Furthermore, the results show that the amount of drug bound can be tailored by altering the concentration of the binding solutions. Thus, loading can be tuned by the concentration of the original drug solution.

The imprinted hydrogels showed a 67%, 76%, 83% increase in maximum loading over the control hydrogels for the FM/T ratio of 10.5, 3.5 and 1.0, respectively, demonstrating the presence of memory sites in the imprinted hydrogels, when placed in a 0.25mg/mL diclofenac solution. All the imprinted hydrogels demonstrate higher average loading as compared to the control hydrogels, although no remarkable differences in the loading capacity for the imprinted hydrogels were found. Similar results were found from the partition coefficient calculations, where the values are 116.6 ± 8.2 , 118.7 ± 7.6 and 122.5 ± 2.9 for the FM/T ratio of 10.5, 3.5 and 1.0, respectively (Table 6.1). These results can be attributed to the fact that all the formulations have the same amount of functional monomer, DEAEM (5% mole), which means that the

different networks probably have the same amount of positive charges available to interact with the negative charge of the template.

Table 6.1: Partition coefficients, binding capacities and affinities for diclofenac sodium in poly(HEMA-co-DEAEM-co-PEG200DMA) hydrogels

FM/T ratio	K_d (Partition coefficient)	K_a (mM^{-1})	Q_{max} ($\times 10^2 \text{ mmol/g}$)
1.0	122.5 ± 2.9	13.83 ± 0.25	8.75 ± 0.06
3.5	118.7 ± 7.6	15.74 ± 0.12	7.75 ± 0.04
10.5	116.6 ± 8.2	17.65 ± 0.22	7.45 ± 0.08
Control	52.3 ± 3.8	10.87 ± 0.20	5.32 ± 0.04

The data are presented as mean \pm SD (n=3).

Calculations of binding parameters are summarized in Table 6.1. Having the same trend as the partition coefficients and with no significant difference, the template binding capacity (Q_{max}) increased as the FM/T ratio was decreased. However, the template binding affinity (K_a) increased as the FM/T ratio was increased. Hydrogels with a FM/T ratio of 10.5 demonstrated a binding affinity of $17.65 \pm 0.22 \text{ mM}^{-1}$, which was 27.6% times higher than the binding capacity of hydrogels with a FM/T ratio of 1 ($K_a = 13.83 \text{ mM}^{-1}$). It is hypothesized that the memory binding sites might have a better conformation where the drug is better retained as the FM/T ratio increases. Therefore, a more higher affinity binding sites were acquired and not necessarily more binding sites were produced (Q_{max}). Moreover, binding parameters revealed an increase in both the number of binding sites (Q_{max}) and binding affinity (K_a) in imprinted hydrogels over the corresponding control hydrogels, indicating the successful creation of macromolecular memory in the imprinted hydrogels.

6.2.2 Dynamic Release Studies

6.2.2.1 Infinite sink release studies

Release studies were first conducted with the infinite sink model in order to sustain the greatest driving force. Infinite sink dynamic cumulative and fractional mass release studies for the diclofenac sodium for imprinted and control (non-imprinted) poly(HEMA-co-DEAEM-co-PEG200DMA) contact lenses are shown in Figure 6.3a and 6.3b, respectively. Among the release studies, the lenses prepared with a FM/T ratio of 10.5, exhibited an extended release profile for duration of 72 hours within artificial lacrimal solution, which resulted in a delay of the template release by 8 fold over that of the control lenses (the drug was completely released in 9 hours). The other imprinted systems demonstrated a complete release by 24 hours (FM/T of 3.5) and 12 hours (FM/T of 1). Thus, as the FM/T ratio increased the release rate of diclofenac decreased. This data along with the data from loading studies provide evidence of macromolecular memory affecting these parameters. Thus, both FM/T ratio and macromolecular memory extend release.

Although no remarkable differences in the loading capacity for the imprinted lenses were found, a delay in transport of the drug was achieved changing the FM/T ratio of the lenses. The differences in the diclofenac release rate could be related to the strength of the non-covalent bond (i.e., binding affinity) between the drug and the functional monomer. It was shown that as the FM/T increased, the template binding affinity increased (Table 6.1). As the FM/T ratio increases from 1 to 10.5, the memory or binding sites have a better conformation that provides the most favorable binding to the drug. The interaction with these better sites delays transport more (higher affinity with less dissociation) than interactions with non-specific binding and lower affinity binding sites (more dissociation).

In order to evaluate the suitability for the Fickian mechanism, the diffusional exponent, n , was calculated by plotting the log of the fractional mass release (M_t/M_∞) against the log of time. The values for n , in the infinite sink release for the imprinted contact lenses, are approximately equal to 0.5 (Table 6.2), which indicates that they are in agreement with a Fickian diffusion mechanism.

Table 6.2: Summary of diffusion coefficients, power law exponents and swelling data

FM/T ratio	Infinite Sink Model		Physiological Flow Model
	Diffusion Coefficient ($\times 10^{10}$ cm ² /s)	Power law exponent (n)	Power law exponent (n)
1.0	7.05 \pm 0.21	0.456	0.798
3.5	5.80 \pm 0.20	0.503	0.890
10.5	3.23 \pm 0.17	0.591	0.935
Control	14.11 \pm 0.80	0.448	N/A

The data are presented as mean \pm SD (n=3).

Within the Fickian diffusion process, the fractional mass released depends linearly on $t^{0.5}/L$ at short times or fractional release less than 0.7 with a slope directly proportional to the diffusion coefficient. Poly(HEMA-co-DEAEM-co-PEG200DMA) contact lenses with a FM/T ratio of 10.5 exhibited a diclofenac sodium diffusion coefficient of $3.23 \pm 0.17 \times 10^{-10}$ cm²/s, which was a factor of 1.8, 2.2, and 4.4 less than FM/T ratio of 3.5, 1.0 and the control contact lenses, respectively (Table 6.2).

6.2.2.2 Release studies under physiological flow conditions

In view of the fact that the pre-corneal volume is very small and the tear turnover fast, the infinite sink method is not consistent with the physiological conditions of the eye. Thus, a microfluidic device (Figure 6.1) was used in order to predict ocular release rates more accurately. Since the imprinting lenses demonstrated control over the release, imprinted lenses, previously

loaded in a 0.25mg/mL diclofenac solution, were used in the microfluidic release studies. Figure 6.4a shows the *in vitro* dynamic drug releases under physiological flow conditions for 6 days. A linear release profile was observed for up to 48 hours for the FM/T ratio of 3.5 and 10.5 contact lenses. By increasing the FM/T ratio from 1 to 10.5, the release rate decreased from 11.72 $\mu\text{g/hr}$ to 6.75 $\mu\text{g/hr}$ during the first 48 hours (Figure 6.4b), this is despite the fact that all imprinted contact lenses have the same water content and consist of exactly the same monomer feed composition. The addition of functional monomers and diclofenac did not have an impact on the optical transmission, with percent transmission of all lenses in the range $96 \pm 1\%$. Thus, these lenses possess the same ocular clarity as commercial contact lenses.

The fractional release at physiological flow rates (Figure 6.4c) for poly(HEMA-co-DEAEM-co-PEG200DMA) contact lenses was calculated as the mass released at a specific time over the mass released from the lens in the infinite sink experiments (or the mass released at infinite time). The results demonstrate that under physiological flow, drug was released at much lower rates and in a much more linear manner than conventional infinite sink release studies suggested (Figure 6.3a and 6.3b), indicating that such contact lenses have the capacity to deliver sustained amounts of drug in a constant manner over an extended time period.

In general, under physiological flow conditions a constant, slower release of the drug is achieved, moving towards a constant, zero-order release (i.e., independent of concentration or time) for approximately 2 days. For the physiological flow method the diffusional exponent, n , was 0.935, 0.890 and 0.795 for an FM/T ratio of 10.5, 3.5 and 1, respectively (Table 6.2). Figure 6.5 shows the log for the fractional drug release plotted against the log of time for the infinite sink and physiological flow methods, for contact lenses with a FM/T ratio of 10.5. Therefore, constant release is achieved by engineering the lens (i.e. FM/T ratios) and by reducing the

concentration gradient through the accumulation of diclofenac in the slow moving fluid at simulated physiological tear turnover rates. Compared to the infinite sink release profile, the cumulative mass released under physiological flow conditions was reduced for all lenses studied. Within infinite sink conditions there are sufficient fluid volumes producing a maximum concentration driving force and stirring which disrupts boundary layers. Within the microfluidic device low flow rates are used, which lead to a concentration boundary layer, which decreases the local diffusion concentration driving force. Thus, mass transfer effects in the fluid cannot be neglected and significant boundary layers will exist. It is clear that boundary layer effects are important to the differences in release comparing the microfluidic and the infinite sink cases. The importance of matching physiological flow is crucial to the characterization of this delivery system.

These results demonstrate that in an *in vitro* environment the release from imprinted lenses is further delayed by matching the ocular volumetric flow rates. This effect may be due to two causes—significant boundary layers due to the finite tear turnover rates, and molecular imprinting strategies which lead to delayed release kinetics despite comparable free volume for drug transport through the polymer chains. Thus, it is imperative to evaluate contact lens release kinetics within finite turnover conditions if they are to mimic the *in vivo* environment.

6.2.2.3 Release analysis for daily disposable lenses

Daily disposable contact lenses are designed to be worn for a single day (16-18 hrs), and then thrown-away. With this in mind we performed a release analysis for the first 24 hours.

When using the physiological flow model, the contact lenses with a FM/T ratio of 10.5, previously loaded in a 0.25mg/mL diclofenac solution, released diclofenac at a constant rate of

8.74 $\mu\text{g/hr}$ for the first 24 hours (Figure 6.6), which corresponded to 28% of the total drug available for release. Furthermore, after 6 days the contact lens had released only 78% of the total drug available for release. The infinite sink model, which showed decreasing rates of release over time, exhibited a release of 52.50 $\mu\text{g/hr}$ for the first 12 hours, which corresponded to 83% of the total drug available for release, resulting in a complete release in 3 days (Figure 6.3a). Similar calculations, for the physiological flow conditions for the first 24 hours, were performed for the contact lenses with FM/T ratios of 3.5 and 1.0, where the lenses released 36% and 49% of the drug available for release at a rate of 11.99 $\mu\text{g/hr}$ and 17.27 $\mu\text{g/hr}$, respectively (Figure 6.6). While for the infinitive sink model, the lenses released 95% and 100% of the drug in 12 hours at a rate of 59.28 $\mu\text{g/hr}$ and 66.76 $\mu\text{g/hr}$, respectively. The microfluidic release rates are lower and more constant when compared to infinite sink. It is clear that boundary layer effects are important to the differences in release kinetics when comparing both methods.

The imprinted loaded contact lenses can be designed to release the drug at the required therapeutic rate (Figure 6.7) without the variation in concentration observed with eye drops. Conventional diclofenac sodium drops deliver approximately 80-160 $\mu\text{g/day}$ (3.33-6.67 $\mu\text{g/hr}$) based on the recommended dosage regimen within a typical peak and valley profile (i.e. Voltaren Ophthalmic[®] solution concentration is 1 mg diclofenac sodium/mL; assuming a typical eye drop volume of 20 μL per drop at the recommended frequency of administration of 4-8 drops per day). Therefore, there is strong potential to release therapeutically relevant concentrations of drug from a contact lens platform. Moreover, the mass of diclofenac released by these contact lenses can be tailored (i.e. changing the loading concentration and the FM/T ratio) to match the current recommended dose from eye drops. The lens with a FM/T ratio of 10.5 released diclofenac at a constant rate of 8.62 $\mu\text{g/hr}$ for 24 hours (Figure 6.6), being close to the maximum dose delivered

by commercial eye drops, making them ideal for use as daily disposable lenses. These therapeutic lenses will release diclofenac sodium in a linear manner without the variation in concentration observed with eye drops for the duration of lens wear. The only drawback will be that no drug will be delivered during sleep; however, this is currently a limitation of using eye drops.

6.2.3 Structural Analysis

In order to verify that molecular imprinting was responsible for the enhanced loading and delayed release, lenses swelling studies and mechanical analysis were performed to obtain information about the network structure. The volume swelling ratio and the polymer volume fraction in the swollen state were calculated for all lenses and are summarized in Table 6.3.

Table 6.3: Equilibrium swelling parameters of poly(HEMA-co-DEAEM-co-PEG200DMA)

FM/T ratio	Q (Equilibrium volume swelling ratio)	$v_{2,s}$ (Equilibrium polymer volume fraction in the swollen state)
1.0	1.538 ± 0.010	0.650 ± 0.005
3.5	1.537 ± 0.009	0.650 ± 0.006
10.5	1.535 ± 0.010	0.651 ± 0.005
Control	1.538 ± 0.002	0.650 ± 0.001

The data are presented as mean ± SD (n=3).

The equilibrium volume swelling ratios were similar for imprinted and non-imprinted lenses, which suggest that similar macromolecular architectures are available for free volume transport. Once again, the equilibrium polymer volume fraction in the swollen state was not statistically different between all the lenses (Table 6.3).

There were no observable trends in the mesh sizes of the lenses. Comparable values were obtained for imprinted and non-imprinted lenses, in the ranges of 27.6–29.5 Å (Table 6.4). The

hydrodynamic radius of diclofenac sodium is 4.3 Å, making it amenable to imprinting via multiple polymer chains and diffusion through the network.

Table 6.4: Structural parameters of poly(HEMA-co-DEAEM-co-PEG200DMA)

FM/T ratio	Young's Modulus (MPa)	Shear Modulus (MPa)	Mc (g/mol)	Mesh Size (Å)
1.0	3.652 ± 0.247	1.298 ± 0.073	1804 ± 89	29.49 ± 0.73
3.5	3.609 ± 0.217	1.295 ± 0.055	1807 ± 78	29.51 ± 0.63
10.5	4.175 ± 0.278	1.481 ± 0.113	1586 ± 127	27.64 ± 1.09
Control	3.695 ± 0.277	1.301 ± 0.102	1805 ± 146	29.49 ± 1.18

The curves obtained to calculate the modulus and Mc had excellent correlation coefficients (>0.99). The data are presented as mean ± SD (n=3).

6.3 Conclusions

All imprinted poly(HEMA-co-DEAEM-co-PEG200DMA) contact lenses demonstrated improved loading over corresponding non-imprinted contact lenses. Furthermore, the imprinting process extends further control over the release kinetics, independent of polymer structure and free volume, resulting in variations in diffusion coefficients. As the FM/T ratio increases the release rate decreases. Thus, by engineering the macromolecular memory sites (i.e. FM/T ratio) in the contact lens, the release rate can be tailored. The conventionally used infinite sink method indicated Fickian concentration dependent kinetics; however, it is inadequate for modeling the small volume and flow conditions found in the eye. We demonstrated that under physiological ocular volumetric flow rates, the release kinetics for the higher FM/T ratio, is zero-order, or concentration independent for an extended time of 2 days, making them ideal for use as daily disposable therapeutic lenses. The imprinted loaded contact lenses can be designed to release the drug at the required therapeutic rate without the variation in concentration observed with eye drops.

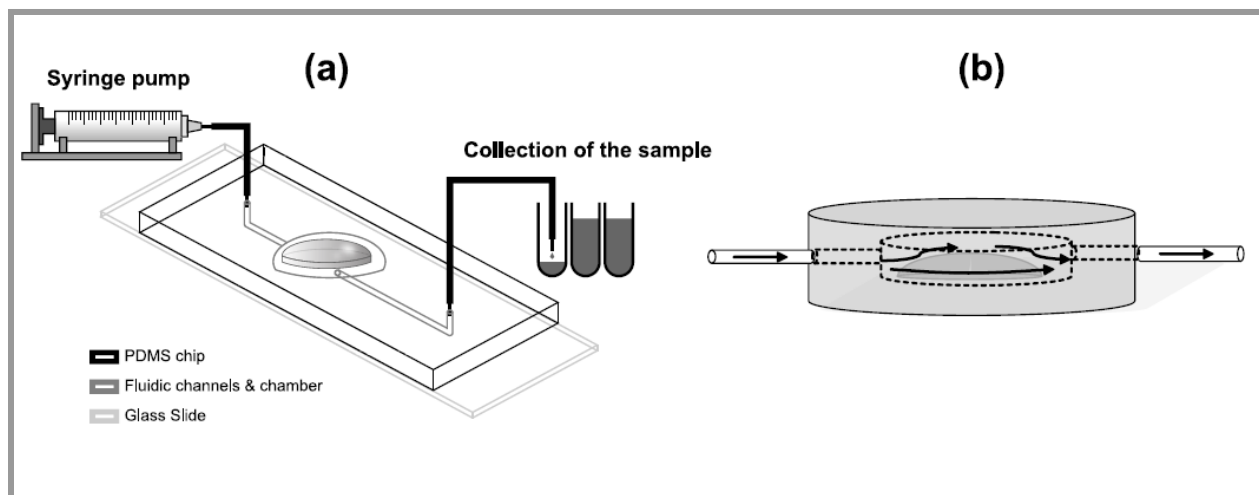


Figure 6.1: Microfluidic chip design with physiological ocular flow

The device mimics the in-vivo drug release profiles by duplicating the physiological flow rate of the eye. **(a)** Schematic of experimental set-up for contact lens drug delivery evaluation. The contact lens is placed in the microfluidic chamber and drug release is measured within artificial lacrimal fluid flow rates. **(b)** The inner chamber has a radius of curvature of 9.00 ± 0.10 mm. A drug-loaded lens is placed over a mount with radius of curvature of 8.75 ± 0.10 mm and the device is sealed against a glass plate.

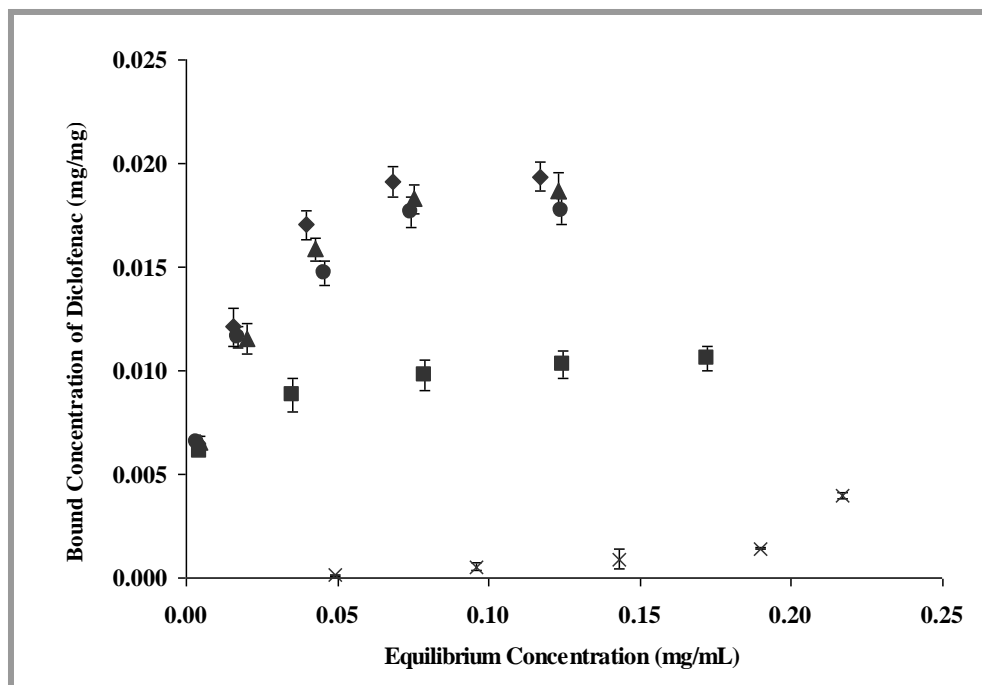


Figure 6.2: Equilibrium binding isotherm for poly(HEMA-co-DEAEM-co-PEG200DMA)

Imprinted hydrogels: FM/T= 1(◆), FM/T = 3.5 (▲) and FM/T = 10.5 (●) bound more diclofenac sodium compare with control (non-imprinted) hydrogels (■) and imprinted poly(HEMA-co-PEG200DMA) hydrogels (×). The data is plotted as the mean \pm SD (n=3).

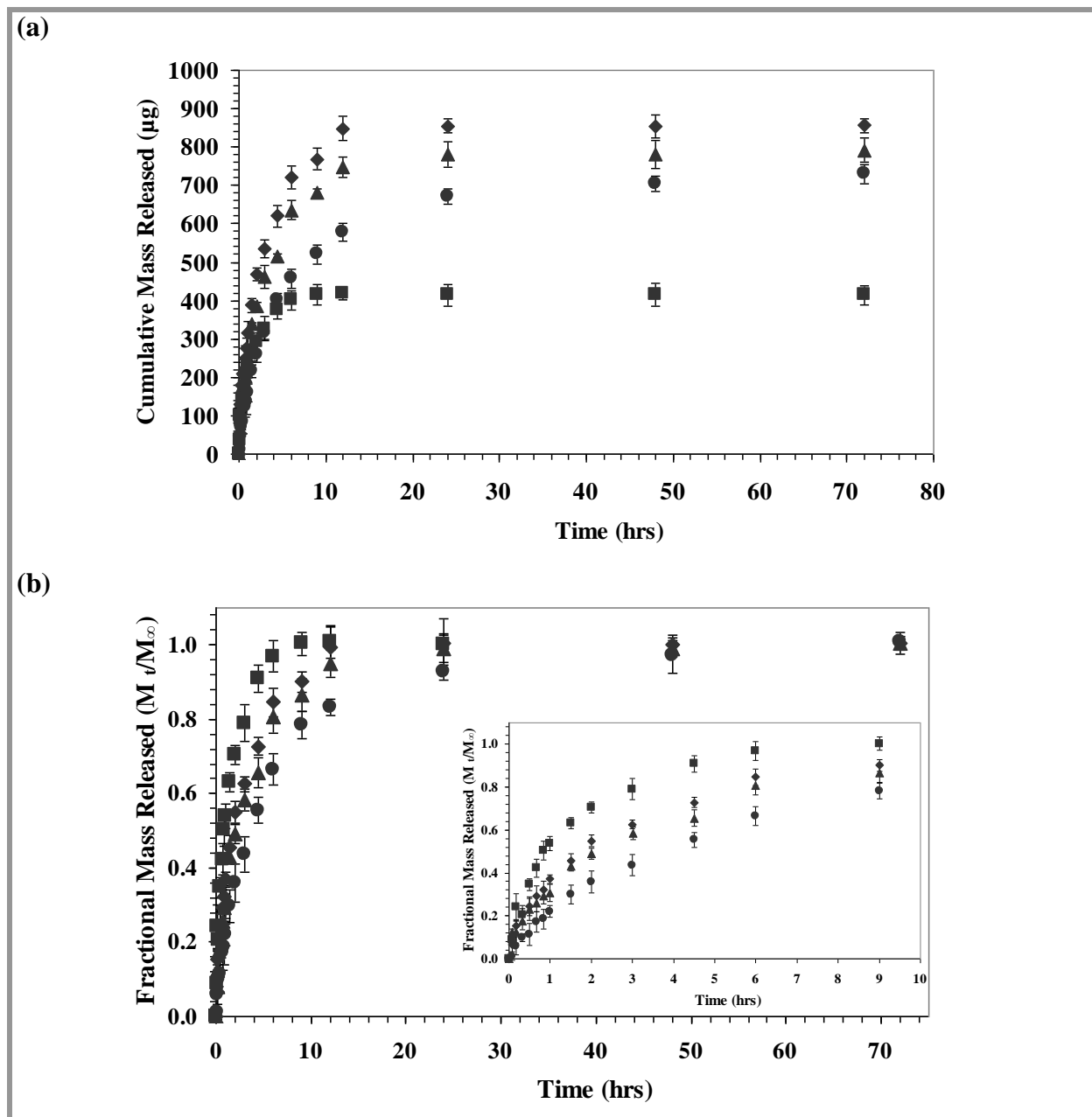


Figure 6.3: Infinite sink drug release of diclofenac sodium for poly(HEMA-co-DEAEM-co-PEG200DMA) contact lenses

(a) Cumulative release and (b) fractional release profiles of diclofenac sodium from therapeutic contact lenses in artificial lacrimal solution. Imprinted contact lenses FM/T= 1(◆), FM/T = 3.5 (▲) and FM/T = 10.5 (●) had extended release in lacrimal solution when compare with the control (■). Lens details: 105±5 µm thickness, diameter 15.0±0.2 mm, base curve of 8.6±0.2 mm, previously loaded in a 0.25mg/mL diclofenac solution. The data is plotted as the mean ±SD (n=3).

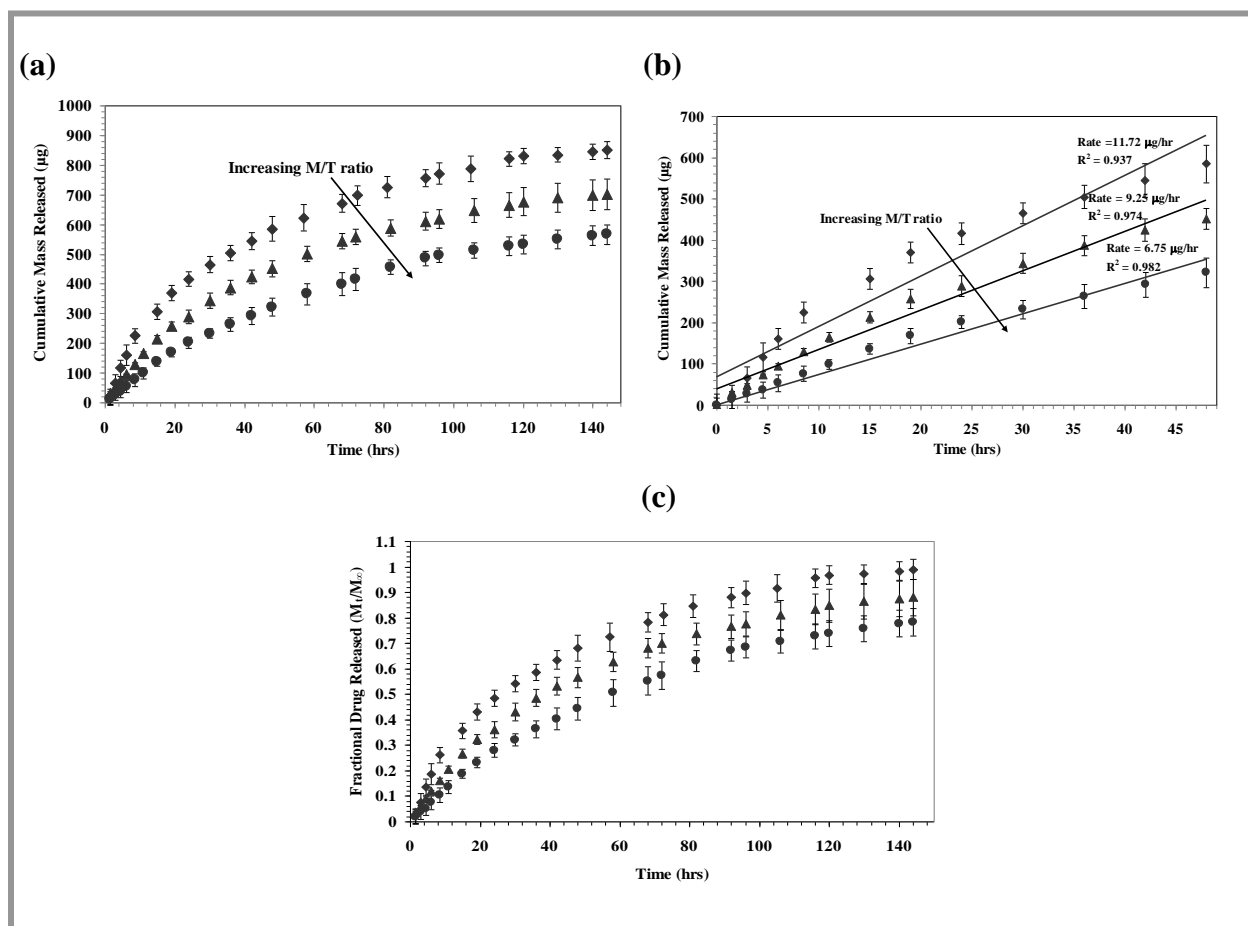


Figure 6.4: Cumulative and fractional diclofenac release from imprinted contact lenses in a physiological flow

(a) Cumulative of diclofenac sodium attained in 6 days, (b) cumulative of diclofenac sodium for 48 hrs, and (c) fractional mass released from poly(HEMA-co-DEAEM-co-PEG200DMA) contact lenses in artificial lacrimal fluid via steady in vitro physiological flow rate of 3 µL/min using the microfluidic device. Imprinted contact lenses FM/T= 1(♦), FM/T = 3.5 (▲) and FM/T = 10.5 (●). As the FM/T ratio increases the release rate decreases. Lens details: 105±5 µm thickness, diameter 15.0±0.2 mm, base curve of 8.6±0.2 mm, previously loaded in a 0.25mg/mL diclofenac solution. The data is plotted as the mean ±SD (n=3).

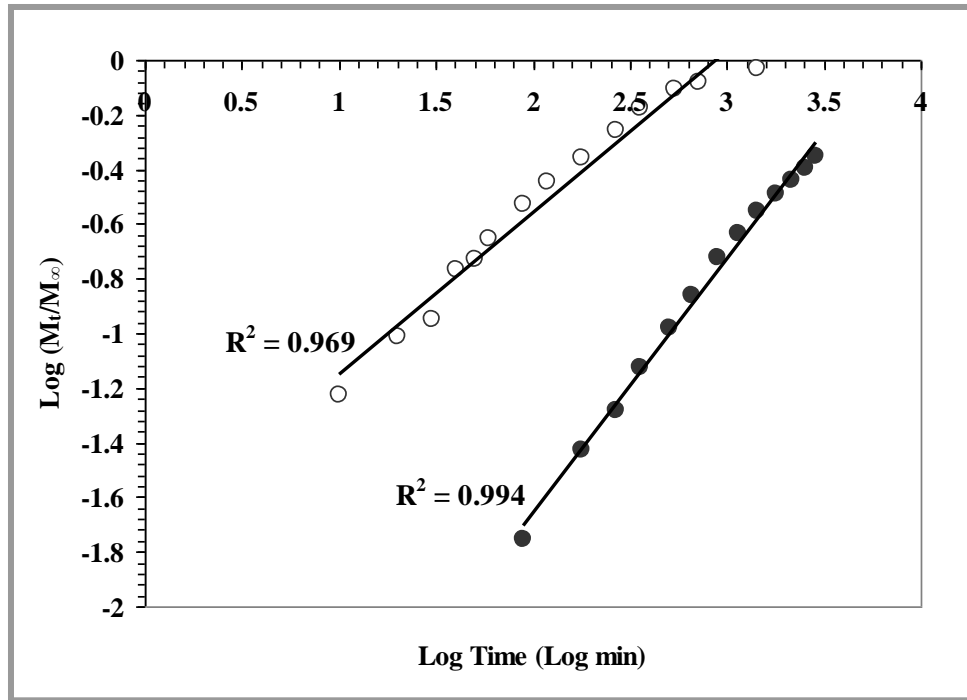


Figure 6.5: Zero-order of release for imprinted lenses in physiological flow

The slope yields n , where $n-1$ is the order of release. For the infinite sink method (○, $n=0.591$) and the physiological flow case utilizing the microfluidic device (●, $n=0.935$, zero-order) for poly(HEMA-co-DEAEM-co-PEG200DMA) FM/T 10.5 contact lenses.

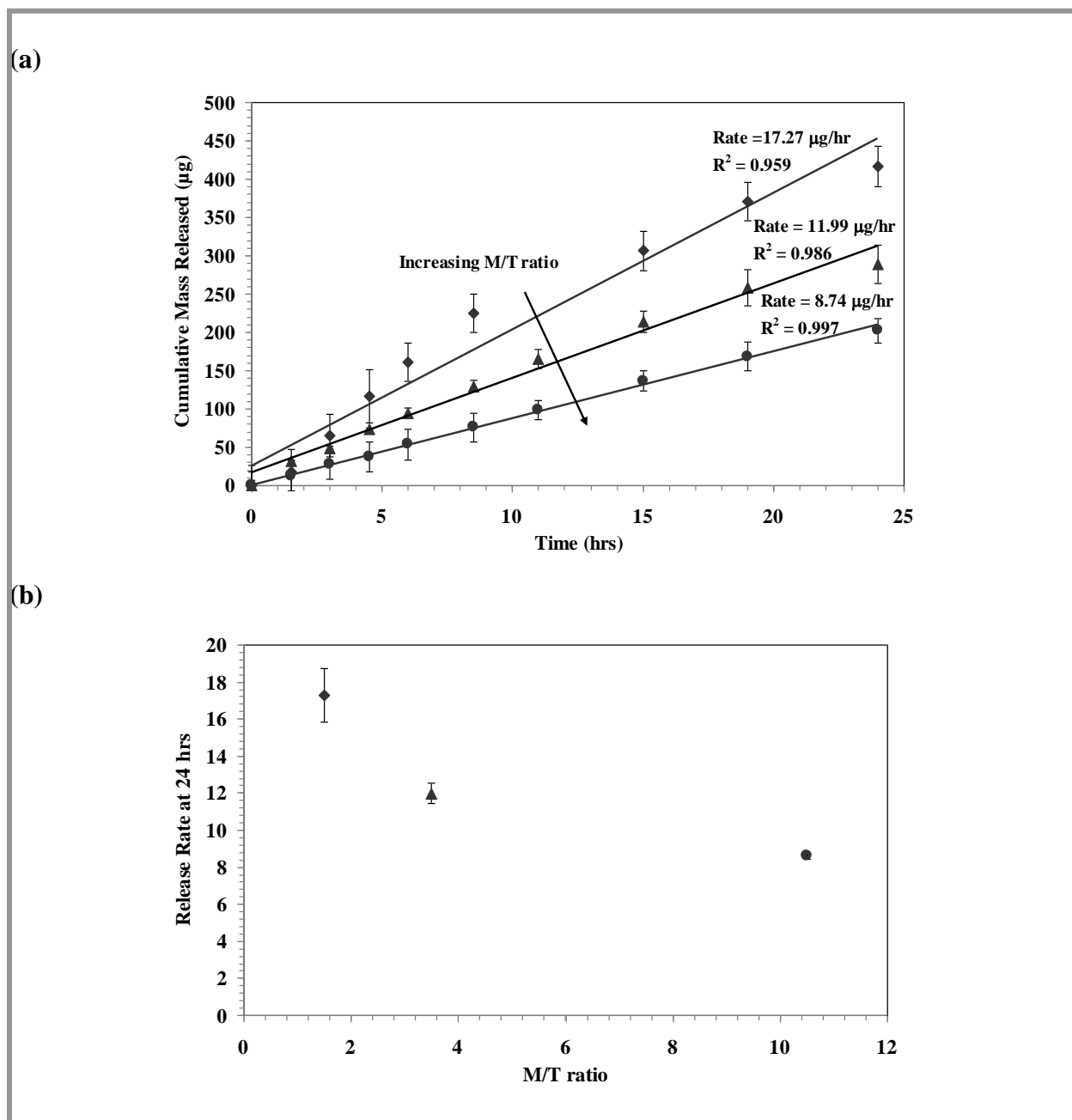


Figure 6.6: Release rate for 24 hours for poly(HEMA-co-DEAEM-co-PEG200DMA) contact lenses

(a) Cumulative release profiles and (b) release rate vs FM/T ratio. Imprinted contact lenses FM/T= 1(\diamond), FM/T = 3.5 (\blacktriangle) and FM/T = 10.5 (\bullet). Error bars represent the standard error for the rate.

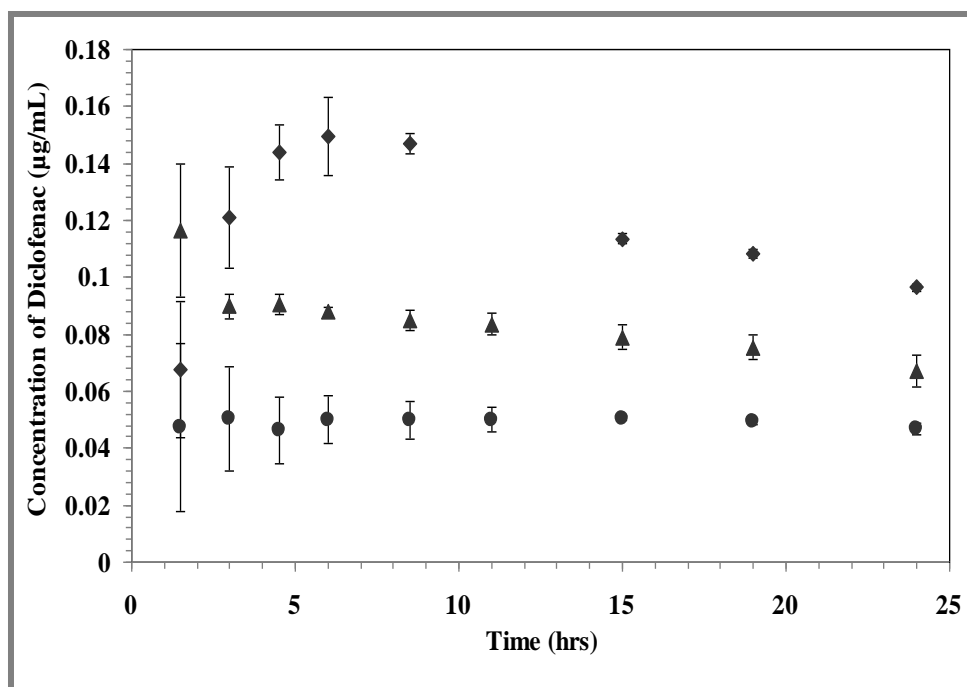


Figure 6.7: Relative constant diclofenac concentration for 24 hours for poly(HEMA-co-DEAEM-co-PEG200DMA) contact lenses

The imprinted loaded contact lenses can be designed to release the drug at the required therapeutic rate without the variation in concentration observed with eye drops. Imprinted contact lenses FM/T = 1 (♦), FM/T = 3.5 (▲) and FM/T = 10.5 (●). The data is plotted as the mean \pm SD (n=3).

Chapter 7

Engineering Therapeutic Contact Lenses for Delivery of Non-Steroidal Anti-Inflammatory Drugs

In the ocular drug market, there is a considerable unmet need and strong motivation for more efficient delivery of ocular therapeutics. This study was sponsored by CIBA Vision, Inc., a major producer of contact lenses and lens care products, to assess the synthesis of a daily disposable contact lens to control the release of diclofenac sodium for an extended period of time, using its patented hydrophilic macromer Nelfilcon A. Nelfilcon A also permitted the study of the imprinting effectiveness on a large hydrophilic network structure. In addition, Lotrafilcon B (LFB), a patented silicone contact lens material used in some CIBA Vision, Inc. lens brands, was used to tailor the release rate of the drug by rationally altering the ratio of hydrophobic to hydrophilic co-monomer composition and network structure of the silicone hydrogel.

Nelfilcon A is primarily used for the synthesis of CIBA Vision Inc. daily-wear disposable contact lenses, such as, Focus® DAILIES® Progressives, Focus® DAILIES® with AquaRelease, Focus® DAILIES® Toric, DAILIES® AquaComfort Plus®, and FreshLook® Color Contact Lenses. The water content of these type of lenses is 69% [211]. Daily disposable lenses are one class of contact lenses currently in the market. They are inexpensive and designed to forego the need for daily cleansing and storage of contact lenses by the user. A new lens is worn daily while the old lens is discarded. Daily disposable lenses are recommended for patients with ocular allergies, to prevent the accumulation of dust and other allergens on the lens [96]. Even though, Nelfilcon A lenses are daily disposable, they have been worn for multiple days

[212]. Up to today, several studies have been performed using Nelfilcon A lenses as drug delivery device. Supercritical solvent impregnation techniques were used in Focus® DAILIES® lenses, where impregnation of the drug (i.e. timolol, flurbiprofen) was minimum. Moreover, a burst release was observed and no control over the release was achieved [115]. On the other hand, release of comfort molecules from Nelfilcon A contact lenses has been achieved. Controlled release of hyaluronic acid (HA) from molecularly imprinted Nelfilcon A lenses demonstrated release at a relatively constant rate for up to 2 days [122]. CIBA Vision Inc. has two Nelfilcon A commercial lenses that release comfort agents to the surface of the eye. Focus® DAILIES® with AquaRelease lenses have an elution rate of polyvinyl alcohol (PVA) for ~15-20 hours [113, 213]. The newer version of these lenses, the DAILIES® AquaComfort Plus®, have been enhanced by the addition of polyethylene glycol (PEG), which binds to the PVA, increasing the molecular weight, hence prolonging the PVA+PEG release. Additionally, these lenses are packed in a solution of hydroxypropyl methylcellulose (HPMC), which promotes initial comfort upon insertion.

The size of the therapeutic and the size of the spaces available for diffusion within the polymer chains also influence the drug release rate. Since HA and PVA are long chain molecules their diffusion from the structure will be highly reduced compared to a small molecular weight molecule. It is important to mention that the release of a small hydrophobic charged molecule, such as diclofenac sodium, represents a major challenge.

Lotrafilcon B (LFB) is a silicone contact lens material used in CIBA Vision, Inc. lens brands, such as, AIR OPTIX® AQUA, AIR OPTIX® for ASTIGMATISM and AIR OPTIX® AQUA MULTIFOCAL. The water content of this type of lens is 33% [211]. Soft contact lenses based on silicone hydrogels are the most recent generation of contact lenses. Unlike traditional

hydrogel lenses, which are largely hydrophilic, silicone hydrogel lenses are biphasic systems. The silicone component (hydrophobic portion) of the lens material provides extremely high oxygen permeability, while the hydrogel component (hydrophilic portion) facilitates flexibility, wettability and ions transport, making them ideal for continuous wear (i.e. 5-7 days) and extended continuous wear (i.e. up to 30 days and nights). However, commercial silicone hydrogel contact lenses may have no appropriate composition to provide extended drug release [124]. Over the past few years, it has been speculated that the release of hydrophobic drugs from a silicone hydrogel lens can be affected by the hydrophobic siloxane components of the lens formulation [125]. Previous studies have shown that lens composition can alter release [214, 215]; however, there is little improvement in the loading when compared to drug soaked lenses. Thus, the release is fast and not very tailorable, and does not deliver therapeutic amounts.

The incorporation of a diffusion barrier (Vitamin E) into Lotrafilcon B discontinued lenses, O₂OPTIX™, to slow the release of loaded drug (i.e. dexamethasone, timolol, fluconazole) was performed. Loading of the barrier drug decreases the volume available for any secondary drug, resulting in lower drug mass uptake. The rate of release is strongly dependent on the concentration of the diffusion barrier [114, 137]. Molecular imprinting contact lenses, were engineered using Lotrafilcon B formulation to release HPMC, a comfort molecule [169]. Controlled release of HPMC was achieved for the duration of lens wear (i.e. up to 60 days).

7.1 Creating Memory in Nelfilcon A Lens.

Nelfilcon A has hydroxyl groups on its side chain and a neutral hydrophilic nature as HEMA. However, Nelfilcon A hydrogels have larger chain building blocks than imprinted

poly(HEMA-co-DEAEM-co-PEGnDMA) hydrogels studied in Chapter 5. Therefore, various approaches were sought to synthesize Nelfilcon A lenses to release diclofenac sodium.

By applying the principles of molecular imprinting functional monomers with similar chemical functionalities to mimic the natural receptor sites of diclofenac sodium were chosen. Acrylate and methacrylate monomers capable of similar non-covalent interactions and similar functional groups as those of tyrosine and serine were sought. Monomers with similar chemical groups are N-vinyl 2-pyrrolidinone (NVP), diethylaminoethyl methacrylate (DEAEM), N,N,N,N-diallyl dimethylammonium chloride (DADMAC), methacrylamide propyltrimethylammonium chloride (MAPTAC), and 2-hydroxyethylmethacrylate (HEMA). NVP, an aromatic lactam, can be seen as an analog to tyrosine for its aromaticity and hydrogen-binding capability. The hydroxyl group of HEMA can be seen as an analog for that of serine. Finally, DEAEM, DADMAC, MAPTAC are cationic monomers and at physiological pH are expected to form a stronger, ionic non-covalent bond with diclofenac sodium. Also, during the research, we focused on using functional monomers to form partial inclusion complexes with diclofenac sodium. It is well document that in solution diclofenac sodium forms an inclusion complex with cyclodextrins (CDs) by insertion of its dichlorophenyl ring [216-218]. Therefore, a functional monomer containing CDs was also used. Given the large mesh size of Nelfilcon A lenses and the small hydrodynamic radius of diclofenac sodium in water ($\sim 4.3 \text{ \AA}$); it was hypothesized that the addition of a large third molecule into the network would serve to physically restrict the transport of diclofenac sodium. Diethylaminoethyl-dextran hydrochloride (DEAE-Dextran), which is a polycationic derivative of Dextran was selected. Lastly, a positively charged surfactant, benzalkonium chloride (BAK), was used. Benzalkonium chloride is the most commonly used preservative among ophthalmic formulations, at an average concentration of

0.01% (range, 0.004%–0.025%), because of its long shelf life and ability to increase corneal drug penetration [219, 220]. Chemical structures of functional monomers are shown in Figure 7.1.

7.2 Materials and Methods

7.2.1 Reagents

Monomers such as 2-hydroxyethylmethacrylate (HEMA), diethylaminoethyl methacrylate (DEAEM), N,N,N,N-diallyl dimethylammonium chloride (DADMAC), methacrylamide propyltrimethylammonium chloride (MAPTAC) (50 wt % solution in water), and N-methylolacrylamide (NMA) (technical quality 48% in water), N,N-dimethyl acrylamide (DMA), ethylene glycol dimethacrylate (EGDMA) and the photo initiator, Darocur 1173 were purchased from Sigma-Aldrich (Milwaukee, WI). Diethylaminoethyl-dextran hydrochloride (DEAE-Dextran, MW~500kDa) and diclofenac sodium salt (DS) were purchased from Sigma-Aldrich (Saint Louis, MO). N-vinyl 2-pyrrolidinone (NVP), β -cyclodextrin, polyethylene glycol (200) dimethacrylate (PEG200DMA), and polyethylene glycol (600) dimethacrylate (PEG600DMA) were purchased from Polysciences, Inc. (Warrington, PA). Benzalkonium chloride (BAK) (alkyl distribution from C₈H₁₇ to C₁₆H₃₃) was purchased from Acros Organics (New Jersey, NJ). Formic acid 88% was purchased from Fisher Chemical (New Jersey, NJ). Methacryloxypropyl-tris-(trimethylsiloxy) silane (TRIS), Lotrafilcon B (a Betacon Macromer) and Nelfilcon A (a PVA macromer) were provided by CIBA Vision, Inc. (Duluth, GA). All components were used as received.

7.2.1.1 Nelfilcon A

Nelfilcon A is a hydrophilic polymeric material consisting of biocompatible polyvinyl alcohol (PVA) in aqueous solution, photocrosslinked into a network structure. PVA contains hydroxyl (OH) groups attached to a repeating polymeric backbone in the 1,3 position. These hydroxyl groups are perfectly positioned to undergo cyclic acetal formation upon reaction with aldehydes, and this mechanism is highly useful for the attachment of moieties necessary for hydrogel formation.

A novel aspect of Nelfilcon A is the lack of monomers in the prepolymerization solution, eliminating the need to purify the prepared lens. Actually, almost every component required for polymerization is attached to the PVA chains, thus, small unreacted monomers do not remain in the final hydrogel. This includes the crosslinkers, the initiator, and the tint where applicable.

The synthesis of Nelfilcon A was performed by CIBA Vision, Inc. (Duluth, GA) according to a two-step procedure [113]. First a diacetal with acrylate functionality, N-acryloylaminoacetaldehyde dimethylacetal (NAAADA), was synthesized by reacting aminoacetaldehyde with acryloyl chloride in a low-temperature alkaline aqueous solution. After neutralization and extraction, the crude product was purified through molecular distillation. In the second step, PVA was transacetylated with NAAADA resulting in PVA chains with a well-controlled number of pendant crosslinking acrylate groups per macromer chain [221]. A number of reactions were taking place at this acid catalyzed stage: the acetal of the crosslinker was hydrolyzed to aldehyde, the aldehyde reacted with the PVA, and some acetate groups remaining on the PVA from its synthesis were converted to hydroxyl groups, as shown in Figure 7.2. The added crosslinker was also modified by attaching the initiator Irgacure 2959. Atmospheric oxygen was used as the stabilizer for the acrylate. To make tinted lenses, a commercial dye such

as Remazol Brilliant Blue RTM was also activated and attached to PVA through acetylation. The reaction was quenched by neutralizing with alkali. The photopolymer was then purified by ultrafiltration to the desired purity and concentration.

7.2.1.2 Lotrafilcon B

Lotrafilcon B (LFB) is a silicone hydrogel material consisting of both hydrophilic and hydrophobic monomers with the main material a silicone-based macromer. The result is a biphasic system, where the silicone section (hydrophobic phase) is responsible for the high oxygen permeability, while the hydrophilic phase allows the transport of ions, protein and enzymes through the lens.

LFB is a mixture of the proprietary silicone hydrogel macromer (Betacon macromer), methacryloxypropyl-tris-(trimethylsiloxy) silane (TRIS), and N,N-dimethyl acrylamide (DMA). In the LFB lens formulations, the Betacon macromer serves as both the oxygen permeable phase and the crosslinking monomer. The synthesis of the Betacon macromer was performed by CIBA Vision, Inc. (Duluth, GA). The structures of the silicone hydrogel monomers are presented in Figure 7.3.

7.2.1.3 Synthesis of acrylanidomethyl-β-cyclodextrin (β-CD-NMA)

Acrylanidomethyl-β-cyclodextrin (β-CD-NMA) was prepared based on a method described by Lee et al. [222]. Briefly, for a NMA:β-CD mol ratio of 10, 5 g of pure β-CD, 390 μL formic acid and 11.78 mL of DI water were added to a three-neck reactor, equipped with a magnetic stirrer, a thermometer, and a condenser. The reaction started by addition of 8.64 mL of NMA solution. The mixture was stirred and heated at 80°C for 30 min and stopped by

precipitation using 100 mL of acetone. The acetone solution was kept at 4°C overnight and the precipitates were filtered (40 Ashless, Whatman®) and washed several times with acetone (four cycles). The precipitate was finally dried at 30°C under vacuum for 2 days and stored at 4°C. FTIR spectra of β -CD-NMA monomer was recorded over the range 400–4000 cm^{-1} in a NXR-FT-Raman spectrometer.

7.2.2 Synthesis of Nelfilcon A Contact Lenses

Nelfilcon A formulation previously prepared by CIBA Vision, Inc. was received and then frozen at -18°C. To produce lenses, the macromer (Nelfilcon A) was defrosted and reconditioned at 65-70°C for 30-35 minutes and left at room temperature (~22°C) to cool down before use.

The simplest system synthesized for the ocular delivery of diclofenac sodium to the eye is a crosslinked network of Nelfilcon A with diclofenac sodium molecules. To prepare a pre-polymerization mixture, 5 g of Nelfilcon A macromer were mixed with 32.5 mg of diclofenac sodium. Lenses were also prepared at other concentrations of diclofenac sodium such as 2 mg DS/g Nelfilcon, 4mg DS/g Nelfilcon, 8 mg DS/g Nelfilcon and 10 mg DS/g Nelfilcon. For additional formulations involving a slightly change in the chemistry of the polymer network, functional monomers such as, DADMAC, HEMA or β -CD-NMA, were also added at this stage, keeping a ratio of 6.5 mg of diclofenac sodium per gram of Nelfilcon A. The mixture was repeatedly stirred, centrifuged, and sonicated until diclofenac sodium was homogeneously incorporated into the pre-polymerization mixture. The sample was mixed overnight on a Rugged Rotator (Glass-Col LLC, Terre Haute, IN) to reach equilibrium. The mixture was finally centrifuged for 5 to 10 minutes to remove air bubbles.

Each formulation was identified by the percentage-by-mass of the total pre-polymerization mixture that was composed of added functional monomers (before the addition of DS). For instance, a formulation containing 95 wt.% of stock Nelfilcon A and 5 wt.% of added functional monomers was referred to as a 5% monomer composition. However, it should be noted that these are feed compositions and the final polymer composition may vary depending on the reactivity ratios of the corresponding monomers.

The pre-polymer mixture was pipetted into the polypropylene (PP) contact lens molds provided by CIBA Vision, Inc. (Series No.: EV86-100 and EV86-BCBP). The lens was polymerized via UV-light free radical polymerization using a UV light source (Novacure 2100, Exfo, Mississauga, Canada) with an intensity of $\sim 15 \text{ mW/cm}^2$ measured by radiometer (International Light IL400A, Peabody, MA). The duration of exposure was from 3.5 to 10 minutes depending of the formulation (separate differential photocalorimetry (DPC) studies revealed exact reaction times). The lenses were then removed from the mold and used immediately. Lenses were produced with a swollen center thickness of $110 \pm 12.5 \text{ }\mu\text{m}$, a diameter of $14.2 \pm 0.2 \text{ mm}$ and a base curve of $8.6 \pm 0.2 \text{ mm}$.

We hypothesized that when the functional monomers are added to the formulation mixture and allowed to equilibrate with the template, the monomers would prefer to be spatially arranged in a low energy configuration. Such a configuration would favor electrostatic and polar interactions between the monomers and the template, much like the interactions between amino acids and template in biological binding sites. When the gel is crosslinked, the functional chemistry of the monomers would be immobilized in these favorable configurations, creating sites within the network with a stronger affinity for template than areas with similar chemical

composition and random configuration. The lens synthesis protocol was modified by adding appropriate amounts of functional monomers.

7.2.3 Synthesis of Silicone Contact Lenses

Silicone hydrogel lenses were produced using a commercial lens formulation known as Lotrafilcon B (LFB). Silicone hydrogel lenses of several compositions were prepared by mixing the individual monomers of the LFB formulation (Betacon Macromer, TRIS and DMA), and if applicable with crosslinking monomers. Table 7.1 shows the composition of the pre-polymer formulations. Ethanol was added to aid in solubilization, and Dorocur 1173 was used as the initiator. The samples were repeatedly vortexed and sonicated until evenly dispersed. The mass ratio of Macromer/TRIS:DMA was varied as well as the percent of crosslinking monomer. The compositions presented herein were chosen in order to demonstrate the full range of control obtained by altering the Macromer/TRIS:DMA mass ratio (i.e. to evaluate the boundaries of release control).

Table 7.1: Silicone contact lens formulations

Lens	Macromer/TRIS:DMA mass ratio	Macromer (mg)	TRIS (mg)	DMA (mg)	EGDMA (mg)	Ethanol (mg)
LFB1	0.76:1	1050	850	2500	--	500
LFB2	1.50:1	1250	1000	1500	--	1150
LFB3	7.50:1	2000	1750	500	--	650
LFB4	2.18:1	1500	1450	1350	100	500

The pre-polymer mixture was pipetted into polypropylene (PP) contact lens molds provided by CIBA Vision, Inc. (Series No.: EV86-100 and EV86-BCBP). The lens was polymerized via UV-light free radical polymerization with an intensity of ~ 25 mW/cm² for duration of 1.5 min. Silicone hydrogel lenses were washed with ethanol for 24 hours and later

placed in deionized water (Millipore, 18.2 MΩcm, pH 6.2) until unreacted monomers could no longer be detected by spectroscopic monitoring (Synergy Biotek UV–Vis Spectrophotometer, BioTek Instruments, Vermont, USA). Swollen clean lenses (n=4) were randomly taken and physical parameters were measured; the results are listed in Table 7.2.

Table 7.2 Physical parameters of the silicone contact lenses in swollen state

Lens	Central thickness (μm)	Diameter (mm)	Weight (mg)
LFB1	118.0±2.0	17.7±0.2	46.2±0.5
LFB2	98.7±2.9	14.8±0.2	30.0±1.1
LFB3	98.0±2.5	14.1±0.2	24.5±0.6
LFB4	98.6±1.9	14.7±0.1	31.2±0.7

The data are presented as mean ± SD (n=4).

Lastly, all silicone lenses were dried at room temperature for 24 hours, followed by vacuum drying (T=30 °C, 28 in. Hg vacuum), until the weight change was less than 0.1 wt%.

7.2.4 Diclofenac Sodium Loading Studies

The unique process used to make Nelfilcon A lenses allows one to formulate most polymeric and high molecular weight ingredients directly into the processing of the final contact lens (the lens does not have to be extracted to remove residual toxic monomers) [221]. Therefore, the final lenses do not have to re-loaded with the desired compound, instead a direct embedding of diclofenac sodium to the pre-polymerization mixture was the method used to load diclofenac sodium into the lenses.

Dry silicone contact lenses were placed into vials with 5 mL of a 0.05 mg/mL solution of diclofenac sodium; the vials were gently agitated for 10 days on an ocelot rotator (Fisher Scientific; Chicago, IL) at 75 rpm and 12° tilt angle. Separate experiments were conducted to assure equilibrium.

7.2.5 Dynamic Release Studies

Dynamic release studies were conducted to measure how long a therapeutic contact lens would release drug *in vitro*. The studies were conducted under infinite sink conditions in order to sustain the greatest driving force, using a dissolution apparatus from SOTAX Inc. (Hopkinton, MA), in which loaded lenses were placed in 200 mL of DI water (Millipore, 18.2 MΩcm, pH 6.4). The release media was stirred at a constant rate 30 rpm by paddles and kept at a constant temperature of 34°C. Samples were taken at various time intervals and analyzed by photospectrometry in a Synergy UV/Vis spectrophotometer (BioTek Instruments, Winooski, VT) at a wavelength of 276 nm. Diclofenac sodium concentration was determined from a standard curve created by measuring the absorbance of known concentrations (0.005, 0.01, 0.05, 0.1, 0.15, 0.20, 0.25 mg/mL) of diclofenac in DI water and artificial lacrimal solution.

For diclofenac sodium containing lenses, benchmark studies were conducted at various stirring rates (Figure A1, Appendix A). Studies were also conducted to validate the sink conditions comparing the dissolution apparatus release profiles with those from an ocelot rotator (Fisher Scientific; Chicago, IL) at 75 rpm and 12° tilt angle (Figures A2 & A3, Appendix A), where after measured time intervals, the lenses were extracted and deposited into fresh DI water. This "replacement protocol" has the advantage that it produces the closest release environment to the "infinite sink" model.

Cumulative mass release curves were plotted for each lens formulation, and the data was used to calculate the rate of diffusion of template from the lens (Equation 4.8). As the length of the exposed surface of the lens was greater than ten times the thickness, edge effects were ignored and assumed the system was planar with diffusion occurring in one-dimension. An empirical power law equation was used to determine the order of release (Equation 4.9).

7.2.5.1 Effect of ionic strength in the release of diclofenac sodium

Most NSAIDs salts are charged molecules at physiological pH. Therefore, diclofenac sodium transport may be affected by the ionic strength. To study this effect release experiments for diclofenac sodium were also performed in a PBS buffer solution, pH 7.0. In these experiments the ionic strength was changed by adding KCl to the PBS buffer to a corresponding ionic strength of 0.5M and 1.0M. Release studies were also performed in artificial lacrimal solution, isotonic with human tears (6.78 g/L NaCl, 2.18 g/L NaHCO₃, 1.38 g/L KCl, 0.084 g/L CaCl₂ 2H₂O, pH 8) [223].

7.2.6 Swelling Studies and Tensile Studies

Hydrogel structural analysis was obtained by swelling and tensile experimental studies. Contact lenses were dried at room temperature for 24 hours and then dried in a vacuum oven at $32 \pm 1^\circ\text{C}$ and 28 in. Hg until the weight change in the lenses was less than 0.1% (at least 7 days).

Contact lenses were subject to the analysis described in section 4.2.1. Dry contact lenses were weighted on a Sartorius scale. Afterward, a density determination kit was installed on the scale. The mass of the dry lens was then weighted in heptane, a non-solvent (density of 0.684 g/mL at a temperature of 25°C). After being weighted in the dry state, lenses were placed in DI water and allowed to swell to equilibrium. The experiment was repeated for swollen lenses. Once measurements were taken, Archimedes buoyancy principle [200] was used to calculate the density of the dry and swollen lenses as shown in equation 4.13. The specific volume of the hydrogel was calculated as the reciprocal of density. The volume swelling ratio (Q) and the polymer volume fraction in the swollen state ($v_{2,s}$) were calculated. Q is the ratio of the swollen

to dry volumes of the hydrogel, $v_{2,s}$ is the inverse of the volume swelling, and $(1 - v_{2,s})$ gives the fractional water content of the hydrogel.

Equilibrium weight swelling ratios (q) were obtained by placing dried lenses in DI water and artificial lacrimal solution until they reached equilibrium. The lenses were then removed from the solutions, patted dry with a soft tissue (Kimwipes[®]), and weighted in air. Weight swelling ratios (q) were calculated as the ratio of the swollen weight at equilibrium to the dry weight. Dynamic swelling studies were conducted by placing dried lenses in DI water or lacrimal solution, removing them at designated time intervals, patting them with a soft tissue, weighing them, and then returning them to the solution.

Stress–strain data were obtained by performing tensile studies with a RSA III Dynamic Mechanical Analyzer (DMA), (TA Instruments, New Castle, DE). A linear load stress at a constant rate of 4 mm/min was applied to hydrated hydrogels prepared in strips (8mm × 30 mm × 0.25mm, in triplicate). The gels were fully hydrated through the experiment, and the modulus was calculated from the initial slope of the stress vs. strain curve.

7.2.7 Optical Clarity Studies

Optical clarity studies were conducted by measuring the percent transmittance of visible light (wavelength range from 450-750nm) through swollen lenses. Lenses from the molds were cut with a No. 3 cork borer and placed in the bottom of a 96 well plate where absorbance values were measured via spectrophotometric monitoring (Biotek, Winooski, VT). Each sample lens was cut into at least three samples to note any local differences within the lens. All films were fully hydrated in 200 μ L of water with care taken that the film was in full contact with the bottom of the well plate and no air bubbles were present. The absorbance value of each well with

DI water was calculated and subtracted from the data. Percent transmission values were calculated from the optical density and absorbance data. Furthermore, in some cases, optical clarity measurements were taken from the pre-polymer mixture, and 200 μL of pre-polymer mixture was placed into a 96 UV well plate. All optical clarity experiments were carried out in triplicate with three separate lenses.

7.3 Results and Discussion

7.3.1 Dynamic Release of Diclofenac Sodium from Nelfilcon A Lenses

Dynamic diclofenac sodium (DS) release was first studied from Nelfilcon A lenses synthesized with diclofenac sodium included in the formulation (6.5 mg DS per gram of Nelfilcon A formulation). Figure 7.4 shows the cumulative mass of diclofenac sodium released from Nelfilcon-DS lenses in DI water. A Fickian or concentration-dependent release profile was demonstrated with most of the loaded diclofenac sodium being released in less than 2 hours. The release rates can be classified into three general zones. Initially, diclofenac sodium was released at a rate of around 641 $\mu\text{g/hr}$ ($\sim 10.7 \mu\text{g/min}$) for the first few minutes. During this period, a significant amount ($\sim 50\%$) of loaded diclofenac sodium was released. A linear release profile delivering $\sim 30.1 \mu\text{g/hr}$ ($\sim 0.5 \mu\text{g/min}$) was demonstrated over a period of ~ 1.5 hours. Finally, the release gradually decreased until very low diclofenac sodium amounts were released.

In order to preliminary assess the release rates, a comparison of topical diclofenac sodium eye drops is needed. Voltaren Ophthalmic[®] Drops is the topical alternative and consists of a 0.1% solution of diclofenac sodium or 1 mg DS/mL. For example, consider the recommended dosage of Voltaren[®] after cataract surgery: 1 drop 4 times daily, beginning 24 hours after surgery and continuing for two weeks. Assuming the volume of a typical eye drop is 20 μL , the delivered

dose would be 20 µg of diclofenac sodium every 6 hours or 3.33 µg/hour. As the bioavailability of a topically applied drug is generally low (<7%), it appears that the Nelfilcon A lens delivers a much higher therapeutic amount of diclofenac sodium. It is also clear that the lenses have an inadequate duration of release and a non-uniform rate. However, an additional level of control over the release rate may be achieved by incorporating functional monomers that interact with diclofenac sodium into the lens. One must also consider that any lens would release diclofenac sodium *in-vivo* at a reduced rate compared to the infinite sink data shown in Figure 5.4 due to the significantly reduced sink *in vivo*. However, diclofenac sodium release would still be non-uniform and not occur for a significant duration, probably approaching 4-6 hours.

Figure 7.5 shows the release curves in DI water obtained from lenses made with formulations containing 2 mg/g, 4 mg/g, 6.5 mg/g, 8 mg/g and 10 mg/g of DS in Nelfilcon. Release profiles are very similar and, in all cases, fractional release was not dependent on diclofenac sodium loading concentration (Figure A4, Appendix A). Along with Figure 5.4, the results indicate that diclofenac sodium can be loaded in amounts that will be needed to sustain an extended release of a therapeutic amount for 24 hours and beyond.

Figures 7.6 shows the percent transmittance from lenses producing with 2 mg/g, 4 mg/g, 8 mg/g and 10 mg/g of DS in Nelfilcon, as well the percent transmittance after these lenses were released in DI water. At relatively low diclofenac sodium concentrations above 2mg/g DS in Nelfilcon, there was a significant decrease in percent transmittance as the loading concentration of diclofenac sodium increased (Figure A.5, Appendix A). It is important to note that the decrease is not due to the absorption of light by diclofenac sodium (data not shown).

The Nelfilcon A formulation was modified by adding different proportions by mass of 2-hydroxyethyl methacrylate (1.3%, 2.7% and 3.81% HEMA) as functional monomer and the

lenses were synthesized in the presence of diclofenac sodium. Dynamic release studies in DI water for lenses prepared with HEMA are presented in Figures 7.7a and 7.7b, which shows that release rate is slower compared to control lenses (Nelfilcon A lenses prepared with diclofenac sodium and no functional monomers). Also, the cumulative diclofenac sodium mass released tends to decrease as the proportion of HEMA is increased or the functional monomer to template (FM/T) ratio is increased (Figure 7.7a). After approximately 1 day, the diclofenac sodium release rate decreased significantly; however the study was continued for one week (Figure A.6, Appendix A). Thus, it is clear that the additional of HEMA was affecting the release rate, but no remarkable differences in the diclofenac sodium diffusion coefficients were found, therefore the fractional release is not dependent on HEMA loading concentration (Figure 7.7b). Also, the addition of HEMA resulted in lenses with decreased optical clarity. Transmittance was approximately 60% in all lenses studied that contained HEMA (Table 7.5).

Due to poor optical clarity of lenses with the addition of HEMA, and the possibility that diclofenac sodium may not be significantly receptive to extra-molecular hydrogen bonding, due to its having an intramolecular hydrogen bond between its carboxyl oxygen and its amino hydrogen [40, 198, 199], another approach was considered. Diclofenac sodium has a pKa value of ~4 and its acidity is such that at physiological pH of 7.4 or more, the molecules are dissociated to more than 99%, exhibiting a negative charge [196]. Quaternary amines, N,N,N,N-Diallyl dimethylammonium chloride (DADMAC) and methacrylamide propyltrimethylammonium chloride (MAPTAC), were selected that exhibit a positive charge and differing strengths of complexation with diclofenac sodium. Lenses were synthesized containing different proportions by-mass of DADMAC (0.5%, 1%, and 2%) and MAPTAC (2% and 5%). Dynamic cumulative and fractional diclofenac sodium release studies in DI water for lenses prepared with DADMAC

functional monomer are presented in Figures 7.8 and 7.9, respectively. The results demonstrate that the incorporation of functional monomers delays the release rate of the template. As the amount of DADMAC was increased in the lens (or FM/T ratio is increased), the cumulative diclofenac sodium mass release rate tended to decrease (Figure 7.8). Optical clarity at visible wavelengths was favorable, with a minimum transmittance of 85% and a maximum of 91% (Table 7.5). For the lenses containing 2% DADMAC, the release rate was the slowest and can be classified into two general zones. Initially, diclofenac sodium was released at a linear rate of around 0.1 $\mu\text{g}/\text{min}$ (6 $\mu\text{g}/\text{hr}$) for 24 hours (Figure A.7, Appendix A). For the following 48 hours, small amounts of diclofenac sodium were released at a rate of 0.004 $\mu\text{g}/\text{min}$ (0.24 $\mu\text{g}/\text{hr}$).

The release profile can be subjected to the analysis described in section 4.1 to determine the order of release and diffusion coefficient of diclofenac sodium from the DADMAC lenses. From Equation 4.8, the M_t/M_∞ versus $(t/L^2)^{1/2}$ can be plotted and the diffusion coefficient can be calculated by setting the slope equal to $4(D/\pi)^{1/2}$. The order of release is $1/n-1$ when n is equal to the slope of $\text{Log}[M_t/M_\infty]$ versus $\text{Log}[t]$ (Figure 5.10). The calculated diclofenac sodium diffusion coefficients and the orders of release for the DADMAC containing lenses are presented in Table 7.3. The 2% DADMAC lens diffusion coefficient of diclofenac sodium was a factor of 3.2 and 16.5 less than the 1% DADMAC lens and 0.5% DADMAC lens, respectively.

Table 7.3: Diclofenac sodium diffusion coefficient and release order from Nelfilcon A lenses with varying DADMAC proportions

Lens	FM/T ratio	Diffusion Coefficient (cm^2/s)	Release Order ($n-1$)
2.0 % DADMAC	6.0	$1.192 \pm 0.001 \times 10^{-10}$	0.36 ± 0.02
1.0 % DADMAC	3.0	$3.820 \pm 0.005 \times 10^{-10}$	0.59 ± 0.03
0.5 % DADMAC	1.5	$1.961 \pm 0.004 \times 10^{-9}$	0.76 ± 0.02

The data are presented as mean \pm SD (n=3).

These results show that therapeutic release can be tailored via the incorporation of functional monomers within the polymer chains, through the type and amount of functionality present within the polymer. By controlling the FM/T ratio, one can control the delivery rate. The fractional release profile (Figure 7.9) and the release order (Table 7.3) show that diclofenac sodium release is more constant, less Fickian, and moving toward zero-order release as the amount of DADMAC is increased in the lens.

From Chapter 5, it is known that the presence of salts and ions in lacrimal solution alters interactions between the anionic template molecule and cationic monomer. Therefore, release studies were conducted in PBS buffer solutions with different ionic strengths (0.5M and 1.0M, pH 7) and artificial lacrimal solution (pH 8). For lenses containing 2% DADMAC, the release was markedly different than the relatively constant release profile demonstrated previously in DI water. The cumulative release profiles are presented in Figure 7.11, which shows a very quick release when the lenses are placed in solutions that contain ions, confirming that a strong, non-covalent ionic bond exists between DADMAC and diclofenac sodium. Moreover, release studies were performed with lenses containing increased amounts of DADMAC monomer in the formulation (10% and 15%) as well as DADMAC:HEMA (2%:1% , and 1.75%:1.75%), to mitigate diclofenac sodium release by providing non-ionic interaction to limit the decomplexation of DADMAC and diclofenac sodium. However, the release in lacrimal solution was not extended, releasing more than 80 % of the template in the first 10 minutes (Figure A.9, Appendix A).

Figure 7.12 highlights the use of another positively charged monomer (MAPTAC), which did not extend the release of diclofenac sodium in DI water compared to the lenses containing DADMAC. Also, there was still a quick diclofenac sodium release when the lenses were placed

in artificial lacrimal solution, and the transmittance of lenses containing MAPTAC was less than 68%. It is interesting to compare the release of lenses containing similar amounts of MAPTAC and DADMAC. A larger amount of MAPTAC is needed to obtain a similar release profile, indicating that the DADMAC-DS non-covalent complexation is much stronger.

To further understand these results, it was necessary to determine if a structural change in the network happened when release occurred in artificial lacrimal solution, as compared to DI water. Equilibrium weight swelling studies in artificial lacrimal solution and DI water were performed using lenses prepared with 2% DADMAC and 5% MAPTAC. These lenses were also compared to pure Nelfilcon A lenses and Nelfilcon A lenses prepared with diclofenac sodium. As shown in Table 7.4, no significant differences in swelling are observed for each lens when it is placed in DI water or lacrimal solution.

Table 7.4: Equilibrium weight swelling values compared for lenses containing DADMAC and MAPTAC

Lens	Equilibrium Weight Swelling Ratio (q) in DI Water	Equilibrium Weight Swelling Ratio (q) in Lacrimal Solution
DADMAC 2 %	3.35 ± 0.05	3.38 ± 0.01
MAPTAC 5 %	2.82 ± 0.01	2.87 ± 0.02
Pure Nelfilcon	3.07 ± 0.03	3.10 ± 0.03
Nelfilcon-DS	3.03 ± 0.03	3.10 ± 0.02

The data are presented as mean ± SD (n=3).

The results are interesting considering the lenses prepared with MAPTAC exhibit the lowest equilibrium swelling ratio and the lenses prepared with DADMAC (which have the slowest release profile) exhibited the highest swelling. These results point toward a loss of ionic complexation as the primary cause for the pre-mature release of diclofenac sodium in artificial lacrimal solution.

It was hypothesized that multiple non-covalent interactions would be needed in order to delay release in artificial lacrimal solution or *in-vivo*. Therefore, our approach was refined to include monomers that can create a cavity with multiple functional sites to interact with the both the phenyl groups and the negative charge on the diclofenac sodium molecule. β -Cyclodextrin (β -CD) was selected as one of these monomers. It contains hydroxyl groups located at the outer surface of the molecule, which makes β -CDs water-soluble (and soluble in Nelfilcon), but simultaneously generates an inner cavity that is relatively hydrophobic. β -CDs can either partially or entirely accommodate suitably sized lipophilic low molecular weight molecules. The main driving force behind the formation of these so-called host-guest inclusion complexes are hydrophobic and van der Waals interactions [73]. In solution, the inclusion of diclofenac sodium occurs by insertion of the dichlorophenyl ring into the cavity of the β -CD [216], still allowing us to potentially exploit the negative charge of the molecule. To produce Nelfilcon A lenses with cyclodextrin covalently attached to the network, a β -CD monomer is needed. In order to synthesize acrylanidomethyl- β -cyclodextrin monomer (β -CD-NMA), conditions were chosen to obtain 1 mmol of $\text{CH}_2=\text{CH}-$ per gram of β -CD (β -CD-NMA). The formation of β -CD-NMA was confirmed by FTIR. Compared to the FTIR spectrum of β -CD, the spectrum of β -CD-NMA showed three clear additional bands around 1670, 1628 and 1570 cm^{-1} , which corresponded to the amide I C=O stretching peak, the C=C vinyl stretching peak, and to the amide II NH stretching peak. β -CD-NMA molecular weight was estimated as 1219 Da (from the molecular weight of one β -CD and one NMA substituent).

Lenses with 2% and 5% of β -CD-NMA monomer were synthesized. As shown in Figure 7.13, the release of diclofenac sodium in DI water was delayed. As β -CD-NMA is increased in the lens, the diclofenac sodium release rate decreased. However, the optical clarity was much

less than the lenses containing DADMAC (Table 7.5), and a larger amount of monomer would be needed to achieve an equivalent reduced release rate. It is important to note that a quick release of diclofenac sodium also occurred in lacrimal solution.

Given the large mesh size of Nelfilcon A lenses (Table 7.6) and the small hydrodynamic radius of diclofenac sodium in water ($\sim 4.3 \text{ \AA}$), it was hypothesized that the addition of a large third molecule into the network would serve to physically restrict the transport of diclofenac sodium. Diethylaminoethyl-dextran hydrochloride (DEAE-Dextran), which is a polycationic derivative of Dextran, was selected. Figure 7.14 highlights lenses using 2% of DEAE-Dextran (MW \sim 500 KDa) as a diffusion barrier. In DI water, similar diclofenac release was achieved as lenses with 2 % DADMAC. The only exception was that there was a delay in release for approximately 60 minutes from the barrier lens. It appears that the lens delivers therapeutic amounts of diclofenac sodium at a controlled rate. The ionic, non-covalent complexation between diclofenac sodium and the DEAE-Dextran leads to longer diffusion transport times in DI water. However, when the lenses were placed in lacrimal solution, a fast diclofenac sodium release occurred. Optical clarity at visible wavelengths was favorable, with a transmittance of 90%.

Lastly, release studies for 24 hours in lacrimal solution were carried out on hydrogels containing 3% BAK. The highest % transmittance, 96 %, and the best qualitative properties are achieved with this formulation. Figure 7.15 shows the dynamic release in DI water and lacrimal solution of DAILIES[®] lenses prepared with BAK. The release of diclofenac sodium in DI water is slower than control lens prepared with Nelfilcon containing diclofenac sodium, but it is faster compared to the imprinted lenses made with DADMAC. Nevertheless, a controlled release in lacrimal solution was achieved. The concentration of BAK used in this formulation is much

higher than the critical micelle concentration of BAK (0.17 g/dL). It is hypothesized that BAK forms complexes with diclofenac sodium and the long carbon chain of BAK shields diclofenac sodium from contact with the species in the aqueous lacrimal solution, leading to a delay in the release. Experiments were done to assess the potential interference of BAK with diclofenac sodium concentration measurements. Results demonstrated that BAK does not interfere with diclofenac sodium concentration determination at the concentrations used in this study (data not shown). The release of BAK was not measured. A major drawback with this system was the cytotoxic side effects of BAK [224]. However, the results are encouraging as to potential directions to provide delayed release in lacrimal solution. Pluronic surfactants (31R1, 17R4 25R4 and 10R5) were also used. Nonetheless, a poor release was observed in both, DI water and lacrimal solution (data not shown), confirming the importance of the ionic interaction.

Chapters 5 and 6 showed that diclofenac sodium can be released from imprinted pHEMA films using ionic interactions. Alvarez-Lorenzo and colleagues released diclofenac sodium from pHEMA films using pendant cyclodextrins [111] and from pHEMA films with the incorporation of chemistry [110]. In some of these studies the incorporation of ions (i.e. NaCl, lacrimal solution) in the release media promoted the dissociation of diclofenac sodium: functional monomer complexes; however, even under these conditions, sustained release was achieved for several hours up to days. The high polymeric density of the pHEMA hydrogels was believed to be a contributing factor [110]. One of the main differences of poly(HEMA-co-DEAEM-co-PEG200DMA) network and Nelfilcon A network is that the former has ~4.4 times smaller mesh size which may allow better proximity to interact with the functional monomers making the multiple non-covalent interactions affect on release more favorable. To enhance the potential of Nelfilcon A hydrogels as drug delivery systems reducing the mesh size was evaluated to enhance

the interactions of the functional monomers with the drug. Formulations with DADMAC and HEMA and the incorporation of crosslinkers, such as polyethylene glycol (200) dimethacrylate (PEG200DMA), and ethylene glycol dimethacrylate (EGDMA) were made, nonetheless the mechanical properties of the hydrogels were completely diminish, and no improvement in the release in lacrimal solution was achieved (data not shown).

7.3.2 Structural Analysis of Nelfilcon A-DS Lenses

There are many theoretical models that enable us to obtain structural and configurational information about a hydrogel from experimental data obtained by swelling and tensile studies. In particular we can obtain information about the mesh size of the hydrogel and determine whether a tighter mesh is responsible for the decrease in the diffusion coefficient of diclofenac sodium through hydrogels. The mesh size is related to the molecular weight between crosslinks according to equation 4.18.

The Nelfilcon macromer mixture contains water as a solvent. Based on the discussion in Section 4.2.2, the Peppas-Merrill model describes the relationship between the average molecular weight between crosslinks (\overline{M}_c) and the equilibrium polymer volume fraction ($v_{2,s}$) for a swollen hydrogel crosslinked in the presence of a solvent.

Equilibrium swelling studies were performed on the hydrogels to determine the weight swelling and volume swelling ratios (q and Q) and the polymer volume fraction in the swollen state ($v_{2,s}$). These parameters were calculated for the contact lenses and are summarized in Table 7.5.

Lenses synthesized with DADMAC have slightly higher weight swelling (q), and volume swelling (Q) ratios than lenses synthesized with other functional monomers. The former also

have lower polymer volume fraction ($v_{2,s}$), indicating higher water content. The presence of DADMAC in the pre-polymer mixture might influence the formation of polymer chains and associated crosslinking points, making the polymer chains more mobile and increasing the hydrogels' capacity to hold water. The results are interesting considering the lenses prepared with DADMAC exhibited the highest swelling, but the slowest release profile.

Table 7.5: Equilibrium swelling parameters and transmittance values of Nelfilcon A-DS lenses with functional monomers

Functional monomer within the lens	Q (Equilibrium volume swelling ratio)	$v_{2,s}$ (Equilibrium polymer volume swelling fraction)	% Transmittance
Nelfilcon-DS (No FM)	4.194 ± 0.039	0.238 ± 0.002	65
2.57% HEMA	3.914 ± 0.061	0.256 ± 0.004	59
3.81 % HEMA	3.862 ± 0.093	0.259 ± 0.006	58
0.5% DADMAC	4.323 ± 0.018	0.231 ± 0.001	85
1.0% DADMAC	4.467 ± 0.029	0.224 ± 0.001	88
2.0% DADMAC	4.633 ± 0.042	0.216 ± 0.002	91
2.0% β -CD-NMA	3.977 ± 0.009	0.251 ± 0.001	45
5.0% β -CD-NMA	3.800 ± 0.086	0.263 ± 0.006	40
2.0% DEAE-Dextran	4.203 ± 0.069	0.238 ± 0.004	90
2.0% BAK	4.397 ± 0.021	0.227 ± 0.003	96

The data are presented as mean ± SD (n=3).

Modulus values which depended on the functional monomer used were also determined and summarized in Table 7.6. Hydrogels, where an ionic interaction occurred between the template and the functional monomers (DADMAC and DEAE-Dextran), showed the lowest moduli. This suggests that the presence of DADMAC and DEAE-Dextran in the prepolymer results in a network with longer chains between crosslinks (based on Equation 4.17).

The slope of τ versus the elongation term ($\alpha-1/\alpha^2$), obtained from the tensile tests, is the Shear modulus and enables one to calculate \overline{M}_c . For this case, the ratio of polymer volume fractions of swollen and relaxed gels is $v_{2,s}/v_{2,r} \approx 1$, the specific polymer volume is $\overline{v} = 0.909$, the

molecular weight of uncrosslinked polymers is $\overline{M}_n \approx 50,000$ Da, the temperature of experimental conditions is $T = 295$ K and the ideal gas constant is $R = 8.314472 \text{ cm}^3 \cdot \text{MPa} \cdot \text{K}^{-1} \cdot \text{mol}^{-1}$. From \overline{M}_c , the mesh size (ξ) can be determined using Equation 4.18 [100], where $l = 1.54 \text{ \AA}$ and M_r is the effective molecular weight of the repeating unit (44 g/mol). The average value of the characteristic ratio used was $C_n = 8.3$ [225].

Table 7.6: Structural parameters of Nelfilcon A-DS lenses with functional monomers

Functional monomer within the lens	Young's Modulus (MPa)	Shear Modulus (MPa)	Mc (g/mol)	Mesh Size (\AA)
Nelfilcon-DS (No FM)	1.041 ± 0.082	0.384 ± 0.027	6851.0 ± 485.3	126.23 ± 4.44
2.57% HEMA	1.398 ± 0.071	0.501 ± 0.035	5289.0 ± 363.6	110.91 ± 3.82
3.81 % HEMA	1.444 ± 0.255	0.521 ± 0.064	5600.6 ± 94.30	114.17 ± 0.96
0.5% DADMAC	1.019 ± 0.146	0.374 ± 0.028	7146.0 ± 412.3	128.93 ± 3.75
1.0% DADMAC	1.039 ± 0.197	0.393 ± 0.088	7321.9 ± 579.5	130.47 ± 5.23
2.0% DADMAC	1.045 ± 0.033	0.380 ± 0.023	7317.8 ± 754.7	130.39 ± 6.70
2.0% β -CD-NMA	1.333 ± 0.047	0.490 ± 0.013	5390.1 ± 141.4	112.00 ± 1.47
5.0% β -CD-NMA	1.560 ± 0.029	0.574 ± 0.004	4612.1 ± 34.90	103.61 ± 1.39
2.0% DEAE-Dextran	1.008 ± 0.034	0.350 ± 0.018	7480.2 ± 372.3	131.92 ± 3.27
2.0% BAK	1.009 ± 0.074	0.351 ± 0.021	7485.4 ± 448.7	131.96 ± 3.92

The curves obtained to calculate the modulus had excellent correlation coefficients (>0.99). The data are presented as mean \pm SD (n=3).

The ionic functional monomer seems to influence the formation of polymer chains and associated crosslink points in the hydrogel resulting in a larger mesh size. This agrees with the results of the swelling studies, in which the Nelfilcon-DADMAC formulation has the lowest polymer volume fraction.

7.3.3 Dynamic Release of Diclofenac Sodium from Lotrafilcon B Lenses

Due to the large mesh size of Nelfilcon A lenses, the multiple non-covalent interactions in the binding site were not able to be stabilized and assisted the ionic interactions (the primarily ones) to delay the release of diclofenac in lacrimal solution, resulting in a fast and not controlled

release; making the drug diffusion the limiting step in the release process. As a result of the large network in Nelfilcon A lenses, there is no barrier to slow the diffusion of the drug; thus, a quick release in lacrimal solution occurs in any of the Nelfilcon formulations. Therefore, to further tailor the release of hydrophobic charged molecules, such as diclofenac sodium, more hydrophobic interactions may be needed to lead a sustained controlled release in the presence of competitive agents.

It has been previously demonstrated in acrylate polymers that adjusting the co-monomer composition of polymeric materials influences the network structure of photopolymerized polymers [226]. Surprisingly, little work has been done tailoring the rate of drug release from silicone hydrogel contact lens by altering the lens composition and network structure. In this study, silicone contact lenses were engineered by rationally altering the ratio of hydrophobic to hydrophilic co-monomer composition in the LFB formulation (Table 7.1) to control the release of diclofenac sodium in lacrimal solution, while maintaining sufficient optical and mechanical properties for clinical use.

Dynamic release studies were performed in DI water (data not shown), where no significant differences were observed with those performed in lacrimal solution. More importantly an extended release of diclofenac sodium was achieved in lacrimal solution, validating the hypothesis that hydrophobic interactions would aid in controlling the release rate of a hydrophobic charged molecule, such as diclofenac sodium. Thus, lacrimal solution was used for all the remainder studies.

Dynamic cumulative and fractional mass release profiles in lacrimal solution for LFBs-DS lenses (LFB 1-3 lenses) are shown in Figure 7.16a and 7.16b, respectively. The results demonstrate that the release rate of the silicone hydrogel contact lenses is dependent on the

hydrophobic:hydrophilic ratio within the lens. As the amount of hydrophobic monomers is increased in the lens, the cumulative diclofenac sodium mass release rate tends to decrease. Diclofenac sodium release was sustained for up to 5 days in lacrimal solution depending on the lens type. Figure 7.16a showed that LFB1 (0.76:1 Macromer/TRIS:DMA mass ratio) and LFB2 (1.5:1 Macromer/TRIS:DMA mass ratio) lenses released for ~24 hours. LFB3 (7.5:1 Macromer/TRIS:DMA mass ratio) lens exhibited an extended release profile for duration of 5 days, which resulted in a delay of the template release profile by 5 fold over LFB1 and LFB2 lenses.

For LFB3 lenses, the release rate can be classified into three general zones. Initially, diclofenac sodium was released at a rate of around 20.0 $\mu\text{g/hr}$ for the first 2 hours. During this period, ~20% of loaded diclofenac sodium is released. A linear release profile delivering 2.8 $\mu\text{g/hr}$ was demonstrated for the next 46 hours. Finally, the release gradually decreased until very low diclofenac sodium amounts were released (0.45 $\mu\text{g/hr}$) for the next 72 hours.

The fractional release profile, Figure 7.16b, shows that diclofenac sodium release was more constant as the amount of hydrophobic monomers was increased in the lens. The calculated diffusion coefficients of diclofenac sodium for the release profile shown in Figure 7.16 are summarized in Table 7.7. LFB3 lens had a significantly lower diffusion coefficient ($1.49 \pm 0.24 \times 10^{-10} \text{ cm}^2/\text{s}$): 35.8 and 27.6 times lower than LFB1 and LFB2 lenses, respectively.

Differences in the release rate could also be due to changes in the network structure. The equilibrium swelling data (Table 7.7) shows that as the Macromer/TRIS:DMA mass ratio increases the equilibrium volume swelling ratio (Q) decreases. As the volume swelling fraction ($v_{2,s}$) represents the inverse of the polymer volume fraction in the swollen state, a higher Q value indicates a decreased polymer volume fraction or an increased free volume within the polymer

structure in the swollen state. Thus, the LFB3 lenses had a higher polymer volume fraction in the swollen state, swelling to a lesser extent (~3.7 weight % water), which could also be responsible for the delay in diclofenac sodium release due to more resistance to the diffusion of diclofenac.

Table 7.7: Diffusion coefficient, equilibrium swelling parameters and structural parameters of silicone contact lenses

Sample	Macromer/TRIS: DMA ratio	Diffusion Coefficient (cm ² /s) x 10 ¹⁰	Q (Equilibrium volume swelling ratio)	v _{2,s} (Equilibrium polymer volume swelling fraction)	Young's Modulus (MPa)	% Transmittance
LFB1	0.76:1	42.18±2.79	2.17±0.04	0.461±0.009	1.313±0.022	89
LFB2	1.50:1	22.94±0.62	1.55±0.05	0.644±0.019	1.071±0.007	93
LFB3	7.50:1	1.49±0.24	1.11±0.01	0.963±0.039	0.192±0.034	85
LFB4	2.27:1 & 2 wt.% EGDMA	1.73±0.58	1.42±0.03	0.704±0.020	1.882±0.119	93

The data are presented as mean ± SD (n=3).

On the other hand, LFB3 lenses showed the smaller Young moduli (0.192 ± 0.034 MPa), which suggests a network with longer chains between crosslinks, where the drug could diffuse freely. Therefore, the observed difference in release might be due to the hydrophobic/hydrophilic ratio of the silicone hydrogel and to a lesser extent to the structural differences within the polymer network resulting from changes in the composition. These experimental results also confirm that LFB3 lenses prepared with a 7.5:1 Macromer/TRIS:DMA mass ratio had the highest hydrophobicity as they swelled to the lowest extent.

Maximum transmittance was 89% and 93% for LFB1 and LFB2 lenses, respectively. Although, LFB3 lenses showed a controlled release, a significant haze was observed and its transmittance value was 85%, which was less than an acceptable 90% target. Moreover, the high hydrophobicity of LFB3 lenses caused unsuitable mechanical properties. Their low water content and low Young's moduli produced a material that manifested typical rubbery behavior, such as

high adhering and poor mechanical properties, which would not deliver the necessary comfort, along with a poor handling, which might translate to difficult manufacture.

To design a lens that complies with current commercial silicone contact lenses, while maintaining an extended controlled release of diclofenac sodium, additional formulations were synthesized, some of them using crosslinking monomers (Table B.1, Appendix B). Incorporation of functional monomers to the pre-polymer formulation was attempted so as to allow interactions between the functional monomers and diclofenac sodium; however, phase separation was observed in all the attempts (Table B.1 and Table B.2, Appendix B). The best results were achieved with the LFB4 formulation (Table 7.1), with a 2.18:1 Macromer/TRIS:DMA mass ratio and 2 wt.% EGDMA, a crosslinking monomer. Figure 7.17 shows the fractional release of diclofenac sodium from LFB4 lenses. There was a similar trend in the release profile of LFB3 lenses and LFB4 lenses. LFB4 lenses have a complete release of diclofenac sodium in 7 days and a diffusion coefficient of $1.73 \pm 0.58 \times 10^{-10} \text{ cm}^2/\text{s}$. Moreover, the LFB4 lenses had water content (~29.6 weight % water), a transmittance value of 93%, and moduli of $1.882 \pm 0.119 \text{ MPa}$ (Table 5.7), which are similar to those of commercial silicone contact lenses. Altering the hydrophobic/hydrophilic ratio and the addition of a crosslinking monomer led to an extended controlled release of diclofenac sodium from silicone hydrogels lenses.

The silicone contact lenses can be designed to release the drug at the required therapeutic rate without the variation in concentration observed with eye drops. LFB4 lenses (2.18:1 Macromer/TRIS:DMA mass ratio and 2 wt.% EGDMA) released diclofenac at a constant rate of $7.23 \mu\text{g/hr}$ for the first 24 hours, during this period, ~50% of loaded diclofenac sodium was released. A linear release profile delivering $0.86 \mu\text{g/hr}$ was demonstrated for the next 120 hours. Finally, the release gradually decreased until very low diclofenac sodium amounts were released

(0.08 $\mu\text{g/hr}$) for the next 24 hours. Conventional diclofenac sodium drops deliver approximately 80-160 $\mu\text{g/day}$ (3.33-6.67 $\mu\text{g/hr}$) based on the recommended dosage regimen within a typical peak and valley profile (assuming 100% bioavailability, i.e. Voltaren Ophthalmic[®] solution concentration is 1 mg diclofenac sodium/mL; assuming a typical eye drop volume of 20 μL per drop at the recommended frequency of administration of 4-8 drops per day). Therefore, there is strong potential to release therapeutically relevant concentrations of drug from a contact lens platform. Moreover, the mass of diclofenac released by these contact lenses can be tailored (i.e. changing the loading concentration (Figure B.1, Appendix B), to match the current recommended dose from eye drops. These therapeutic lenses will release diclofenac sodium in a linear manner without the variation in concentration observed with eye drops for the duration of lens wear. Another tremendous advantage is that silicone lenses can be engineered to be worn during sleep. Thus, the patient will be receiving an extended continuous treatment. Such lens has the potential to greatly enhance patient ocular health by overcoming the inherent inefficiencies of topical eye drops.

7.4 Conclusions

In this work, we tested the feasibility of controlling diclofenac sodium release from Nelfilcon A lenses and silicone contact lenses (lenses synthesized with modifications to the Lotrafilcon B formulation). Various directions were undertaken to produce Nelfilcon A lenses, having the best results when non-covalent ionic interactions were presented. Nelfilcon A lenses demonstrated controlled release of diclofenac sodium in DI water for up to 72 hours and adequate optical clarity when synthesized with 2 wt.% of DADMAC. The only hurdle is to stabilize the ionic interaction so it is not as easily disrupted in lacrimal solution. Additionally,

silicone contact lenses were engineered by varying both the hydrophobic to hydrophilic monomer ratio and the weight percent of additional crosslinking monomers in LFB lenses. The silicone hydrogel contact lenses had good optical clarity, mechanical properties and contained siloxane compositions similar to highly oxygen permeable silicone hydrogel lenses currently on the market. More importantly, an extended and controlled release in lacrimal solution of diclofenac sodium was achieved for up to 7 days. The results demonstrate that silicone lenses can be used to release therapeutically relevant concentrations of diclofenac sodium for extended periods of time. Such a lens has the potential to greatly enhance patient ocular health by overcoming the inherent inefficiencies of topical eye drops.

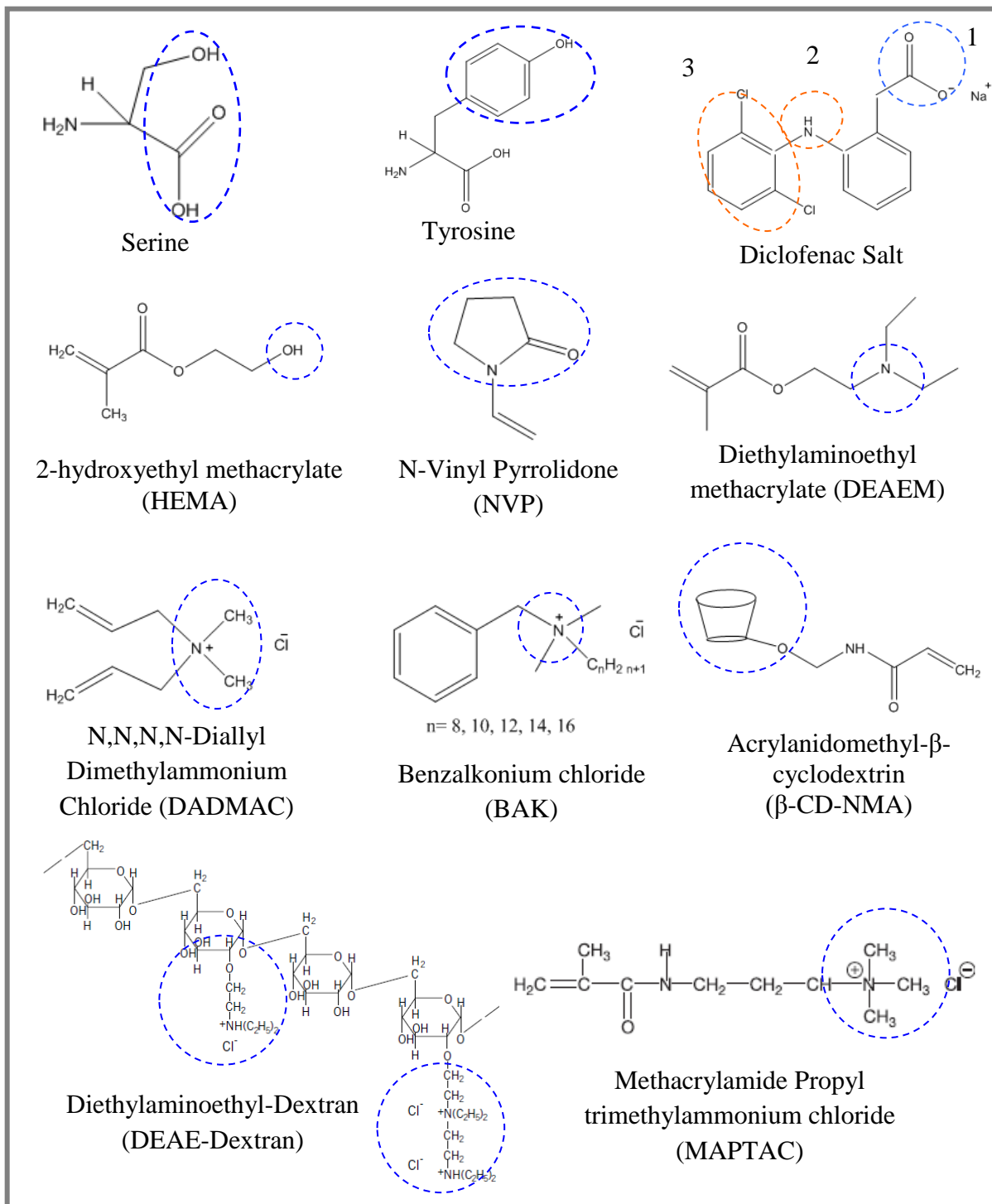


Figure 7.1: Chemical structures of interest in diclofenac releasing Nelfilcon A lenses

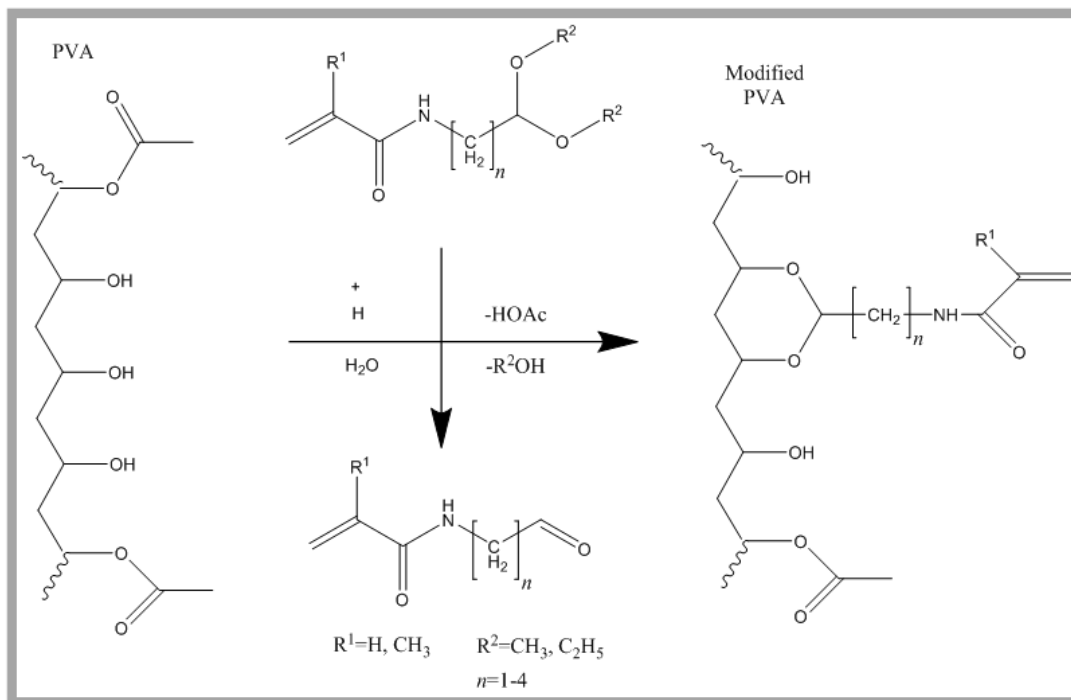


Figure 7.2: Synthesis of Nelfilcon A macromer from PVA

Nelfilcon A is synthesized using poly(vinyl alcohol) (PVA) as a starting material. N-acryloyl-aminoacetaldehyde-dimethylacetal (NAAADA) is reacted with the PVA through transacetylation under acidic aqueous conditions. The product is a PVA macromer with pendant acrylate groups at well-defined intervals. The trans-acetylation process can be used to attach initiator and tint to the macromer. The product is purified by diafiltration.

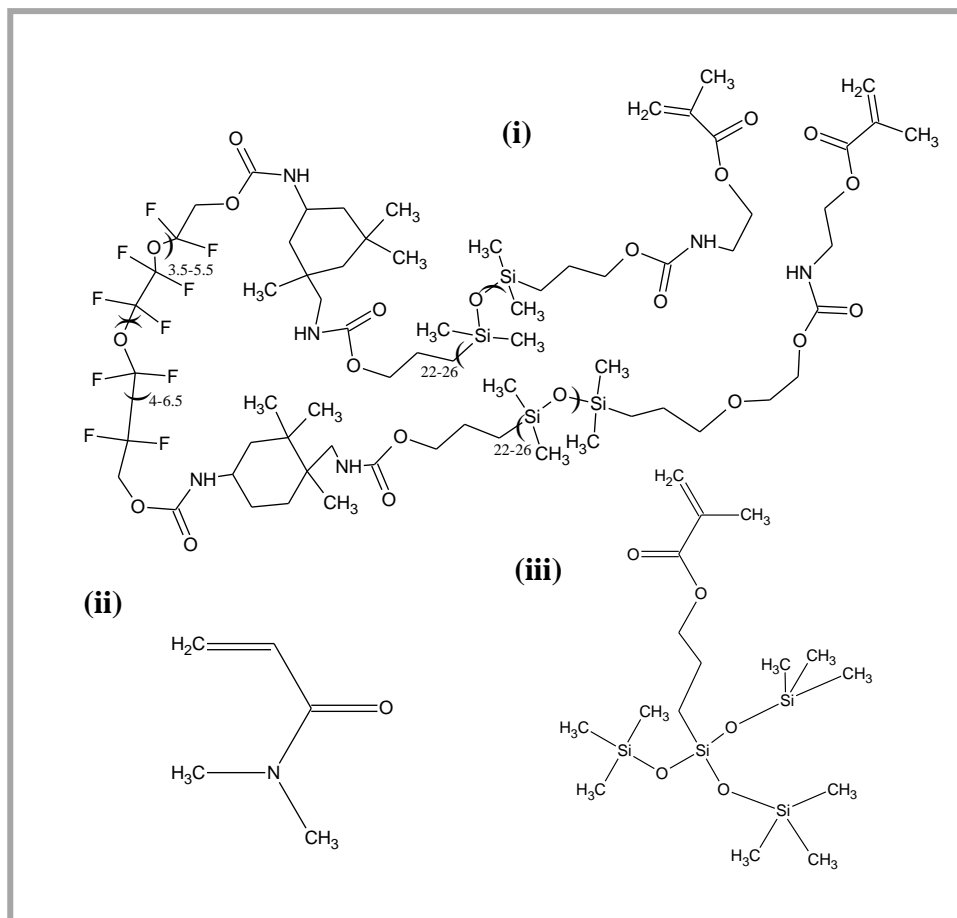


Figure 7.3: Monomers in the LFB formulation

The silicone hydrogel contact lens formulation, Lotrafilcon B, is made up of three major components (i) 26% Betacon Macromer, (ii) 30% DMA and (iii) 19% TRIS. The balance of the formulation is initiator and solvent. TRIS and the macromer are the hydrophobic section of the lens and responsible for oxygen permeability. DMA makes up the hydrophilic, ion permeable phase of the lens.

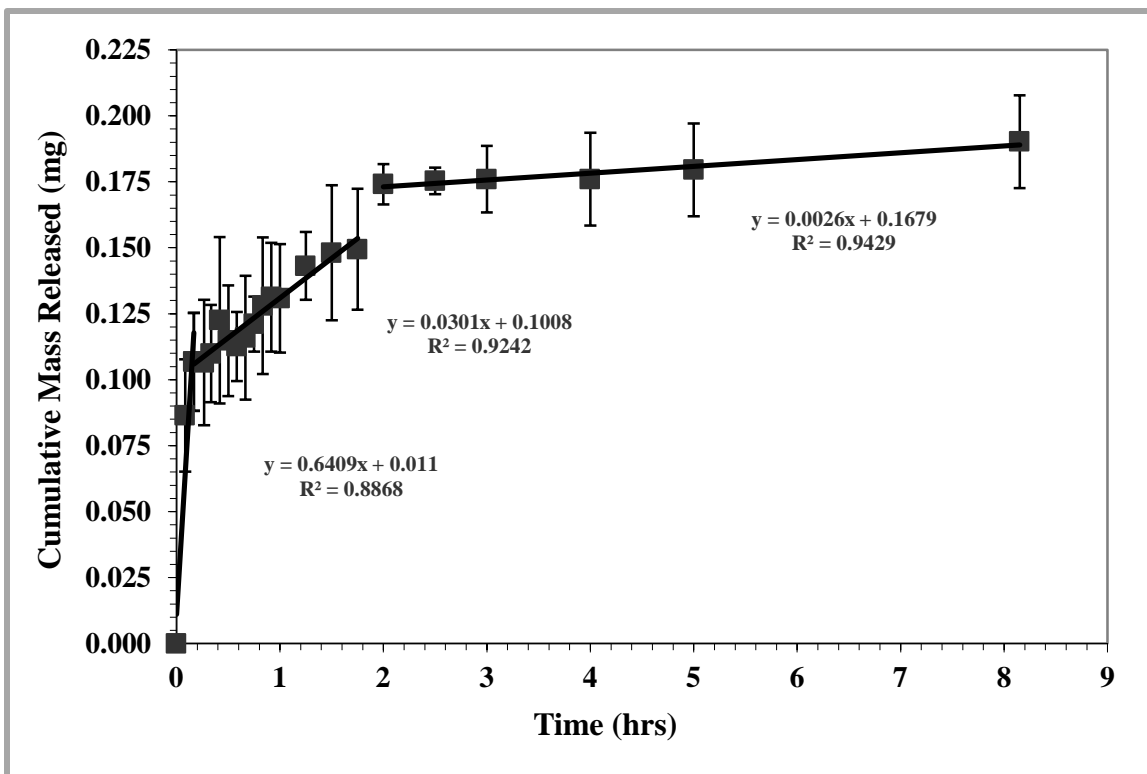


Figure 7.4: Cumulative mass release of diclofenac from Nelfilcon A contact lenses

Dynamic release study in DI water was conducted on lenses prepared from a pre-polymer containing 6.5 mg of DS per gram of Nelfilcon formulation. No functional monomers were added. N= 2, T = 34°C. The duration of the release is not adequate and the rate is non-uniform. The Fickian release DS diffusion coefficient is $3.97 \times 10^{-8} \text{ cm}^2/\text{sec}$. Optical clarity measured by % transmittance at visible wavelengths was ~65%.

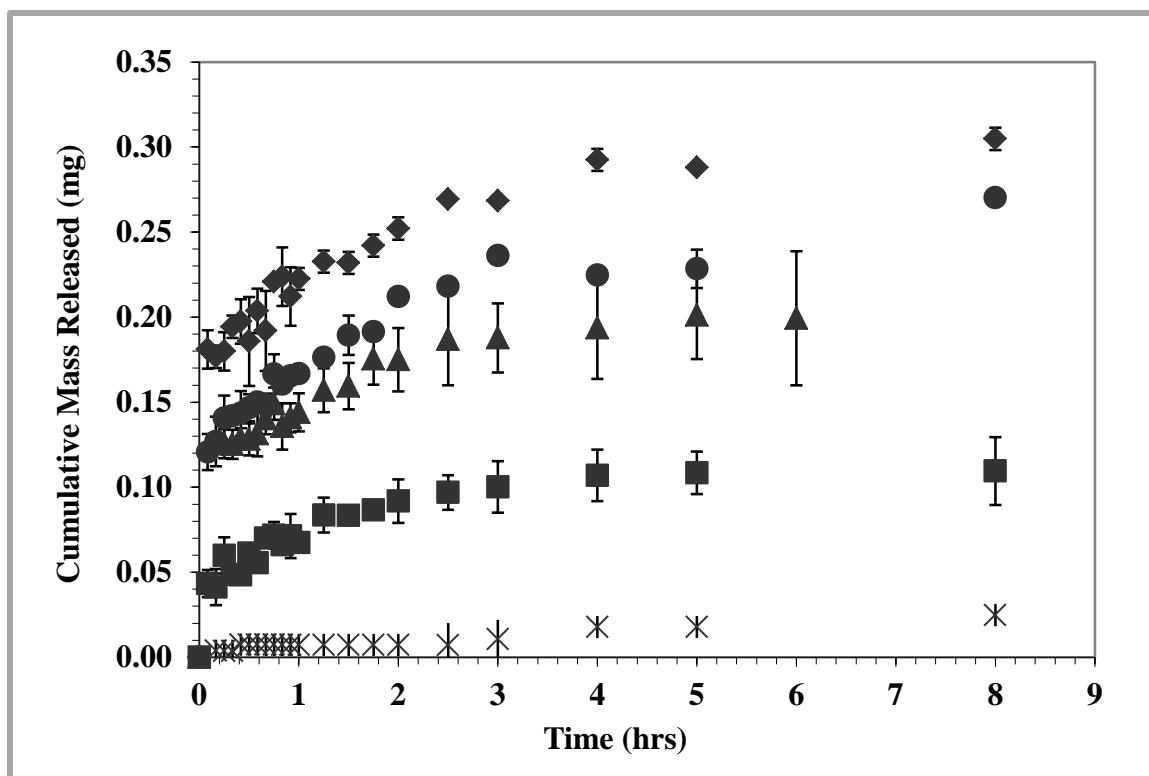


Figure 7.5: Cumulative mass release of diclofenac from Nelfilcon A lenses comparing different loading concentrations of diclofenac

Dynamic release studies in DI water were conducted on DAILIES[®] lenses synthesized with different amounts of DS per gram of Nelfilcon formulation: 10.0 mg/g (◆), 8.0 mg/g (●), 6.5 mg/g (▲), 4.0 mg/g (■), 2.0 mg/g (×). No functional monomers were added. Loading of DS can be achieved in amounts to sustain an extended release for 24 hours. N= 2, and T = 34°C. Optical clarity measured by % transmittance at visible wavelengths was ~89% for 2.0 mg/g (×), ~68% for 4.0 mg/g (■), ~65% for 6.5 mg/g (▲), ~60% for 8.0 mg/g (●), and ~61% for 10.0 mg/g (◆).

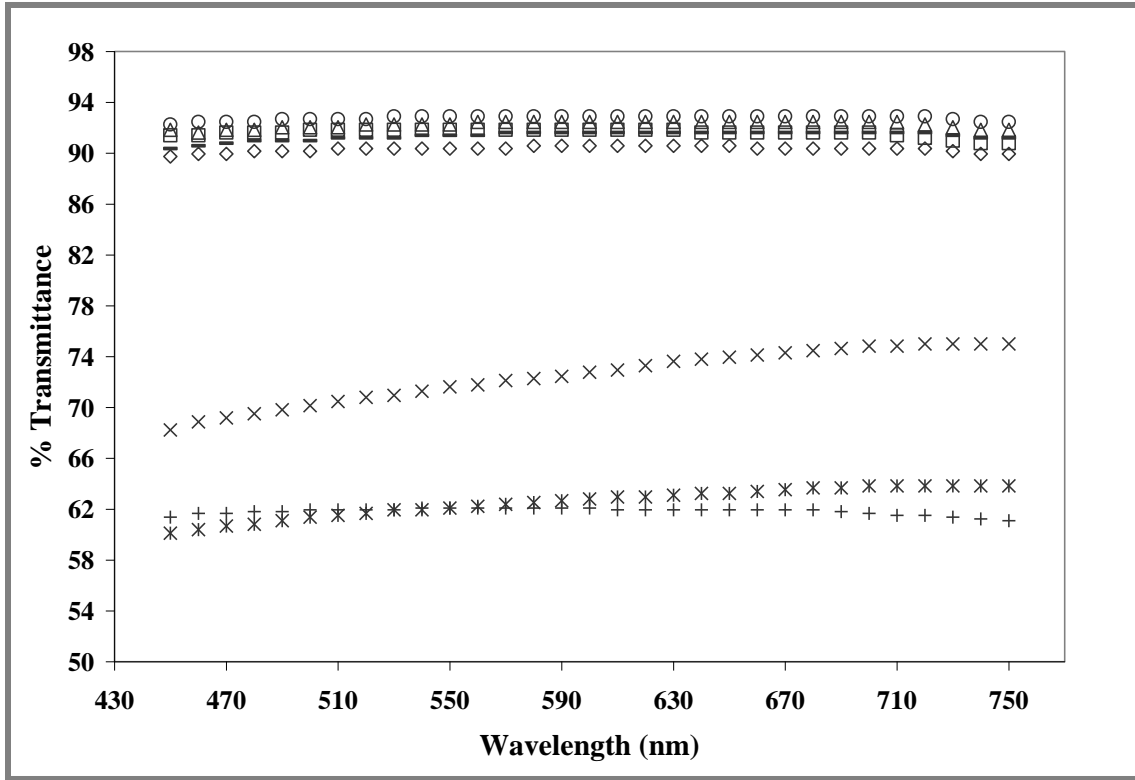


Figure 7.6: Optical clarity of Nelfilcon A lenses synthesized with diclofenac

The pre-release lenses: 2 mg/g (◇), 4 mg/g (×), 8 mg/g (*), 10 mg/g (+), have a low percent transmittance, while the post-release lenses have a high percent transmittance 2 mg/g (□), 4 mg/g (Δ), 8 mg/g (○), 10 mg/g (-).

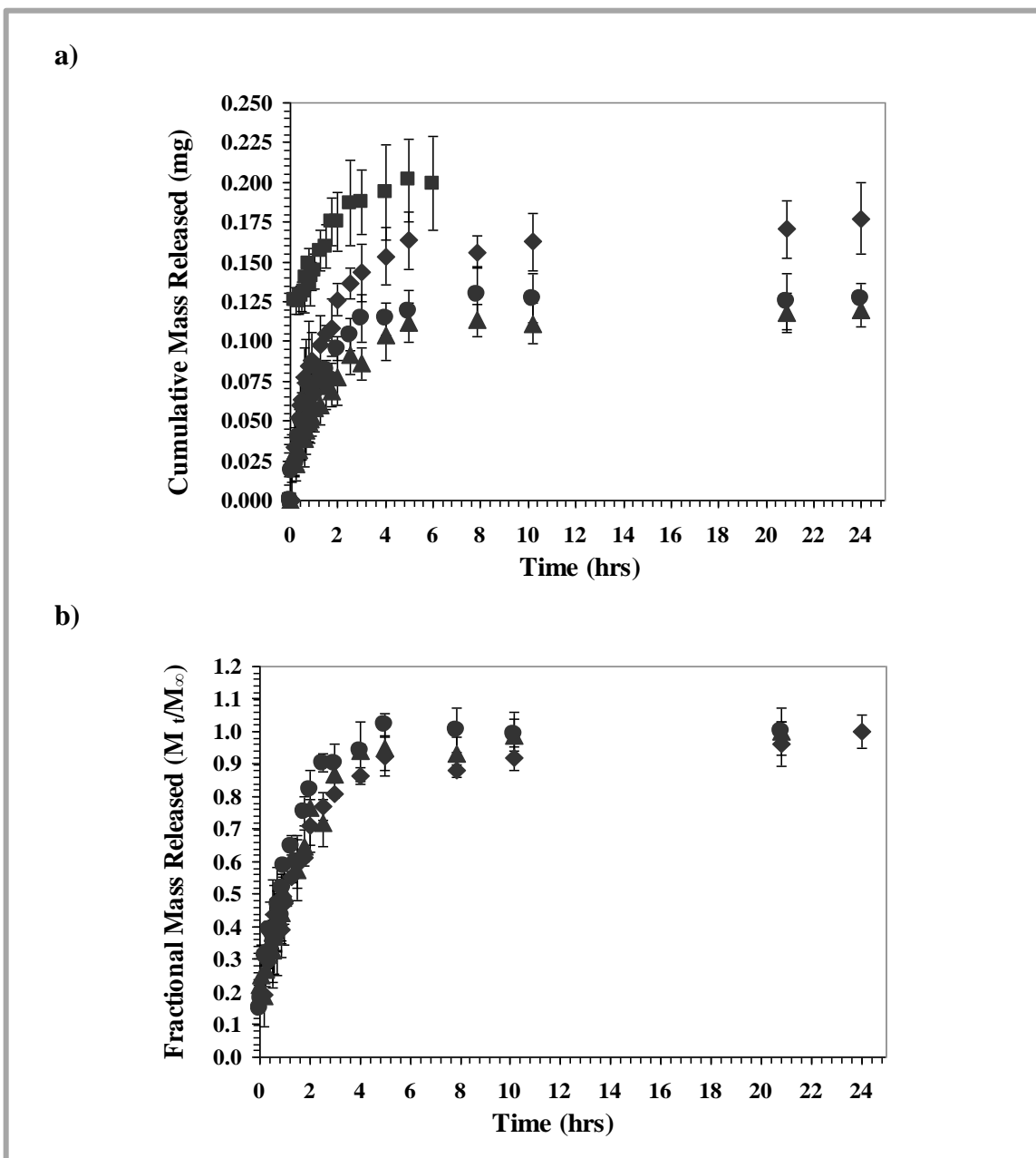


Figure 7.7: Cumulative and fractional diclofenac release from Nelfilcon A lenses with different proportions of HEMA

(a) Cumulative release, and (b) fractional release profiles of diclofenac sodium in DI water. Lenses were prepared from pre-polymers containing different proportions of HEMA functional monomer: 1.30 wt.% HEMA (FM/T~5) (◆), 2.57 wt.% HEMA (FM/T~10) (●), and 3.81 wt.% HEMA (FM/T~15) (▲). For comparison, a plot of a Nelfilcon A lenses with no functional monomer (0 wt.% HEMA) containing 6.5 mg of DS per gram of Nelfilcon formulation is also shown (■). HEMA may provide interaction that slows release compared to control. Fractional release (DS diffusion coefficient) is not dependent on HEMA loading concentration or FM/T ratio. Transmittance is less than 60%. N= 3, and T = 34°C.

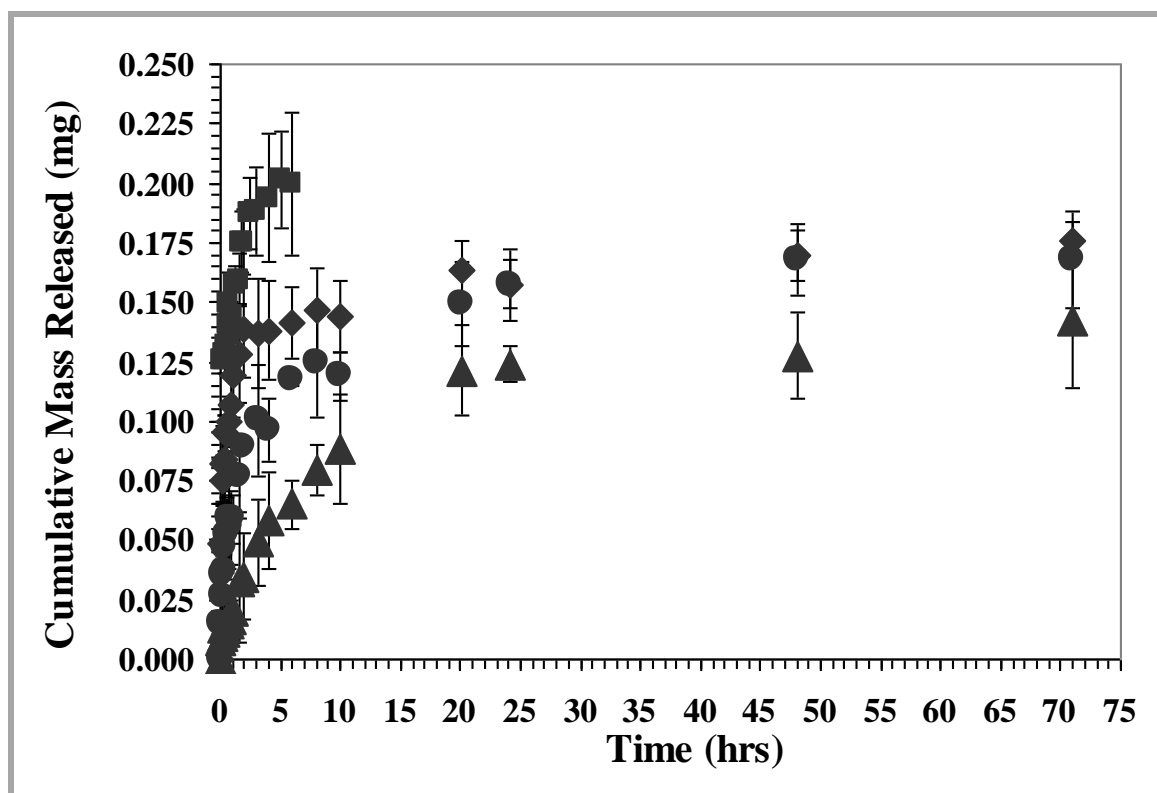


Figure 7.8: Cumulative release of diclofenac from Nelfilcon A lenses with different proportions of DADMAC

Dynamic release studies in DI water were conducted on lenses prepared from pre-polymers containing different proportions of DADMAC functional monomer: ~0.5 wt.% DADMAC (FM/T~1.5) (◆), ~1.0 wt.% DADMAC (FM/T~3.0) (●) and ~2.0 wt.% DADMAC (FM/T~6.0) (▲). For comparison, a plot of a DAILIES® lenses with no functional monomer (0 wt.% DADMAC) containing 6.5 mg of DS per gram of Nelfilcon formulation is also shown (■). As DADMAC is increased in the lens, there is a significant delay in DS release. Optical clarity at visible wavelengths ranged from 85-91%. N= 2, and T = 34°C.

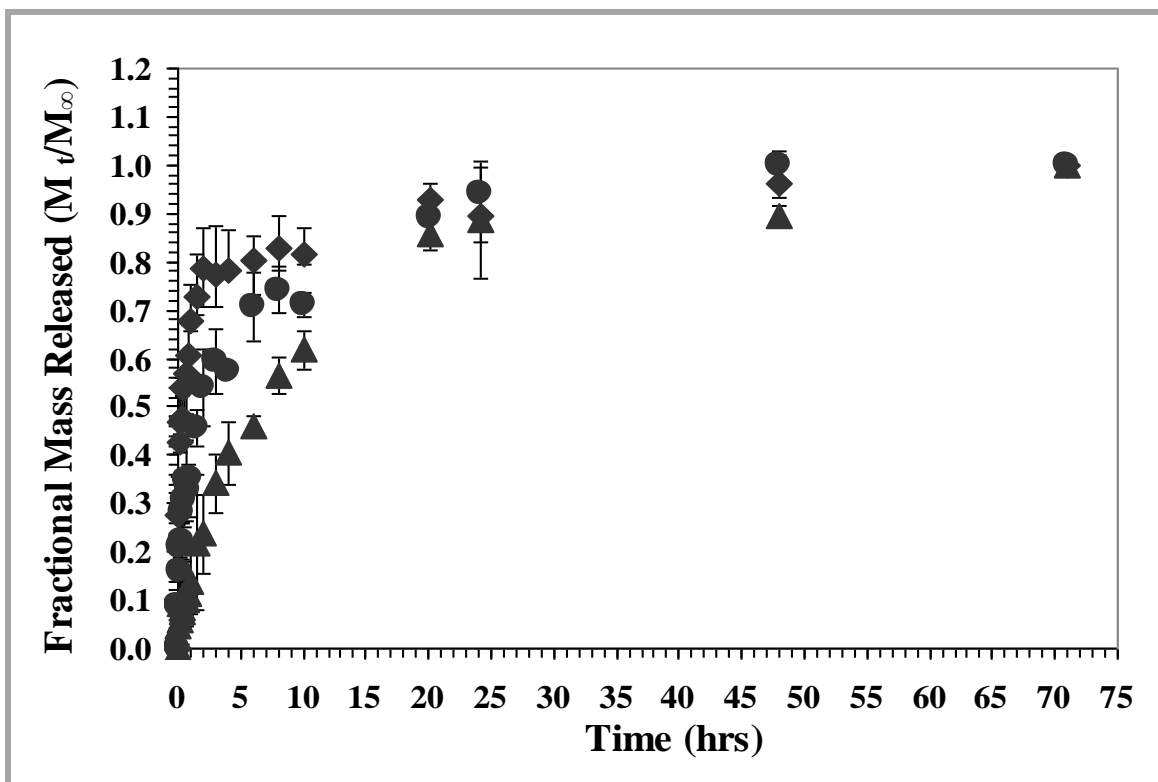


Figure 7.9: Fractional release of diclofenac from Nelfilcon A lenses with different proportions of DADMAC

Dynamic release studies in DI water were conducted on lenses prepared from pre-polymers containing different proportions of DADMAC functional monomer: ~0.5 wt.% DADMAC (FM/T~1.5) (◆), ~1.0 wt.% DADMAC (FM/T~3.0) (●) and ~2.0 wt.% DADMAC (FM/T~6.0) (▲). As DADMAC is increased in the lens, the release becomes more constant moving from Fickian towards a zero-order release profile. The study was carried out for 72 hours (data not shown). N= 2, and T = 34°C

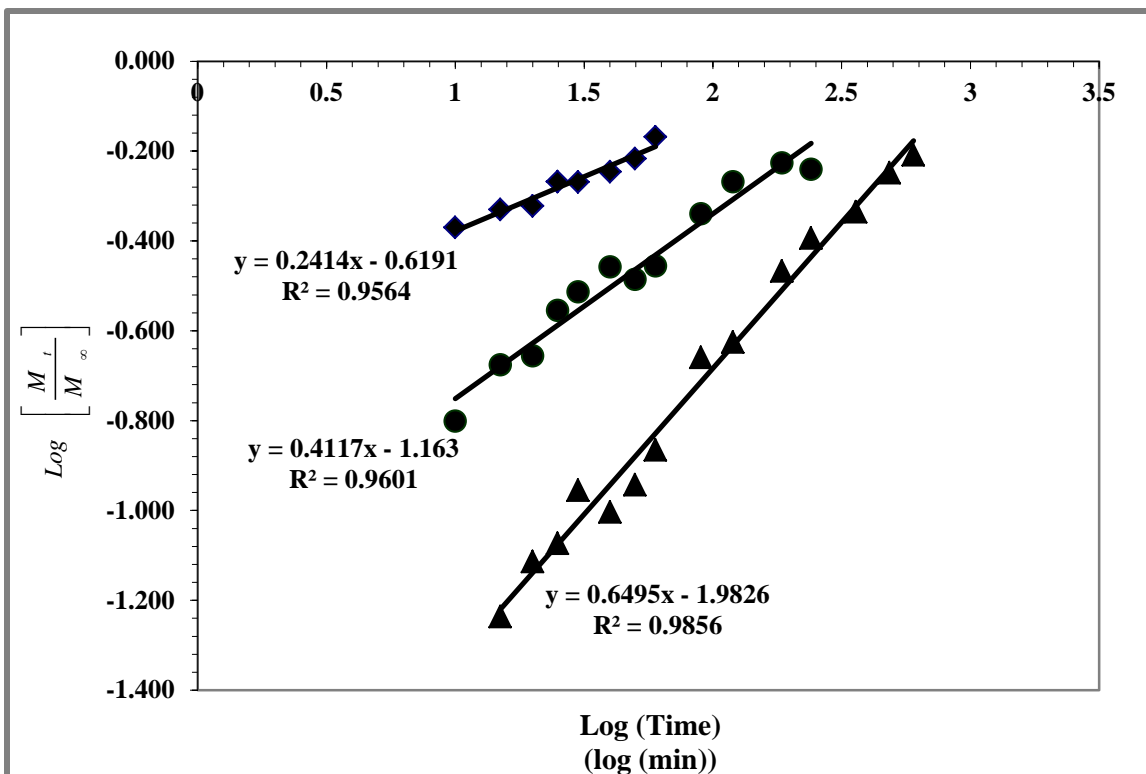


Figure 7.10: Zero-order release analysis from Nelfilcon A lenses with different proportions of DADMAC

Diclofenac fractional release in DI water for lenses prepared from pre-polymers containing different proportions of DADMAC functional monomer: ~0.5 wt.% DADMAC (FM/T~1.5) (◆) with $n=0.24$, ~1.0 wt.% DADMAC (FM/T~3.0) (●) with $n=0.41$ and ~2.0 wt.% DADMAC (FM/T~6.0) (▲) with $n=0.64$. As n moves closer to 1, the release profile moves towards zero-order, or constant, release. $N=2$, and $T=34^{\circ}\text{C}$. The order of release is $n-1$.

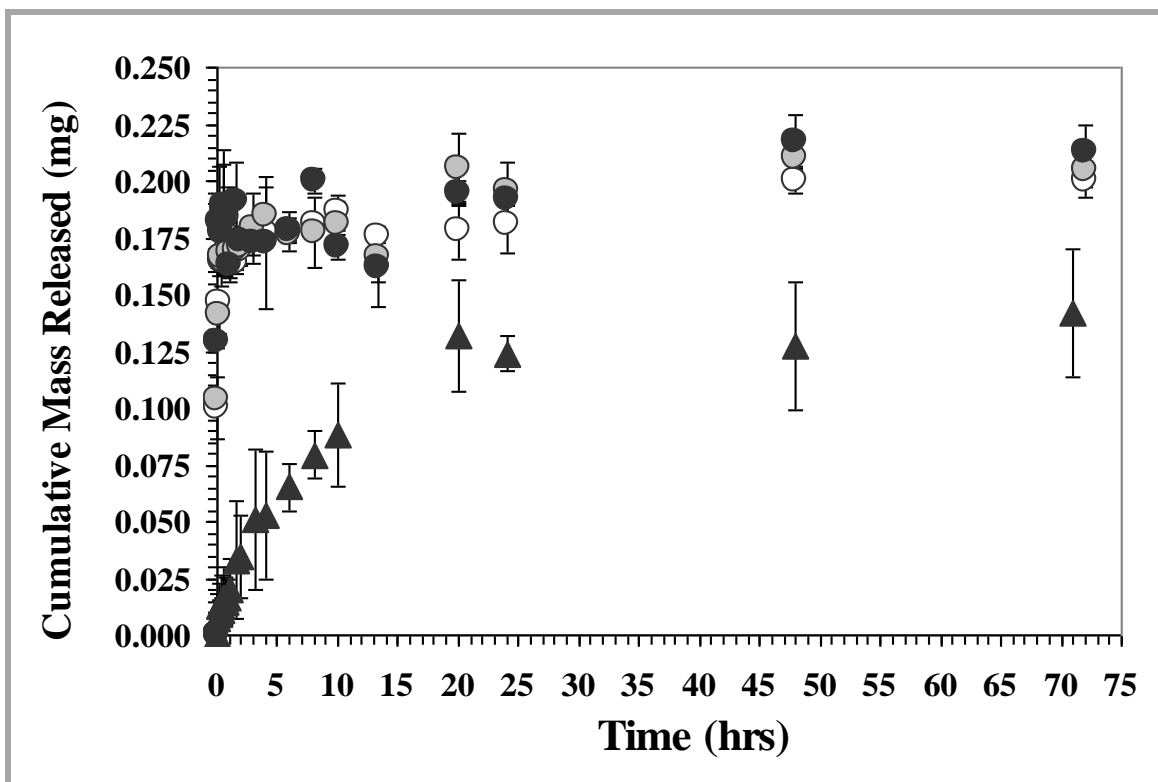


Figure 7.11: Effect of ionic strength on diclofenac release profiles from Nelfilcon A lenses

Dynamic release studies were conducted on lenses prepared with ~2.0wt.% DADMAC (FM/T~6.0) in different release solutions: 1.0M buffer solution, pH 7.0 (○), 0.5M buffer solution, pH 7.0 (●), artificial lacrimal solution, pH 8.0 (●) and DI water (▲). A quick release occurred when the lenses were placed in artificial lacrimal solution and solutions containing ions. N= 2-3, and T = 34°C.

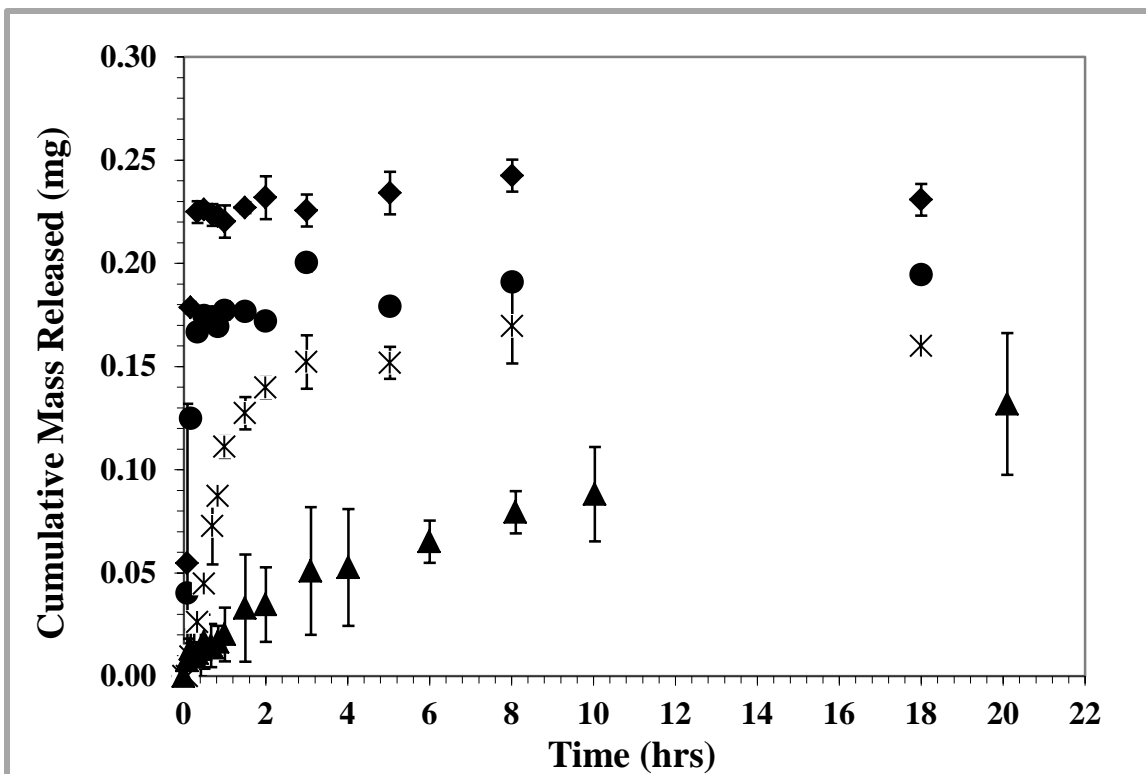


Figure 7.12: Cumulative release of diclofenac from Nelfilcon A lenses with MAPTAC

Dynamic release studies were conducted on lenses prepared from pre-polymers containing different proportions of MAPTAC functional monomer. The release was carried out in lacrimal solution: 5 wt.% MAPTAC (FM/T~25.0) (♦) and 2 wt.% MAPTAC (FM/T~9.0) (●), and in DI water: 5 wt.% MAPTAC (FM/T~25.0) (×). For comparison, a plot of a lens prepared with ~ 2 wt.% DADMAC (FM/T~6.0) (▲) releasing in DI water is also shown. Using a different positively charged monomer, DS release in water was not improved, and release in lacrimal solution was quick. Also, the strength of complexation is an important indicator of release. Transmittance values of lenses containing MAPTAC were less than 68%. N= 2, and T = 34°C.

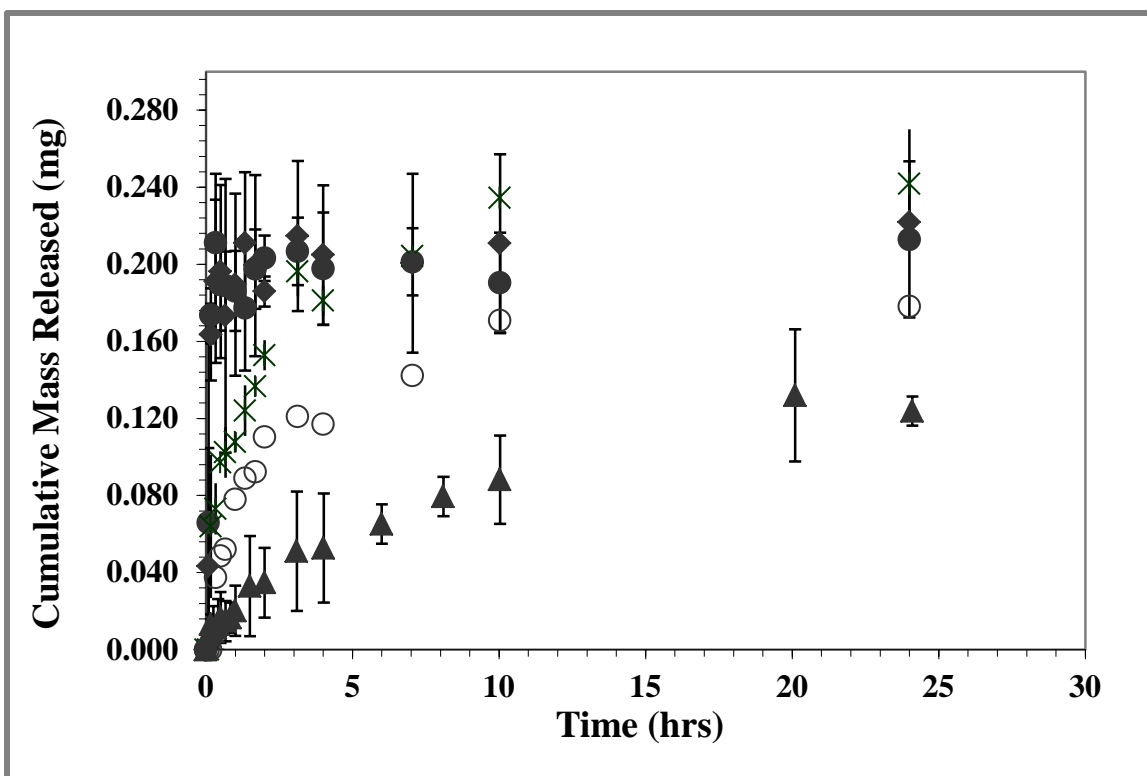


Figure 7.13: Cumulative release of diclofenac from Nelfilcon A lenses with β -CD-NMA10

Dynamic release studies were conducted on lenses prepared with different proportions of β CD-NMA. The release was carried out in lacrimal solution (N=2): 5 wt.% β CD-NMA (\blacklozenge) and 2 wt.% β CD-NMA10 (\bullet), and DI water (N=1): 5 wt.% β CD-NMA10 (\circ) and 2 wt.% β CD-NMA10 (\times). For comparison, a plot of a lens prepared with \sim 2 wt.% DADMAC (FM/T \sim 6.0) (\blacktriangle) in DI water are also shown. DS release is delayed in water as β CD-NMA is increased; however, the release rate is much higher in lacrimal solution. Transmittance values of lenses containing β CD-NMA10 were less than 60 %. T = 34°C.

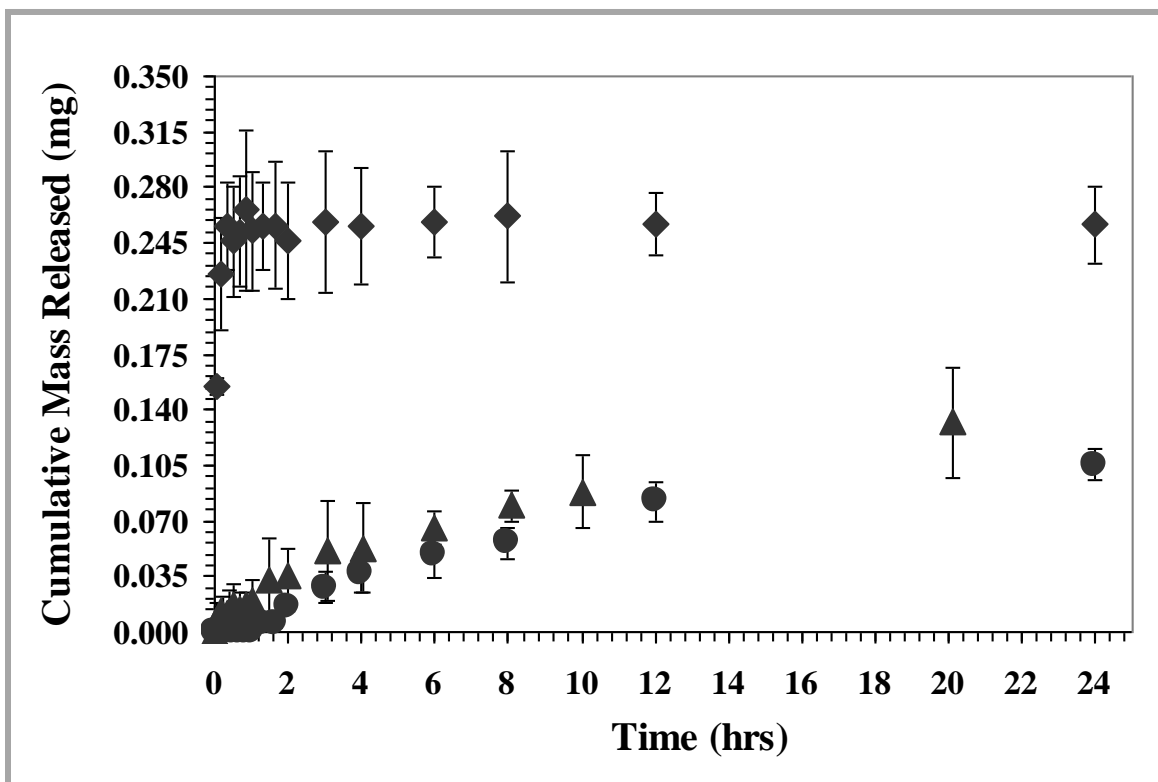


Figure 7.14: Cumulative release of diclofenac from Nelfilcon A lenses with DEAE-Dextran as diffusion barrier

Dynamic release studies were conducted on lenses prepared from pre-polymers containing 2 wt. % DEAE-Dextran. Release was carried out in lacrimal solution (♦) and DI water (●). For comparison, a plot of a lens prepared with ~ 2 wt. % DADMAC (FM/T~6.0) (▲) releasing in DI water is also shown. Similar release results are achieved compared to lenses containing DADMAC. N= 2, T = 34°C.

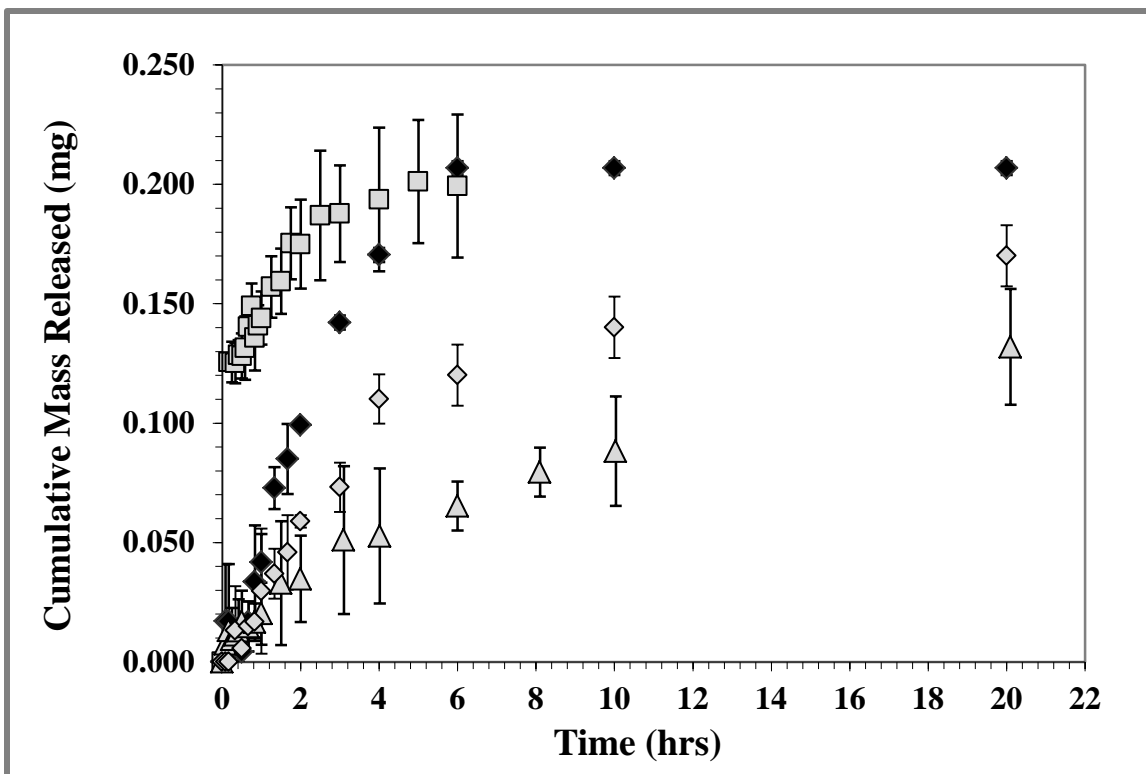


Figure 7.15: Cumulative release of diclofenac from Nelfilcon A lenses with BAK

Dynamic release studies were conducted on lenses prepared from pre-polymers containing 3 wt % BAK. Release was carried out in lacrimal solution (◆) and in DI water (◊). For comparison, a plot of a lens prepared with ~ 2 wt.% DADMAC (FM/T~6.0) (▲) and a plot of a DAILIES® lens with no functional monomers containing 6.5 mg of DS per gram of Nelfilcon formulation (■) releasing in DI water are also shown. The addition of BAC slows the release of DS in DI water and also in lacrimal solution. N= 2, T = 34°C.

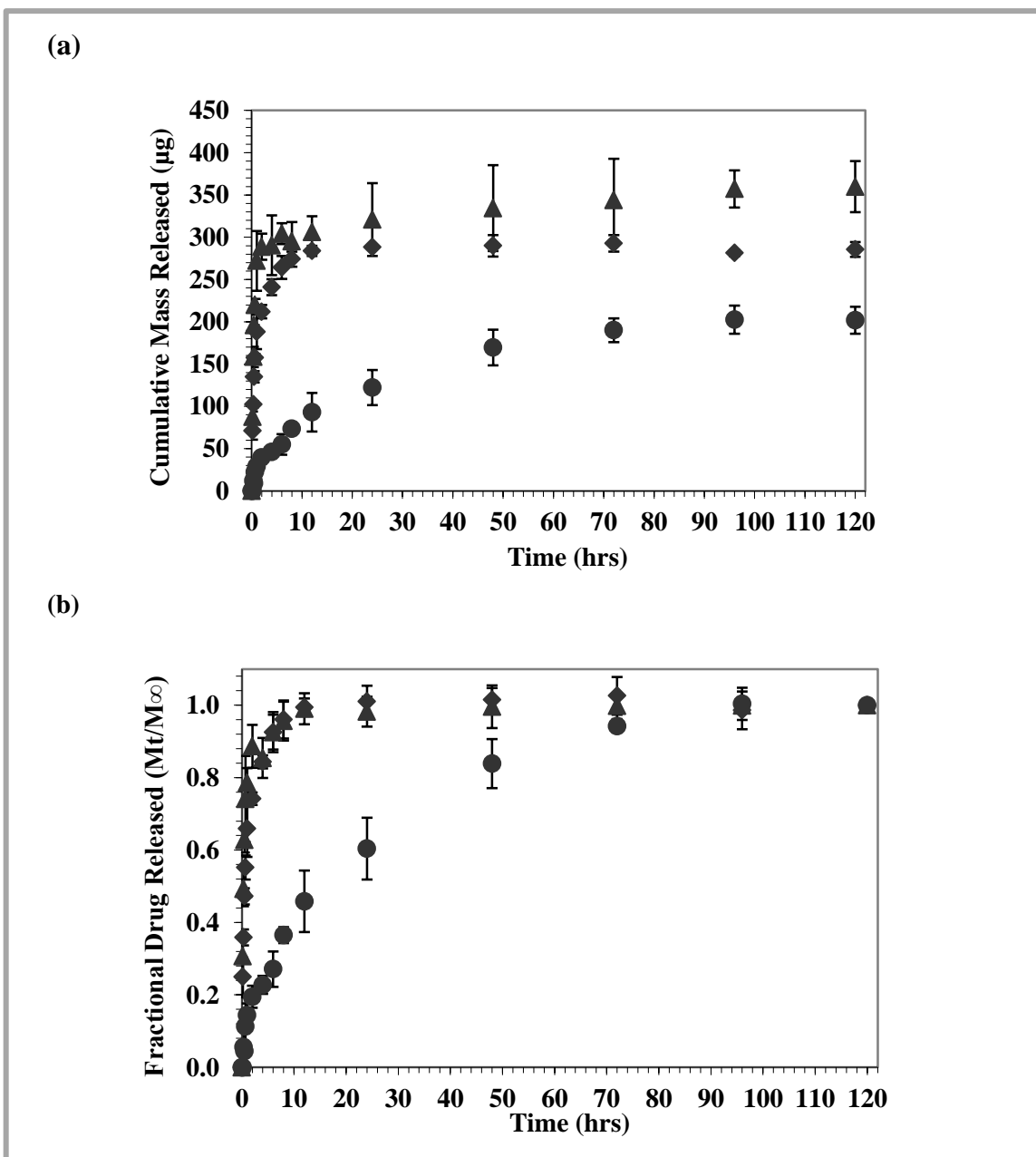


Figure 7.16: Cumulative and fractional diclofenac release from LFBs lenses with different hydrophobic:hydrophilic ratios

(a) Cumulative release, and (b) fractional release profiles of diclofenac sodium in lacrimal solution. Silicone lenses were prepared from pre-polymers containing different proportions of hydrophobic:hydrophilic ratios: LFB1 (0.76:1) (▲), LFB2 (1.50:1) (◆), and LFB3 (7.50:1) (●). Hydrophobic interactions may slow the release of diclofenac sodium. Fractional release (DS diffusion coefficient) is dependent on the hydrophobic:hydrophilic ratios. N= 3, and T = 34°C.

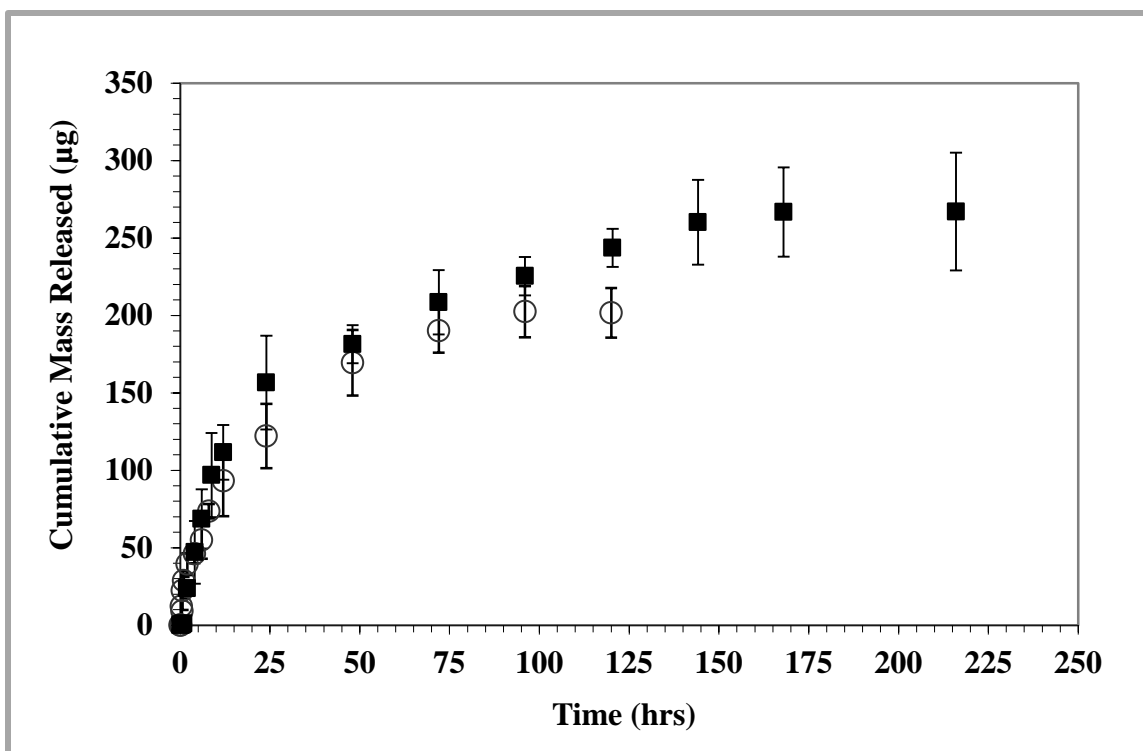


Figure 7.17: Cumulative release from LFB4 lenses with a 2.18:1 Macromer/TRIS:DMA mass ratio and 2 wt.% EGDMA

Dynamic release studies in lacrimal solution were conducted on LFB4 prepared with a 2.18:1 Macromer/TRIS:DMA mass ratio and 2 wt.% EGDMA (■). For comparison, a plot of a LFB3 lenses prepared with 7.50:1 Macromer/TRIS:DMA mass ratio and no crosslinker is also shown (○). As DADMAC is increased in the lens, there is a significant delay in DS release. N= 3, and T = 34°C.

Chapter 8

Sustained *In Vivo* Release of Ketotifen Fumarate from Imprinted Therapeutic Contact Lenses

The motivation for this work was to design a contact lens that allowed a steady, effective concentration of drug in the tear film for an extended period of time for the entire duration of lens wear. The objectives sought to compare the *in vivo* release of ketotifen fumarate from molecularly imprinted therapeutic contact lenses with topical eye drop administration.

In 2006, our group produced biomimetic hydrogel contact lenses for the enhanced loading and extended release of the anti-histamine, ketotifen fumarate [121, 167, 168]. Such lenses could be worn with comfort by allergic conjunctivitis patients to relieve itching and discomfort due to seasonal or perennial allergies [227]. In biomimetic imprinting, monomers chosen to mimic receptors in the drug's biological binding molecule are complexed non-covalently to the drug and crosslinked into a hydrogel matrix. The drug's heightened interaction with these memory pockets slows its release from the hydrogel. Multiplicity of monomer-template interactions were achieved with four functional monomers chosen from an analysis of histamine ligand-binding pockets leading to significantly enhanced loading and an increased duration of release compared to less functionalized systems [167]. Therapeutically relevant amounts of drug were released *in vitro* over multiple days from a contact lens platform [167]. This included relatively constant release in artificial lacrimal solution with ocular flow rates [168]. Since conditions within the eye are difficult to match *in vitro*, *in vivo* studies are needed to

confirm the increased efficacy and efficiency of this delivery method. The results described herein are the first *in vivo* study of these lenses.

The first *in vivo* release from imprinted contact lenses was published in 2005 showing the release of timolol in rabbit eyes using 14 mm wide diameter, 80 μm thick lenses [166]. Imprinted lenses showed higher timolol concentration in the tear layer of the rabbits but did not manage to extend release past 90 minutes. Thus, these imprinted lenses showed marginal improvement over conventional eye drops with enhanced bioavailability, but only loaded 35 μg of timolol/lens [166].

The technology represented by controlled release imprinted contact lenses is one of the most promising areas in ocular drug delivery. Afocal or non-correcting cosmetic lenses can be used by non-lens wearing patients and elute drug for the duration of wear. Controlled, sustained delivery will remove patient non-compliance as a hindrance to effective delivery and represents a more convenient and comfortable platform for drug delivery than traditional topical delivery.

8.1 Materials and Methods

8.1.1 Rabbit Purchase, Handling, and Ophthalmic Evaluation

Male New Zealand white rabbits, approximately 3 months old and weighing between 2.3-2.5 kg, were purchased from Myrtles Rabbitry (Thompsons Station, TN). Upon arrival, rabbits were acclimatized for at least 7 days to reduce stress and achieve psychological, nutritional, and physiological stability. All animal facilities used in this project were certified and inspected by AAALAC and the USDA. All rabbits were treated according to the ARVO Statement for the use of Animals in Ophthalmic and Vision Research and NIH standards. Prior to experimental work, protocols were reviewed and approved by the Auburn University Institutional Animal Care and

Use Committee (IACUC). Care was taken to assure animals were acclimated to the handling in this study. Prior to experimental manipulation, rabbits were handled on a regular basis starting on the second day after arrival in a non-threatening situation (e.g. petting, giving food treats) [228]. The rabbits were individually housed in a light controlled room (12 hour light-dark cycle) maintained at $20\pm 2^{\circ}\text{C}$ with a relative humidity of $50\pm 3\%$ with no restriction of food and water intake.

Procedures were non-painful and a commercially available rabbit restrainer (Otto Environmental, LLC) was used. The rabbits were adapted to the restraint device. The rabbits were placed in the device for successively longer intervals until the maximum time of restraint was achieved without causing distress to the rabbit. Rabbits in restraints were also continuously monitored. Rabbits were housed in stainless steel cages with slatted-floor provided by Auburn University Division of Laboratory Animal Health.

All rabbits received an ophthalmic examination with slit beam biomicroscopy (SL-15 Kowa portable slit lamp, Japan) at the beginning of the project. Tear film quality and typical tear fluid flow (TFF) of both eyes was determined by 1-minute Schirmer tear test (STT standardized strips, Schering-Plough). A small strip of calibrated filter paper was placed inside the lower eyelid and left in place for one minute. The distance to which the tears flow along the filter paper is a measure of the volume of tears produced. Corneas were stained with fluorescein-impregnated strips (Ful-Glo, Akorn) and evaluated with a slit beam of cobalt blue light. Whenever corneal surface cells are disrupted, fluorescein diffuses in the fluid spaces between cells and causes greenish staining (when viewed with a blue light). A positive or negative grade was given for the whole cornea. Rabbits with corneal disruption and a positive grade were not included in this study.

8.1.2 Synthesis of Imprinted Lenses and Ketotifen Loading

Acrylic acid (AA), acrylamide (AM), 2-hydroxyethylmethacrylate (HEMA) and azobisisobutyronitrile (AIBN) were purchased from Sigma-Aldrich (Milwaukee, WI). N-vinyl 2-pyrrolidone (NVP) and polyethylene glycol (200) dimethacrylate (PEG200DMA) was purchased from Polysciences, Inc. (Warrington, PA); ketotifen fumarate was purchased from MP Biomedicals. All chemicals were used as received.

Hydrogel contact lenses were synthesized in a temperature controlled, non-oxidative environment using free radical UV photopolymerization, according to previously published procedures [5]. Polymer composition consisted of 95 mole% functional monomer (92 mole% of the backbone functional monomer, HEMA, and the balance 3 mole% as combinations of other functional monomers), and 5 mole% crosslinking monomer. The monomer solution was pipetted into polypropylene contact lens molds (donated by Ciba Vision, Inc. (Duluth, GA)) with a diameter of 11.0 ± 0.2 mm, a base curve of 8.6 ± 0.2 mm, and power of zero. The polymerization reaction was carried out for 9 minutes with a light intensity of 40 mW/cm^2 at a constant temperature of 35°C . Non-imprinted (control) contact lenses were synthesized exactly in the same manner except ketotifen fumarate was not included in the formulation. Lenses were washed with deionized water until the template, unreacted monomers, and unincorporated photoinitiator (AIBN) could no longer be detected by spectroscopic monitoring (Synergy Biotek UV-Vis Spectrophotometer, BioTek Instruments, Vermont, USA).

Imprinted and non-imprinted poly(HEMA-co-AA-co-AM-co-NVP-co-PEG200DMA) contact lenses were loaded with ketotifen fumarate by placing each lens in a solution of ketotifen fumarate with a concentration of 0.3 mg/mL at room temperature. After equilibrium, the bound concentration in the lens was determined by mass balance.

The effect of heat and sterilization conditions on ketotifen fumarate was also assessed. In 10mL centrifuge tubes, 3 mL samples of ketotifen fumarate solutions of 0.15 mg/mL and 0.3 mg/mL were heated to 120 °C for 40 min. Loaded contact lenses were autoclaved in their equilibrium solution for 40 min at 120°C. They were sealed until fitting.

8.1.3 Transport and Structural Characterization Studies

For these studies, imprinted and non-imprinted thin films were prepared and washed as mentioned before. Then, each polymer sample was dried at 30°C under vacuum until no further weight loss was observed. The ketotifen partition coefficient (K_d) was calculated as the ratio of the equilibrium ketotifen concentration within the lens to the equilibrium solution concentration. This was found by soaking the networks in an aqueous drug solution until an equilibrium weight uptake was achieved [121].

The hydrogel films were subject to the analysis described in section 4.2 and the volume swelling ratio (Q), and the polymer volume fraction in the swollen state ($v_{2,s}$) were determined. Q is the ratio of the swollen to dry volumes of the hydrogel, $v_{2,s}$ is the inverse of the volume swelling, and $(1 - v_{2,s})$ gives the fractional water content of the hydrogel. The volume of the gel in the swollen or dry state was calculated by using Archimedes buoyancy principle [200].

Stress–strain data were obtained by performing tensile studies on a RSA III Dynamic Mechanical Analyzer (TA Instruments, New Castle, DE). Hydrogels were cut into thin sheets and a linear load stress was applied. Based on the discussion in section 4.2.2, Equation 4.16 describes the relationship between the average molecular weight between crosslinks ($\overline{M_c}$) and $v_{2,s}$ for a swollen hydrogel crosslinked in the absence of solvent [173, 229]. The slope of τ versus the elongation term $(\alpha - 1/\alpha^2)$ and tension values obtained from the tensile tests, is the Shear

modulus and enables to calculate $\overline{M_c}$. From $\overline{M_c}$, the mesh size (ξ) can be determined using equation 4.18 [230], where $C_n=11$ for this structure, $l=1.54 \text{ \AA}$ and $M_r=128.78 \text{ g/mol}$

Ketotifen fumarate permeation studies through gels were conducted using PermeGear side-by-side diffusion cells (Bethlehem, PA, USA) at 25°C. Each thin film was pre-swollen in deionized water until equilibrium was reached and placed between two half diffusion cells. The receptor cell was filled with 3.1 mL of deionized water, and the donor cell was filled with 3.1 mL of a 0.4 mg/mL ketotifen fumarate solution. To determine the rate of permeation of ketotifen through the flat lens, samples were taken from the receptor cell at scheduled intervals. Care was taken to add the equivalent amount of pure water to maintain a constant water volume within the cell. The samples were analyzed for ketotifen concentration and compared to Fick's first law of diffusion for one dimensional transport. The permeability coefficient, P , was then determined [121]. Throughout the experiment, the concentration of the donor cell was monitored to ensure a concentration driving force. The diffusion coefficient of the solute in the gel, D , was calculated by the ratio of the permeability coefficient times the thickness of the swollen gel and the partition coefficient of the solute in the gel.

8.1.4 In vitro Dynamic Therapeutic Release Studies

Dynamic release studies were conducted with the conventional or infinite sink model in order to sustain the greatest driving force, using a dissolution apparatus (Sotax Inc., Horsham, PA). In the infinite sink studies, loaded imprinted and non-imprinted contact lenses were placed in 300 mL of artificial lacrimal solution (6.78 g/L NaCl, 2.18 g/L NaHCO₃, 1.38 g/L KCl, 0.084 g/L CaCl₂·2H₂O, pH 8). The release media was stirred at a constant rate of 30 rpm and kept at a constant temperature of 34°C. Samples were taken at various time intervals and analyzed by

spectroscopic monitoring at 300 nm by drawing 200 μL of fluid into 96-well Corning Costar UV-transparent microplate and placing them in the BioTek spectrophotometer. Absorbances were recorded for three samples and averaged. Preliminary experiments were conducted to determine the amount of fluid needed to approximate infinite sink analysis. The drug loading capacity of the lenses was calculated as the total amount of drug released.

8.1.5 Fitting of Lenses and In vivo Release Studies

Sterile, ketotifen fumarate loaded contact lenses were used. Commercially available saline solution (Ocu Fresh, Optics Laboratory, Inc.) was used to remove the excess of ketotifen solution on the lens surface by soaking the lens in 10 mL of the saline solution for 15-20 seconds. The lens was placed on the right cornea of each rabbit. Retention and fit was evaluated by slit lamp biomicroscopy in both eyes using non-drug soaked lenses. Lenses were carefully placed on the cornea of the rabbits without anesthetization using a rabbit restrainer (Otto Environmental, LLC). At regular time intervals, 3-5 μL of tear fluid was collected via capillary action from the lower eyelid and conjunctival sac by using 5 μL disposable glass capillaries. During sampling, rabbits were transferred to the rabbit restrainer, and care was taken to not cause lacrimation during sampling. No nictitating membranectomy was needed. However, to prevent drying of the lens on the surface of the eye, slight partial tarsorrhaphy was performed using surgical tape. Rabbits wore Elizabethan collars during this period of the study. The contact lens was worn up to 26 hours, and after taking out the lens, an ophthalmic exam and corneal stain was conducted again as previously discussed.

Precipitation of proteins in the tear fluid occurred by treating 2 μL of the tear sample with 20 μL of 6.0 N HCl and 40 μL of DI water. The samples were centrifuged (13000 rpm) at 4°C

for 5 min. After centrifugation the supernatant was collected and ketotifen fumarate was detected by spectroscopic monitoring (Biotek Synergy H4 Hybrid Multi-Mode Microplate Spectrophotometer) using a Biotek Take3™ multivolume quartz, microreader plate with 16 spot wells of 2 μ L each. Measurements were taken by running the spectrum between 200-900 nm. Concentration measurements were taken at 300 nm wavelength, the wavelength of maximum absorption. This procedure was performed on tear fluid without ketotifen fumarate and no peak was observed. For the topical eye drop study, one drop (50 μ L) of commercially available 0.025% ketotifen eye drops (Zaditor®, Novartis), equivalent to 0.035% ketotifen fumarate, was applied to the contralateral rabbit's eye (left eye), and the above procedure for the tear fluid samples was followed.

8.1.6 Pharmacokinetic Parameters of Ketotifen Fumarate in Tear Fluid

The area under the concentration time curve (AUC) and the area under the first moment of the concentration versus time curve (AUMC) were calculated according to the linear trapezoidal rule. The mean residence time (MRT) was calculated from the ratio between the AUMC and the AUC [231].

8.2 Results and Discussion

Previous work conducted by our lab highlights that the best results in loading and delayed *in vitro* release corresponded to the most structurally diverse polymer network [167]. The inclusion of four functional monomers into the formulation created the most stable monomer/drug complexes, which allowed the formation of memory sites within the poly(HEMA-co-AA-co-AM-co-NVP-co-PEG200DMA) network through the arrangement, type,

and amount of functionality [121, 167]. Thus, a high degree of control could be achieved over the release rate of ketotifen fumarate through application of molecular imprinting techniques.

The $\log P_{\text{octanol/water}}$ of ketotifen fumarate is -0.3 , indicating that ketotifen is mildly hydrophilic. The aqueous solubility of ketotifen fumarate is 3.4 mg/mL at pH 7 and 20°C [168].

Figure 8.1 demonstrates that therapeutic transport and loading can be tailored via the memory within the polymer chains. Transport was significantly delayed from the imprinted gels compared to non-imprinted gels despite having very similar structures as determined experimentally. It is clear that imprinting affected transport compared to controls and was not due to structural differences. The imprinted poly(HEMA-co-AA-co-AM-co-NVP-co-PEG200DMA) network exhibited a ketotifen fumarate diffusion coefficient of $(7.08 \pm 0.24) \times 10^{-10} \text{ cm}^2/\text{s}$ (via permeation studies), a partition coefficient (K_d) of 45.05, an equilibrium volume swelling (Q) of 1.646 ± 0.136 , and a polymeric volume fraction in the swollen state ($v_{2,s}$) of 0.608 ± 0.050 . The imprinted network had a much greater loading (4 times more) and a considerably slower transport (19 times slower) than non-imprinted networks at approximately equivalent volume fraction in the swollen state and average molecular weight between crosslinks.

To assess the effect of sterilization conditions on ketotifen fumarate, 3 mL samples of ketotifen fumarate solutions of 0.15 mg/mL and 0.3 mg/mL were heated to 120°C for 40 min. Before and after the samples were autoclaved, ketotifen concentration was measured. The concentration of ketotifen did not change and no other absorbance peaks were detected. The autoclaved samples had slightly elevated concentrations ($4.0 \pm 0.2\%$) due to water evaporation.

Dynamic release studies were performed under infinite sink conditions in order to maintain a maximum concentration driving force. Figure 8.2a shows the cumulative release

profiles in artificial lacrimal solution from imprinted and non-imprinted poly(HEMA-co-AM-co-AA-co-NVP-co-PEG200DMA) contact lenses. The imprinted lenses exhibited an extended release of ketotifen fumarate for a duration of 72 hours (85% of the drug was released in approximately 24 hours). In contrast, the non-imprinted lens released 100 % of the drug in less than 6 hours (Figure 8.2b). The results showed that the imprinted lenses have a much slower release rate, moving towards zero order release, than non-imprinted lenses. The mass of ketotifen fumarate loaded into poly(HEMA-co-AA-co-AM-co-NVP-co-PEG200DMA) imprinted lenses was 115 ± 10 $\mu\text{g}/\text{lens}$ and 39 ± 2 $\mu\text{g}/\text{lens}$ for non-imprinted lenses. All contact lenses had high optical clarity and adequate mechanical properties for use as contact lenses.

Exam slit beam biomicroscopy was unremarkable and STT results were normal for all rabbits in the study. Rabbits had no corneal abrasions prior to the study and were graded as negative. Figure 8.3 shows the *in vivo* dynamic release of ketotifen fumarate from imprinted and non-imprinted poly(HEMA-co-AM-co-AA-co-NVP-co-PEG200DMA) contact lenses.

The *in vivo* release profile for the imprinted lenses showed an initial pulse characterized by a rapid concentration increase up to a maximum value, C_{max} , (Table 8.1), followed by a steady drug release. The results clearly demonstrate an extended release and relatively constant tear concentration of ketotifen fumarate for 26 hours. The lenses delivered an average constant concentration of 170 ± 30 $\mu\text{g}/\text{mL}$. The controlled and sustained release of ketotifen fumarate from the imprinted contact lenses maintained a stable drug concentration in the tear fluid, despite the tear drainage and tear-film turnover rate. Furthermore, the hydrogel lens protected the reservoir of drug inside the lens from being quickly washed away by the lacrimal system. Prolonged retention in the precorneal area increases the ocular bioavailability of ketotifen fumarate.

Table 8.1: Pharmacokinetic parameters calculated from the concentration time profiles of ketotifen fumarate in tear fluid

Delivery Mechanisms	C _{max} (µg/mL)	t _{max} (min)	AUC _{0-26 h} (µg*hr/mL)	MRT (hr)
Imprinted Lens	214 ± 63	240	4365 ± 1070	12.60 ± 0.37
Non-Imprinted Lens	140 ± 35	60	493 ± 180	3.36 ± 0.17
0.035% eye drops (50 µL)	143 ± 18	0	46.6 ± 24.5	0.25 ± 0.07

The data are presented as mean ± SD (n=3-5).

In order to assess the release rates of the imprinted contact lenses, a comparison of non-imprinted contact lenses was needed. As Figure 8.3 shows, when the non-imprinted lenses were used the concentration of ketotifen fumarate in tear fluid increased quickly to a C_{max} of 140±35 µg/mL and exponentially decreased and disappeared from the tear fluid within 10 hours. It is important to mention that due to the chemistry of the non-imprinted lenses (i.e. 3 mol% of functional monomers), random interactions can occur between ketotifen and the functionalities within the lens, which can slow the diffusion rate of the drug. However, the non-imprinted lenses do not maintain a stable drug concentration in the tear fluid, and the effective dose (ED₅₀) of ~30 µg/mL [232] was maintained for just 7 hours.

A comparison of topical ketotifen fumarate eye drops was also performed. Figure 8.3 shows the *in vivo* concentration profile of ketotifen fumarate after application of one drop of topical 0.035% ketotifen fumarate solution (50 µL, 17.5 µg of ketotifen fumarate, Zaditor®, Novartis) into the rabbit's eye. The concentration of ketotifen fumarate in tear fluid, after installation, increased quickly to a C_{max} of 143±18 µg/mL and exponentially decreased and disappeared from the tear fluid within 45 min. This means that upon installation of ketotifen fumarate eye drops, most of the installed drug is quickly eliminated from the precorneal area due to tear drainage. It is important to note that ED₅₀ is 30 µg/mL [232], and this concentration is reached in approximately 30 minutes. However, after wearing the imprinted contact lens for 26 hours, the concentration of ketotifen fumarate in the tear fluid was still high at a value of 160

$\mu\text{g/mL}$. Tear concentration values of ketotifen fumarate were substantially higher in the imprinted contact lens group indicating that the lenses release a clinically effective amount of ketotifen fumarate [232, 233]. This is the first demonstration of a steady concentration of drug being maintained in the tear film for an extended period of time via release from a contact lens.

To appreciate the average time that the drug stayed in tear fluid, the mean residence time (MRT) of ketotifen fumarate in rabbit eyes was calculated. The MRT of ketotifen fumarate from the imprinted contact lenses was 12.60 ± 0.37 hours, 3.75 times greater than the MRT of non-imprinted and almost 50 times greater than the MRT of the topical eye drops (Table 8.1). The imprinted contact lenses exhibited a AUC value of $4365 \pm 1070 \mu\text{g} \cdot \text{hr/mL}$, which is almost 9 times greater than non-imprinted lenses and 94 times greater than topical eye drops (Table 8.1).

The bioavailability of ketotifen fumarate in the tear fluid for the contact lenses relative to the eye drops was calculated as the ratio between the AUC of the lenses to the AUC of the eye drops, normalized for dose. The relative bioavailability for the imprinted lenses is 14.25 ± 2.62 , which is 3 times greater than the relative bioavailability for non-imprinted lenses (4.75 ± 0.50). This indicates that the imprinted lenses are much more effective and efficient drug delivery devices than non-imprinted lenses and eye drops.

Control over drug loading and release from molecularly imprinted contact lenses has greatly improved since the publication of the first *in vivo* release. Release of timolol from poly(DEAA-co-EGDMA-co-MAA) imprinted lenses showed an AUC of $57 \mu\text{g} \cdot \text{hr/mL}$ which was only a 3.5 fold increase over the AUC from topically applied eye drops for a duration of only 90 minutes (Figure 8.4a) [166]. Thus, these imprinted lenses showed marginal improvement over conventional eye drops with enhanced bioavailability, but they only loaded $35 \mu\text{g}$ of timolol/lens [166]. However, the field has learned much over the last 5 years and our imprinted

gels have demonstrated substantial increases in the amounts of drug loaded as well as imprinting mechanisms delaying release [121, 167, 170]. The early timolol imprinted lenses showed 50% increase in drug loading comparing imprinted lenses to control with no differences in drug transport. For the study presented herein, imprinted lenses loaded 175% more and also showed delayed transport compared to non-imprinted lenses.

Moreover, our imprinted contact lenses performed remarkably better than ketotifen fumarate silicone contact lenses, which showed decreasing rates of release over time and lacked of any sort of controlled release mechanism (Figure 8.4b) [214]. It was reported that the silicone contact lenses had an $AUC_{0-35\text{hrs}}$ value of $988.03 \pm 67.75 \mu\text{g} \cdot \text{hr}/\text{mL}$ [214], which is 4 times less than the value for the imprinted contact lenses ($4365 \pm 1070 \mu\text{g} \cdot \text{hr}/\text{mL}$). Also, an effective dose (ED_{50}) of $\sim 30 \mu\text{g}/\text{mL}$ [232] was maintained for less than 8 hours. The imprinted lenses demonstrated controlled release of an effective concentration for the entire duration of lens wear, which is 24 hours for a daily wear lens.

This data is very exciting as it demonstrates controlled release under *in vivo* conditions, and comparison to human physiology and anatomy is warranted. The normal lacrimal volume in rabbits has been reported as $7.5 \pm 2.5 \mu\text{L}$ [234]. The same parameter in humans has been reported as $7 \mu\text{L}$ [235]. Moreover, the tear film thickness is comparable between the rabbit cornea ($45 \mu\text{m}$) and human cornea ($41\text{--}46 \mu\text{m}$) [43]. However, the most different parameters are lacrimation and tear turnover rate as well as blinking times. The human lacrimal fluid turnover rate is twice as large as that found for rabbits ($\sim 16\%/ \text{min}$ in humans and $\sim 7.1\%/ \text{min}$ in rabbits). Humans blink approximately once every 5 seconds and rabbits may not blink for up to 15 minutes [234, 235]. Thus, this suggests that the residence time and release duration may be slightly less in human eyes compared to rabbit eyes.

Other competing platforms are drug eluting inserts that are designed to reside under the lid or in the cul de sac of the eye. However, inserts can cause irritation and discomfort and usually cannot be placed by the consumer, as opposed to contact lenses which can readily be placed and removed. In addition, patients may not notice if an insert is expelled from the eye. It can also be reasonably stated that public confidence in and awareness of contact lenses is much higher than ocular inserts.

Duration of action depends on pharmacokinetics, bioavailability, and receptor kinetics. The inhibition effect of ketotifen decreases significantly in the hours after administration and is less than 8 hours [232]. Imprinted lenses can deliver a constant drug concentration at a high effectiveness level for extended periods leading to significantly increased duration of action. The enormous advantage of using imprinting mechanisms is that the release rate, and thus the concentration reached, can be altered by changing the engineering design of such systems [167, 168, 170, 236].

8.3 Conclusions

In summary, we demonstrated that imprinted poly(HEMA-co-AA-co-AM-co-NVP-co-PEG200DMA) contact lenses can controllably deliver a sustained effective concentration of ketotifen fumarate under *in vivo* conditions. Previous work by our group has demonstrated that *in vitro* drug release rates can be tailored to deliver for extended periods of time. For the first time, we demonstrate that contact lenses can be used to release a constant, effective drug concentration in tear fluid for up to 26 hours, making them ideal for use as daily wear or disposable delivery devices. The imprinted lenses demonstrated much longer precorneal retention times and much higher tear fluid bioavailability compared to commercially available ketotifen fumarate eye

drops or drug soaked lenses. This work demonstrates the high value of imprinted mechanisms toward the formation of combination devices, such as a contact lens that also relieves itching and discomfort due to seasonal or perennial allergies.

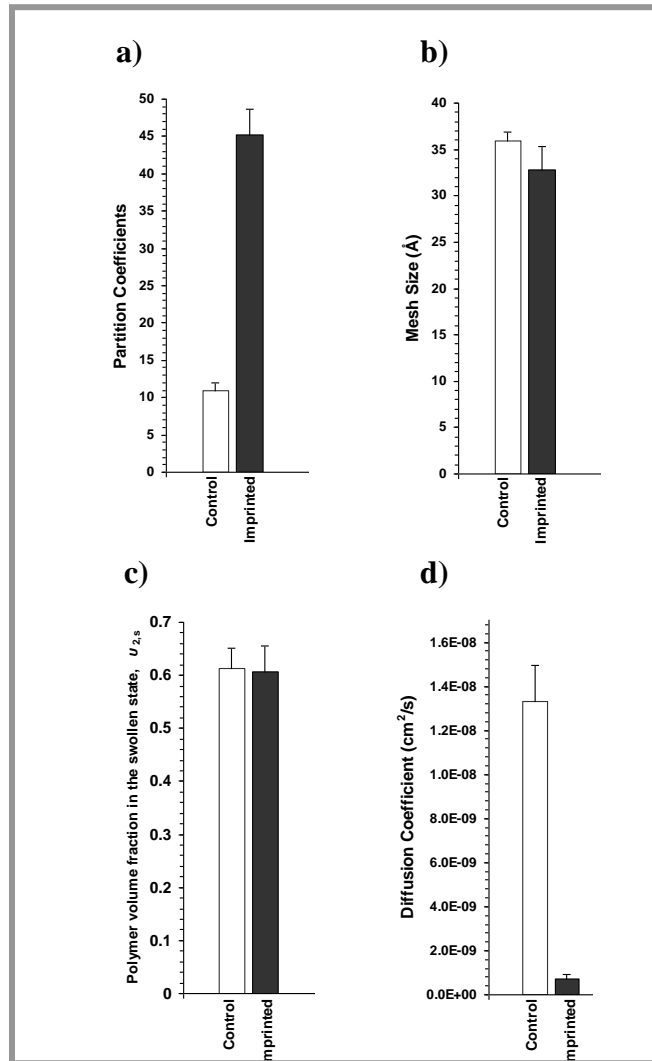


Figure 8.1: Loading, transport, and structure of imprinted networks

(a) Partition coefficients, (b) Mesh sizes obtained via tensile studies, (c) Equilibrium polymer volume fractions in the swollen state, (d) Diffusion coefficients obtained via permeation studies, for poly(HEMA-co-AA-co-AM-co-NVP-co-PEG200DMA) networks with a crosslinking percentage of 5 mole %. $N = 3$, and $T = 25\text{ }^\circ\text{C}$.

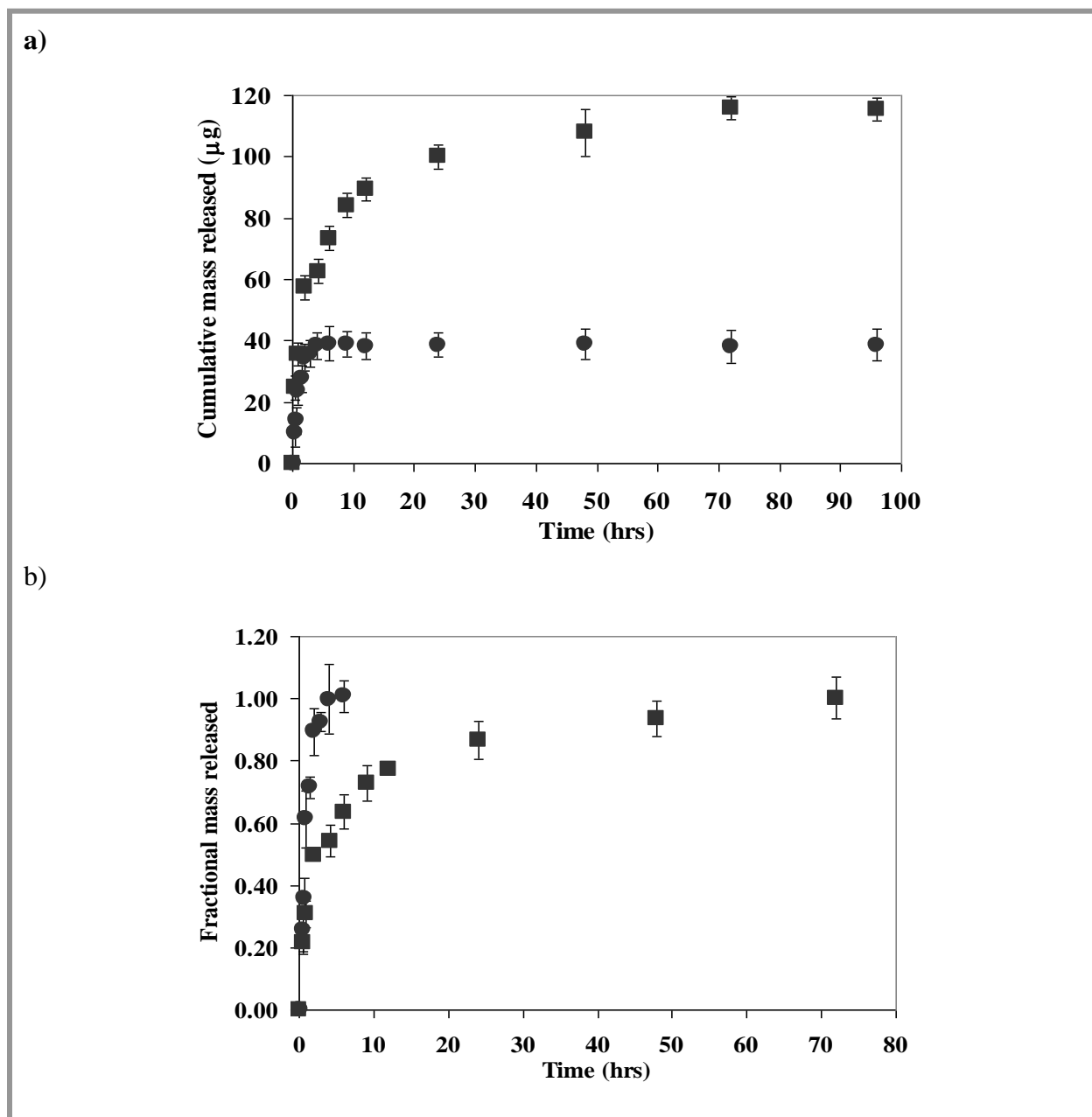


Figure 8.2: Conventional infinite sink drug release from imprinted (■) and non-imprinted (●) poly(HEMA-co-AA-co-AM-co-NVP-co-PEG200DMA) contact lenses

(a) Cumulative release of ketotifen fumarate from therapeutic contact lenses in artificial lacrimal solution at 34°C. The total amount of ketotifen fumarate released from the contact lenses was considered as the drug loading capacity. (b) Fractional release profiles of ketotifen fumarate from therapeutic contact lenses. Lens details: 100±5 µm thickness, diameter 11.8 mm, no power, loaded at 0.3mg/mL ketotifen concentration. The data is plotted as the mean ±SD (N=3).

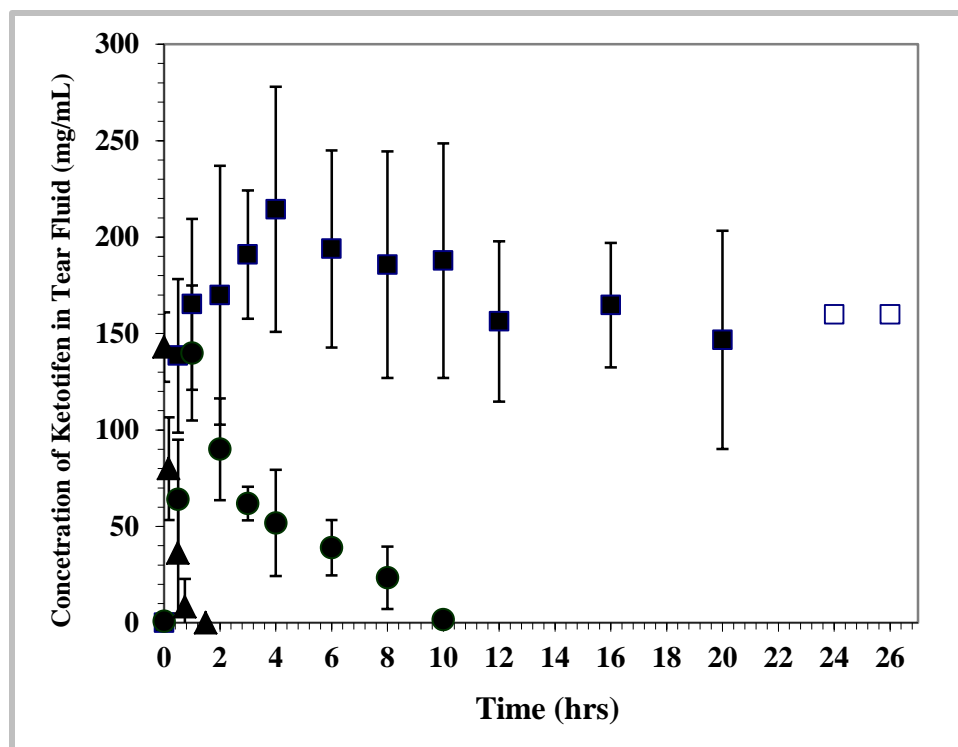


Figure 8.3: *In vivo* ketotifen fumarate tear fluid concentration profile from contact lenses and topical eye drops in a white New Zealand rabbit

Dynamic ketotifen fumarate release from poly(HEMA-co-AA-co-AM-co-NVP-co-PEG200DMA) contact lenses, Imprinted (■,□) and non-imprinted (●) (lens details: 100 ± 5 μm thickness, diameter 11.8 mm, no power, loaded at 0.3mg/mL ketotifen concentration). Release from one eye drop (0.035% solution Zaditor® Novartis) (▲). Imprinted contact lenses clearly demonstrate an extended release of ketotifen fumarate, a significantly increased ketotifen fumarate residence time, and a significantly increased bioavailability of ketotifen fumarate in the tear fluid for an extended duration compared to non-imprinted lenses and topical drop therapy. Solid data points represent the mean \pm SD (N=3-5) and hollow data points represent single run (N=1).

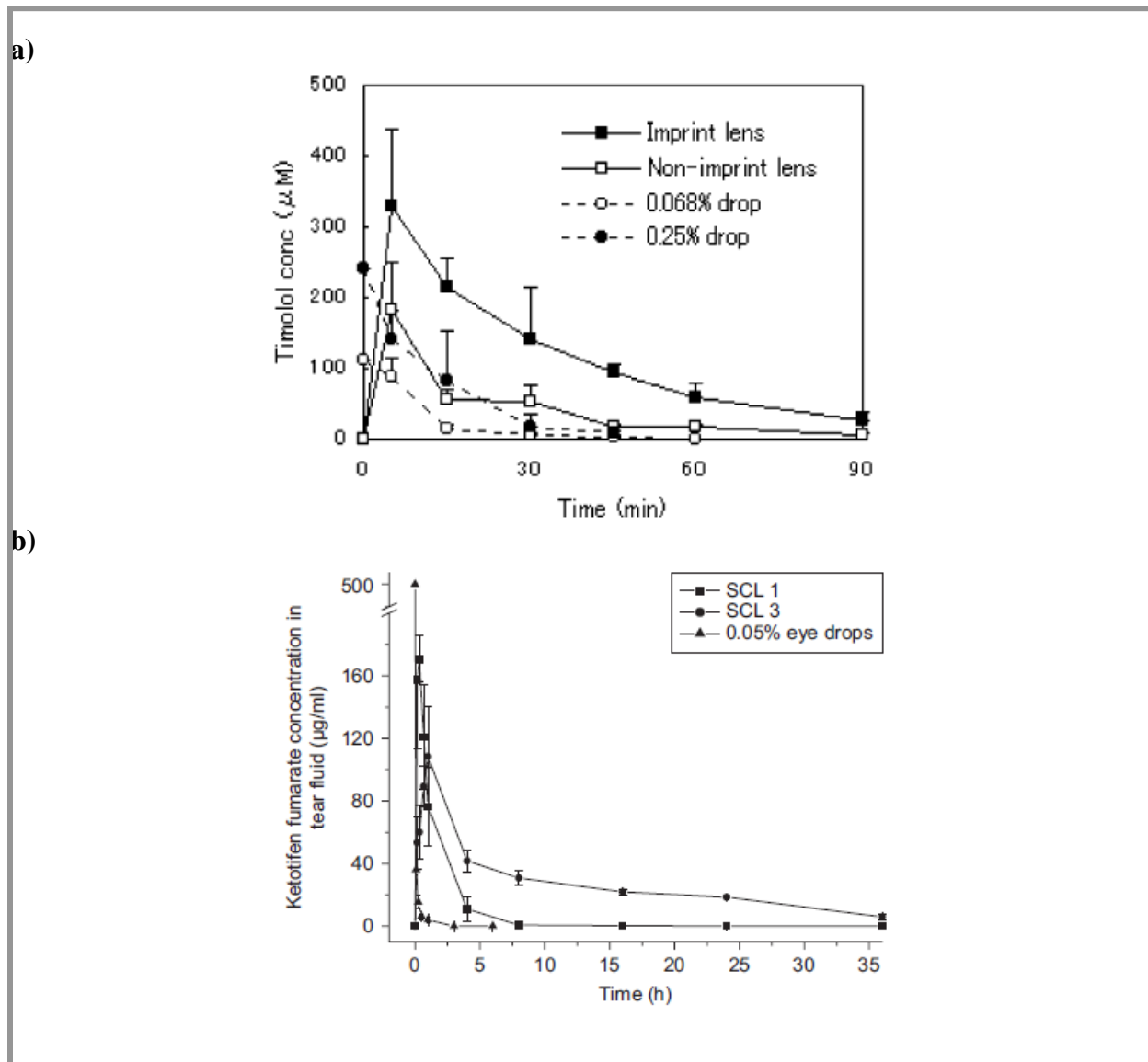


Figure 8.4: In vivo drug release results: (a) First study of imprinted lenses releasing timolol, and (b) silicone hydrogel lenses releasing ketotifen fumarate

Soaking commercial silicone hydrogel and hydrogel contact lenses in ketotifen fumarate solutions does not result in sufficient loading or release duration for effective delivery from contact lenses. Figure 8.4a, reproduced from reference [166], shows release of timolol from poly(DEAA-co-EGDMA-co-MAA) imprinted lenses with a bioavailability of $57 \mu\text{g}\cdot\text{hr}/\text{mL}$ which was only a 3.5 fold increase over the bioavailability from topically applied eye drops for a duration of only 90 minutes. Figure 8.4b reproduced from reference[214], shows *in vivo* release from a silicone hydrogel of an effective concentration (ED_{50}) in ~ 8 hrs. Ketotifen loading was very low, with a peak ketotifen concentration of $133 \mu\text{g}/\text{lens}$. Very low control over release rate is observed and low loading.

Chapter 9

Effects of Sink Conditions on Release Kinetics of Ocular Therapeutic from Contact Lenses

In the last 50 years, several methods have been proposed to achieve an extended and controlled release of ocular therapeutics from soft contact lenses. Developing an effective method that allows for controlled and extended controlled drug release via contact lenses may revolutionize the ocular therapeutics field as well as have a huge impact on the market. Unfortunately, there is an issue hindering progress in the field. Release conditions (e.g. volumes, temperature, and mixing rate) and their effects on release kinetics are not well studied or presented well in the literature, which leads to false conclusions of long release durations as the vast majority of lens release systems have failed during *in vivo* studies by not demonstrating considerable differences compared to topical drop therapy. Using different conditions for the study of drug release kinetics have created a system that allows for no true basis of comparison, and therefore leads to issues assessing which techniques are more effective than others. At this stage in the field, proper comparisons among different release mechanisms are vital.

Currently, the *in vitro* release studies in the field can be generalized into three separate categories: small volume, large volume, and microfluidic flow devices. Some researchers use the term release sink, which refers to the volume of solvent in which the lenses are placed during release studies. A small sink is typically an aqueous volume approximately between 2-30 mL with no forced mixing and with or without a timed interval of water exchange. For release studies conducted in small sinks, solvent exchange is required to reestablish the driving force for

mass diffusion. A large sink is typically a solvent volume of 200 mL or more that is mixed, where, at times, can be classified as an infinite sink where the majority of drug release is achieved without the necessity for solvent exchange. The infinite sink is defined as an environment where the accumulation of drug in the solution surrounding the lens is considered to be negligible, attaining the greatest driving force possible and corresponding to the fastest possible release. It allows for the quickest comparison between formulations of a certain method or various methods to control release. The microfluidic device consists of a small chamber where the contact lens sits, and it is designed to mimic the continuous, volumetric flow rate of tear fluid [237].

Most drug-eluting lens systems described in the literature to date have used small volumes (i.e., 2-10 mL), which are not well mixed (Figure 9.1) [93]. We hypothesize that this stems from characteristics pertaining to the fluid flowrates of the eye. The tear turnover rate within the eye is 0.5-2.2 $\mu\text{L}/\text{min}$ [6, 23]. This flowrate, although not constant *in vivo*, can be used to calculate the total amount of tear fluid that comes into contact with the eye during a 24 hour period – an average of 2 mL, making the assumption that a small sink is a good setting for drug release kinetic studies. Moreover, the turnover rate during contact lens wear can be 2.82 ± 1.45 $\mu\text{L}/\text{min}$ [23], meaning that the eye surface can be flushed with an average of 4.1 mL of tear fluid a day. However, we hypothesize that a stagnant, small sink is neither a suitable environment for testing extended release nor a reliable representation of the ocular environment. The continuous tear turnover rate of the actual eye is expected to lead to very different diffusion kinetics than a stagnant volume. A common, incorrect assumption made with small volumes, is to proclaim them as perfect sinks or infinite sinks. In some cases the Higuchi equation [238, 239] is misused to calculate the release kinetics parameters such as the diffusion coefficient.

The focus of the work presented in this chapter is to explore the effect of release conditions on the release rate as well as the reasons why so many promising *in vitro* studies have failed to show extended release during *in vivo* studies.. Variations in the release conditions (e.g. volumes, temperature, and mixing rate) and their effect on drug release were examined for a wide spectrum of both hydrophilic and hydrophobic drugs (ketotifen fumarate, diclofenac sodium, timolol maleate and dexamethasone) (Figure 9.2) from conventional hydrogel lenses and silicone hydrogel lenses.

9.1. Materials and Methods

9.1.1 Materials and Reagents.

Diethylaminoethyl methacrylate (DEAEM), acrylic acid (AA), acrylamide (AM), methacrylic acid (MAA) 2-hydroxyethylmethacrylate (HEMA), N-vinyl-2-pyrrolidone (NVP), ethylene glycol dimethacrylate (EGDMA), azobisisobutyronitrile (AIBN), timolol maleate salt (TMS), ketotifen fumarate (KF), dimethyl acrylamide (DMA), and Darocur 1173 were purchased from Sigma-Aldrich (Milwaukee, WI). Diclofenac sodium salt (DS) was purchased from Sigma-Aldrich (Saint Louis, MO). Tris(hydroxymethyl)aminomethane (TRIS), and 900-1200 MW methacryloxypropyl-terminated polydimethylsiloxane (PDMS) were purchased from Gelest, Inc. (Morrisville, PA). Dexamethasone (DEX), and ethanol (97%) was purchased from VWR International (Radnor, PA). Polyethylene glycol (200) dimethacrylate (PEG200DMA) was purchased from Polysciences, Inc. (Warrington, PA). All chemicals were used in their respective forms as received.

9.1.2 Synthesis of Therapeutic Hydrogels Films.

Therapeutic hydrogel films were synthesized using molecular imprinting techniques, where macromolecular framework or memory for the drug is produced during polymer synthesis. Imprinted networks have been shown to improve loading and considerably extend and control release. Excellent review articles give background of the field [22-24] with some specifically written in regard to contact lenses [25, 26]. A wide spectrum of both hydrophilic and hydrophobic drugs (ketotifen fumarate, diclofenac sodium, timolol maleate and dexamethasone) (Figure 9.2) were used to synthesize both platforms of hydrogels currently used in experimental papers, silicone and hydrophilic, conventional (pHEMA) hydrogels. Several formulations were made as describe in Table 9.1 and Table 9.2.

Table 9.1: Formulation of hydrophilic, conventional hydrogel films

Sample	Drug	Monomers						Crosslinkers		Initiator
		HEMA	AA	AM	NVP	DEAEM	MAA	EGDMA	PEG200DMA	AIBN
KF-HEMA	0.5	91	1	1	1				5	0.5
DS-HEMA	0.5	89				5			5	0.5
TMS-HEMA	1.5	90					3	5		0.5

Feed composition of the pre-polymerization solutions. Amounts represent mole% of the total solution.

Table 9.2: Formulation of silicone hydrogel films

Sample	Drug	Monomers				Ethanol	Initiator
		PDMS	TRIS	DMA	AA		Darocur 1173
KF-PDMS	0.3	3.9	7.3	44.1	9.8	33.7	0.9
DEX-PDMS	0.3	2.6	5.1	32.7		58.6	0.7

Feed composition of the pre-polymerization solutions. Amounts represent mole% of the total solution. Ethanol was added to aid in solubilization.

All the solutions were vortexed and sonicated until no phase separation occurred in the mixture. The solutions were transferred to a MBraun Labmaster 130 1500/1000 glovebox, which provided an inert (nitrogen) atmosphere. The films were prepared by pipetting the monomer solution into glass plates (15.25 cm x 15.25 cm) coated with hydroxy-terminated

polydimethylsiloxane (to prevent strong adherence of the polymer matrix to the glass), and separated by 0.145 mm Teflon spacers. Free-radical UV photopolymerization was carried out in a temperature controlled non-oxidative environment for 9 minutes for the HEMA hydrogels and 2 minutes for the silicone hydrogels, with a light intensity of $41.0 \pm 0.5 \text{ mW/cm}^2$, measured using a radiometer (International Light IL1400A). The glass plates were submerged into a deionized water bath; the thin film was peeled from the glass surface and cut into circular films of 16.75 mm diameter.

9.1.3 Drug Loading of Hydrogel Films

Silicone hydrogel films were washed with ethanol for up to 5 days, and subsequently conventional and silicone hydrogel films were washed with deionized water (Millipore, 18.2 M Ω cm, pH 6.2) until the respective drug and unreacted monomers could no longer be detected by spectroscopic monitoring (Synergy Biotek UV–Vis Spectrophotometer, BioTek Instruments, Winooski, VT). Stock solutions were prepared with the different drugs in DI water (0.30 mg of KF/mL, 0.20 mg of DS/mL, 0.08 mg of DEX/mL, and 0.20 mg of TMS/mL). Initial absorbances of each concentration were measured using a Synergy UV–Vis spectrophotometer at 300 nm for ketotifen fumarate, 276 nm for diclofenac sodium, 240 nm for dexamethasone, and 295 nm for timolol maleate, the wavelength of maximum absorption. After the initial absorbance was taken, a washed hydrogel film was inserted into 5 mL of solution placed in a vial, and the vials were gently agitated on an ocelot rotator (Fisher Scientific; Chicago, IL) at 75 rpm and 12° tilt angle. Separate experiments were conducted to assure equilibrium was reached. After equilibrium was reached, the solutions were vortexed for 10 seconds; the bound concentration in the gel was determined by mass balance. All hydrogels were analyzed in triplicate.

9.1.4 Dynamic Therapeutic Release Study

To analyze the difference among the release studies, the first set of experiments were to replicate the volume and mixing rates used throughout literature. All the experiments were performed at room temperature (~20°C). The releases in the large volumes were performed using a dissolution apparatus (Sotax Inc., Horsham, PA) in which loaded hydrogel films were placed in 200 mL, 300mL or 400 mL of DI water (pH 6.4) and continuously agitated at 30 rpm, with no exchange of solvent.. For the releases in the small volumes (one of the most used throughout literature), loaded hydrogel films were placed into 2 mL, 5 mL or 30 mL with no forced mixing and solvent exchange every 24 hours. Release of the drugs was monitored at specific time intervals using a Synergy UV-Vis Spectrophotometer (BioTek, Winooski, VT) at 300 nm for ketotifen fumarate, 276 nm for diclofenac sodium, 295 nm for timolol maleate, and 240 nm for dexamethasone. The absorbance was recorded for three samples, averaged, and corrected by subtracting the respective controls. After the readings were performed all samples were placed back into the respective sinks. Studies were ended after 96 hours. Other variables that could affect the release rate of the drug, such as temperature and mixing rate, were studied in the 200 mL volume case. Release studies were conducted using the hydrophilic, conventional hydrogel films loaded with ketotifen fumarate, where mixing rate was set at 30 rpm and 160 rpm with all other variables held constant (20°C, and no water exchange), and the temperature at 20°C and 34°C with all other variables held constant (30 rpm, and no water exchange). Studies were ended after 48 hours.

9.2 Results and Discussion

9.2.1 Release Studies from Hydrophilic, Conventional Hydrogels

Figure 9.3a exhibits the release profile obtained for lenses that release ketotifen fumarate in a 2 mL small volume with no forced mixing and solvent exchange every 24 hours. The results show that the release profile was being affected by the experimental set-up, where equilibrium was reached promptly. As time increased, the driving force decreased slowing down the release rate until equilibrium was reached. As noted by the steep climb and then almost immediate flattening of the data, equilibrium was reached well before the time for solvent exchange (within a few hours after solvent exchange). If the differential time and mass are calculated for each 24 hour period (with Δm being the change in mass released of each fresh solvent, with the initial solvent 1 through the final solvent 4), a decrease in differential mass release with each fresh solvent is quite notable. The largest differential mass release occurred in the first solvent exchange (the first 24 hours) and each of the following solvent exchanges decreased substantially in differential mass released (Figure 9.3b).

If the release volume and the boundary conditions are not well understood and enough data points are not obtained to assure equilibrium is not close to being reached, the data can be misinterpreted as it is often done in the literature, resulting in false conclusions. Figure 9.3c shows the data points for the cumulative mass released every 24 hours if the data point was taken immediately before solvent exchange. The trend, especially from the 24 hour to 96 hour points, could be mistaken as a linear extended controlled release profile. This would be an inaccurate conclusion. Thus, our results prove that to produce accurate release data in a volume of 2 mL, the exchange of solvent should be performed at very short time intervals (e.g. 1 hour or under 1 hour). As the release rates will also depend on solubility of drug in the bulk solution and within

the polymer, it is warranted for each investigator to assess time for equilibrium to occur for their particular polymer/drug system and choose a solvent exchange time well before equilibrium is reached. Typically, this data is not supplied or presented in the literature to support the overall drug release profile.

A relatively small increase in volume can lead to a different result. When increasing the volume of the release media from 2 mL to 5 mL (Figure 9.4), the total ketotifen fumarate released at 48 hours increased by approximately 55%. Thus, for a given molecule that has a given solubility, the release rate is very sensitive to the volume of the release media available as well as the drug concentration in the bulk fluid.

Figure 9.5 compares various release media volumes that span a much wider range. It highlights 2 mL and 30 mL volumes with no forced mixing and solvent exchange every 24 hours, as well as, 200 mL, 300 mL and 400 mL volumes with a mixing rate of 30 rpm and no solvent exchange. Among the release studies, the large volumes with mixing exhibited a dramatic increase in the release rate. Comparing the 30 mL and 200 mL volumes, they reached the same cumulative mass of ketotifen fumarate released, but at much different rates. The hydrogels releasing in the 30 mL volume exhibited a much slower release rate, and these results could potentially be misunderstood if samples were only taken once every 24 hours. Also, the same trend of decreasing differential mass release with each new solvent was observed, with the first 24 hours exhibiting the largest differential mass release.

The cumulative mass released at 96 hours from the 2 mL small volume was 0.028 ± 0.001 mg, whereas for the 200 mL and 300 mL large volumes, was 0.118 ± 0.011 mg and 0.162 ± 0.008 mg, respectively. At 96 hours, the hydrogels releasing in the 200 mL and 300 mL volumes had released about 4 and 6 times as much of the ketotifen fumarate as had the hydrogels in the 2 mL

volume. While an increase in the cumulative mass released was observed in the results of the 300 mL volume when compared to release of the 200 mL volume, there is not a statistically significant difference between the releases of the 300 mL and 400 mL volumes. Therefore, one can conclude that the 300 mL volume would be enough to maintain a high concentration driving force and possibly the highest concentration driving force, and potentially achieve infinite sink conditions until the completion of the release.

If one were to only consider the data taken at each solvent exchange (every 24 hours), for the 2 mL volume case (Figure 9.3c), and extrapolated, a power trend fit the data ($y = 0.0067x^{0.3083}$, $R^2 = 0.997$, Figure 9.6). With a power law equation reported, the release of ketotifen fumarate in the 2 mL volume case would take 5,566 hours or 232 days to release 0.096 mg, the equivalent to the 200 mL volume case at 24 hours, and 10,915 hours or 1.25 years to release 0.118 mg, the equivalent to the 200 mL volume case at 96 hours. Thus, extrapolating the data highlights the extremely slow rate of release in small volume with solvent exchange made only every 24 hours, which is significantly slower than release in the large volume.

These results reflect the drastic difference between release kinetics when the experimental conditions, such as volume and mixing rate are varied. When the release study is performed in small volumes with no forced mixing, a boundary layer between the film and the surrounding solvent is formed. The bulk concentration of the drug in the solvent is non-negligible, and increases as drug releases with time. The release becomes delayed as this concentration gradient (driving force) decreases. When the release is close to equilibrium, the concentration gradient becomes low, resulting in a very low release rate and extending the duration of the release, making difficult to compare the results achieved in larger volumes or infinite sink conditions. There was a continuous increase of the cumulative mass released in the

mixed large volume, demonstrating that equilibrium was not reached during the experiment. Therefore, the concentration gradient and the fastest possible driving force throughout the majority of the release can be realized.

For further release studies, the 2 mL volume with no forced mixing and solvent exchange every 24 hours, and the 200 mL volume with a mixing rate of 30 rpm were set to be the standards. Next, drugs with similar molecular weights and different solubilities were tested (Figure 9.2). Figure 9.7a and 9.7b show the large and small volume release profiles for diclofenac and timolol from hydrophilic, conventional hydrogel films. The results demonstrated similar trends as demonstrated in the ketotifen releasing hydrophilic hydrogel films. Both systems show substantial differences between the various release conditions with strong evidence of equilibrium being reached well before solvent exchange in the small volume cases. The films in the large sinks (200 mL with a mixing rate of 30 rpm) exhibited cumulative mass release amounts that were approximately 12 times greater for diclofenac and 3 times greater for timolol than the cumulative mass release amounts in their respective small sinks (2 mL with no forced mixing and solvent exchange every 24 hours).

9.2.2 Release Studies from Silicone Hydrogels

Silicone hydrogels are biphasic systems; they contain both hydrophilic and hydrophobic regions. Therefore, the partitioning of the drug within the silicone hydrogel network is expected to be different than the drug partitioning within purely hydrophilic hydrogels, resulting in different transport properties. Consequently, release studies were also performed using silicone hydrogels. Figure 9.8a exhibits the release profiles of ketotifen fumarate from silicone hydrogels in both the 2 mL volume with no forced mixing and solvent exchange every 24 hours and the

and 200 mL volume with a mixing rate of 30 rpm. At 96 hours, the silicone hydrogels releasing in the 200 mL volume had released about 9 times as much of the ketotifen as had the silicone hydrogels in the 2 mL volume. This ratio is over 2 times more the amount of ketotifen released from the conventional hydrogels, indicating that the release is even more affected by the use of a small volume. The same observations as before can be made for the small volume data points – equilibrium was reached well before the 24 hour solvent exchange point.

Figure 9.8b exhibits the release profiles for dexamethasone from silicone hydrogel films. Comparing release in the 2 mL and 200 mL volumes, the films reached the same cumulative mass of dexamethasone released, but at much different rates. The hydrogels releasing in the 2 mL volume exhibited a much slower release rate, reaching equilibrium well before the 24 hour time point for solvent exchange. Once again, these results could potentially be misunderstood if samples were only taken once every 24 hours. Dexamethasone is an extremely hydrophobic drug with an aqueous solubility of only about 0.08 mg/mL (Figure 9.2). Because of its extremely low solubility, dexamethasone will only occupy a low percentage of the solvent volume available, regardless of how large the sink is. Thus, the same cumulative mass is released in both systems leading to conclusions that the 200 mL sink is not an infinite sink. While 200 mL volume is not an accurate semi-infinite or “large” sink for dexamethasone, a sufficiently large volume would allow more of the drug to be released. Release in a 500 mL volume with a mixing rate of 30 rpm was carried out (data not shown). Equilibrium was reached during the 72 hours indicating that a sink much larger than 500 mL would be needed to maintain the concentration gradient between the volume of the sink and the film itself. There was no statistical difference in the cumulative mass released of the 200 and 500 mL sinks. Because of the lower limit of detection, no larger

volume past 500 mL was attempted. Thus, for hydrophobic molecules, a proper sink would require a large mixed volume that has solvent exchange.

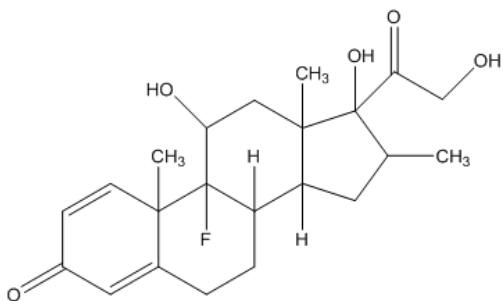
9.2.3 Effect of Temperature and Mixing Rate

To study the effect of the mixing rate and temperature in the kinetics of the release, hydrophilic, conventional hydrogel films loaded with ketotifen fumarate were used in the 200 mL volume case. Experiments with mixing rates of 30 and 160 rpm, and temperatures of 20 °C and 34 °C were performed separately. Figure 9.9a shows that an increase in mixing rate led to an increase in the total mass released from the hydrogel films. The fractional mass released at 48 hours with a mixing rate of 160 rpm was approximately 40% more than the fractional mass released with a mixing rate of 30 rpm. The mixing of the solvent reduces the boundary layer effect and therefore increases the driving force of the concentration gradient between film and bulk solvent. As expected, an increase in temperature led to an increase in the total mass released from the hydrogel films (Figure 9.9b). The fractional mass released at 48 hours and 34°C was approximately 20% more than the fractional mass released at 20°C. When the temperature is raised, the drug molecules had more kinetic energy, increasing the driving force and leading to a faster diffusional transport, regardless of other factors. Also, solubility is a function of temperature, with molecules becoming more soluble as temperature increases. However, these results suggest that sink volume had the most substantial influence on the release kinetics.

9.3 Conclusions

The results demonstrated that the experimental conditions used to study the release kinetics of therapeutic hydrogel films had a huge effect. The results showed that volume is the

most significant experimental variable affecting the release. While the increase in temperature and mixing rate increased the fractional mass released by 1.2 and 1.4 times, respectively, a much higher increase (up to 12 times more) occurred when the conditions were changed from 2 mL volume with no forced mixing to 200 mL volume with a mixing rate of 30rpm. Releases performed in small volumes reached equilibrium promptly, decreasing the concentration gradient, and causing the driving force for mass transfer of the drug molecules to be severely diminished. Not only are small volumes inadequate for testing extended controlled release but also they could lead to false conclusions about the extent of the release. The lack of standard conditions will continue to hinder the development of effective methods. Therefore, consistent experimental conditions are needed, for comparison of various controlled drug release methods, validation of the potential of lenses as an efficient and effective means of drug delivery, as well as increasing the likelihood of only the most promising methods leading to *in vivo* studies.

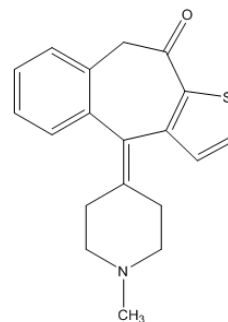


Dexamethasone

Solubility: 0.08 mg/mL

MW = 392.47 g/mol

log P = 1.89

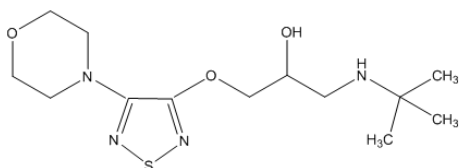


Ketotifen Fumarate

Solubility: 3.4 mg/mL

MW = 309.43 g/mol

log P = -0.3

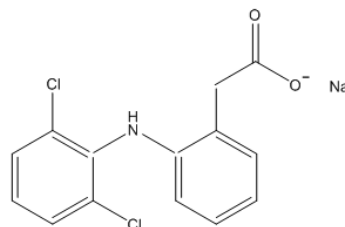


Timolol Maleate

Solubility: 4.3 mg/mL

MW = 432.49 g/mol

log P = -0.2



Diclofenac Sodium Salt

Solubility: 14.18 mg/mL

MW = 318.14 g/mol

log D_{7.4} = 1.1

Figure 9.2: Chemical structures and physicochemical properties of drugs

Drugs exhibit different physicochemical properties, such as solubilities.

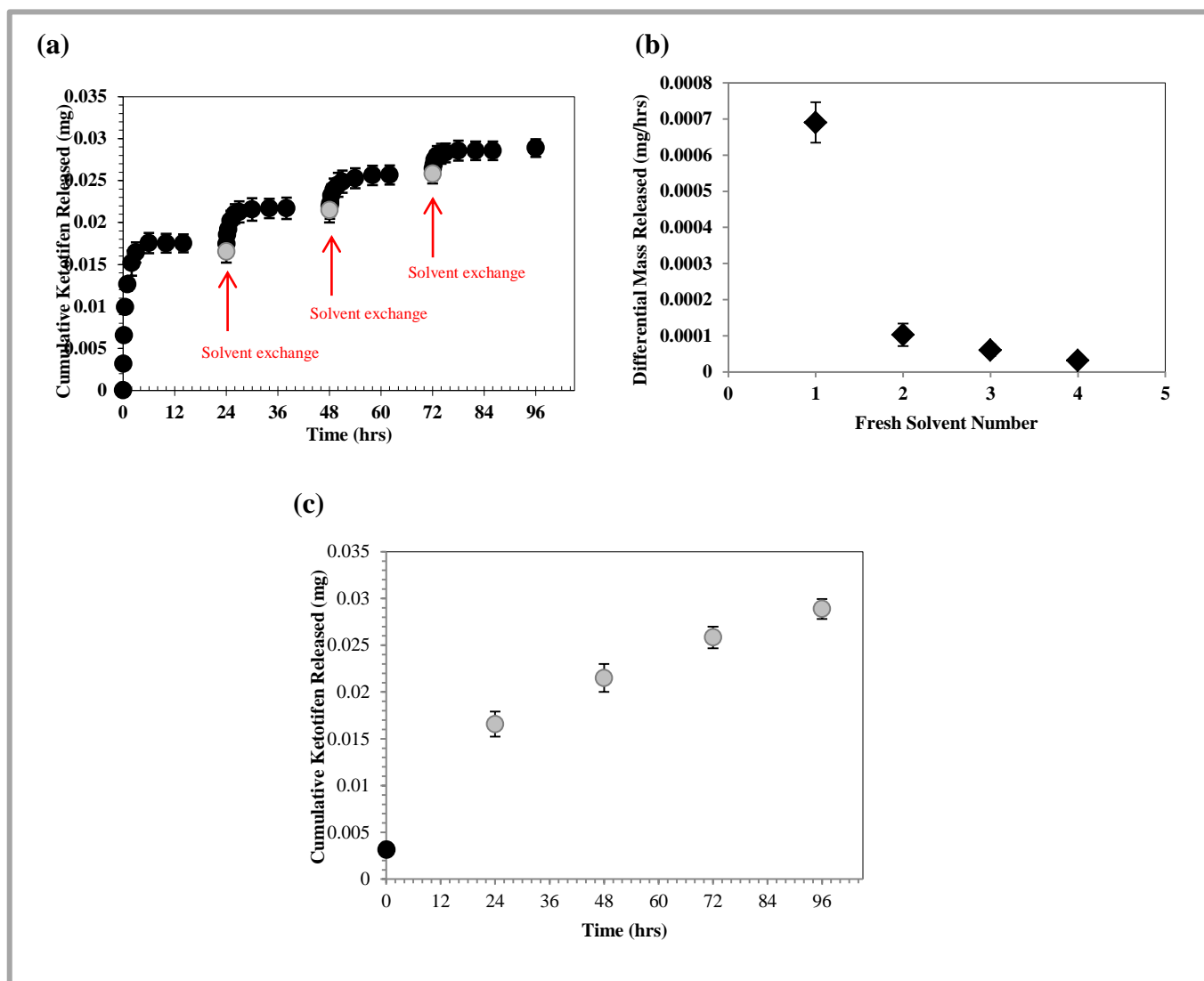


Figure 9.3: Drug release in small volumes from hydrophilic, conventional hydrogel films

Release study in DI water of ketotifen fumarate from pHEMA films in a 2 mL with no forced mixing and solvent exchange every 24 hours. **(a)** Equilibrium is reached well before 24 hours in the small volume, as is evident by the steep flattening of each individual curve. The differential mass released for each new solvent decreases significantly as well. **(b)** The differential mass released decreases with each new solvent. The largest differential mass release occurred in the first solvent exchange (the first 24 hours). **(c)** Cumulative mass released every 24 hours. The trend could be mistaken as a linear extended controlled release, which would be an inaccurate conclusion. $T=20\text{ }^{\circ}\text{C}$ and $n=3$.

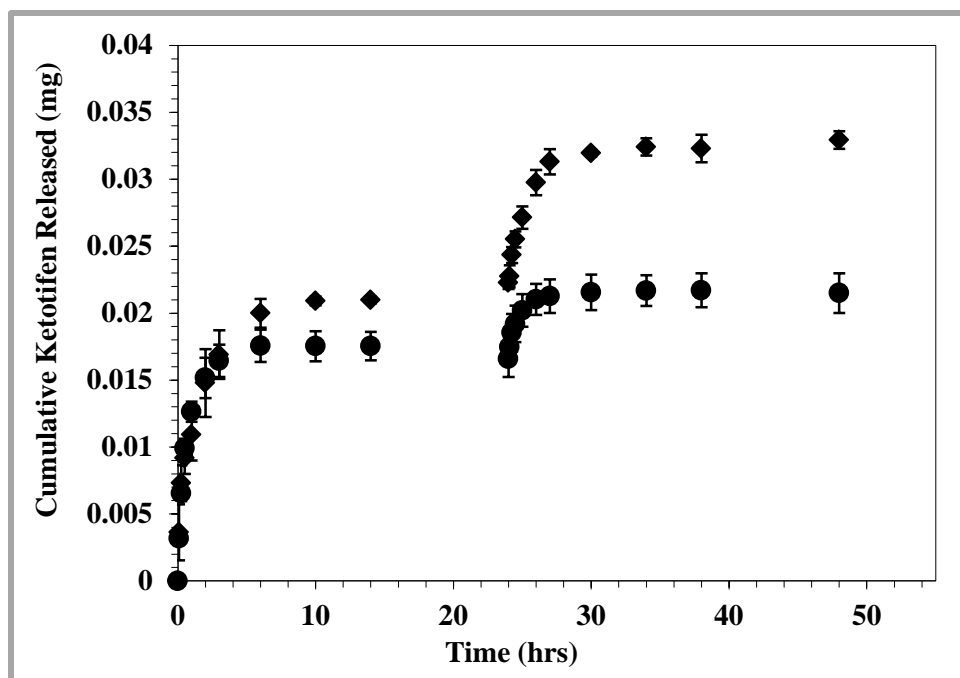


Figure 9.4: Release of ketotifen fumarate from hydrophilic, conventional hydrogel films in 2 mL and 5 mL small volumes

Release study in DI water of ketotifen fumarate from pHEMA films in a 2 mL (●) and 5 mL (◆) volumes with no forced mixing. The 75% increase in total drug released from 2 to 5 mL is evidence of the sensitivity of release rate to sink volume available and corresponding concentration gradient. T=20 °C and n =3.

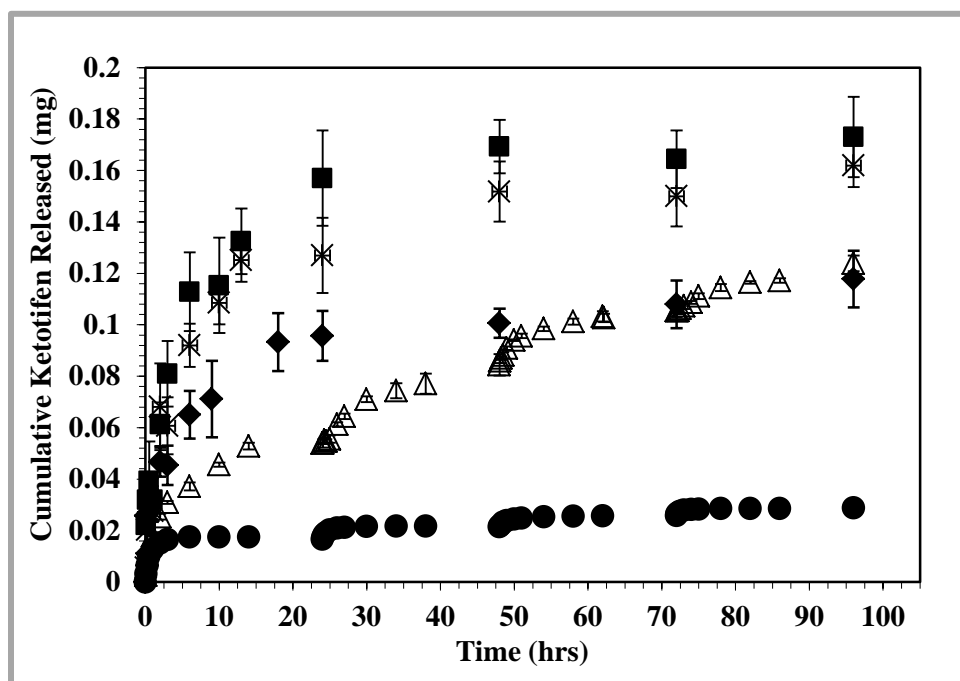


Figure 9. 5: Release of ketotifen fumarate from hydrophilic, conventional hydrogel films in small and large volumes

Comparison of volumes used in release studies of ketotifen fumarate from pHEMA hydrogel films. (■) represents 400 mL large volume with 30 rpm mixing, (*) represents 300 mL large volume with 30 rpm mixing, (◆) represents 200 mL large volume with 30 rpm mixing, (△) represents 30 mL small volume with no forced mixing, (●) represents 2 mL volume with no forced mixing. Release studies were performed in DI water at 20 °C and n =3.

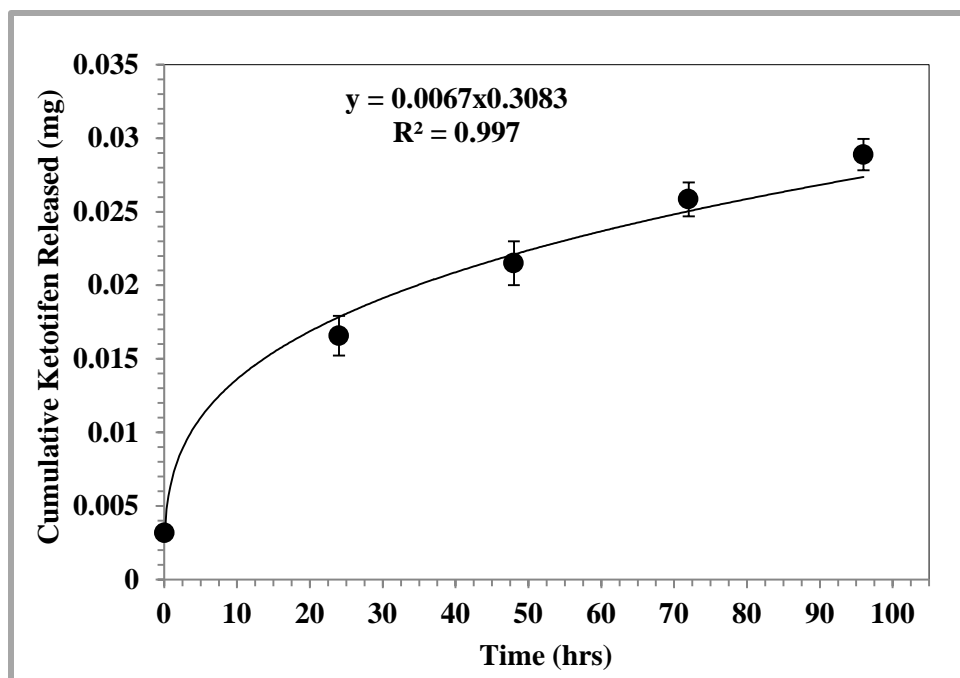


Figure 9.6: Data fit for hydrophilic, conventional hydrogel films releasing ketotifen fumarate in the 2 mL volume.

The data points represent the cumulative mass released every 24 hours for the 2 mL volume with no forced mixing and solvent exchange every 24 hours. A power trend fit the data. With the equation given, the release of ketotifen fumarate would take 5,566 hours or 232 days to release 0.096 mg, the equivalent released in the 200 mL volume at 24 hours and 10,915 hours or 1.25 years to release 0.118 mg, the equivalent released in the 200 mL volume at 96 hours. Thus, extrapolating the data highlights the extremely slow rate of release in small volumes with solvent exchange made only every 24 hours, which is significantly slower than release in the large volume.

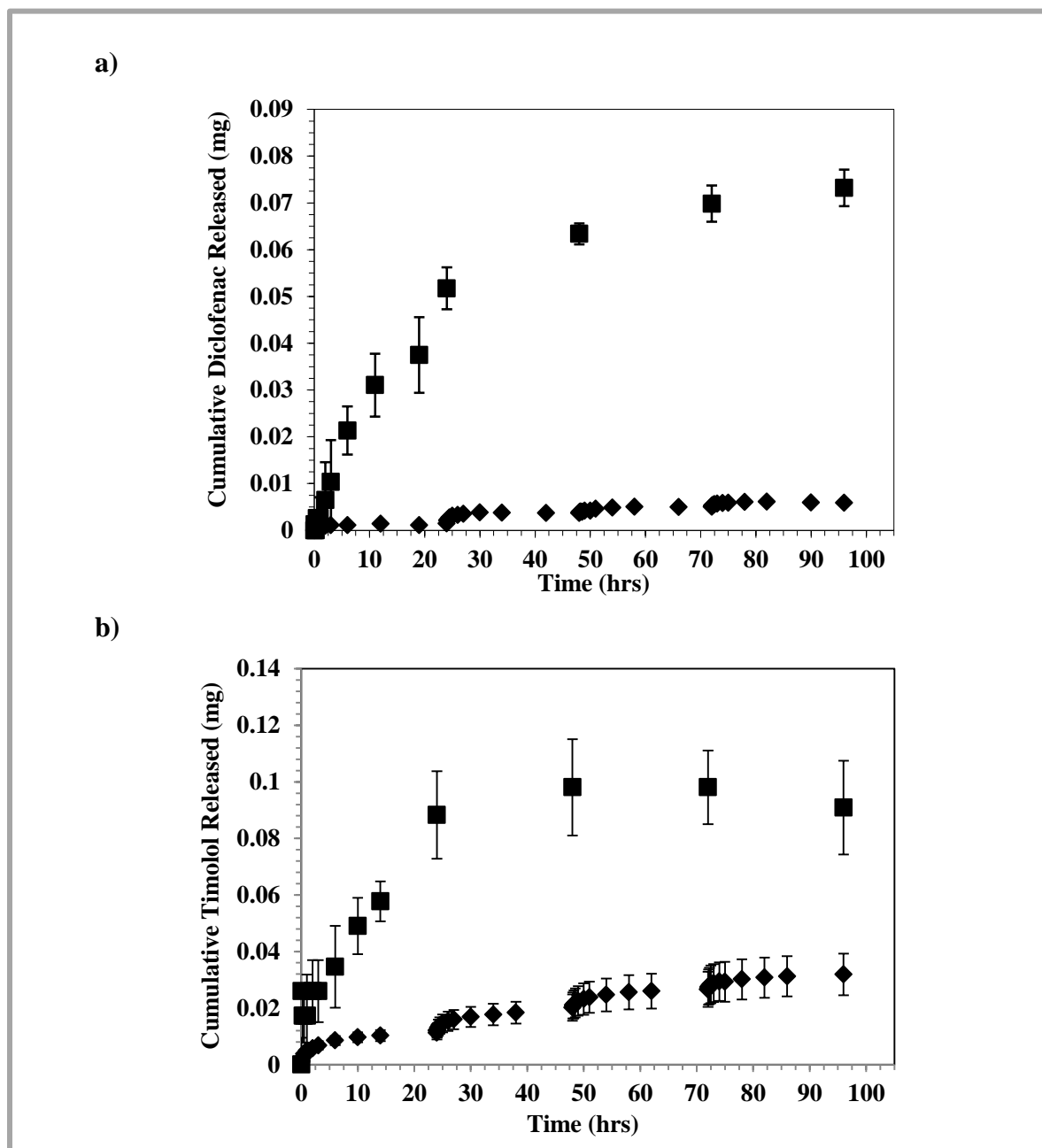


Figure 9.7: Cumulative mass released of diclofenac and timolol from hydrophilic, conventional hydrogel films

(a) Cumulative diclofenac sodium release from pHEMA hydrogel films. At 96 hours, the films in the 200 mL large volume released ~12 times more diclofenac than films in the the 2 mL small volume. (b) Cumulative timolol maleate release from pHEMA hydrogel films. At 96 hours, the films in the 200 mL large volume released ~3 times more timolol than the films in the 2 mL small volume. (■) 200 mL large volume with 30 rpm mixing, (◆) 2 mL small volume with no forced mixing. T=20 °C and n =3.

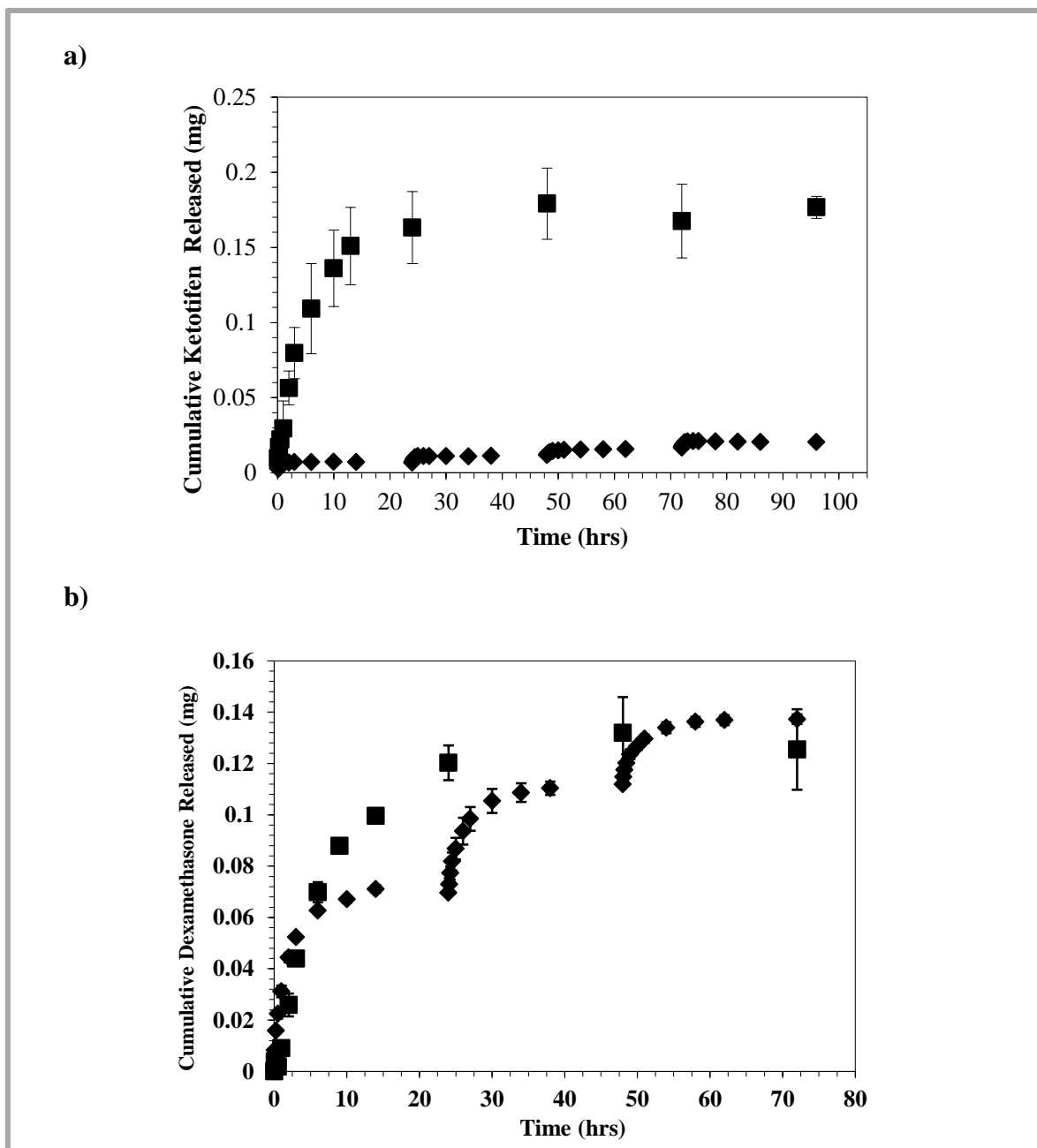


Figure 9.8: Cumulative mass released of ketotifen and dexamethasone from silicone hydrogel films

(a) Cumulative ketotifen fumarate release from silicone hydrogels. At 96 hours, the films in the 200 mL large volume released ~9 times more ketotifen than in the 2 mL small volume (b) Cumulative dexamethasone release from silicone hydrogels. The film in the small 2 mL volume exhibited a slower release rate, reaching equilibrium well before the 24 hour time point for solvent exchange. (■) 200 mL large volume with 30 rpm mixing, (◆) 2 mL small volume with no forced mixing. T=20 °C and n=3.

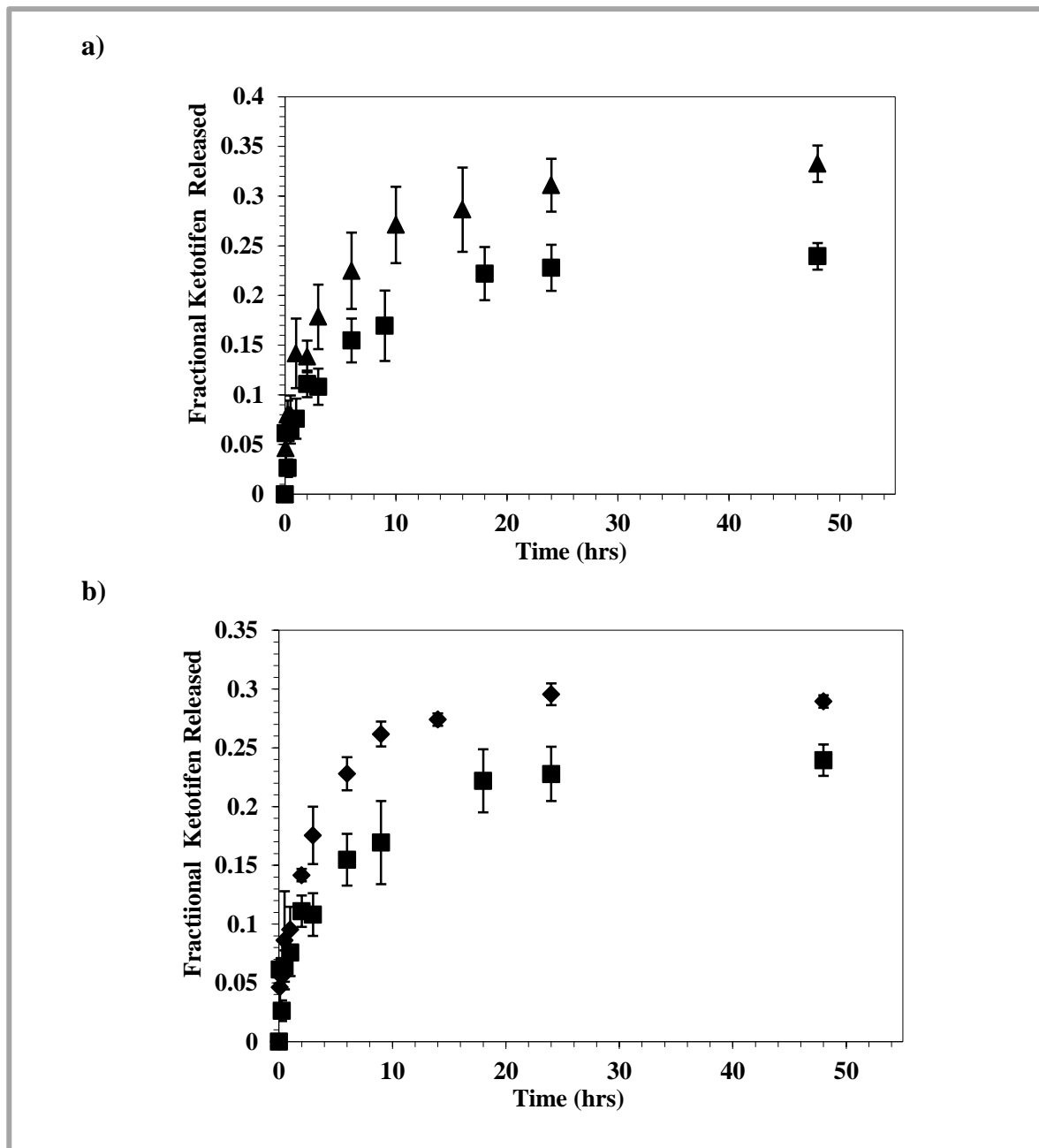


Figure 9.9: Effect of mixing rate and temperature on release kinetics

(a) Fractional ketotifen fumarate release from pHEMA hydrogels at 30 rpm (■) and 160 rpm (▲) in 200 mL volume at 20°C. The release performed at 160 rpm was ~40% faster than the release performed at 30 rpm. (b) Fractional ketotifen fumarate release from pHEMA hydrogels at 20°C (■), and 34°C (◆) in 200 mL volume with 30 rpm mixing. A ~ 20% faster release was observed, when the temperature of the release was increased from 20°C to 34°C. n = 3.

Chapter 10

Conclusions

In this study, various (poly(HEMA-co-DEAEM-co-PEGnDMA) hydrogels imprinted with diclofenac sodium, a small hydrophobic charged molecule, were engineered exploiting non-covalent interactions. The effects of varying compositional parameters on the structure of imprinted hydrogels and subsequently their drug binding and transport properties were investigated. It was found that an increase in the length of the crosslinker resulted in decreased binding affinity and faster template transport through the hydrogel, which corresponded with increased equilibrium swelling ratios, lower polymer volume fractions and increased mesh size. Increase in the amount of crosslinking in the hydrogels resulted in a decrease in the template binding capacity and a slower template transport with smaller reductions in template binding affinity, which corresponded with lower equilibrium swelling ratios and smaller mesh size of the hydrogels. It was found that imprinted networks, demonstrated improved loading over corresponding non-imprinted (control). Thus, by engineering the macromolecular memory sites and the mesh size, drug transport through the hydrogel network can be tailored.

It was found that among the different length and amount of crosslinking monomers, imprinted hydrogels with a mesh size around 30 Å (i.e., poly(HEMA-co-DEAEM-co-PEG200DMA) hydrogels prepared with 5 mole% crosslinking monomer) had an optimal conformation of the macromolecular memory sites, which provided the most favorable binding to the drug (i.e., binding capacity and affinity was maximized). The results showed similar drug

diffusion coefficients in DI water, than imprinted hydrogels with smaller mesh size (i.e., hydrogels prepared with 5% EGDMA, 10% PEG200DMA and 50%PEG200DMA).

Moreover, the presence of salts and ions in artificial lacrimal solution altered interactions between the anionic template molecule and the cationic functional monomer, resulting in a fast release rate. The ionic interaction appeared to be the most important interaction when compared to the hydrogen bonding interactions. Nonetheless, an extended release for up to 72 hours was still achieved in artificial lacrimal solution, due to hydrogel networks with a relatively small mesh size ($\sim 20\text{-}40 \text{ \AA}$) allow for the stabilization of the macromolecular site through multiple non-covalent interactions.

To further control the transport of diclofenac sodium through the hydrogel network, imprinted poly(HEMA-co-DEAEM-co-PEG200DMA) contact lenses with 5 mole% of the crosslinking monomer were engineered by varying the functional monomer to template (FM/T) ratio. As the FM/T ratio was increased in the imprinted contact lenses, the template binding affinity increased, decreasing the release rate. Furthermore, the imprinting process extended further control over the release kinetics independent of polymer structure and free volume, resulting in variations in diffusion coefficients. Thus, by engineering the macromolecular memory sites through changes in the FM/T ratio, the release rate could also be tailored. It was also demonstrated that under physiological ocular volumetric flow rates the release kinetics, for higher FM/T ratios, was zero-order, or concentration independent, for an extended time of 2 days, making them ideal for use as daily disposable therapeutic lenses. The imprinted contact lenses can be designed to release drug at the required therapeutic rate without the significant variation in concentration observed with eye drops.

Additionally, a polyvinyl alcohol (PVA) macromer, Nelfilcon A, which permitted the study of the imprinting effectiveness on a large network structure, was used as a backbone monomer to engineer a daily disposable lens to tailor the release rate of diclofenac sodium. The diffusion coefficient of diclofenac sodium in DI water was controlled by adjusting the FM/T ratio. When Nelfilcon A lenses were placed in lacrimal solution the release of diclofenac was really fast, lasting just for ~ 10 min. This may be due to the macromolecular sites architecture within the network of Nelfilcon A lenses, which have ~4.4 times larger mesh size than poly(HEMA-co-DEAEM-co-PEG200DMA) networks, and where multiple non-covalent interactions were not able to be stabilized and assist the ionic interactions (the primarily ones) to delay the release, resulting in a fast and not controlled release.

In addition, silicone hydrogels contact lenses were engineered by rationally altering the ratio of hydrophobic to hydrophilic co-monomer composition and network structure to study hydrophobic interactions for diclofenac sodium. The results demonstrated that the release rate was dependent on the hydrophobic:hydrophilic ratio within the silicone hydrogel lens. As the amount of hydrophobic monomers was increased in the lens, the cumulative diclofenac sodium mass release rate decreased. The silicone hydrogel contact lenses had good optical clarity, mechanical properties and contained siloxane compositions similar to highly oxygen permeable silicone hydrogel lenses currently on the market. More importantly, an extended and controlled release in lacrimal solution of diclofenac sodium was achieved for the entire duration of lens wear (up to 7 days).

Furthermore, an *in vivo* study was performed in a New Zealand Rabbit model, where imprinted poly(HEMA-co-AA-co-AM-co-NVP-co-PEG200DMA) contact lenses were used. Previous work by our group has demonstrated that *in vitro* ketotifen fumarate release rates can be

tailored to deliver for extended periods of time. In this work, these imprinted lenses successfully and controllably deliver a sustained effective concentration of ketotifen fumarate *in vivo*. For the first time, it was demonstrated that contact lenses can be used to release a constant, effective drug concentration in tear fluid for up to 26 hours, making them ideal for use as daily wear or disposable delivery devices. The imprinted lenses demonstrated much longer precorneal retention times and much higher tear fluid bioavailability compared to commercially available ketotifen fumarate eye drops or drug soaked lenses.

The contact lenses engineered during this study have the potential to greatly enhance patient ocular health by overcoming the inherent inefficiencies of topical eye drops. This work highlights the potential for achieving better control of hydrogel properties in molecularly imprinted hydrogels. These developments will contribute to the ability to rationally design imprinted hydrogels in order to tailor binding and transport properties. It also demonstrates the complex relationship between the spacing of functionality chemistry with the imprinted network in relation to loading and release control.

In conclusion, imprinted contact lenses as a platform for drug delivery offer a more effective method of ocular therapy by providing a constant and optimal dosage of medication with increased drug bioavailability to the eye. This novel system has great potential for use with a wide spectrum of drugs and enormous potential in the design and engineering of the next generation of drug delivery carriers. A thorough understanding of weakly crosslinked imprinted hydrogels might lead to the rational design of imprinted polymer networks for not just drug delivery but for a wide variety of other applications.

Finally, variations in release conditions, such as volume, temperature and mixing rates, as well as their effect on the release kinetics were examined. Conventional and silicone hydrogels

were synthesized to release a wide spectrum of both hydrophilic and hydrophobic drugs (ketotifen fumarate, diclofenac sodium, timolol maleate and dexamethasone). Volume had the biggest effect on the release profile, which incidentally is the least consistent variable throughout the literature. Increases in mixing rate and temperature resulted in relatively small increases in fractional mass released. The results strongly demonstrated the necessity of proper and thorough analysis of release data to assure that equilibrium is not significantly affecting the release kinetics. This is paramount for comparison of various controlled drug release methods, validation of the potential of lenses as an efficient and effective means of drug delivery, as well as increasing the likelihood of only the most promising methods entering clinical trials.

References

- [1] M. Elder, *Ophthalmic Therapeutic Drugs: Technologies and Global Markets*. New York, NY: BBC Publisher, 2010.
- [2] J. C. Lang, "Ocular drug delivery conventional ocular formulations," *Advanced Drug Delivery Reviews*, vol. 16, pp. 39-43, 1995.
- [3] D. Ghate and H. F. Edelhauser, "Ocular drug delivery," *Expert Opinion on Drug Delivery*, vol. 3, pp. 275-287, 2006.
- [4] M. Ali and M. E. Byrne, "Challenges and solutions in topical ocular drug-delivery systems," *Expert Review of Clinical Pharmacology*, vol. 1, pp. 145-161, 2008.
- [5] D. H. Geroski and H. F. Edelhauser, "Drug delivery for posterior segment eye disease," *Investigative Ophthalmology Visual Science*, vol. 41, pp. 961-964, 2000.
- [6] R. D. Schoenwald, "Ocular pharmacokinetics," in *Textbook of ocular pharmacology*, T. J. Zimmerman, K. Kooner, and M. Sharir, et. al., Eds., ed Philadelphia: Lippincott-Raven, 1997.
- [7] A. J. Winfield, D. Jessiman, A. Williams, and L. Esakowitz, "A study of the causes of non-compliance by patients prescribed eyedrops," *British Journal of Ophthalmology*, vol. 74, pp. 477-480, 1990.
- [8] M. Elder, *Ophthalmic Devices, Diagnostics, and Surgical Equipment: Global Markets*. New York, NY: BBC Research, 2013.

- [9] J. A. Shoemaker, D. S. Friedman, N. Congdon, J. Kempen, and J. M. Tielsch, *Vision problems in the U.S. : prevalence of adult vision impairment and age-related eye disease in America*. Bethesda, MD; Schaumburg, Ill.: National Eye Institute ; Prevent Blindness America, 2002.
- [10] P. M. Hughes, O. Olejnik, J. E. Chang-Lin, and C. G. Wilson, "Topical and systemic drug delivery to the posterior segments," *Advanced Drug Delivery Reviews*, vol. 57, pp. 2010-2032, 2005.
- [11] M. Hornof, E. Toropainen, and A. Urtti, "Cell culture models of the ocular barriers," *European Journal of Pharmaceutics and Biopharmaceutics*, vol. 60, pp. 207-225, 2005.
- [12] R. Gaudana, J. Jwala, S. Boddu, and A. Mitra, "Recent perspectives in ocular drug delivery," *Pharmaceutical Research*, vol. 26, pp. 1197-1216, 2009.
- [13] R. D. Schoenwald and H. S. Huang, "Corneal penetration behavior of beta-blocking agents 1. Physicochemical factors," *Journal of Pharmaceutical Sciences*, vol. 72, pp. 1266-1272, 1983.
- [14] R. D. Schoenwald, "Ocular drug delivery: pharmacokinetic considerations," *Clinical Pharmacokinetics*, vol. 18, pp. 255-269, 1990.
- [15] D. H. Geroski and H. F. Edelhauser, "Drug delivery for posterior segment eye disease," *Investigative Ophthalmology & Visual Science*, vol. 41, pp. 961-964, 2000.
- [16] E. Mannermaa, K. S. Vellonen, and A. Urtti, "Drug transport in corneal epithelium and blood-retina barrier: Emerging role of transporters in ocular pharmacokinetics," *Advanced Drug Delivery Reviews*, vol. 58, pp. 1136-1163, 2006.

- [17] G. Rieger, "The importance of the precorneal tear film for the quality of optical imaging," *British Journal of Ophthalmology* *British Journal of Ophthalmology*, vol. 76, pp. 157-158, 1992.
- [18] F. J. Holly, "Tear film physiology," *American Journal of Optometry and Physiological Optics*, vol. 57, pp. 252-257, 1980.
- [19] B. A. Nichols, M. L. Chiappino, and C. R. Dawson, "Demonstration of the mucous layer of the tear film by electron-microscopy," *Investigative Ophthalmology & Visual Science*, vol. 26, pp. 464-473, 1985.
- [20] F. J. Holly and M. A. Lemp, "Tear physiology and dry eyes," *Survey of Ophthalmology*, vol. 22, pp. 69-87, 1977.
- [21] A. Sharma and E. Ruckenstein, "Mechanism of tear film rupture and its implications for contact lens tolerance," *American Journal of Optometry and Physiological Optics*, vol. 62, pp. 246-253, 1985.
- [22] M. G. Doane, "Blinking and the mechanics of the lacrimal drainage system," *Ophthalmology*, vol. 88, pp. 844-51, 1981.
- [23] M. J. Glasson, F. Stapleton, L. Keay, and M. D. P. Willcox, "The effect of short term contact lens wear on the tear film and ocular surface characteristics of tolerant and intolerant wearers," *Contact Lens and Anterior Eye*, vol. 29, pp. 41-47, 2006.
- [24] C. L. Bourlais, L. Acar, H. Zia, P. A. Sado, T. Needham, and R. Leverage, "Ophthalmic drug delivery systems--recent advances," *Progress in Retinal and Eye Research*, vol. 17, pp. 33-58, 1998.

- [25] N. A. Brennan, "Corneal oxygenation during contact lens wear: comparison of diffusion and EOP-based flux models," *Clinical & Experimental Optometry: Journal of the Australian Optometrical Association*, vol. 88, pp. 103-8, 2005.
- [26] K. Hosoya, V. H. L. Lee, and K. J. Kim, "Roles of the conjunctiva in ocular drug delivery: a review of conjunctival transport mechanisms and their regulation," *European Journal of Pharmaceutics and Biopharmaceutics*, vol. 60, pp. 227-240, 2005.
- [27] K. Jarvinen, T. Jarvinen, and A. Urtti, "Ocular absorption following topical delivery," *Advanced Drug Delivery Reviews*, vol. 16, pp. 3-19, 1995.
- [28] D. A. Dartt, "Regulation of mucin and fluid secretion by conjunctival epithelial cells," *Progress in Retinal and Eye Research*, vol. 21, pp. 555-576, 2002.
- [29] M. R. Prausnitz and J. S. Noonan, "Permeability of cornea, sclera, and conjunctiva: A literature analysis for drug delivery to the eye," *Journal of Pharmaceutical Sciences*, vol. 87, pp. 1479-1488, 1998.
- [30] K. M. Hamalainen, K. Kananen, S. Auriola, K. Kontturi, and A. Urtti, "Characterization of paracellular and aqueous penetration routes in cornea, conjunctiva, and sclera," *Investigative Ophthalmology & Visual Science*, vol. 38, pp. 627-634, 1997.
- [31] D. M. Maurice and S. Mishima, "Ocular pharmacokinetics.," in *Handbook of Experimental Pharmacology*. vol. 69, M. C. Sears, Ed., ed Berlin-Heidelberg: Springer-Verlag, pp. 19-116, 1984
- [32] S. Duvvuri, S. Majumdar, and A. K. Mitra, "Role of metabolism in ocular drug delivery," *Current Drug Metabolism*, vol. 5, pp. 507-515, 2004.

- [33] R. J. Prankerd and V. J. Stella, "The use of oil-in-water emulsions as a vehicle for parenteral drug administration," *Journal of parenteral science and technology : a publication of the Parenteral Drug Association*, vol. 44, 1990.
- [34] M. de la Fuente, M. Raviña, P. Paolicelli, A. Sanchez, B. Seijo, and M. J. Alonso, "Chitosan-based Nanostructures: A Delivery Platform for Ocular Therapeutics," *Advanced Drug Delivery Reviews*, vol. In Press, Accepted Manuscript.
- [35] A. Urtti, "Challenges and obstacles of ocular pharmacokinetics and drug delivery," *Advanced Drug Delivery Reviews*, vol. 58, pp. 1131-1135, 2006.
- [36] M. R. Prausnitz, A. Edwards, J. S. Noonan, D. E. Rudnick, H. F. Edelhauser, and D. H. Geroski, "Measurement and prediction of transient transport across sclera for drug delivery to the eye," *Industrial & Engineering Chemistry Research*, vol. 37, pp. 2903-2907, 1998.
- [37] D. H. Geroski and H. F. Edelhauser, "Transscleral drug delivery for posterior segment disease," *Advanced Drug Delivery Reviews*, vol. 52, pp. 37-48, 2001.
- [38] I. Ahmed and T. F. Patton, "Importance of the noncorneal absorption route in topical ophthalmic drug delivery," *Investigative Ophthalmology & Visual Science*, vol. 26, pp. 584-587, 1985.
- [39] R. D. Schoenwald, G. S. Deshpande, D. G. Rethwisch, and C. F. Barfknecht, "Penetration into the anterior chamber via the conjunctival/scleral pathway," *Journal of Ocular Pharmacology and Therapeutics*, vol. 13, pp. 41-59, 1997.
- [40] Y. Horibe, K. Hosoya, K. J. Kim, T. Ogiso, and V. H. L. Lee, "Polar solute transport across the pigmented rabbit conjunctiva: Size dependence and the influence of 8-bromo

- cyclic adenosine monophosphate," *Pharmaceutical Research*, vol. 14, pp. 1246-1251, 1997.
- [41] J. Liaw and J. R. Robinson, "Ocular penetration enhancers," in *Ophthalmic Drug Delivery Systems*. vol. 58, A. K. Mitra, Ed., ed Nee York: Marcel Dekker, pp. 369-381. 1993.
- [42] S. W. Friedrich, Y. L. Cheng, and B. A. Saville, "Theoretical corneal permeation model for ionizable drugs," *Journal of Ocular Pharmacology*, vol. 9, pp. 229-249, 1993.
- [43] J. H. Liaw, Y. Y. Rojanasakul, and J. R. Robinson, "The effect of drug charge type and charge density on corneal transport," *International Journal of Pharmaceutics*, vol. 88, pp. 111-124, 1992.
- [44] Y. Y. Rojanasakul and J. R. Robinson, "Transport mechanisms of the cornea: characterization of barrier permselectivity," *International Journal of Pharmaceutics*, vol. 55, pp. 237-246, 1989.
- [45] L. Pitkanen, V. P. Ranta, H. Moilanen, and A. Urtti, "Permeability of retinal pigment epithelium: Effects of permeant molecular weight and lipophilicity," *Investigative Ophthalmology & Visual Science*, vol. 46, pp. 641-646, 2005.
- [46] K. I. Hosoya and M. Tachikawa, "Inner Blood-Retinal Barrier Transporters: Role of Retinal Drug Delivery," *Pharmaceutical Research*, vol. 26, pp. 2055-2065, 2009.
- [47] R. R. Tamesis, A. Rodriguez, W. G. Christen, Y. A. Akova, E. Messmer, and C. S. Foster, "Systemic drug toxicity trends in immunosuppressive therapy of immune and inflammatory ocular disease," *Ophthalmology*, vol. 103, pp. 768-775, 1996.
- [48] D. M. Albert and D. D. Edwards, *The history of ophthalmology*. Cambridge, Mass., USA: Blackwell Science, 1996.

- [49] M. B. Sintzel, S. F. Bernatchez, C. Tabatabay, and R. Gurny, "Biomaterials in Ophthalmic Drug Delivery," *European Journal of Pharmaceutics and Biopharmaceutics*, vol. 42, pp. 358-374, 1996.
- [50] E. Barbu, L. Verestiuc, T. G. Nevell, and J. Tsibouklis, "Polymeric materials for ophthalmic drug delivery: trends and perspectives," *Journal of Materials Chemistry*, vol. 16, pp. 3439-3443, 2006.
- [51] H. R. Lin and K. C. Sung, "Carbopol/pluronic phase change solutions for ophthalmic drug delivery," *Journal of Controlled Release*, vol. 69, pp. 379-388, 2000.
- [52] A. Bernkop-Schnürch, "Thiomers: a new generation of mucoadhesive polymers," *Advanced drug delivery reviews*, vol. 57, pp. 1569-82, 2005.
- [53] A. Ludwig, "The use of mucoadhesive polymers in ocular drug delivery," *Advanced drug delivery reviews*, vol. 57, pp. 1595-639, 2005.
- [54] S. K. Sahoo, F. Diinawaz, and S. Krishnakumar, "Nanotechnology in ocular drug delivery," *Drug Discovery Today*, vol. 13, pp. 144-151, 2008.
- [55] Y. Diebold, M. Jarrin, V. Saez, E. L. S. Carvalho, M. Orea, M. Calonge, *et al.*, "Ocular drug delivery by liposome–chitosan nanoparticle complexes (LCS-NP)," *Biomaterials*, vol. 28, pp. 1553-1564, 2007.
- [56] N. Li, C. Zhuang, M. Wang, X. Sun, S. Nie, and W. Pan, "Liposome coated with low molecular weight chitosan and its potential use in ocular drug delivery," *International journal of pharmaceutics*, vol. 379, pp. 131-138, 2009.
- [57] S. Wang, J. Zhang, T. Jiang, L. Zheng, Z. Wang, J. Zhang, *et al.*, "Protective effect of Coenzyme Q10 against oxidative damage in human lens epithelial cells by novel ocular drug carriers," *International Journal of Pharmaceutics*, vol. 403, pp. 219-229, 2011.

- [58] K. M. Hosny, "Preparation and evaluation of thermosensitive liposomal hydrogel for enhanced transcorneal permeation of ofloxacin," *AAPS PharmSciTech*, vol. 10, pp. 1336-1342, 2009.
- [59] I. P. Kaur, D. Aggarwal, H. Singh, and S. Kakkar, "Improved ocular absorption kinetics of timolol maleate loaded into a bioadhesive niosomal delivery system," *Graefe's Archive for Clinical and Experimental Ophthalmology*, vol. 248, pp. 1467-1472, 2010.
- [60] G. Abdelbary, "Ocular ciprofloxacin hydrochloride mucoadhesive chitosan-coated liposomes," *Pharmaceutical Development and Technology*, vol. 16, pp. 44-56, 2011.
- [61] E. Gavini, P. Chetoni, M. Cossu, M. G. Alvarez, M. F. Saettone, and P. Giunchedi, "PLGA microspheres for the ocular delivery of a peptide drug, vancomycin using emulsification/spray-drying as the preparation method: in vitro/in vivo studies," *European Journal of Pharmaceutics and Biopharmaceutics*, vol. 57, pp. 207-212, 2004.
- [62] S. K. Motwani, S. Chopra, S. Talegaonkar, K. Kohli, F. J. Ahmad, and R. K. Khar, "Chitosan–sodium alginate nanoparticles as submicroscopic reservoirs for ocular delivery: Formulation, optimisation and in vitro characterisation," *European Journal of Pharmaceutics and Biopharmaceutics*, vol. 68, pp. 513-525, 2008.
- [63] H. Gupta, M. Aqil, R. K. Khar, A. Ali, A. Bhatnagar, and G. Mittal, "Biodegradable levofloxacin nanoparticles for sustained ocular drug delivery," *Journal of drug targeting*, vol. 19, pp. 409-417, 2011.
- [64] H. Gupta, M. Aqil, R. K. Khar, A. Ali, A. Bhatnagar, and G. Mittal, "Sparfloxacin-loaded PLGA nanoparticles for sustained ocular drug delivery," *Nanomedicine: Nanotechnology, Biology and Medicine*, vol. 6, pp. 324-333, 2010.

- [65] E. Barbu, L. Verestiuc, M. Iancu, A. Jatariu, A. Lungu, and J. Tsibouklis, "Hybrid polymeric hydrogels for ocular drug delivery: nanoparticulate systems from copolymers of acrylic acid-functionalized chitosan and N-isopropylacrylamide or 2-hydroxyethyl methacrylate," *Nanotechnology*, vol. 20, p. 225108, 2009.
- [66] F. Rafie, Y. Javadzadeh, A. R. Javadzadeh, L. A. Ghavidel, B. Jafari, M. Moogooee, *et al.*, "In vivo evaluation of novel nanoparticles containing dexamethasone for ocular drug delivery on rabbit eye," *Current eye research*, vol. 35, pp. 1081-1089, 2010.
- [67] G. Spataro, F. Malecaze, C.-O. Turrin, V. Soler, C. Duhayon, P.-P. Elena, *et al.*, "Designing dendrimers for ocular drug delivery," *European journal of medicinal chemistry*, vol. 45, pp. 326-334, 2010.
- [68] W. Yao, K. Sun, H. Mu, N. Liang, Y. Liu, C. Yao, *et al.*, "Preparation and characterization of puerarin-dendrimer complexes as an ocular drug delivery system," *Drug Development and Industrial Pharmacy*, vol. 36, pp. 1027-1035, 2010.
- [69] C. Durairaj, R. S. Kadam, J. W. Chandler, S. L. Hutcherson, and U. B. Kompella, "Nanosized dendritic polyguanidilyated translocators for enhanced solubility, permeability, and delivery of gatifloxacin," *Investigative ophthalmology & visual science*, vol. 51, pp. 5804-5816, 2010.
- [70] I. Pepić, N. Jalšenjak, and I. Jalšenjak, "Micellar solutions of triblock copolymer surfactants with pilocarpine," *International Journal of Pharmaceutics*, vol. 272, pp. 57-64, 2004.
- [71] Y. Kadam, U. Yerramilli, A. Bahadur, and P. Bahadur, "Micelles from PEO-PPO-PEO block copolymers as nanocontainers for solubilization of a poorly water soluble drug hydrochlorothiazide," *Colloids and Surfaces B: Biointerfaces*, vol. 83, pp. 49-57, 2011.

- [72] I. Pepić, A. Hafner, J. Lovrić, B. Pirkić, and J. Filipović-Grčić, "A nonionic surfactant/chitosan micelle system in an innovative eye drop formulation," *Journal of pharmaceutical sciences*, vol. 99, pp. 4317-4325, 2010.
- [73] F. van de Manakker, T. Vermonden, C. F. van Nostrum, and W. E. Hennink, "Cyclodextrin-based polymeric materials: synthesis, properties, and pharmaceutical/biomedical applications," *Biomacromolecules*, vol. 10, pp. 3157-3175, 2009.
- [74] J. Zhang, L. Wang, C. Gao, L. Zhang, and H. Xia, "Ocular pharmacokinetics of topically-applied ketoconazole solution containing hydroxypropyl beta-cyclodextrin to rabbits," *Journal of Ocular Pharmacology and Therapeutics*, vol. 24, pp. 501-506, 2008.
- [75] M. A. Halim Mohamed and A. A. Mahmoud, "Formulation of indomethacin eye drops via complexation with cyclodextrins," *Current Eye Research*, vol. 36, pp. 208-216, 2011.
- [76] A. A. Mahmoud, G. S. El-Feky, R. Kamel, and G. E. A. Awad, "Chitosan/sulfobutylether- β -cyclodextrin nanoparticles as a potential approach for ocular drug delivery," *International Journal of Pharmaceutics*, vol. 413, pp. 229-236, 2011.
- [77] M. F. Armaly and K. R. Rao, "The effect of pilocarpine Ocusert with different release rates on ocular pressure," *Investigative Ophthalmology*, vol. 12, pp. 491-6, 1973.
- [78] J. U. Prause, "Treatment of keratoconjunctivitis sicca with Lacrisert," *Scandinavian Journal of Rheumatology*, pp. 261-263, 1986.
- [79] V. Baeyens, O. Felt-Baeyens, S. Rougier, S. Pheulpin, B. Boisrame, and R. Gurny, "Clinical evaluation of bioadhesive ophthalmic drug inserts (BODI (R)) for the treatment of external ocular infections in dogs," *Journal of Controlled Release*, vol. 85, pp. 163-168, 2002.

- [80] U. L. Patel, N. P. Chotai, and C. D. Nagda, "Design and evaluation of ocular drug delivery system for controlled delivery of," *Pharm Dev Technol*, vol. 17, pp. 15-22, Jan-2012.
- [81] P. Bhagav, V. Trivedi, D. Shah, and S. Chandran, "Sustained release ocular inserts of brimonidine tartrate for better treatment in open-angle glaucoma," *Drug Delivery and Translational Research*, vol. 1, pp. 161-174, 2011.
- [82] G. Wei, P. T. Ding, J. M. Zheng, and W. Y. Lu, "Pharmacokinetics of timolol in aqueous humor sampled by microdialysis after topical administration of thermosetting gels," *Biomedical Chromatography*, vol. 20, pp. 67-71, 2006.
- [83] Y. X. Cao, C. Zhang, W. B. Shen, Z. H. Cheng, L. L. Yu, and Q. N. Ping, "Poly(N-isopropylacrylamide)-chitosan as thermosensitive in situ gel-forming system for ocular drug delivery," *Journal of Controlled Release*, vol. 120, pp. 186-194, 2007.
- [84] W.-D. Ma, H. Xu, C. Wang, S.-F. Nie, and W.-S. Pan, "Pluronic F127-g-poly(acrylic acid) copolymers as in situ gelling vehicle for ophthalmic drug delivery system," *International Journal of Pharmaceutics*, vol. 350, pp. 247-256, 2008.
- [85] Y. Sultana, M. Aqil, A. Ali, and S. Zafar, "Evaluation of carbopol-methyl cellulose based sustained-release ocular delivery system for pefloxacin mesylate using rabbit eye model," *Pharmaceutical Development and Technology*, vol. 11, pp. 313-319, 2006.
- [86] H. Gupta, T. Velpandian, and S. Jain, "Ion-and pH-activated novel in-situ gel system for sustained ocular drug delivery," *Journal of drug targeting*, vol. 18, pp. 499-505, 2010.
- [87] Y. Sultana, M. Aqil, and A. Ali, "Ion-Activated, Gelrite®-Based in Situ Ophthalmic Gels of Pefloxacin Mesylate: Comparison with Conventional Eye Drops," *Drug Delivery*, vol. 13, pp. 215-219, 2006.

- [88] M. R. Gokulgandhi, D. M. Modi, and J. R. Parikh, "In Situ Gel Systems for Ocular Drug Delivery: A Review," *DRUG DELIVERY TECHNOLOGY*, vol. 7, pp. 30-37, 2007.
- [89] B. K. Nanjawade, F. V. Manvi, and A. S. Manjappa, "In situ.-forming hydrogels for sustained ophthalmic drug delivery," *Journal of Controlled Release*, vol. 122, pp. 119-134, 2007.
- [90] Y. Sultana, R. Jain, M. Aqil, and A. Ali, "Review of Ocular Drug Delivery," *Current Drug Delivery*, vol. 3, pp. 207-217, 2006.
- [91] O. Wichterle and D. Lim, "Cross-linked hydrophilic polymers and articles made therefrom," United States Patent, 1965.
- [92] O. Wichterle and D. Lim, "Hydrophilic gels for biological use," *Nature*, vol. 185, pp. 117-118, 1960.
- [93] C. J. White, A. Tieppo, and M. E. Byrne, "Controlled drug release from contact lenses: a comprehensive review from 1965-present," *Journal of Drug Delivery Science and Technology*, vol. 21, pp. 369-384, 2011.
- [94] C. Alvarez-Lorenzo, H. Hiratani, and A. Concheiro, "Contact lenses for drug delivery: achieving sustained release with novel systems," *American Journal of Drug Delivery*, vol. 4, pp. 131-151, 2006.
- [95] L. Xinming, C. Yingde, A. W. Lloyd, S. V. Mikhalovsky, S. R. Sandeman, C. A. Howel, *et al.*, "Polymeric hydrogels for novel contact lens-based ophthalmic drug delivery systems: A review," *Contact Lens and Anterior Eye*, vol. 31, pp. 57-64, 2008.
- [96] V. Y. Hayes, C. M. Schnider, and J. Veys, "An evaluation of 1-day disposable contact lens wear in a population of allergy sufferers," *Contact Lens and Anterior Eye*, vol. 26, 2003.

- [97] C. C. S. Karlgard, L. W. Jones, and C. Moresoli, "Survey of bandage lens use in North America, October-December 2002," *Eye & contact lens*, vol. 30, pp. 25-30, 2004.
- [98] R. Morrison and J. P. Shovlin, "A review of the use of bandage lenses," *Metabolic, pediatric, and systemic ophthalmology*, vol. 6, p. 117, 1982.
- [99] S. S. Tuli, G. S. Schultz, and D. M. Downer, "Science and strategy for preventing and managing corneal ulceration," *The ocular surface*, vol. 5, pp. 23-39, 2007.
- [100] N. A. Peppas, *Hydrogels in medicine and pharmacy*. Boca Raton, Fla.: CRC Press, 1986.
- [101] N. A. Peppas, P. Bures, W. Leobandung, and H. Ichikawa, "Hydrogels in pharmaceutical formulations," *European Journal of Pharmaceutics and Biopharmaceutics*, vol. 50, pp. 27-46, 2000.
- [102] M. E. Byrne, K. Park, and N. A. Peppas, "Molecular imprinting within hydrogels," *Advanced Drug Delivery Reviews*, vol. 54, pp. 149-161, 2002.
- [103] N. A. Peppas, K. M. Wood, and J. O. Blanchette, "Hydrogels for oral delivery of therapeutic proteins," *Expert Opinion on Biological Therapy*, vol. 4, pp. 881-887, 2004.
- [104] N. A. Peppas, J. Z. Hilt, A. Khademhosseini, and R. Langer, "Hydrogels in biology and medicine: From molecular principles to bionanotechnology," *Advanced Materials*, vol. 18, pp. 1345-1360, 2006.
- [105] R. Langer and D. A. Tirrell, "Designing materials for biology and medicine," *Nature*, vol. 428, pp. 487-492, 2004.
- [106] P. C. Nicolson and J. Vogt, "Soft contact lens polymers: an evolution," *Biomaterials*, vol. 22, pp. 3273-3283, 2001.

- [107] B. A. Holden and G. W. Mertz, "Critical oxygen levels to avoid corneal edema for daily and extended wear contact lenses," *Investigative Ophthalmology and Visual Science*, vol. 25, pp. 1161-7, 1984.
- [108] R. Uchida, T. Sato, H. Tanigawa, and K. Uno, "Azulene incorporation and release by hydrogel containing methacrylamide propyltrimethylammonium chloride, and its application to soft contact lens," *Journal of Controlled Release*, vol. 92, pp. 259-264, 2003.
- [109] T. Sato, R. Uchida, H. Tanigawa, K. Uno, and A. Murakami, "Application of polymer gels containing side-chain phosphate groups to drug-delivery contact lenses," *Journal of Applied Polymer Science.*, vol. 98, p. 731, 2005.
- [110] P. Andrade-Vivero, E. Fernandez-Gabriel, C. Alvarez-Lorenzo, and A. Concheiro, "Improving the loading and release of NSAIDs from pHEMA hydrogels by copolymerization with functionalized monomers," *Journal of Pharmaceutical Sciences*, vol. 96, pp. 802-13, 2007.
- [111] J. F. Rosa dos Santos, C. Alvarez-Lorenzo, J. J. Torres-Labandeira, A. Concheiro, M. Silva, L. Balsa, *et al.*, "Soft contact lenses functionalized with pendant cyclodextrins for controlled drug delivery," *Biomaterials*, vol. 30, pp. 1348-1355, 2009.
- [112] J. Xu, X. Li, and F. Sun, "Cyclodextrin-containing hydrogels for contact lenses as a platform for drug incorporation and release," *Acta Biomaterialia*, vol. 6, pp. 486-493, 2010.
- [113] L. C. Winterton, J. M. Lally, K. B. Sentell, and L. L. Chapoy, "The elution of poly (vinyl alcohol) from a contact lens: the realization of a time release moisturizing agent/artificial

- tear," *Journal of Biomedical Materials Research. Part B, Applied Biomaterials*, vol. 80, pp. 424-432, 2007.
- [114] C. C. Peng, J. Kim, and A. Chauhan, "Extended delivery of hydrophilic drugs from silicone-hydrogel contact lenses containing vitamin E diffusion barriers," *Biomaterials*, vol. 31, pp. 4032-47, 2010.
- [115] V. P. Costa, M. E. M. Braga, J. P. Guerra, M. H. Gil, H. C. de Sousa, A. R. C. Duarte, *et al.*, "Development of therapeutic contact lenses using a supercritical solvent impregnation method," *Journal of Supercritical Fluids*, vol. 52, pp. 306-316, 2010.
- [116] M. E. Braga, F. Yañez, C. Alvarez-Lorenzo, A. Concheiro, C. M. Duarte, M. H. Gil, *et al.*, "Improved drug loading/release capacities of commercial contact lenses obtained by supercritical fluid assisted molecular imprinting methods," *Journal of Controlled Release*, vol. 148, pp. 102-104, 2010.
- [117] R. Garhwal, S. F. Shady, E. J. Ellis, J. Y. Ellis, C. D. Leahy, S. P. McCarthy, *et al.*, "Sustained ocular delivery of ciprofloxacin using nanospheres and conventional contact lens materials," *Invest Ophthalmol Vis Sci*, vol. 53, pp. 1341-52, 2012.
- [118] J. B. Ciolino, T. R. Hoare, N. G. Iwata, I. Behlau, C. H. Dohlman, R. Langer, *et al.*, "A drug-eluting contact lens," *Invest Ophthalmol Vis Sci*, vol. 50, pp. 3346-52, 2009.
- [119] J. B. Ciolino, S. P. Hudson, A. N. Mobbs, T. R. Hoare, N. G. Iwata, G. R. Fink, *et al.*, "A prototype antifungal contact lens," *Invest Ophthalmol Vis Sci*, vol. 52, pp. 6286-91, 2011.
- [120] H. Hiratani and C. Alvarez-Lorenzo, "The nature of backbone monomers determines the performance of imprinted soft contact lenses as timolol drug delivery systems," *Biomaterials*, vol. 25, pp. 1105-13, 2004.

- [121] S. Venkatesh, J. Saha, S. Pass, and M. E. Byrne, "Transport and structural analysis of molecular imprinted hydrogels for controlled drug delivery," *European Journal of Pharmaceutics and Biopharmaceutics*, vol. 69, pp. 852-860, 2008.
- [122] M. Ali and M. E. Byrne, "Controlled release of high molecular weight hyaluronic acid from molecularly imprinted hydrogel contact lenses," *Pharmaceutical Research*, vol. 26, pp. 714-726, 2009.
- [123] O. Wichterle and D. Lim, "Cross-linked hydrophilic polymers and articles made therefrom," US Patent: 3220960 Patent, 1965.
- [124] C. C. Karlgard, N. S. Wong, L. W. Jones, and C. Moresoli, "In vitro uptake and release studies of ocular pharmaceutical agents by silicon-containing and p-HEMA hydrogel contact lens materials," *International Journal of Pharmaceutics*, vol. 257, pp. 141-151, 2003.
- [125] C. C. Karlgard, L. W. Jones, and C. Moresoli, "Ciprofloxacin interaction with silicon-based and conventional hydrogel contact lenses," *Eye and Contact Lens*, vol. 29, pp. 83-89, 2003.
- [126] M. R. Jain, "Drug delivery through soft contact lenses," *British Journal of Ophthalmology*, vol. 72, pp. 150-154, 1988.
- [127] M. Kanemoto, T. Sato, A. Aoyama, T. Matsunaga, K. Uno, H. Toshida, *et al.*, "The interaction and compatibility between a soft contact lens and an ophthalmic drug," *Eye and Contact Lens*, vol. 32, pp. 192-196, 2006.
- [128] G. A. Lesher and G. G. Gunderson, "Continuous drug delivery through the use of disposable contact lenses," *Optometry and Vision Science*, vol. 70, pp. 1012-1018, 1993.

- [129] E. M. Hehl, R. Beck, K. Luthard, R. Guthoff, and B. Drewelow, "Improved penetration of aminoglycosides and fluoroquinolones into the aqueous humour of patients by means of Acuvue contact lenses," *European Journal of Clinical Pharmacology*, vol. 55, pp. 317-323, 1999.
- [130] A. Hui, A. Boone, and L. Jones, "Uptake and release of ciprofloxacin-HCl from conventional and silicone hydrogel contact lens materials," *Eye and Contact Lens*, vol. 34, pp. 266-271, 2008.
- [131] A. Boone, A. Hui, and L. Jones, "Uptake and release of dexamethasone phosphate from silicone hydrogel and group I, II, and IV hydrogel contact lenses," *Eye and Contact Lens*, vol. 35, pp. 260-267, 2009.
- [132] D. S. Hull, H. F. Edelhauser, and R. A. Hyndiuk, "Ocular penetration of prednisolone and the hydrophilic contact lens," *Archives of Ophthalmology*, vol. 92, pp. 413-6, 1974.
- [133] A. Soluri, A. Hui, and L. Jones, "Delivery of ketotifen fumarate by commercial contact lens materials," *Optometry & Vision Science*, vol. 89, pp. 1140-1149, 2012.
- [134] C. L. Schultz and D. W. Morck, "Contact lenses as a drug delivery device for epidermal growth factor in the treatment of ocular wounds," *Clinical and Experimental Optometry*, vol. 93, pp. 61-65, 2010.
- [135] V. P. Costa, M. E. M. Braga, C. M. M. Duarte, C. Alvarez-Lorenzo, A. Concheiro, M. H. Gil, *et al.*, "Anti-glaucoma drug-loaded contact lenses prepared using supercritical solvent impregnation," *Journal of Supercritical Fluids*, vol. 53, pp. 165-173, 2010.
- [136] F. Yañez, L. Martikainen, M. E. M. Braga, C. Alvarez-Lorenzo, A. Concheiro, C. M. M. Duarte, *et al.*, "Supercritical fluid-assisted preparation of imprinted contact lenses for drug delivery," *Acta Biomaterialia*, vol. 7, pp. 1019-1030, 2011.

- [137] J. Kim, C. C. Peng, and A. Chauhan, "Extended release of dexamethasone from silicone-hydrogel contact lenses containing vitamin E," *Journal of Controlled Release*, vol. 148, pp. 110-116, 2010.
- [138] C. C. Peng and A. Chauhan, "Extended cyclosporine delivery by silicone-hydrogel contact lenses," *Journal of Controlled Release*, vol. 154, pp. 267-274, 2011.
- [139] C. C. Peng, M. T. Burke, and A. Chauhan, "Transport of Topical Anesthetics in Vitamin E Loaded Silicone Hydrogel Contact Lenses," *Langmuir*, vol. 28, pp. 1478-1487, 2012.
- [140] C.-C. Peng, M. T. Burke, B. E. Carbia, C. Plummer, and A. Chauhan, "Extended drug delivery by contact lenses for glaucoma therapy," *Journal of Controlled Release*, vol. 162, pp. 152-158, 2012.
- [141] C.-C. Peng, A. Ben-Shlomo, E. O. Mackay, C. E. Plummer, and A. Chauhan, "Drug delivery by contact lens in spontaneously glaucomatous dogs," *Current eye research*, vol. 37, pp. 204-211, 2012.
- [142] D. Nguyen, A. Hui, A. Weeks, M. Heynen, E. Joyce, H. Sheardown, *et al.*, "Release of ciprofloxacin-HCl and dexamethasone phosphate by hyaluronic acid containing silicone polymers," *Materials*, vol. 5, pp. 684-698, 2012.
- [143] M. Fahmy, B. Long, T. Giles, and C.-H. Wang, "Comfort-enhanced daily disposable contact lens reduces symptoms among weekly/monthly wear patients," *Eye & contact lens*, vol. 36, pp. 215-219, 2010.
- [144] J. K. Xu, X. S. Li, F. Q. Sun, and P. T. Cao, "PVA Hydrogels Containing beta-Cyclodextrin for Enhanced Loading and Sustained Release of Ocular Therapeutics," *Journal of Biomaterials Science-Polymer Edition*, vol. 21, pp. 1023-1038, 2010.

- [145] T. Sato, R. Uchida, H. Tanigawa, K. Uno, and A. Murakami, "Application of polymer gels containing side-chain phosphate groups to drug-delivery contact lenses," *Journal of Applied Polymer Science*, vol. 98, p. 731, 2005.
- [146] K. Kakisu, T. Matsunaga, S. Kobayakawa, T. Sato, and T. Tochikubo, "Development and efficacy of a drug-releasing soft contact lens," *Invest Ophthalmol Vis Sci*, vol. 54, pp. 2551-61, 2013.
- [147] D. Gulsen and A. Chauhan, "Ophthalmic drug delivery through contact lenses," *Investigative Ophthalmology and Visual Science*, vol. 45, pp. 2342-2347, 2004.
- [148] D. Gulsen, C.-C. Li, and A. Chauhan, "Dispersion of DMPC liposomes in contact lenses for ophthalmic drug delivery," *Current Eye Research*, vol. 30, pp. 1071-1080, 2005.
- [149] C. C. Li, M. Abrahamson, Y. Kapoor, and A. Chauhan, "Timolol transport from microemulsions trapped in HEMA gels," *Journal of Colloid and Interface Science*, vol. 315, pp. 297-306, 2007.
- [150] Y. Kapoor, J. C. Thomas, A. Chauhan, G. Tan, and V. T. John, "Surfactant-laden soft contact lenses for extended delivery of ophthalmic drugs," *Biomaterials*, vol. 30, pp. 867-878, 2009.
- [151] H. J. Jung and A. Chauhan, "Temperature sensitive contact lenses for triggered ophthalmic drug delivery," *Biomaterials*, vol. 33, pp. 2289-2300, 2012.
- [152] H. J. Jung, M. Abou-Jaoude, B. E. Carbia, C. Plummer, and A. Chauhan, "Glaucoma therapy by extended release of timolol from nanoparticle loaded silicone-hydrogel contact lenses," *J Control Release*, vol. 165, pp. 82-89, 2013.

- [153] A. Danion, H. Brochu, Y. Martin, and P. Vermette, "Fabrication and characterization of contact lenses bearing surface-immobilized layers of intact liposomes," *Journal of Biomedical Materials Research. Part A*, vol. 82, pp. 41-51, 2007.
- [154] A. Danion, I. Arsenault, and P. Vermette, "Antibacterial activity of contact lenses bearing surface-immobilized layers of intact liposomes loaded with levofloxacin," *Journal of Pharmaceutical Sciences*, vol. 96, pp. 2350-63, 2007.
- [155] M. E. Davis, A. Katz, and W. R. Ahmad, "Rational catalyst design via imprinted nanostructured materials," *Chemistry of materials*, vol. 8, pp. 1820-1839, 1996.
- [156] K. Haupt and K. Mosbach, "Molecularly imprinted polymers and their use in biomimetic sensors," *Chemical Reviews*, vol. 100, pp. 2495-2504, 2000.
- [157] Q. He, X. Chang, Q. Wu, X. Huang, Z. Hu, and Y. Zhai, "Synthesis and applications of surface-grafted Th (IV)-imprinted polymers for selective solid-phase extraction of thorium (IV)," *Analytica chimica acta*, vol. 605, pp. 192-197, 2007.
- [158] J. Z. Hilt and M. E. Byrne, "Configurational biomimesis in drug delivery: molecular imprinting of biologically significant molecules," *Advanced Drug Delivery Reviews*, vol. 56, pp. 1599-1620, 2004.
- [159] N. M. Bergmann and N. A. Peppas, "Molecularly imprinted polymers with specific recognition for macromolecules and proteins," *Progress in Polymer Science*, vol. 33, pp. 271-288, 2008.
- [160] D. Cunliffe, A. Kirby, and C. Alexander, "Molecularly imprinted drug delivery systems," *Advanced drug delivery reviews*, vol. 57, pp. 1836-1853, 2005.

- [161] G. Wulff, "Molecular imprinting in cross-linked materials with the aid of molecular templates - a way towards artificial antibodies," *Angewandte Chemie International Edition*, vol. 34, pp. 1812-1832, 1995.
- [162] B. Sellergren, "Noncovalent molecular imprinting: Antibody-like molecular recognition in polymeric network materials," *Trends in Analytical Chemistry*, vol. 16, pp. 310-320, 1997.
- [163] M. E. Byrne and V. Salián, "Molecular imprinting within hydrogels II: Progress and analysis of the field," *International Journal of Pharmaceutics*, vol. 364, pp. 188-212, 2008.
- [164] M. E. Byrne, J. Z. Hilt, and N. A. Peppas, "Recognitive biomimetic networks with moiety imprinting for intelligent drug delivery," *Journal of Biomedical Materials Research Part A*, vol. 84A, pp. 137-147, 2008.
- [165] C. Alvarez-Lorenzo and A. Concheiro, "Molecularly imprinted polymers for drug delivery," *Journal of Chromatography B-Analytical Technologies in the Biomedical and Life Sciences*, vol. 804, pp. 231-245, 2004.
- [166] H. Hiratani, A. Fujiwara, Y. Tamiya, Y. Mizutani, and C. Alvarez-Lorenzo, "Ocular release of timolol from molecularly imprinted soft contact lenses," *Biomaterials*, vol. 26, pp. 1293-1298, 2005.
- [167] S. Venkatesh, S. P. Sizemore, and M. E. Byrne, "Biomimetic hydrogels for enhanced loading and extended release of ocular therapeutics," *Biomaterials*, vol. 28, pp. 717-724, 2007.

- [168] M. Ali, S. Horikawa, S. Venkatesh, J. Saha, J. W. Hong, and M. E. Byrne, "Zero-order therapeutic release from imprinted hydrogel contact lenses within in vitro physiological ocular tear flow," *Journal of Controlled Release*, vol. 124, pp. 154-162, 2007.
- [169] C. J. White, M. K. McBride, K. M. Pate, A. Tieppo, and M. E. Byrne, "Extended release of high molecular weight hydroxypropyl methylcellulose from molecularly imprinted, extended wear silicone hydrogel contact lenses," *Biomaterials*, vol. 32, pp. 5698-5705, 2011.
- [170] A. D. Vaughan, J. B. Zhang, and M. E. Byrne, "Enhancing Therapeutic Loading and Delaying Transport via Molecular Imprinting and Living/Controlled Polymerization," *Aiche Journal*, vol. 56, pp. 268-279, 2010.
- [171] B. Amsden, "Solute diffusion within hydrogels. Mechanisms and models," *Macromolecules*, vol. 31, pp. 8382-8395, 1998.
- [172] J. Crank, *The mathematics of diffusion*. New York: Oxford University Press, 1975.
- [173] P. J. Flory, *Principles of Polymer Chemistry*. Ithaca: Cornell University Press, 1953.
- [174] P. J. Flory and J. Rehner, "Statistical mechanics of cross-linked polymer networks II. Swelling," *J. Chem. Phys*, vol. 11, pp. 521-526, 1943.
- [175] J. Ricka and T. Tanaka, "Swelling of ionic gels: quantitative performance of the Donnan theory," *Macromolecules*, vol. 17, pp. 2916-2921, 1984.
- [176] L. Brannon-Peppas and N. A. Peppas, "Equilibrium swelling behavior of pH-sensitive hydrogels," *Chemical Engineering Science*, vol. 46, pp. 715-722, 1991.
- [177] A. M. Rampey, R. J. Umpleby, G. T. Rushton, J. C. Iseman, R. N. Shah, and K. D. Shimizu, "Characterization of the imprint effect and the influence of imprinting conditions on affinity, capacity, and heterogeneity in molecularly imprinted polymers

- using the Freundlich isotherm-affinity distribution analysis," *Analytical chemistry*, vol. 76, pp. 1123-1133, 2004.
- [178] R. J. Umpleby, M. Bode, and K. D. Shimizu, "Measurement of the continuous distribution of binding sites in molecularly imprinted polymers," *Analyst*, vol. 125, pp. 1261-1265, 2000.
- [179] C. Lübke, M. Lübke, M. J. Whitcombe, and E. N. Vulfson, "Imprinted polymers prepared with stoichiometric template-monomer complexes: efficient binding of ampicillin from aqueous solutions," *Macromolecules*, vol. 33, pp. 5098-5105, 2000.
- [180] O. Kimhi and H. Bianco-Peled, "Study of the interactions between protein-imprinted hydrogels and their templates," *Langmuir*, vol. 23, pp. 6329-6335, 2007.
- [181] Y.-q. Xia, T.-y. Guo, M.-d. Song, B.-h. Zhang, and B.-l. Zhang, "Hemoglobin recognition by imprinting in semi-interpenetrating polymer network hydrogel based on polyacrylamide and chitosan," *Biomacromolecules*, vol. 6, pp. 2601-2606, 2005.
- [182] B. M. Espinosa-García, W. M. Argüelles-Monal, J. Hernández, L. Félix-Valenzuela, N. Acosta, and F. M. Goycoolea, "Molecularly imprinted chitosan-genipin hydrogels with recognition capacity toward o-xylene," *Biomacromolecules*, vol. 8, pp. 3355-3364, 2007.
- [183] R. J. Umpleby, S. C. Baxter, M. Bode, J. K. Berch Jr, R. N. Shah, and K. D. Shimizu, "Application of the Freundlich adsorption isotherm in the characterization of molecularly imprinted polymers," *Analytica Chimica Acta*, vol. 435, pp. 35-42, 2001.
- [184] Y. Chen, M. Kele, I. Quiñones, B. Sellergren, and G. Guiochon, "Influence of the pH on the behavior of an imprinted polymeric stationary phase — supporting evidence for a binding site model," *Journal of Chromatography A*, vol. 927, pp. 1-17, 2001.

- [185] X. Li and S. M. Husson, "Adsorption of dansylated amino acids on molecularly imprinted surfaces: A surface plasmon resonance study," *Biosensors and Bioelectronics*, vol. 22, pp. 336-348, 2006.
- [186] H. Kim, K. Kaczmarek, and G. Guiochon, "Mass transfer kinetics on the heterogeneous binding sites of molecularly imprinted polymers," *Chemical Engineering Science*, vol. 60, pp. 5425-5444, 2005.
- [187] R. J. Umpleby, S. C. Baxter, A. M. Rampey, G. T. Rushton, Y. Chen, and K. D. Shimizu, "Characterization of the heterogeneous binding site affinity distributions in molecularly imprinted polymers," *Journal of Chromatography B*, vol. 804, pp. 141-149, 2004.
- [188] E. Turiel, C. Perez-Conde, and A. Martin-Esteban, "Assessment of the cross-reactivity and binding sites characterisation of a propazine-imprinted polymer using the Langmuir-Freundlich isotherm," *Analyst*, vol. 128, pp. 137-141, 2003.
- [189] R. J. Umpleby, S. C. Baxter, Y. Chen, R. N. Shah, and K. D. Shimizu, "Characterization of Molecularly Imprinted Polymers with the Langmuir–Freundlich Isotherm," *Analytical Chemistry*, vol. 73, pp. 4584-4591, 2001.
- [190] W.-Y. Chen, C.-S. Chen, and F.-Y. Lin, "Molecular recognition in imprinted polymers: thermodynamic investigation of analyte binding using microcalorimetry," *Journal of Chromatography A*, vol. 923, pp. 1-6, 2001.
- [191] B. M. Espinosa-García, W. M. Argüelles-Monal, J. Hernández, L. Félix-Valenzuela, N. Acosta, and F. M. Goycoolea, "Molecularly Imprinted Chitosan–Genipin Hydrogels with Recognition Capacity toward o-Xylene," *Biomacromolecules*, vol. 8, pp. 3355-3364, 2007.

- [192] U. G. Spizzirri and N. A. Peppas, "Structural Analysis and Diffusional Behavior of Molecularly Imprinted Polymer Networks for Cholesterol Recognition," *Chemistry of Materials*, vol. 17, pp. 6719-6727, 2005.
- [193] N. Djourelov, Z. Ateş, O. Güven, M. Misheva, and T. Suzuki, "Positron annihilation lifetime spectroscopy of molecularly imprinted hydroxyethyl methacrylate based polymers," *Polymer*, vol. 48, pp. 2692-2699, 2007.
- [194] D. A. Spivak, "Optimization, evaluation, and characterization of molecularly imprinted polymers," *Advanced Drug Delivery Reviews*, vol. 57, pp. 1779-1794, 2005.
- [195] S. W. Rowlinson, J. R. Kiefer, J. J. Prusakiewicz, J. L. Pawlitz, K. R. Kozak, A. S. Kalgutkar, *et al.*, "A novel mechanism of cyclooxygenase-2 inhibition involving interactions with Ser-530 and Tyr-385," *Journal of Biological Chemistry*, vol. 278, pp. 45763-45769, 2003.
- [196] P. Moser, A. Sallmann, and I. Wiesenberg, "Synthesis and quantitative structure-activity relationships of diclofenac analogs," *Journal of Medicinal Chemistry*, vol. 33, pp. 2358-2368, 1990.
- [197] B. Chuasuwan, V. Binjesoh, J. E. Polli, H. Zhang, G. L. Amidon, H. E. Junginger, *et al.*, "Biowaiver Monographs for Immediate Release Solid Oral Dosage Forms: Diclofenac Sodium and Diclofenac Potassium," *Journal of Pharmaceutical Sciences*, vol. 98, pp. 1206-1219, 2009.
- [198] A. R. Sallmann, "The history of diclofenac," *American Journal of Medicine*, vol. 80, pp. 29-33, 1986.

- [199] I. M. Kenawi, "DFT analysis of diclofenac activity and cation type influence on the theoretical parameters of some diclofenac complexes," *Journal of Molecular Structure-Theochem*, vol. 761, pp. 151-157, 2006.
- [200] B. Kim and N. A. Peppas, "Synthesis and characterization of pH-sensitive glycopolymers for oral drug delivery systems," *Journal of Biomaterials Science-Polymer Edition*, vol. 13, pp. 1271-1281, 2002.
- [201] D. Hariharan and N. A. Peppas, "Characterization, dynamic swelling behaviour and solute transport in cationic networks with applications to the development of swelling-controlled release systems," *Polymer*, vol. 37, pp. 149-161, 1996.
- [202] N. J. Kavimandan, E. Losi, and N. A. Peppas, "Novel delivery system based on complexation hydrogels as delivery vehicles for insulin–transferrin conjugates," *Biomaterials*, vol. 27, pp. 3846-3854, 2006.
- [203] J. Berger, M. Reist, J. M. Mayer, O. Felt, N. A. Peppas, and R. Gurny, "Structure and interactions in covalently and ionically crosslinked chitosan hydrogels for biomedical applications," *European Journal of Pharmaceutics and Biopharmaceutics*, vol. 57, pp. 19-34, 2004.
- [204] D. A. Smith, M. L. Wallwork, J. Zhang, J. Kirkham, C. Robinson, A. Marsh, *et al.*, "The effect of electrolyte concentration on the chemical force titration behavior of omega-functionalized SAMs: Evidence for the formation of strong ionic hydrogen bonds," *Journal of Physical Chemistry B*, vol. 104, pp. 8862-8870, 2000.
- [205] R. Srinivasan, J. S. Feenstra, S. T. Park, S. J. Xu, and A. H. Zewail, "Direct determination of hydrogen-bonded structures in resonant and tautomeric reactions using

- ultrafast electron diffraction," *Journal of the American Chemical Society*, vol. 126, pp. 2266-2267, 2004.
- [206] D. B. Moore, A. Harris, and B. Siesky, "The world through a lens: the vision of Sir Harold Ridley," *British Journal of Ophthalmology*, vol. 94, pp. 1277-1280, 2010.
- [207] K. D. Solomon, L. E. F. de Castro, H. P. Sandoval, J. M. Biber, B. Groat, K. D. Neff, *et al.*, "LASIK World Literature Review Quality of Life and Patient Satisfaction," *Ophthalmology*, vol. 116, pp. 691-701, 2009.
- [208] H. S. Dua, D. G. Said, and A. M. Otri, "Are we doing too many cataract operations? Cataract surgery: a global perspective," *British Journal of Ophthalmology*, vol. 93, pp. 1-2, 2009.
- [209] S. P. Srinivas, "In situ measurement of fluorescein release by collagen shields in human eyes," *Current Eye Research*, vol. 13, pp. 281-288, 1994.
- [210] P. Ritger and N. Peppas, "A simple equation for description of solute release I. Fickian and non-fickian release from non-swellable devices in the form of slabs, spheres, cylinders or discs," *Journal of Controlled Release*, vol. 5, pp. 23-36, 1987.
- [211] P. White. Contact lenses and solutions summary. *Contact Lens Spectrum Supplement*, 2011
- [212] L. Michaud and C. J. Giasson, "Overwear of contact lenses: Increased severity of clinical signs as a function of protein adsorption," *Optometry and Vision Science*, vol. 79, pp. 184-192, 2002.
- [213] R. C. Peterson, J. S. Wolffsohn, J. Nick, L. Winterton, and J. Lally, "Clinical performance of daily disposable soft contact lenses using sustained release technology," *Contact Lens and Anterior Eye*, vol. 29, pp. 127-134, 2006.

- [214] J. Xu, X. Li, and F. Sun, "In vitro and in vivo evaluation of ketotifen fumarate-loaded silicone hydrogel contact lenses for ocular drug delivery," *Drug Delivery*, vol. 18, pp. 150-158, 2011.
- [215] J. Kim, A. Conway, and A. Chauhan, "Extended delivery of ophthalmic drugs by silicone hydrogel contact lenses," *Biomaterials*, vol. 29, pp. 2259-2269, 2008.
- [216] S. K. Mehta, K. K. Basin, and S. Dham, "Energetically favorable interactions between diclofenac sodium and cyclodextrin molecules in aqueous media," *Journal of Colloid and Interface Science*, vol. 326, pp. 374-381, 2008.
- [217] M. L. Manca, M. Zaru, G. Ennas, D. Valenti, C. Sinico, G. Loy, *et al.*, "Diclofenac- β -cyclodextrin binary systems: physicochemical characterization and in vitro dissolution and diffusion studies," *Aaps Pharmscitech*, vol. 6, pp. E464-E472, 2005.
- [218] R. Chadha, N. Kashid, A. Kumar, and D. V. S. Jain, "Calorimetric studies of diclofenac sodium in aqueous solution of cyclodextrin and water-ethanol mixtures," *Journal of pharmacy and pharmacology*, vol. 54, pp. 481-486, 2002.
- [219] N. L. Burstein, "Preservative cytotoxic threshold for benzalkonium chloride and chlorhexidine digluconate in cat and rabbit corneas," *Invest Ophthalmol Vis Sci*, vol. 19, pp. 308-13, 1980.
- [220] J. Murube, A. Murube, and C. Zhuo, "Classification of artificial tears. II: Additives and commercial formulas," *Adv Exp Med Biol*, vol. 438, pp. 705-15, 1998.
- [221] N. Buhler, H. P. Haerri, M. Hofmann, C. Irrgang, A. Muhlebach, B. Muller, *et al.*, "Nelfilcon A, a new material for contact lenses," *Chimia*, vol. 53, pp. 269-274, 1999.

- [222] M. H. Lee, K. J. Yoon, and S.-W. Ko, "Synthesis of a vinyl monomer containing beta-cyclodextrin and grafting onto cotton fiber," *Journal of Applied Polymer Science*, vol. 80, pp. 438-446, 2001.
- [223] N. J. Van Haeringen, "Clinical biochemistry of tears," *Survey of Ophthalmology*, vol. 26, pp. 84-96, 1981.
- [224] R. Noecker, "Effects of common ophthalmic preservatives on ocular health," *Adv Ther*, vol. 18, pp. 205-15, 2001.
- [225] L. F. Gudeman and N. A. Peppas, "pH-sensitive membranes from poly(vinyl alcohol)/poly(acrylic acid) interpenetrating networks," *Journal of Membrane Science*, vol. 107, pp. 239-248, 1995.
- [226] A. R. Kannurpatti, J. W. Anseth, and C. N. Bowman, "A study of the evolution of mechanical properties and structural heterogeneity of polymer networks formed by photopolymerizations of multifunctional (meth)acrylates," *Polymer*, vol. 39, pp. 2507-2513, 1998.
- [227] L. Bielory, "Role of antihistamines in ocular allergy," *American Journal of Medicine*, vol. 113, pp. 34S-37S, 2002.
- [228] A. G. Swennes, L. C. Alworth, S. B. Harvey, C. A. Jones, C. S. King, and S. L. Crowell-Davis, "Human Handling Promotes Compliant Behavior in Adult Laboratory Rabbits," *Journal of the American Association for Laboratory Animal Science*, vol. 50, pp. 41-45, 2011.
- [229] L. H. Sperling, *Introduction to physical polymer science*. New York: Wiley, 1986.
- [230] C. S. Brazel and N. A. Peppas, "Modeling of drug release from swellable polymers," *European Journal of Pharmaceutics and Biopharmaceutics*, vol. 49, pp. 47-58, 2000.

- [231] M. Rowland and T. N. Tozer, *Clinical pharmacokinetics : concepts and applications*. Baltimore: Williams & Wilkins, 1995.
- [232] C. Beauregard, D. Stephens, L. Roberts, D. Gamache, and J. Yanni, "Duration of action of topical antiallergy drugs in a guinea pig model of histamine-induced conjunctival vascular permeability," *Journal of Ocular Pharmacology and Therapeutics*, vol. 23, pp. 315-320, 2007.
- [233] A. J. Aguilar, "Comparative study of clinical efficacy and tolerance in seasonal allergic conjunctivitis management with 0.1% olopatadine hydrochloride versus 0.05% ketotifen fumarate," *Acta Ophthalmologica Scandinavica. Supplement*, pp. 52-55, 2000.
- [234] S. S. Chrai, T. F. Patton, A. Mehta, and J. R. Robinson, "Lacrimal and instilled fluid dynamics in rabbit eyes," *Journal of Pharmaceutical Sciences*, vol. 62, pp. 1112-1121, 1973.
- [235] S. Mishima, A. Gasset, S. D. Klyce, Jr., and J. L. Baum, "Determination of tear volume and tear flow," *Investigative ophthalmology*, vol. 5, pp. 264-76, 1966.
- [236] H. Hiratani, Y. Mizutani, and C. Alvarez-Lorenzo, "Controlling drug release from imprinted hydrogels by modifying the characteristics of the imprinted cavities," *Macromolecular Bioscience*, vol. 5, pp. 728-733, 2005.
- [237] A. Tieppo, K. M. Pate, and M. E. Byrne, "In vitro controlled release of an anti-inflammatory from daily disposable therapeutic contact lenses under physiological ocular tear flow," *European Journal of Pharmaceutics and Biopharmaceutics*, vol. 81, pp. 170-177, 2012.
- [238] D. R. Paul, "Elaborations on the Higuchi model for drug delivery," *International Journal of Pharmaceutics*, vol. 418, pp. 13-17, 2011.

- [239] J. Siepmann and N. A. Peppas, "Higuchi equation: Derivation, applications, use and misuse," *International Journal of Pharmaceutics*, vol. 418, pp. 6-12, 2011.

**Appendix A:
Nelfilcon A Lenses**

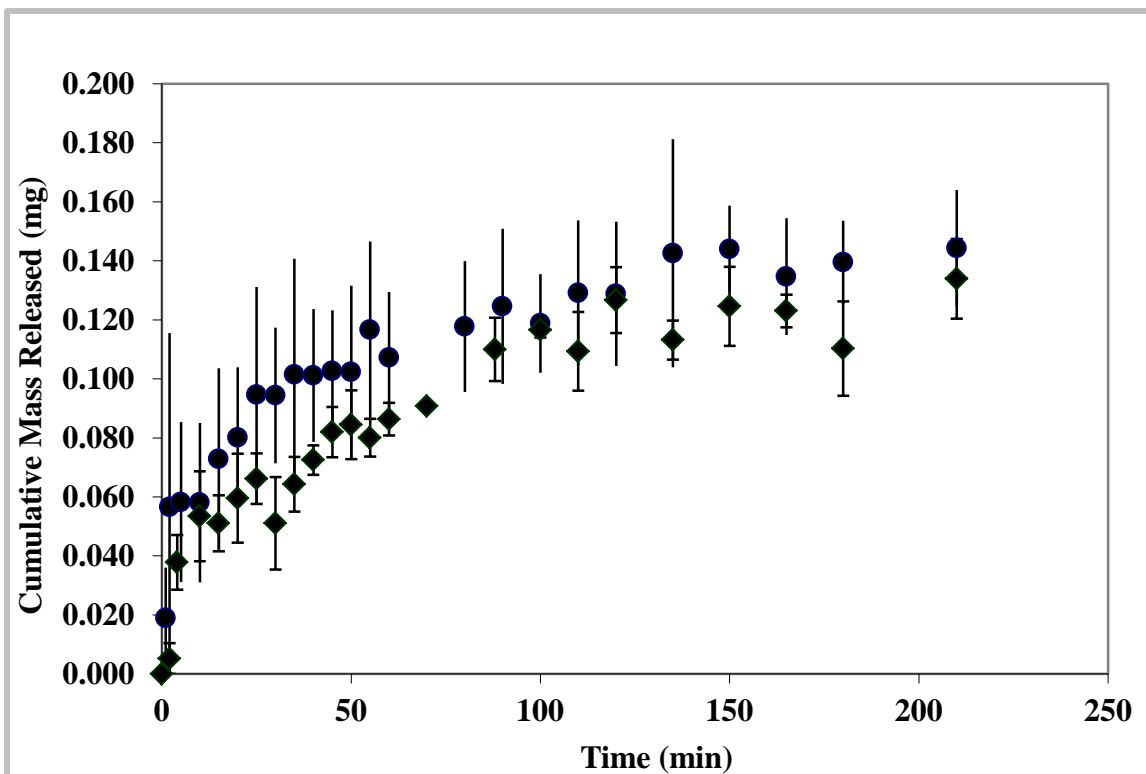


Figure A.1: Cumulative mass release of diclofenac from Nelfilcon A lenses at different stir rates

Dynamic release study in DI water was conducted on lenses prepared from a pre-polymer containing 6.5 mg of DS per gram of Nelfilcon formulation. No functional monomers were added. For comparison, we plot the release profiles of hydrogels at different stir rates: 30 rpm (●), 25 rpm (◆). N= 2, and T = 34°C.

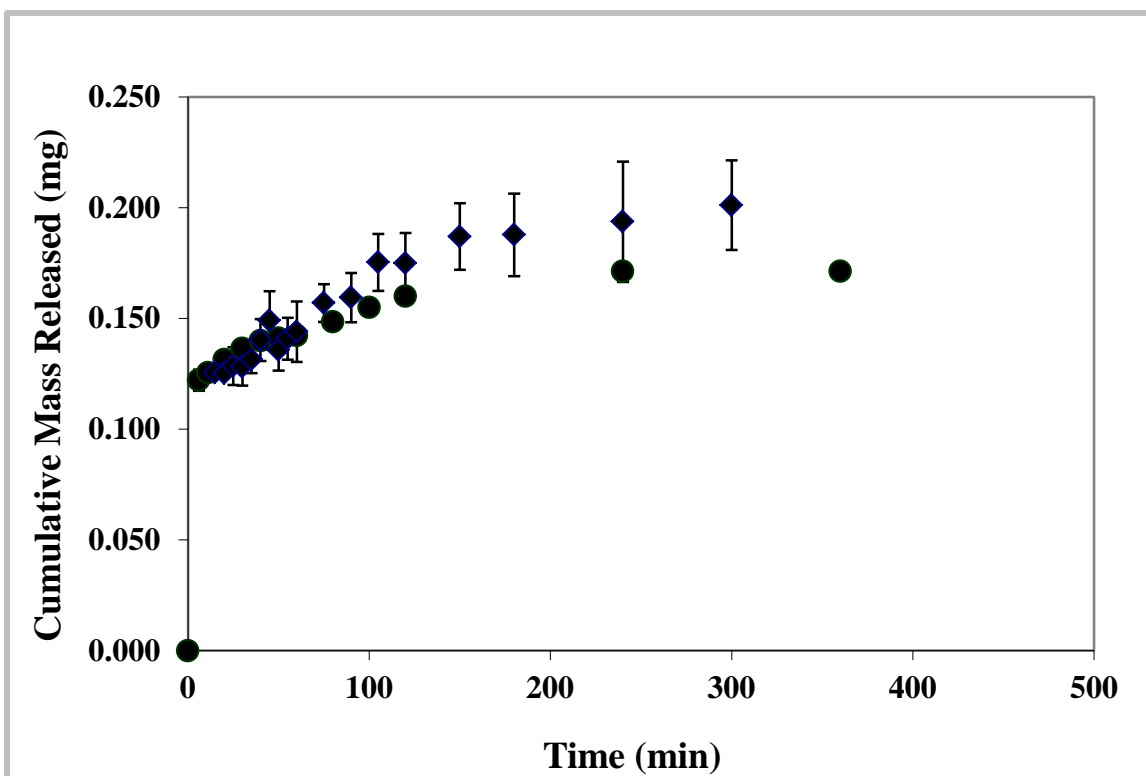


Figure A.2: Comparison of dissolution apparatus protocol and replacement method for the release of diclofenac from Nelfilcon A lenses

Dynamic release study in DI water carried out in the Sotax Apparatus (30 rpm) (◆) and Orbital Shaker with Replacement Method (●) on lenses prepared from a pre-polymer containing 6.5 mg of DS per gram of Nelfilcon formulation. No functional monomers were added. $N=2$, $T=34^{\circ}\text{C}$. In order to prove that an infinite sink can be achieved using the Sotax Dissolution Apparatus, it was necessary to compare the Sotax protocol against the replacement method. For the replacement method, lenses were placed in 50 mL centrifuge tubes with 30 mL of DI water and incubated at 34°C on an orbital shaker. After measured time intervals, the lenses were extracted and deposited into 30 mL of fresh DI water. The results prove a perfect infinite sink model using the Sotax apparatus.

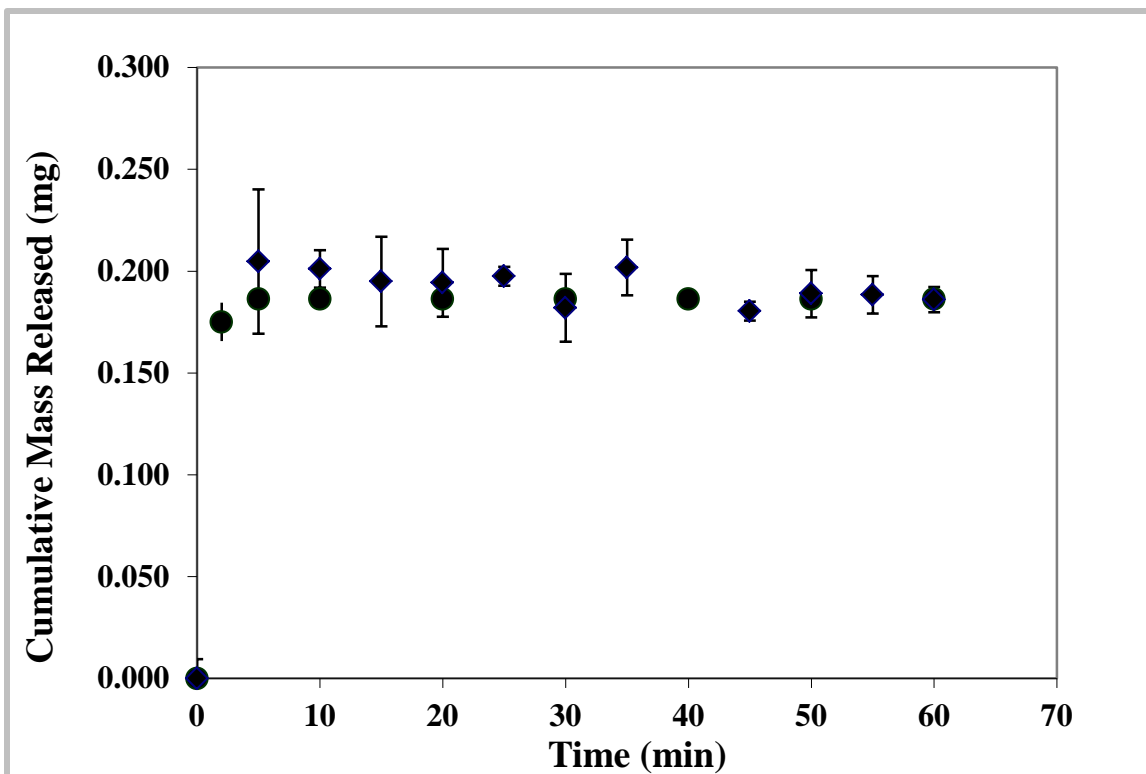


Figure A.3: Comparison of dissolution apparatus protocol and replacement method for the release of diclofenac from Nelfilcon A lenses with different proportions of NVP and DEAEM

Dynamic release study in DI water carried out on the Sotax (30 rpm) (◆) and Orbital Shaker with Replacement Method (●) on lenses prepared from containing NVP and DEAEM functional monomers at a fixed ratio of other monomers [HEMA:NVP:DEAEM] of [0:1:2] 8.91 wt.% (M/T~30).N= 2, and T = 34°C. The results prove a perfect infinite sink model using the Sotax apparatus.

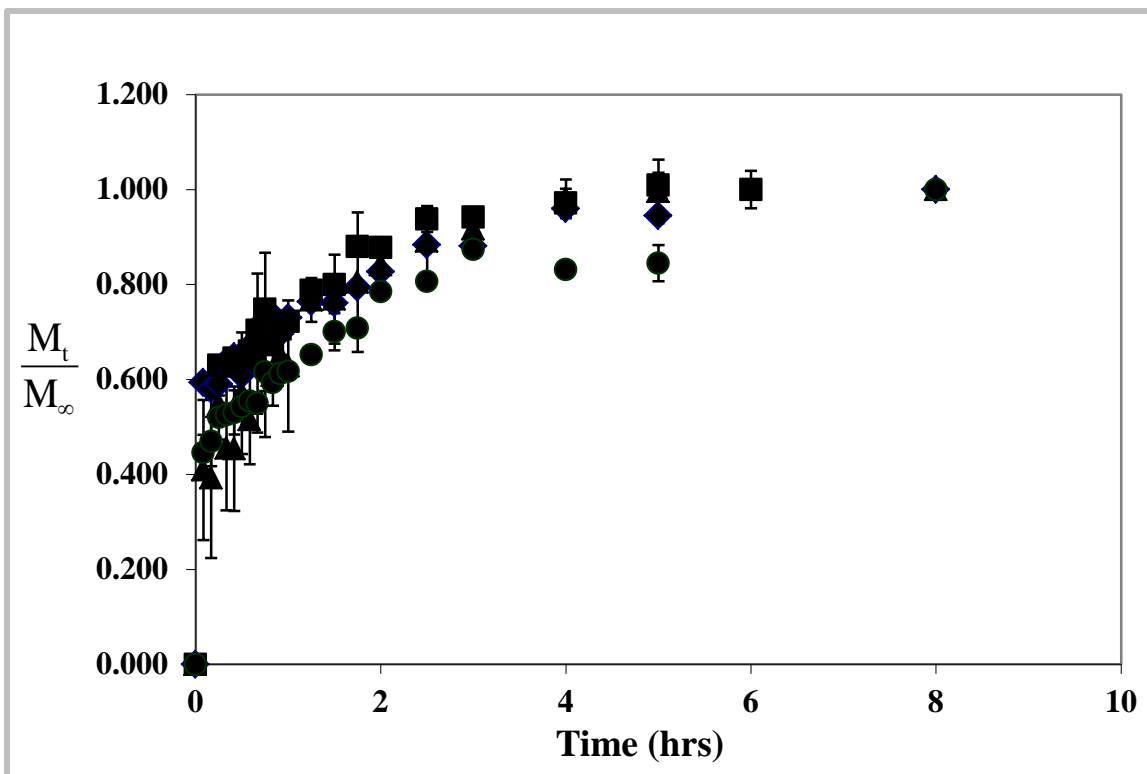


Figure A.4: Fractional mass release of diclofenac from Nelfilcon A lenses with different loading concentrations of DS

Dynamic release studies in DI water were conducted on Nelfilcon lenses containing different amounts of DS per gram of Nelfilcon: 10.0 mg/g (♦), 8.0 mg/g (●), 6.5 mg/g (■), 4.0 mg/g (▲), 2.0 mg/g (×). No functional monomers were added. Fractional release (DS diffusion coefficient) is not dependent on DS loading concentration. N = 2, T = 34°C.

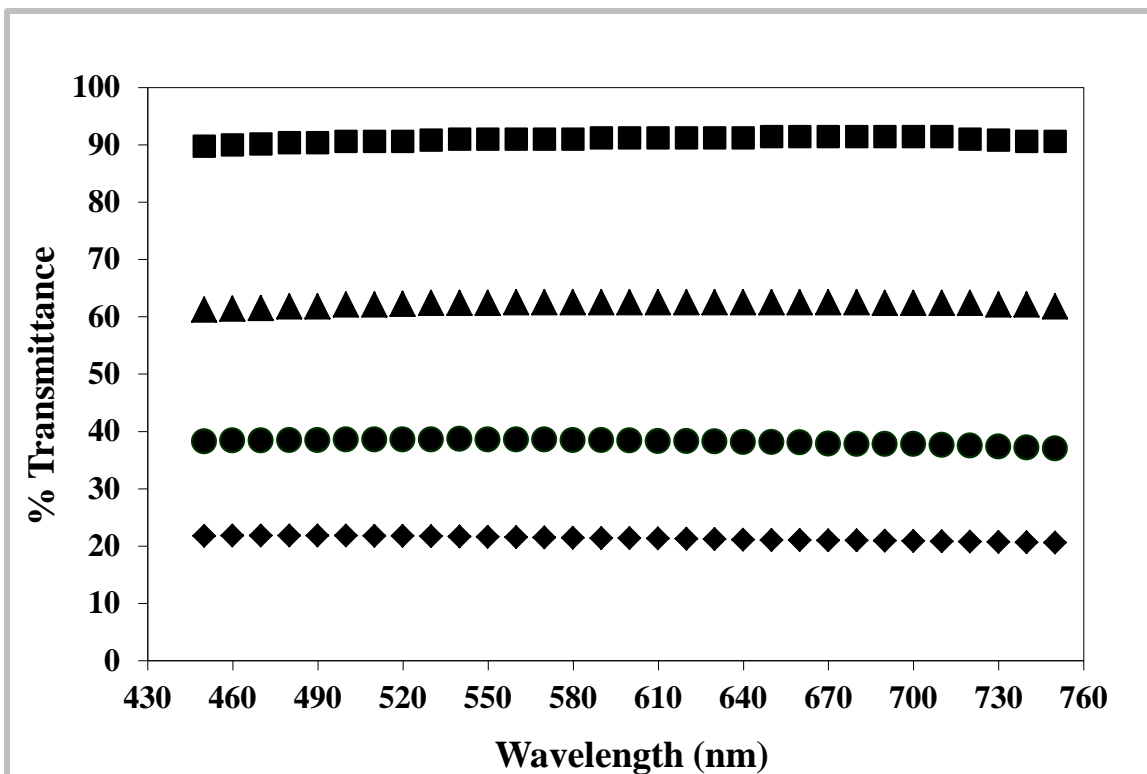


Figure A.5: Optical clarity of Nelfilcon A pre-polymer solutions

Pure Nelfilcon A (■), 4 mg/g (▲), 8.0 mg/g (●), 10 mg/g (◆). As concentration of DS increases, the % transmittance of Nelfilcon-DS solutions decreases. The decrease is not due to the absorption of light by DS.

Dynamic Release of Nelfilcon A Lenses Synthesized with HEMA

Because a large percentage of the drug is sequestered in HEMA lenses (25%-40%) when performing the release for 24 hours, it was necessary to know whether more diclofenac sodium could be released from the lenses. Therefore, a 7 day release was carried out for the lenses imprinted with 3.81% HEMA and 1.30% HEMA. Figure A.6 shows that the majority of diclofenac sodium is released from the lenses at long times (85.8% of diclofenac sodium is released from the lenses imprinted with 3.81% HEMA lenses and a 92.2% is released from the lenses imprinted with 1.3% HEMA).

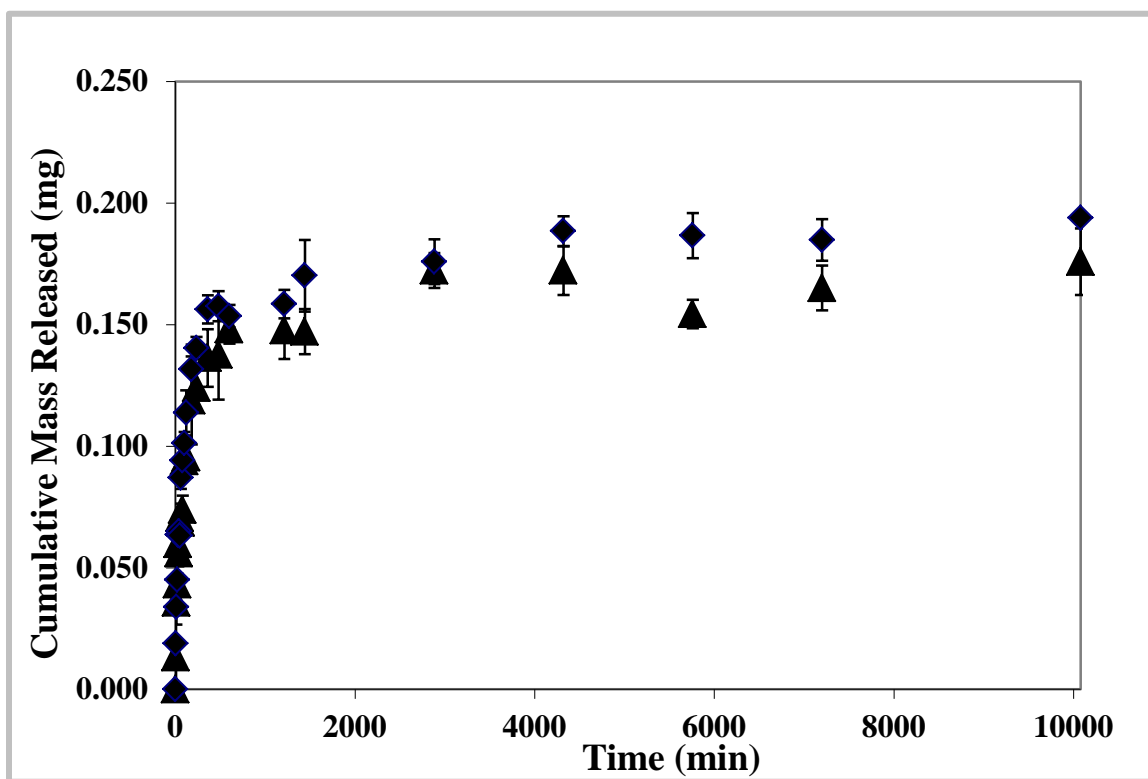


Figure A.6: Long time cumulative mass release of diclofenac from Nelfilcon A lenses with different proportions of HEMA

Dynamic release studies in DI water were conducted on lenses prepared from pre-polymers containing different proportions of HEMA functional monomer at a fixed ratio of other monomers [HEMA:NVP:DEAEM] of [1:0:0]. 1.30 wt.% HEMA (M/T~5) (◆), and 3.81 wt.% HEMA (M/T~15) (▲). At longer times, the majority of the loaded DS is released from the lens. N= 2, and T = 34°C.

Dynamic Release of Nelfilcon A Lenses Synthesized with DADMAC

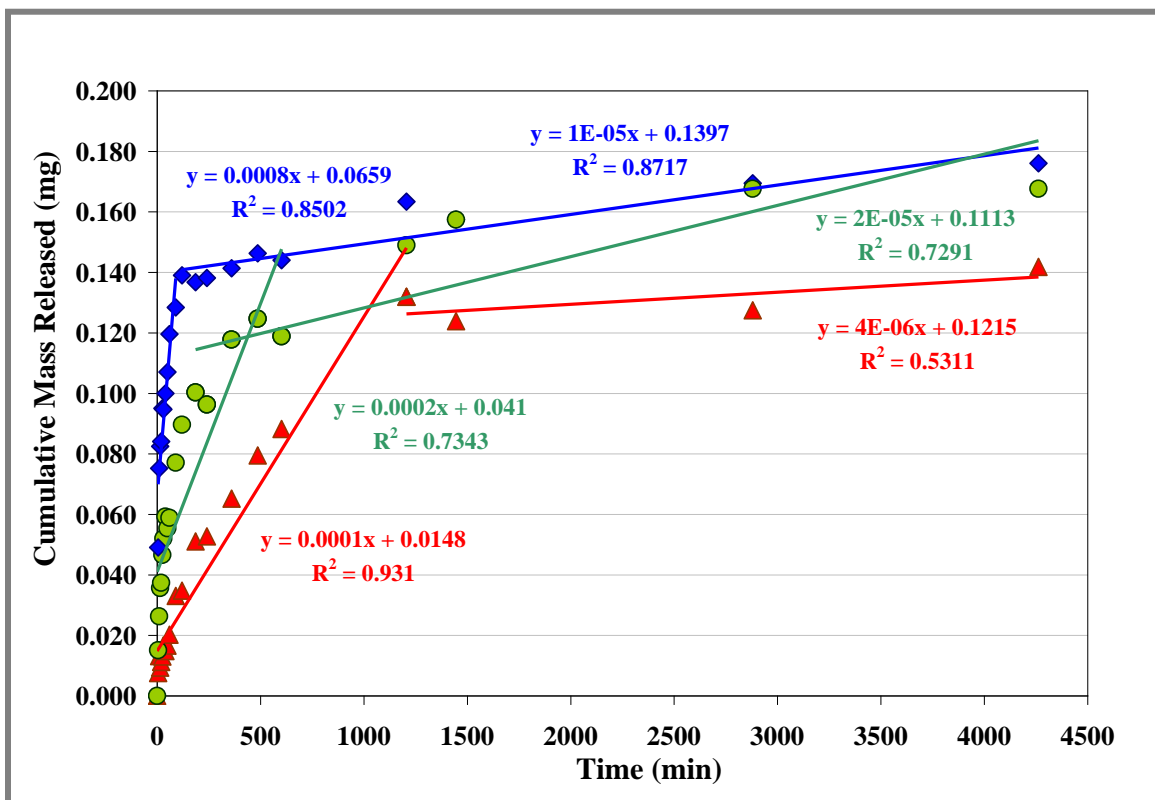


Figure A.7: Cumulative release of diclofenac sodium from Nelfilcon A lenses with different proportions of DADMAC

Dynamic release studies in DI water were conducted on lenses prepared from pre-polymers containing different proportions of DADMAC functional monomer at a fixed ratio of other monomers [DADMAC: DEAEM] of ~0.5 wt.% DADMAC (M/T~1.5) (♦), ~1.0 wt.% DADMAC (M/T~3.0) (●) and ~2.0 wt.% DADMAC (M/T~6.0) (▲). N= 2, and T = 34°C. The cumulative DS mass release tends to decrease as the proportion of DADMAC is increased. For each lens, there are two distinct release rates. For the lenses containing ~0.5 wt.% DADMAC (♦), the initial release of DS is linear with a rate around 0.8 µg/min (48 µg/hr) for 2 hours, and for the next 70 hours, 0.01 µg/min (0.6 µg/hr) of DS is released. For the lens containing ~1 wt% DADMAC (●), DS is released at a rate of around 0.2 µg/min (12 µg/hr) for 10 hours, and for the next 62 hours, small amounts of DS are released (0.02 µg/min or 1.2 µg/hr). For the lens containing ~2 wt.% DADMAC (▲), DS is released at a linear rate of around 0.1 µg/min (6 µg/hr) for 24 hours, and for the next 48 hours, small amounts of DS are released (0.004 µg/min or 0.24 µg/hr).

Dynamic Release of Nelfilcon A Lenses Synthesized with Diclofenac Sodium

Release studies were carried out with Nelfilcon A lenses with no functional monomer containing 6.5 mg of DS per gram of Nelfilcon formulation in different release media. Figure A.8 shows that the release in lacrimal solution is a fast release; the template was released over 20 minutes compared to the 360 minutes that took for the template to release in DI water.

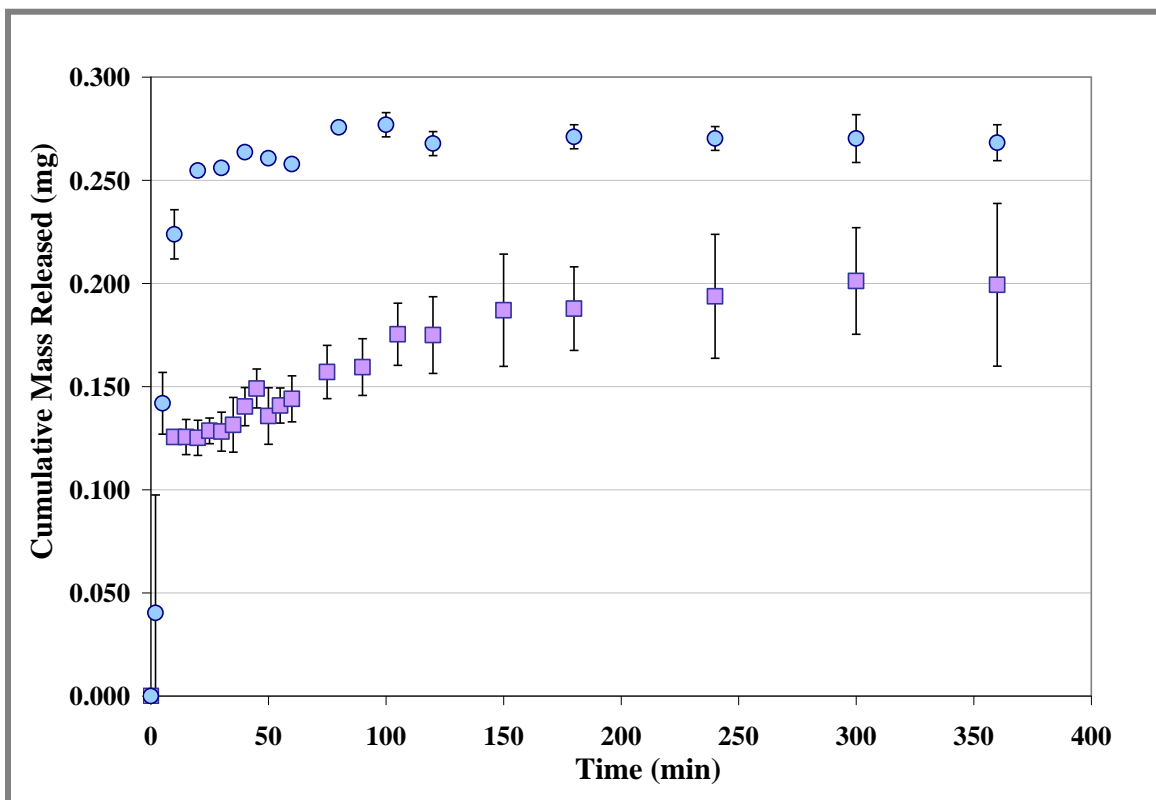


Figure A.8: Cumulative release of diclofenac from Nelfilcon A lenses in artificial lacrimal solution

Dynamic release studies in artificial lacrimal solution and DI water were conducted on lenses prepared from a pre-polymer containing 6.5 mg of DS per gram of Nelfilcon formulation. Lacrimal Solution (●) and DI water (■). No functional monomers were added. N= 2, T = 34°C. An artifact in the data is the total amount of DS in the lens. The lenses tested in lacrimal solution contained more DS due to a difference in the weight attributed to the use of a new set of the same mold.

Dynamic Release in Lacrimal Solution of Nelfilcon A Lenses Synthesized with DADMAC

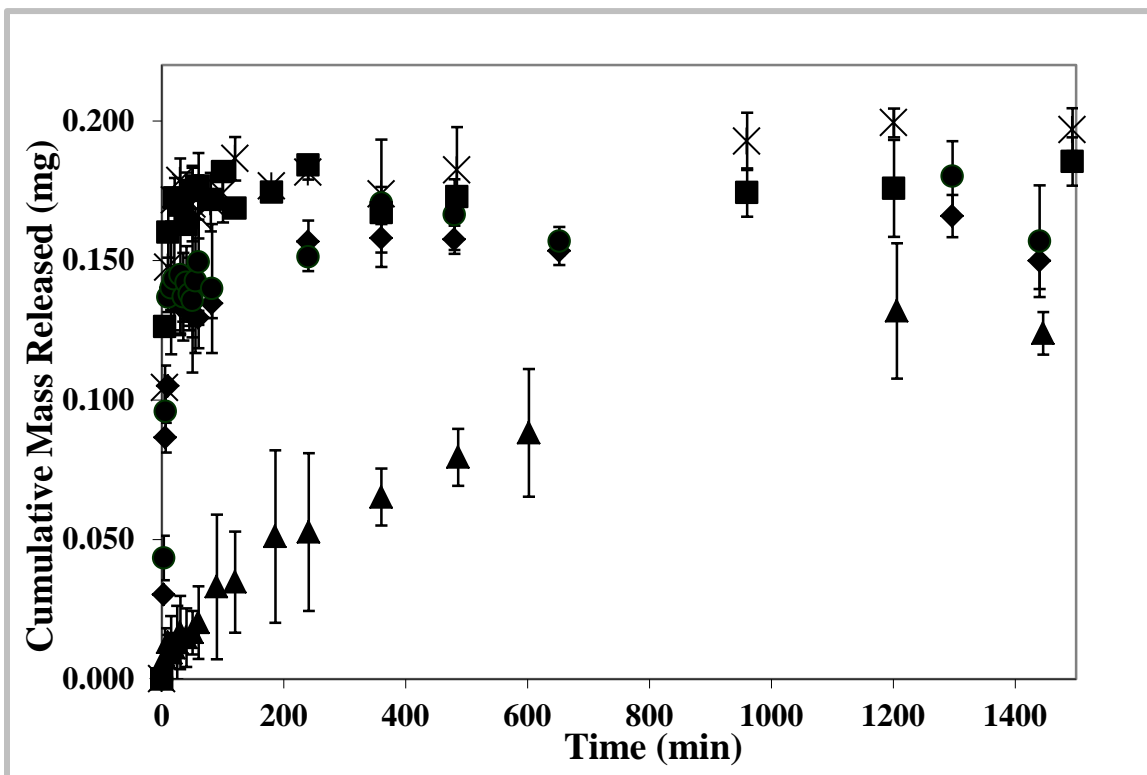


Figure A.9: Cumulative release of diclofenac from Nelfilcon A lenses with DADMAC and HEMA in artificial lacrimal solution

Dynamic release studies in lacrimal solution were conducted on lenses prepared from pre-polymers containing different proportions of functional monomers of ~15 wt.% DADMAC (M/T~45.7) (◆), ~10 wt.% DADMAC (M/T~30.5) (●), [DADMAC:HEMA] of [1:1] ~3.5 wt.% (M/T~12.2) (×), and [1:0.5] ~2.73 wt.% (M/T~9.2) (■). For comparison, a plot of a lens prepared with ~2 wt.% DADMAC (M/T~6.1) with release in DI water is also shown (▲). Significantly increasing the amount of DADMAC or adding HEMA (to increase hydrogen bonding) did not extend the release in lacrimal solution. N= 2, and T = 34°C.

Appendix B: Silicone Lenses

Additional Silicone Lens Formulation

Silicone hydrogel lenses of several compositions were prepared by mixing the individual monomers of the LFB formulation (Betacon Macromer, TRIS and DMA), and if applicable with crosslinking monomers. Table B.1, Table B.2 and Table B.3 show the composition of the pre-polymer formulations. Ethanol was added to aid in solubilization, and Dorocur 1173 was used as the initiator. The lens was polymerized via UV-light free radical polymerization with an intensity of $\sim 25 \text{ mW/cm}^2$ for duration of 1.5 min.

Table B.1: Silicone Lens Formulations

Sample	Macromer	TRIS	DMA	Ethanol	PEG(200)DMA	EGDMA	Initiator	DS
1	2200	1700	500	0	250	250	50	50
2	1500	1400	1500	0	250	250	50	50
3	500	500	3400	0	250	250	50	50
4	1250	1000	1500	1250	0	0	50	50
5	500	2500	500	1250	0	0	50	50
6	2000	2000	500	0	0	500	50	50
7	2000	500	2500	0	0	0	50	50
8	1500	1250	1250	500	0	250	50	50
9	1750	1400	1250	0	500	0	50	50
10	2250	500	500	1250	500	0	50	50
11	2000	500	2500	0	0	0	50	50
12	2650	650	1150	0	250	250	50	50
13	2250	500	500	1250	0	500	50	50
14	500	1500	2500	0	0	0	50	50
15	2500	500	1000	500	250	250	50	50
16	1250	1250	1500	500	250	250	50	50
17	2250	500	500	1250	0	500	50	50
18	1750	1750	500	500	0	500	50	50
19	1750	1750	500	500	250	250	50	50
20	1750	1750	500	500	500	0	50	50
21	1750	1500	750	500	250	250	50	50
22	1500	1500	750	750	250	250	50	50
23	1500	1250	1000	750	250	250	50	50
24	1500	1500	1000	500	0	250	50	50
25	1250	1250	1500	900	0	0	50	50
26	1750	1750	750	650	0	0	50	50
27	1500	1500	1000	900	0	0	50	50
28	1750	1500	1000	750	0	0	50	50

Sample	Macromer	TRIS	DMA	Ethanol	PEG(200)DMA	EGDMA	Initiator	DS
29	1750	1750	500	500	0	0	50	50
30	1850	1850	600	600	0	0	50	50
31	1750	1750	650	500	0	250	50	50
32	1750	1750	650	500	125	125	50	50
33	1750	1750	650	500	250	0	50	50
34	1600	1550	1100	500	0	150	50	50
35	1500	1450	1300	500	0	150	50	50

All quantities represent mg of the compound.

Incorporation of functional monomers to the pre-polymer formulation was attempted to allow interactions between the functional monomers and diclofenac sodium; however, phase separation was observed in all the attempts.

Table B.2: Silicone Lens Formulations with Functional Monomers

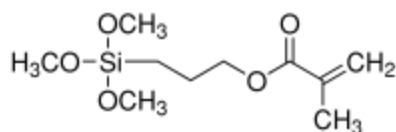
Sample	Macromer	TRIS	DMA	Ethanol	DADMAC	DEAEM	MAPTAC	Dextran	Initiator	DS
1	1500	1500	750	500	100	0	0	0	50	50
2	1750	1650	750	500	0	100	0	0	50	50
3	1750	1650	750	500	0	0	100	0	50	50
4	1750	1650	750	500	0	0	0	100	50	50

All quantities represent mg of the compound

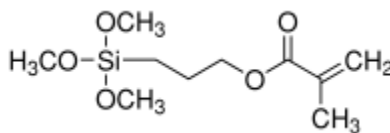
Table B.3: Silicone Lens Formulations with Functional Monomers

Sample	Macromer	TRIS	DMA	Ethanol	TMPM	METAC	AATAC	Initiator	DS
1	1500	1500	750	500	0	0	0	50	50
2	1750	1650	750	500	100	0	0	50	50
3	1750	1650	750	500	0	100	0	50	50
4	1750	1650	750	500	0	0	100	50	50

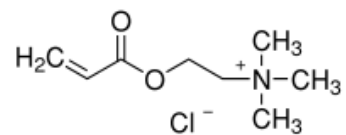
All quantities represent mg of the compound.



3-(Trimethoxysilyl) propyl methacrylate (TMPM)



2-(Methacryloyloxy)ethyl] trimethylammonium chloride (METAC)



3-(Acrylamidopropyl) trimethylammonium chloride (AATAC)

Template Binding Experiments

A variety of concentrations of diclofenac sodium in DI water (0.05, 0.10, and 0.20, mg/mL) were prepared. Initial absorbances of each concentration were measured using a Synergy UV–Vis spectrophotometer at 276 nm, the wavelength of maximum absorption. After the initial absorbance was taken, a dried silicone hydrogel lens was inserted into 5 mL of solution placed in a vial, and the vials were gently agitated on an ocelot rotator (Fisher Scientific; Chicago, IL) at 75 rpm and 12° tilt angle. After equilibrium was reached, the solutions were vortexed for 10 seconds. The bound concentration in the silicone lens was determined by mass balance. All silicone lenses were analyzed in triplicate, and all binding values are based upon the dry weight of the lens.

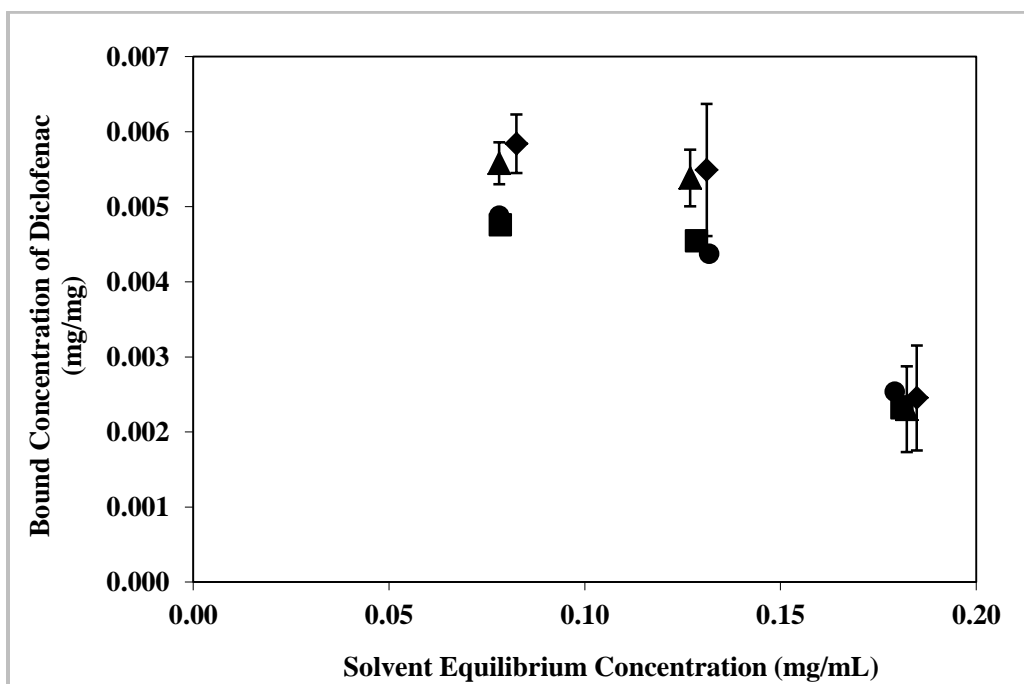


Figure B.1: Equilibrium binding isotherms for diclofenac sodium by silicone hydrogel lenses

Silicone lenses were prepared from pre-polymers containing different proportions of hydrophobic:hydrophilic ratios: LFB1 (0.76:1) (▲), LFB2 (1.50:1) (◆), LFB3 (7.50:1) (●), and LFB4 (2.18:1, and 2 wt.% EGDMA) (■). Changing the loading concentration, the mass of diclofenac loaded to silicone contact lenses can be tailored. The data is plotted as the mean \pm SD (n=3).